A review of the Mastacembeloidei, a suborder of synbranchiform teleost fishes
Part I: Anatomical descriptions

Robert A. Travers
Department of Zoology, British Museum (Natural History), Cromwell Road, London SW7 5BD[1]

Contents

[1]This research was carried out in the Department of Zoology, British Museum (Natural History) and was submitted in partial fulfilment of the requirements for the degree of Doctor of Philosophy in the Faculty of Science, University of London. The author's present address: Department of Anatomy & Cell Biology, St. Mary's Hospital Medical School, Norfolk Place, London W2 1PG.

Bull. Br. Mus. nat. Hist. (Zool.) **46** (1) : 1–133 Issued 26 January 1984

Synopsis

The Mastacembeloidei or spiny eels (comprising the families Mastacembelidae, Chaudhuriidae and Pillaiidae) is a distinctive group of about 70 freshwater species with a tropical and subtropical Oriental and Ethiopian distribution, currently recognised as a suborder of the perciform fishes. The majority of its 70 species have been placed in a single genus, *Mastacembelus*, without regard to their genealogical relationships, and the sub-order as a whole has not been the subject of a detailed taxonomic or anatomical review. A revision of the genera and families within the suborder, and a reconsideration of its interrelationships within the Percomorpha, are the overall objectives of this study.

The present work consists of anatomical descriptions of all available mastacembeloid species. The osteology of *Mastacembelus mastacembelus, Chaudhuria caudata* and *Pillaia indica* is described in detail, and is compared with that in the majority of described species. Myological studies are restricted to the cephalic region (jaw and opercular muscles only), and the arrangement in *Mastacembelus mastacembelus* is described and compared with that found in the other mastacembeloids examined.

Introduction

The Mastacembelidae, or spiny eels, a family of eel-like percomorph fishes is widely distributed in tropical and subtropical regions of Africa, SE. Asia and the Middle East (Ethiopian and Oriental zoogeographic regions). The eel-like appearance of mastacembelids is enhanced by lack of pelvic fins, a long body with numerous vertebrae, a tendency for the dorsal and anal fins to be confluent with the caudal fin, and a narrow, tapered cranium terminating in a pointed rostral appendage. Anterior to the rayed dorsal fin in almost all species is a long series of isolated spines.

The present state of mastacembélid taxonomy is confused. No revision of the entire family has ever been undertaken. Since the first scientific description of this group (Russell, 1756; Gronovius, 1763 & Scopoli, 1777) numerous species have been described, most of which were placed in the genus *Mastacembelus* Scopoli, 1777. Exceptionally, one species, originally described by Bloch (1786, & see Sufi, 1956: 100) was placed in a separate genus, *Macrognathus* Lacépède, 1800 (Bloch's *Ophidium*).

The most recent synoptic review of *Mastacembelus* was published by Boulenger (1912) who recognised 14 Asian, 1 Middle Eastern and 30 African species. Since then, numerous descriptions of new species, particularly from Africa, have appeared in the literature (Table 1), and one was assigned to a new genus (Poll, 1958). However, the validity of this generic distinction was questioned by Roberts & Stewart (1976). Many unidentifiable African specimens lodged in the collections of major national museums including the British Museum (Natural History); Museum of Comparative Zoology, Harvard, and Koninklijk Museum Voor Midden-Afrika, Tervuren, justify the need for a revision of the African mastacembelids.

The state of Oriental mastacembelid taxonomy is little better, although it has been the subject of a more recent revision (Sufi, 1956). Sufi (op. cit.) recognised 15 oriental *Mastacembelus* species and a single *Macrognathus* species on the basis of superficial anatomical and morphometric characters.

Macrognathus remained monotypic until recently (Roberts, 1980). Evidence in support of splitting the single *Macrognathus* species into 3 taxa and expanding this genus to include other species is provided here.

The interrelationships of the mastacembelids with other teleostean fishes have had no less a long and obscure history. Major general classifications treating the Mastacembelidae and their affinities are summarised in Table 2. Their appearance caused the early describers in the latter part of the eighteenth and early nineteenth century to associate them with the true eels (Anguilliformes). By the middle of the nineteenth century Günther (1861) had noticed their many affinities to acanthopterygian fishes and considered them 'acanthopterous eels' distantly related to the Blenniidae. However, it was not until Boulenger (1904) that they were given separate subordinal status, as the Opisthomi, within the Teleostei. Following this, Regan (1912) elevated them to ordinal rank, although he could not trace their affinity to any particular group. Berg (1947: 494) followed Regan (op. cit.) in giving the mastacembelids separate ordinal status (Mastacembeliformes) within the teleosts, but Greenwood, Rosen, Weitzman & Myers (1966) in their phyletic study of teleostean fishes reduced the taxon to subordinal status and included the Mastacembeloidei as one of their 20 suborders in the order Perciformes. This arrangement, apart from slight changes, has remained to the present day.

In addition to the Mastacembelidae, two monotypic families have been included in the suborder Mastacembeloidei. Annandale (1918) erected the family Chaudhuriidae to accommodate a small eel-like fish collected from the Inle Lake, Burma (and recently also collected from Thailand; Roberts, 1980). He considered this small eel-like taxon to be a member of the true eels (Anguilliformes) but was unable to assign it to any known family, partly as a result of its distinct 'fan-shaped' caudal fin (Whitehouse, 1918). Regan (1919), considering the characters described for Chaudhuriidae, showed its affinity to mastacembelids rather than to true eels and placed it in the Mastacembeliformes (his Opisthomi). On the basis of this and new anatomical descriptions, Annandale & Hora (1923) followed his classification as did Mitra & Ghosh (1931) on the basis of the soft anatomy. Berg (1947), however, considered

Table 1 African species assigned to the genus *Mastacembelus* (in chronological order of their description).

Species	Authority	Date
**Mastacembelus cryptacanthus*	Günther	1867
Mastacembelus niger	Sauvage	1878
Mastacembelus marchii	Sauvage	1892
Mastacembelus marmoratus	Perugia	1892
Mastacembelus tanganicae	Günther	1893
Mastacembelus ophidium	Günther	1893
Mastacembelus liberiensis	Steindachner	1894
Mastacembelus loennbergii	Lönnberg	1895
Mastacembelus congicus	Boulenger	1896
Mastacembelus shiranus	Günther	1896
Mastacembelus flavomarginatus	Boulenger	1898
Mastacembelus nigromarginatus	Boulenger	1898
Mastacembelus moorii	Boulenger	1898
Mastacembelus brachyrhinus	Boulenger	1899
Mastacembelus ellipsifer	Boulenger	1899
Mastacembelus paucispinis	Boulenger	1899
Mastacembelus frenatus	Boulenger	1901
Mastacembelus greshoffi	Boulenger	1901
Mastacembelus goro	Boulenger	1902
Mastacembelus sclateri	Boulenger	1903
**Mastacembelus ansorgii*	Boulenger	1905
**Mastacembelus signatus*	Boulenger	1905
Mastacembelus cunningtoni	Boulenger	1906
Mastacembelus longicauda	Boulenger	1907
Mastacembelus batesii	Boulenger	1911
Mastacembelus brevicauda	Boulenger	1911
Mastacembelus reticulatus	Boulenger	1911
**Mastacembelus trispinosus*	Steindachner	1911
Mastacembelus ubangensis	Boulenger	1911
**Mastacembelus moeruensis*	Boulenger	1914
Mastacembelus stappersii	Boulenger	1914
**Mastacembelus laticauda*	Ahl	1937
Mastacembelus albomaculatus	Poll	1953
†*Mastacembelus brichardi*	Poll	1958
Mastacembelus platysoma	Poll & Matthes	1962
**Mastacembelus flavidus*	Matthes	1962
Mastacembelus micropectus	Matthes	1962
Mastacembelus plagiostomus	Matthes	1962
Mastacembelus zebratus	Matthes	1962
**Mastacembelus sanagali*	Thys van den Audenaerde	1972
**Mastacembelus seiteri*	Thys van den Audenaerde	1972
Mastacembelus aviceps	Roberts & Stewart	1976
Mastacembelus crassus	Roberts & Stewart	1976
**Mastacembelus latens*	Roberts & Stewart	1976
Mastacembelus vanderwaali	Skelton	1976
Mastacembelus sp. nov.	Roberts & Travers	(in prep.)

*Unavailable for dissection
†*Caecomastacembelus*

N.B. *Mastacembelus taeniatus* Boulenger, 1901
Mastacembelus victoriae Boulenger, 1903
Mastacembelus mellandi Boulenger, 1914
Mastacembelus mutombotomba Pellegrin 1936
} Synonymised with *M. frenatus* (Matthes, 1962 and Skelton, 1976)

Table 2 Proposed affinities of the Mastacembelidae.

Authority	Date	Relationship
Gronovius	1763	Apodes (Anguilliformes)
Bloch	1786	Apodes (Anguilliformes)
Linneaus	1758	Apodes (Anguilliformes)
Lacépède	1800	Apodes (Anguilliformes)
Schneider (Ed.) *in* Bloch	1801	Apodes (Anguilliformes)
Cuvier & Valenciennes	1831	Notacanthidae
Müller	1844	Scombroidei
Bleeker	1859	*Alostoma* & *Notacanthus*
Günther	1861	'Acanthopterous eels' (in the Blenniformes)
Boulenger	1904	Blenniidae (given separate subordinal status: Opisthomi)
Goodrich	1909	Blenniidae
Regan	1912	Percomorphi (could not trace affinity to any particular group; given separate ordinal status: Opisthomi)
Frost	1930	Percidae
Job	1941	Nandidae
Berg	1940	Acanthopterygii (given separate ordinal status as Mastacembeliformes)
Bertin & Arambourg	1958	Acanthopterygii (given separate ordinal status as Mastacembeliformes)
Bhargava	1953 & 1963*a*	Blennidae
Freihofer	1963	Percoidei
Greenwood *et al*	1966	Perciformes (given separate subordinal rank: Mastacembeloidei)
McAllister	1968	Synbranchidae
Gosline	1971	Synbranchidae

Chaudhuriidae '... so specialised that it plainly deserves the rank of a special order' and assigned it to the Chaudhuriiformes. Sufi (1956) was inclined to agree with Berg (op. cit.), although Greenwood *et al* (1966) retained Chaudhuriidae in the mastacembeloids.

Most recently, Yazdani (1972 & 1975) erected a new genus *Pillaia* for a small eel-like fish collected from the Kasi Hills, Meghalaya. Following more detailed anatomical description and comparison with the Mastacembelidae and Chaudhuriidae, Yazdani (1976*a*) concluded that this genus could be placed in the Mastacembeloidei and erected the Pillaiidae partly as a 'link' between the Mastacembelidae and Chaudhuriidae (Yazdani 1978) and also because of a number of anatomical specialisations including the presence of a single upper jaw element (Yazdani 1976*b*). A second species of Pillaiidae (Talwar, Yazdani & Kundu, 1977) was described from two specimens collected from north east India.

A taxonomic revision of the mastacembelid fishes requires a comprehensive study of their anatomy, particularly that of the African taxa, since existing descriptions, apart from those by Regan (1912: 217–219), Gregory (1933: 353–354), Sufi (1956: 95–96), Poll (1973: 221–230) and Taverne (1973 & 1980), are restricted mainly to accounts dealing with species from the Indian fauna. These include descriptions of cranial development and osteology (Bhargava, 1957*a* & *b*, 1958 & 1963*a*; Maheshwari, 1963 & 1965*a*; Dalela, 1968; Dalela & Garg, 1968; and Yazdani, 1976*a* & *b*), cephalic sensory canals (Maheshwari, 1971), myology (Dubale, 1952), the olfactory system (Bhargava, 1962*a* & *b*), nervous system (Maheshwari, 1965*b*), vascular system (Saxena, 1956; Bhargava, 1963*b*; Agrawal & Dalela, 1966*a*; Maheshwari, 1966*a*; and Dalela, 1967*b*), digestive system (Nagar & Khan, 1957; Agrawal & Tyagi, 1963; Agrawal & Dalela, 1966*b*; and Sriwastwa, 1970), endocrine system

(Khanna & Gill, 1973), excretory system (Chandrasekhar, 1961; and Dalela, 1967*a*), reproductive system (Swarup, Srivastava & Das, 1971; and Maheshwari, 1966*b*) and respiratory system (Datta Munshi, 1964).

This literature contains only scattered and incomplete accounts of the internal anatomy, there are no comprehensive osteological descriptions, and virtually no account of the myology exists.

The Chaudhuriidae and Pillaiidae also lack detailed anatomical coverage, and the numerous errors perpetuated in the literature (e.g. Annandale, 1918; Whitehouse, 1918; Annandale & Hora, 1923; Yazdani, 1976*a* & 1978) and questionable hypothesis regarding their relationships, both taxonomic and phyletic, necessitate a thorough anatomical description of these taxa as well.

This study, therefore, is devoted to detailed osteological descriptions of *Mastacembelus mastacembelus* (and a partial investigation of its cranial myology), *Chaudhuria caudata* and *Pillaia indica*. These descriptions will then form part of a comparative anatomical analysis (including osteology and relevant aspects of cranial myology) of all available mastacembeloid species to provide a basis for a phylogenetic analaysis of the taxa (see Part II; Travers, 1984).

Nomenclatural note

The taxonomic assignment of mastacembeloid species in current use is followed here. However, the succeeding phylogenetic analysis dictates the reclassification of most of these species. Details of these taxonomic changes, including the characters that make them necessary, are given elsewhere (Part II; Travers, 1984).

Material and methods

Material

The spirit collection, stained specimens and dry skeletons of mastacembeloids held at the British Museum (Natural History) together with several specimens presented as gifts, loans from other institutions and a personal collection from Lake Tanganyika, provided the material on which this study is based.

The material examined is listed in full in Table 3, the species arranged alphabetically under their current generic names. All specimens are listed with their registered numbers, together with codes indicating the type of examination or preparation involved, (all are BM(NH) registered specimens unless otherwise indicated). A key to these codes is given in the list of abbreviations on p. 12.

Methods

Osteological studies involved the use of formalin fixed specimens cleared and double stained with Alizarin Red (for bone) and Alcian Blue (for cartilage) following the methods of Dingerkus and Uhler (1977). Myological studies, on the other hand, involved the use of formalin fixed and alcohol preserved specimens. To maximise the usefulness of specimens, where alizarin/alcian transparencies were required, myological examination was performed prior to maceration. Analyses of vertebral structures, fin spines and rays was aided by the use of radiographs. A series of triple-stained transverse histological sections and double-stained longitudinal sections was prepared for more detailed analyses of internal structures.

All specimens were examined with the aid of a Zeiss IVb zoom binocular microscope, fitted with a Schott fibre optic illuminator. Where necessary a substage illumination unit and a camera lucida drawing tube were employed.

The osteological nomenclature is based upon that of Harrington (1955) and Patterson (1977) supplemented by reference to numerous other relevant studies including: Patterson & Rosen (1977) for the ethmoid region, Patterson (1975) for the braincase, Nelson (1969)

Table 3 List of Study Material.

Species	Reg. No.	Preparation
Oriental mastacembeloid taxa		
Genus: *Mastacembelus*		
Mastacembelus alboguttatus	1891.11.30:135–138 (Types)	AP
Mastacembelus armatus	1978.3.2:306–7	A/A
,, ,,	1955.6.22:16–17	MD
,, ,,	LACM 38127–2	MD
,, ,,	1891.11.30:134	DS
Mastacembelus caudiocellatus	1893.6.30:130–132 (Types)	R
Mastacembelus circumcinctus	1980.10.10:274	A/A
,, ,,	1955.6.22:12	MD
,, ,,	1980.10.10:274	R
Mastacembelus erythrotaenia	Unreg	A/A
,, ,,	Unreg	R
Mastacembelus guentheri	1865.7.17:18	MD
,, ,,	1893.3.6:156–157	R
,, ,,	1912.7.20:27	R
Mastacembelus keithi	1938.12.1:267 (Type)	R
Mastacembelus maculatus	1978.3.20:312–314	A/A
,, ,,	1970.9.3:543–552	A/A
,, ,,	1955.6.22:10–11	A
,, ,,	1970.9.3:534–552	A
,, ,,	1970.9.3:543–551	MD
,, ,,	1978.3.20:315	R
Mastacembelus mastacembelus	1974.2.22:1799–1806	A/A, MD & R
,, ,,	1892.9.1:25	DS
,, ,,	1891.6.19:3	R
,, ,,	1955.6.25:4–6 (Types)	R
,, ,,	1975.11.21:8	R
Mastacembelus oatesii	1893.6.30:113–118	A/A
,, ,,	Unreg.	R
Mastacembelus pancalus	1889.2.1:3642–3	A/A
,, ,,	Unreg.	A/A
,, ,,	1935.10.18:71	MD
Mastacembelus sinensis	1927.10.1:19	A/A
,, ,,	1888.3.23:60–2 (Types)	R
,, ,,	1895.5.31:13–14 (Types)	R
,, ,,	IHW-h Gift	R
Mastacembelus unicolor	1978.3.20:317	A/A
,, ,,	1955.6.22:24	R
,, ,,	1978.3.20:318	R
,, ,,	IHW-h Gift	R
Mastacembelus zebrinus	MCZ 9027	A/A
,, ,,	1891.11.30:115–124	A/A & DS
Genus: *Macrognathus*		
Macrognathus aculeatus	Unreg.	A/A
,, ,,	1883.11.28:15	MD
,, ,,	1889.11.12:52	MD
,, ,,	1922.5.19:115	MD & R
Macrognathus aral	1889.2.1:3622–5	A/A
,, ,,	1858.8.15:51–3	R
,, ,,	1872.4.7:38	R
Macrognathus siamensis	Unreg.	A/A
,, ,,	Unreg.	MD
,, ,,	1898.4.2:127–8	R

Table 3 Continued.

Species	Reg. No.	Preparation
Oriental mastacembeloid taxa		
Genus: *Chaudhuria*		
Chaudhuria caudata	MCZ 47058	A/A & AP
,, ,,	1923.3.10:1–3 (Types)	A & AP
,, ,,	ZSI F10822/1	A/A
Genus: *Pillaia*		
Pillaia indica	ZSI (9 ex.)	A/A, A, MD, R & AP
Pillaia khajuriai	ZSI FF816 (Paratype)	AP
African mastacembeloid taxa		
Genus: *Mastacembelus*		
Mastacembelus albomaculatus	Pers. coll.	A/A
,, ,,	MCZ 49212	A/A
,, ,,	Unreg.	R
Mastacembelus ansorgii	1905.5.29:59 (Type)	R
Mastacembelus aviceps	MCZ 50565	A/A
Mastacembelus batesii	1912.6.29:10–16	A/A & MD
,, ,,	1907.5.22:246	DS
Mastacembelus brachyrhinus	MCZ 50563	A/A
Mastacembelus brevicauda	1904.7.1:250	A/A
,, ,,	1906.5.28:193–196 (Types)	R
Mastacembelus brichardi	1976.5.21:99–108	A/A & MD
,, ,,	MCZ 50255	A/A
Mastacembelus congicus	1975.6.20:696–697	A/A
,, ,,	1901.12.26:64	MD
,, ,,	1899.6.28:23	DS
Mastacembelus crassus	MCZ 50258	A/A
Mastacembelus cryptacanthus	1866.6.26:11 (Type)	R
Mastacembelus cunningtoni	Unreg.	A & R
Mastacembelus ellipsifer	Pers. coll.	A/A & MD
Mastacembelus flavidus	RG 130435–439	R
,, ,,	1906.9.8:273 (Type)	R
Mastacembelus flavomarginatus	1912.4.1:575–579	A/A & MD
Mastacembelus frenatus	1961.12.1:356–7	A/A
,, ,,	1977.6.9:134–6	A/A
,, ,, (*mellandi*)	RG 79-01-P-6335–339	A/A
,, ,, (*taeniatus*)	RG 91437	A/A
Mastacembelus goro	1937.4.16:18–22	A/A
Mastacembelus greshoffi	1958.9.8:287	A/A
,, ,,	Unreg.	R
Mastacembelus liberiensis	RG 73.10.P-7363-372	A/A
Mastacembelus loennbergii	1969.3.26:68–69	A/A
,, ,,	1904.1.20:71	R
,, ,,	Unreg.	HS
Mastacembelus longicauda	1910.2.23:7–10	A/A & MD
,, ,,	1908.5.20:189 (Type)	R
Mastacembelus marchii	MCZ 50590	A/A
Mastacembelus marmoratus	RG 118712–719	A/A
Mastacembelus micropectus	MCZ 49210	A/A
,, ,,	RG 130804–812	A/A
Mastacembelus moorii	1955.12.20:1685	A/A
,, ,,	MCZ 50838	A/A

Table 3 Continued.

Species	Reg. No.	Preparation
African mastacembeloid taxa		
Mastacembelus niger	137360–365	A/A
Mastacembelus nigromarginatus	1969.4.28:11–12	A/A
Mastacembelus ophidium	1968.123.30:4	A/A
,, ,,	1936.6.15:1753–6	A/A
Mastacembelus paucispinis	1976.5.21:119–129	A/A
,, ,,	RG 178099	A
Mastacembelus plagiostomus	Pers. coll	A/A
Mastacembelus platysoma	RG 78–25–P.34–38	A/A
Mastacembelus reticulatus	1932.5.18:105–6	A/A
,, ,,	Unreg.	R
Mastacembelus sclateri	904.7.1:104–105	A/A
,, ,,	1911.5.30:35	DS
,, ,,	1909.4.29:111	R
,, ,,	1911.5.30:38	R
Mastacembelus shiranus	Unreg.	A/A
,, ,,	1969.2.20:3–12	A/A
Mastacembelus signatus	1905.11.10:13 (Type)	R
Mastacembelus stappersii	RG 152167	A
Mastacembelus tanganicae	Pers. coll.	A/A
,, ,,	1968.12.30:2–3	A/A
,, ,,	MCZ 49209	A/A
Mastacembelus ubangensis	RG 124267–268	A/A
Mastacembelus vanderwaali	1977.2.3:168–172	A/A
,, ,,	AM 3450	A
Mastacembelus zebratus	MCZ 49211	A/A
,, ,,	RG 130800–801	R
Mastacembelus sp. nov.	CAS Gift	A/A

for the branchial arches, and Greenwood & Rosen (1971) and Rosen (1973) for the caudal skeleton. The nomenclature of muscles follows that of Winterbottom (1974), and cranial nerves that of Freihofer (1978).

Abbreviations

Abbreviations used in text figures and tables.

Skeletal elements

Aa	Anguloarticular
AAPP	*Adductor arcus palatini* process
ACh	Anterior ceratohyal
ADPt	Anal fin distal pterygiophore
AFR	Anal fin ray
AHS	Autogenous haemal spine
AP	Anterior process
AP+MPt	Anal proximal and medial pterygiophores
AS	Anal spine
ASPt	Anal spine supporting pterygiophore
Bb 1–4	Basibranchial 1 to 4
Bblk	Basibranchial 1 keel
BblkC	Basibranchial 1 keel with cartilaginous ventral edge
Bb2VP	Basibranchial 2 ventral process
Bb2VPA	Basibranchial 2 ventral process arched

Bh	Basihyal
BLF	Baudelot's ligament fossa
Bo	Basioccipital
Bpt	Basipterygia
BR	Branchiostegal ray
Bs	Basisphenoid
C	Cleithrum
Cb 1–5	Ceratobranchial 1 to 5
Cb5MP	Ceratobranchial 5 muscular process
Cb5Tp	Ceratobranchial 5 toothplate
Ck	Cleithrum keel
Cmen	Cartilage meniscus
CMF	Cancellous medial face of lateral ethmoid
CN	Cartilage nubbin
Com	Coronomeckelian
Cor	Coracoid
CVt 1	1st Caudal vertebra
D	Dentary
DCP	Dentary coronoid process
DDPt	Dorsal fin distal pterygiophore
DFR	Dorsal fin ray
DHh	Dorsal hypohyal
DP	Dorsal process
DP+MPt	Dorsal proximal and medial pterygiophore
DPP	Dentary posterior process
DPt	Distal pterygiophore
DS	Dorsal spine
DSP	Dentary symphysial process
DSPt	Dorsal spine supporting pterygiophore
E 1–3	Epural 1 to 3
Eb 1–4	Epibranchial 1 to 4
EC	Ethmoid cartilage
EcR	Epicentral rib
Ect	Ectopterygoid
End	Endopterygoid
EndAP	Endopterygoid anterior process
ENS	Expanded (anteroposteriorly) neural spine
Ep	Epioccipital
EpR	Epipleural rib
Ex	Exoccipital
ExDP	Exoccipital dorsal perforations
Exsc	Extrascapula
ExVE	Exoccipital ventral extension
F	Frontal
FDL	Frontal descending lamina
FF	Facial foramen
Fn	Fenestra
FP	Frontal pedicel
FPb2	Fragmented pharyngobranchial 2
FPmAS	Fragmented premaxilla alveolar surface
FTp	Fused toothplate
GTS	Gutter in lateral ethmoid for *truncus supraorbitalis*
H 1–6	Hypural 1 to 6
HAF	Hyoid artery foramen
Hb 1–3	Hypobranchial 1 to 3
Hb3AP	Hypobranchial 3 anterior (descending) process
Hb3Tp	Hypobranchial 3 toothplate
HHAVt (1)	Hemispherical head of 1st abdominal vertebra
HP	Hypural plate

HS	Haemal spine
Hyo	Hyomandibula
HyoAF	Hyomandibular anterior flange
HyoS	Hyomandibular spur
ICF	Internal carotid foramen
Ih	Interhyal
InP	Interdigitating process
Io 1–6	Infraorbital 1–6
IoAP	Infraorbital 1 anterior process
IoPP	Infraorbital 1 posterior process
LC	Lateral commissure
LCF	Lateral commissure flange
LE	Lateral ethmoid
LEVF	Lateral ethmoid ventral facet
LEVP	Lateral ethmoid ventral process
LP	Lateral parapophysis
MC	Meckel's cartilage
Met	Metapterygoid
Mx	Maxilla
N	Nasal
NA	Neural arch
NAF	Neural arch foramen
NS	Neural spine
Op	Operculum
OPM	Opening for the posterior myodome
P	Parasphenoid
Pal	Palatine
PaLS	Palatine spur
PalSF	Palatine suborbital flange
PalT	Palatine teeth
Par	Parietal
Pb 2–4	Pharyngobranchial 2 to 4
PCh	Posterior ceratohyal
PCR	Principal caudal fin rays
PFR	Pectoral fin rays
Ph	Parhypural
Pm	Premaxilla
PmAP	Premaxilla ascending process
Pop	Preoperculum
Poz	Postzygapophysis
PP	Postorbital process
PPP	Parasphenoid posterior process
Pr	Prootic
PR	Pleural rib
PrAP	Prootic anterior process
Prorb S	Preorbital spine
PrS	Prootic spur
PrSh	Prootic shelf
Prz	Prezygapophysis
Pt	Pterosphenoid
PtN	Pterosphenoid notch
PtP	Pterosphenoid pedicel
PtT	Posttemporal tubule
Pu 2 & 3	Preural centra 2 to 3
Pu+U	Fused ural and 1st preural centra
Q	Quadrate
R 1–4	Radials (actinosts) 1–4
Ra	Retroarticular
ROSFF	*Ramus opercularis superficialis facialis* foramen

SB	Saccular bulla
Sc	Scapula
ScaF	Scapular foramen
Snl	Supraneural lamina
So	Supraoccipital
SoC	Supraoccipital commissure
Sop	Suboperculum
SorC	Supraorbital sensory canal commissure
Sph	Sphenotic
SphAF	Sphenotic anterior flange
StSC	Supratemporal sensory canal
Sue	Supraethmoid
Sym	Symplectic
TF	Trigeminal foramen
TFF	Trigeminal and facial foramen confluent
TP4	Toothplate 4
TPOlfT	Tubular passage for olfactory tract
U 1–2	Uroneural 1 to 2
Uh	Urohyal
UhAP	Urohyal ascending process
UhF	Urohyal facet
Unc	Uncinate process
UTp	Unfused toothplate
V	Vomer
VCPH	Vascular canal in head of parhypural
VHh	Ventral hypohyal

Muscles and soft tissues

A_1, A_2, A_3 & A_w	Parts of the *adductor mandibulae*
$A_{2\alpha}$ & $A_{2\beta}$	Deep and superficial subdivisions, respectively, of part A_2 of the *adductor mandibulae*
AAP	*Adductor arcus palatini*
A_wApo	Tendinous aponeurosis of part A_w of the *adductor mandibulae*
A Hyo	*Adductor hyomandibulae*
AO	*Adductor operculi*
B Lig	Baudelot's ligament
DO	*Dilatator operculi*
Epax	*Epaxialis* musculature
Hyo Abd	*Hyohyoidei abductores*
Hyo Add	*Hyohyoidei adductores*
Int	*'Musculus intraoperculi'*
LAP	*Levator arcus palatini*
LO	*Levator operculi*
MmLig	Maxillo-mandibular ligament
ObSup	*Obliquus superioris*
Olft	*Nervus olfactorius*
Pseu	Pseudobranch
RMT	*Ramus mandibularis trigeminus*
tA_1, $tA_{2\alpha}$, $tA_{2\beta}$, tA_3 & tA_w	Tendons from parts of the *adductor mandibulae*
TI	*Truncus infraorbitalis*

Note on the figures: even stipple-dots indicate the presence of cartilage. The scale on all figures indicates 1 mm.

Table of study material

A/A	Double alizarin red/alcian blue stained transparency
A	Alizarin stained transparency
HS	Histologically stained and sectioned
MD	Muscle dissection (cheek and opercular region)

DS	Dry skeleton preparation
R	Radiograph
AP	Alcohol preserved specimen not available for dissection or preparation (superficial gross morphology examined only)
Unreg.	Unregistered specimen held at BM (NH)
Pers. coll.	Personally collected specimen held at BM(NH)

Institutional abbreviations

AM	Albany Museum, Grahamstown
BM(NH)	British Museum (Natural History)
CAS	California Academy of Sciences
IHW-h	Institute of Hydrobiology, Wuhan (China)
LACM	Natural History Museum of Los Angeles County
MCZ	Museum of Comparative Zoology, Harvard
RG	Koninklijk Museum voor Midden-Afrika, Tervuren
ZSI	Zoological Survey of India

Osteology of *Mastacembelus mastacembelus*

Although *Mastacembelus mastacembelus* (Banks & Solander, *in* Russell, 1794) is the type species of the genus (Wheeler 1956) it has not been subjected to a detailed anatomical study. This description is based on two double stained specimens (standard length 212 mm. and 217 mm.) and a single skeletal preparation (see Table 3).

Neurocranium

Ethmovomerine region

Of the two median endochondral ethmoid bones identified by Patterson & Rosen (1977) only the *supraethmoid* is present in *M. mastacembelus.* The supraethmoid is a laterally compressed bone that caps the anterodorsal part of the ethmoid region (Fig. 1a). It consists of two regions; anteriorly, a thin median septum separates the olfactory sacs and posteriorly a long posterodorsally directed process lies between the anteromedial face of each frontal. The anteroventral edge of the median septum is fused to the vomer, and the anterodorsal edge is enlarged to form an ovoid prominance for the attachment of ligaments which help govern the movement of the rostral appendage. Below the posterodorsal process the lower corner of the supraethmoid is cartilaginous and extends as a septal cartilage along the anterodorsal surface of the parasphenoid (below the lateral ethmoids) into the orbital cavity (Fig. 1a).

The *vomer* is a long bone and consists of a broad faceted head region and a long posterior shaft (Fig. 1a & b). Both the anterior and anterolateral faces of the vomerine head are faceted; they articulate with the rostral appendage and medial face of the short ascending process from the premaxilla, respectively. The vomerine shaft lies in a groove on the underside of the parasphenoid and extends posteriorly to a point adjacent to the anterior edge of the pterosphenoid. The dorsal surface, posterior to the median supraethmoid septum, contacts the ventral surface of the posterior cartilaginous region of the supraethmoid. Vomerine teeth are absent.

Each *Lateral ethmoid* is connected to its partner in the midline, and together they saddle the cartilaginous region of the supraethmoid. There is no anterior myodome between the lateral ethmoids. The medial wall is compressed into a cancellous bony sheet that contacts its partner in the midline anterodorsal to the cartilaginous end of the supraethmoid. This wall, together with the outwardly convex lateral wall gives the lateral ethmoid a tubular central region (Fig. 2). The olfactory sac is hypertrophied and its posterior end lies within the anterior entrance to this tubular centre of the lateral ethmoid. The posterior opening accommodates the broad *nervus olfactorius* (Freihofer, 1978), which runs directly from the olfactory bulb to the nasal organ.

The dorsal edge of the lateral ethmoid consists of an anterior arm which lies below the posteroventral surface of the nasal, and a posterior arm that lies below the anteroventral surface of the frontal. A gutter runs longitudinally along the dorsomedial face and carries part of the *truncus supraorbitalis* nerve prior to its separation into two main rami. A large rounded condyle on the lateral face of the lateral ethmoid articulates syndesmotically with the posterior ascending process on the 1st infraorbital bone. Ventral to this condyle is a facet which articulates synchrondrally with the anterior end of the suspensorium (the anterodorsal edge of the ectopterygoid and anterior tip of the endopterygoid).

The *nasal* is a large, thin, flattened bone inclined to the vertical, and overlies the long olfactory cavity (Fig. 1a & c). The medial edge is joined by connective tissue to the dorsolateral margin of the supraethmoid. Posteriorly, it overlaps the anterodorsal process of the lateral ethmoid and contributes, with the 1st infraorbital, to the rim of the posterior nostril.

The dorsolateral margin of the 1st infraorbital is overlapped by the lateral edge of the nasal, and the two are joined by connective tissue.

The nasal encloses the anterior region of the supraorbital sensory canal which forks anteriorly, the short lower arm terminating in a pore on its anterolateral surface.

Orbital region

The *pterosphenoid* is a major contributor to the long, precommissural lateral wall of the braincase. Its anterior edge contributes to the posterior rim of the orbital cavity and partly surrounds the optic foramen (Fig. 1a & b). The anterodorsal edge of the lateral wall is grooved, and accommodates the ventral edge of the frontal descending lamina. Posteriorly, the dorsal margin of the pterosphenoid is partly overlapped by the posterior margin of the frontal lamina and the anterolateral flange of the sphenotic.

The ventral edge of the pterosphenoid is curved medially and sutured to its partner in the midline. Together, these bones form the ventral rim of the optic foramen and roof the small posterior myodome, giving this region of the neurocranium a somewhat tubular shape.

The posterior edge of the pterosphenoid lies between the sphenotic and prootic, and contributes to the rim of the trigeminal foramen. The lateral face of the pterosphenoid is overlain by a long anterior process on the prootic. Dorsal to this process the pterosphenoid is grooved longitudinally to accommodate the nerves issuing from the trigeminal foramen.

The *basisphenoid*, the smallest bone in the neurocranial complex is depressed and Y-shaped. Its small size is the result of its compression between the ventral face of the median pterosphenoid symphsis and the dorsal surface of the parasphenoid (Fig. 1a). The tip of each dorsal arm of the basisphenoid contacts a pterosphenoid. A short ventral shaft extends downwards towards the parasphenoid as a thin process dividing the posterior myodome.

The *parasphenoid* is the longest bone in the neurocranium and extends from below the lateral ethmoids to the posterior edge of the basicranium (Fig. 1a & b). It consists of two main regions: a long anterior process bridging the orbital cavity (between the otic and nasal areas) and a longitudinal, trough-like, posterior region. The ventral surface of the anterior region is grooved to accomodate the vomerine shaft. A dorsal median ridge on the anterior part of the parasphenoid meets the membranous interorbital septum. The lateral wall of the posterior trough-like region overlaps the ventrolateral margin of the prootic; it is not developed into an ascending process. A notch in the dorsal edge of the parasphenoid (ventral to the lateral commissure in the prootic) forms, with the ventral edge of the prootic, the internal carotid foramen. The posteroventral face of the parasphenoid divides into a pair of processes which lie longitudinally on either side of a basioccipital ridge and extend to the posterior margin of that bone.

The *infraorbital* series consist of one large element–the 1st infraorbital (lachrymal)–and 5 small tubules (2nd to 6th infraorbitals). The infraorbital sensory canal is enclosed within these elements (Fig. 3).

The 1st infraorbital is expanded posteriorly and tapered anteriorly, extending to the tip of the nasal. Two large pores are present, as well as several irregular branches of the infraorbital sensory canal system which terminate in small pores on the lateral face of the bone.

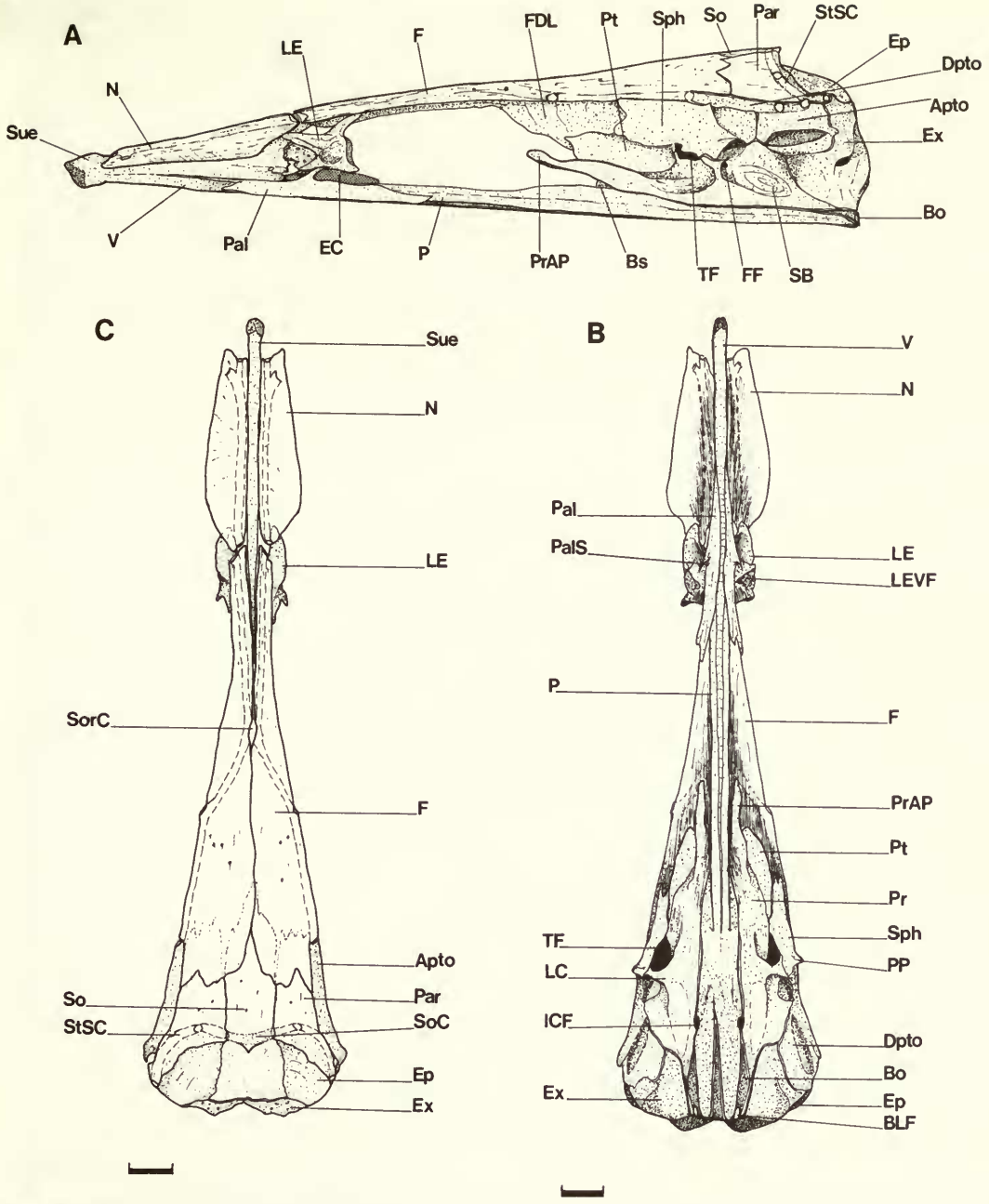

Fig. 1 *Mastacembelus mastacembelus*, neurocranium in: (a) lateral view of left side; (b) ventral view and (c) dorsal view.

The posterodorsal edge of this bone is developed into two ascending processes. The dorsomedial face of the larger posterior process is faceted and joined syndesmotically with the rounded condyle on the lateral ethmoid. A small lip on the anterior edge of the ascending process also contacts the lateral ethmoid. The smaller ascending process is joined by epidermal tissue to the posteroventral edge of the nasal; together with the larger process it forms the ventral rim of the posterior nasal opening.

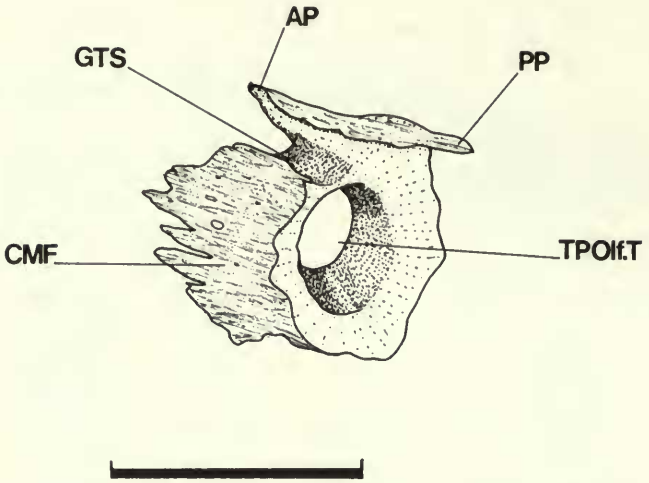

Fig. 2 *Mastacembelus mastacembelus,* right lateral ethmoid in posteromedial view.

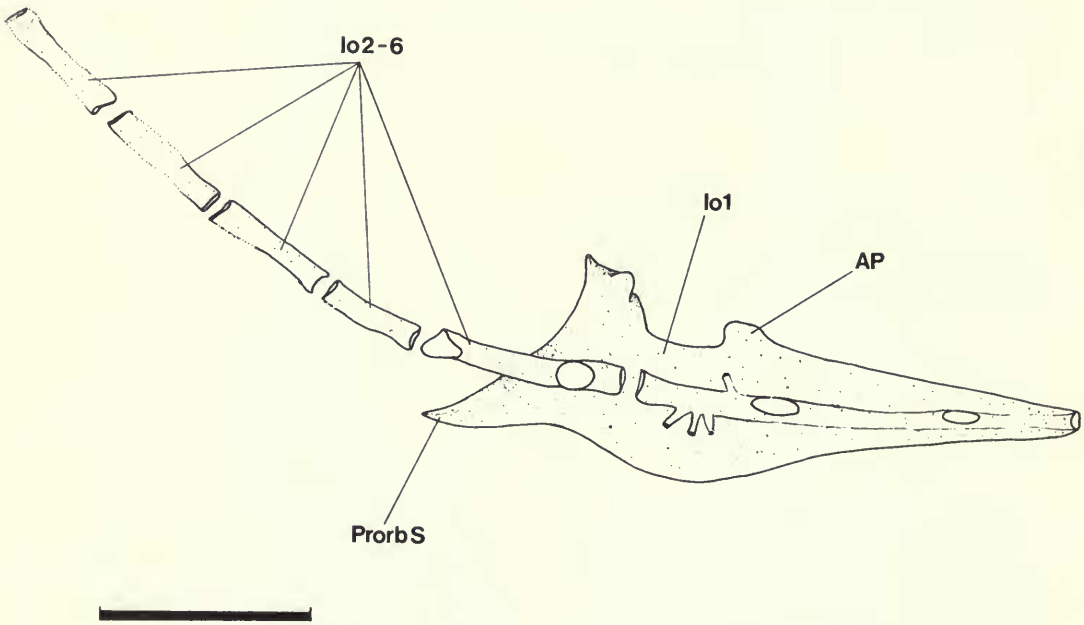

Fig. 3 Infraorbital series of *Mastacembelus mastacembelus.*

The ventral edge of the bone tapers posteriorly to a distinct, pointed process (preorbital spine; Fig. 3), which pierces the integument ventral to the 2nd infraorbital tubule.

The remaining infraorbital bones are reduced to ossifications around the sensory canal. The 2nd element partly overlaps the posterolateral face of the 1st, and has a single large pore midway along its length. The sensory canal portions of the 4th, 5th and 6th infraorbitals are decreasingly ossified.

Otic region

The *prootic* is the largest endochondral bone enclosing the cranial cavity, and in addition to its main posterior region has a prominent anterior process extending into the orbit (Fig. 1a & b).

This region of the prootic overlaps the dorsolateral margin of the parasphenoid and in so doing obscures the basisphenoid laterally. A fossa in the dorsolateral margin of the prootic combines with a similar one in the ventrolateral margin of the sphenotic to form the socket for the anterior hyomandibular condyle. Posterior to the socket, the prootic is bevelled posteroventrally and is connnected dorsally to the pterotic by a number of dentate sutures; ventrally it is connected to the anterolateral edge of the exoccipital and the anterodorsal edge of the basioccipital.

The posterolateral face of the bone is bullate and accommodates the small sacculus in its entirety. The trigeminofacialis chamber is situated anterior to the saccular bulla. The large trigeminal foramen lies anterior to the slender lateral commissure (Fig. 1a), whilst the facial foramen, which is small (relative to the size of the trigeminal foramen), generally pierces the prootic medial to the lateral commissure.

The trigeminal foramen is bounded by the sphenotic (dorsally) and the prootic (ventrally). A short descending spur from the ventral edge of the sphenotic lies above the tip of a similar spur rising from the dorsal edge of the prootic. These spurs do not contact one another; together with the posterior edge of the pterosphenoid they form the rim of the trigeminal foramen. Medial to the trigeminofacialis chamber the prootic bears a vertical strut pierced by the inner opening of the facial foramen. Dorsally, this medial strut contacts the sphenotic, and ventrally it meets its partner in the midline. A hollow, gutter-like channel longitudinally indents the ventromedial face of the strut. The internal carotid artery runs along this channel from the small, posterior myodome and leaves through a foramen situated along the prootic/parasphenoid junction, ventral to the lateral commissure. A narrow, longitudinal ridge on the anterolateral face of the prootic is continuous with the lower edge of a groove in the ventrolateral face of the pterosphenoid, and supports the *truncus infraorbitalis*.

The large *sphenotic* is a major element in the dorsolateral wall of the braincase (Fig. 1a & b). It is characterised by a prominent, anterolateral flange which overlies its medial, sutured, connection to the pterosphenoid. Anterolaterally, the sphenotic contacts the frontal descending lamina by which it is excluded from contributing to the orbital border. Dorsally the sphenotic is grooved and accommodates the ventrolateral edge of the frontal. The posterolateral edge of this groove forms the postorbital process (dorsal to the lateral commissure), from which the *dilatator operculi* muscle originates. The posterior position of this postorbital process (relative to the orbit) illustrates the extreme attenuation of the precommissural region of the neurocranium. The posterior and posterodorsal edge of the sphenotic is overlapped by the prootic. A wide dorsomedial flange extends below the pterotic, to contact the ventral surface of the parietal. Below its postorbital process the sphenotic is sutured to the dorsal surface of the lateral commissure and anterior to this forms the upper border of the trigeminal foramen. The medial face of the sphenotic accommodates the anterior semicircular canal which is looped through the bone, forming the *pons moultoni*.

The *pterotic* consists of two portions; the ventral autopterotic and the dorsal dermopterotic (Fig. 1a & c). The autopterotic is connected to the sphenotic anteriorly, the prootic ventrally, with the exoccipital and epioccipital posteriorly. The dorsal edge of this region is fused to the ventral edge of the dermal portion of the pterotic.

The main body of the pterotic encloses the horizontal semicircular canal, and as a result its lateral face is bullate; its ventral surface is grooved to accommodate the posterior hyomandibular head.

There is no posttemporal fossa although the ventral margin of the pterotic forms part of a recess in the lateral wall of the basicranium.

The dermopterotic extends anteriorly between the sphenotic and frontal. Its anterior tip and posterodorsal edge are sutured to the lateral edge of the parietal. The temporal junction between the supraorbital, preopercular and posttemporal sensory canals is contained in the dermopterotic.

The *epioccipital* is small and forms, with the exoccipital and supraoccipital, the posterodorsal wall of the basicranium (Fig. 1a & c).

Dorsally, it is overlapped by the posterior edge of the parietal. An artery which supplies

the *epaxialis* musculature leaves the cranial cavity *via* a small foramen midway along the parietal/epioccipital border. Ventrally, the epioccipital is bounded largely by the exoccipital, to which it is sutured, and partly by the pterotic.

The inner aspect of the epioccipital contains the posterior semicircular canal and this imparts a bullate appearance to the bone's posteroventral face. The dorsal surface of this bulla forms the floor of a shallow fossa on the posterior face of the epioccipital (lateral to the posterodorsal foramen). A large, partly ossified tendon from the epaxial musculature inserts in this fossa.

Each *exoccipital* is an irregularly shaped bone and is a major contributor to the posterior wall of the neurocranium (Fig. 1a). Above the foramen magnum a dorsomedially directed process is connected in the midline to its partner by a pair of dentate processes. This symphysis, combined with a ventromedial one, results in the exoccipitals completely surrounding the foramen magnum.

The complex anterior edge of the exoccipital connects, by thin interdigitating sheets of bone, with the epioccipital dorsally, the pterotic laterally, and the prootic ventrally. The junction between these elements lies within the recess in the lateral wall of the basicranium (from which originate the branchial levator muscles).

The ventral surface of each exoccipital is flat and abuts against the dorsolateral surface of the basioccipital. Posteroventrally, they have prominent, concave, deltoid facets. These facets, in combination with a similar shaped facet on the posterior face of the basioccipital, form the occipital facet (a concave socket) which articulates with the 1st abdominal vertebra.

The inflated appearance of the anterolateral wall is a result of an inner recess in the exoccipital.

Three major foramina perforate the exoccipital. The small glossopharyngeal foramen pierces the bullate anterolateral wall, a large subdivided foramen, for branches of the occipito-spinal nerve, lies posterior to that for the glossopharyngeal nerve, whilst between, and slightly dorsal to them, lies the vagal foramen.

The stout *basioccipital* is approximately rectangular in outline (Fig. 1b). Its dorsal surface is pyramidal, with the four raised faces converging dorsally to form a longitudinal ridge. The anterodorsal face is excavated to form a pair of pit-like fossae, the *cavum utriculae.* The faceted and concave posterodorsal face contributes to the tripartite occipital facet (see above). The ventral surface of the basioccipital is flat except for a low, central, longitudinal ridge which separates the posterior processes of the parasphenoid.

The *posterior myodome* is small in comparison with that in other perciforms. It is roofed by the medial process of the pterosphenoids and divided in the midline by the ventral shaft of the basisphenoid.

The *supraoccipital* is a flattened bone and may be divided topographically into two regions: (1) the anterior horizontal part and (2) the sloped posterior region which is inclined at 45° to the former (Fig. 1c).

A supraoccipital crest is absent. The dorsal surface is transversely convex and bounded on either side by the parietals and by a posterior portion of the frontals. All these surrounding bones cover the supraoccipital margin. Crossing its posterior surface is a gutter-like channel which accommodates the supratemporal sensory canal commissure. The posterior portion of the supraoccipital is bordered laterally by the epi- and exoccipitals. Ventrally, its tip meets the exoccipital dorsal symphysis by which it is excluded from the foramen magnum.

The *frontal* is the major roofing bone of the cranium and is comprised of two regions: dorsally a flat, horizontal roofing region and ventrally a descending vertical lamina (Fig. 1a & c).

The dorsal region of the frontal is particularly attenuated and narrows above the orbit. Its flat surface lacks crests or any form of sculpturing. Anteriorly, it overlies the posterior tip of the ventral ethmoid, and posteriorly it overlaps the anterior margin of the supraoccipital. Beneath the anterior end of the frontal, and joined to it by connective tissue, is the posterodorsal arm of the lateral ethmoid (see above). The posterior end of the dorsal region of the frontal, overlaps a wide bony lip on the anterior edge of the parietal and con-

nects posterolaterally with the dorsal edge of the pterotic and the sphenotic. The lateral edge of the frontal curves ventrally and is concave above the orbit. Medially, the frontals meet along a straight suture.

The frontal sensory canal (supraorbital branch of cephalic system) passes along the lateral margin of the bone. Posterior to the orbit the ascending infraorbital canal connects with the supraorbital canal, its junction indicated by a large pore in the lateral edge of the frontal.

Anterior to this point the supraorbital canal opens through a medial pore which marks an anterior commissure between the canals from either side of the neurocranium (Fig. 1c).

The frontal descending lamina contributes to the postorbital lateral wall of the braincase (Fig. 1a). Its anterior edge forms, with the pterosphenoid, the posterior rim of the orbit. The ventral lamina, together with the dorsal region of the frontal and the pterosphenoids enclose the optic foramen. The ventral edge of the lamina overlaps the lateral face of the pterosphenoid, and posteriorly is sutured to the anterolateral edge of the sphenotic.

The *parietal* is approximately square in outline except for a short posterolateral arm (Fig. 1a & c). Anteriorly, a wide bony lip is overlapped by the frontal; posteriorly it is sutured to the dorsal edge of the epioccipital. Laterally, the parietal is joined to the pterotic and posterodorsal flange of the sphenotic, whilst medially it contacts the supraoccipital.

The unsculptured dorsal surface of the parietal is flat except for a slight curvature of its ventrolateral aspect. A sensory canal (supratemporal branch) crosses within the posterodorsal margin, from its lateral (pterotic/posttemporal) to its medial (commissure) connections. A single, large pore on this canal pierces the posterodorsal surface of the parietal.

Extrascapular bones are absent.

Two small ossified dermal tubules lie equally spaced along the postcranial sensory canal between the tip of the posterolateral arm of the parietal and the dorsal tip of the supracleithrum. These tubules represent the only ossified remnants of the *posttemporal* bone (Fig. 11).

Jaws

Upper Jaw

The *premaxilla* is a weakly curved, rod-like element, characterised by its short ascending process (Fig. 4). The bone's dorsal edge is tightly joined to the ventral face of the maxilla

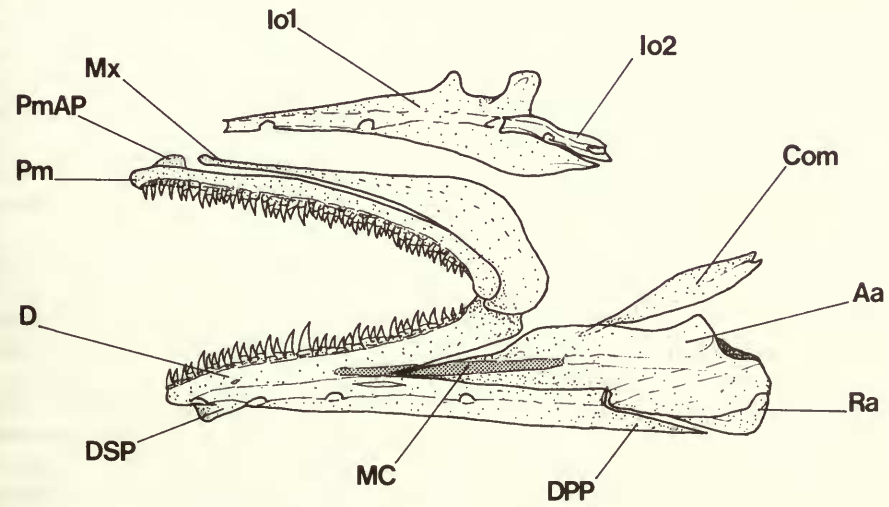

Fig. 4 *Mastacembelus mastacembelus,* lateral view of left upper and lower jaw bones with 1st and 2nd infraorbitals.

by a broad sheet of connective tissue. Anteriorly, each premaxilla curves medially (below and beyond the anterior end of the maxilla) to form a midline symphysis. The short stump-like ascending process articulates (*via* a facet on its medial face) with the faceted anterolateral end of the vomer. The premaxillae are not protrusible.

Its posteroventral end is laterally compressed and partly overlaps the ventral flange of the maxilla. The tooth-bearing alveolar surface of the premaxilla is broadest anteriorly and tapers posteriorly. The dentition is in the form of large, acrodont, caniniform teeth with posteriorly directed tips. Tooth attachment (to the premaxilla, dentary and pharyngeal bones) is by a ring of collagen between the tooth base and bone, in a mode equivalent to type 2 described by Fink (1981). The teeth are arranged in 1–8 irregular rows (depending upon the position along the premaxilla) and decrease in size medially.

The *maxilla* tapers anteriorly to a blunt tip which is connected, *via* a short ligament, to the posterior edge of the premaxillary ascending process and medially to the lateral facet on the head of the vomer. Posteriorly, the maxilla is thickened and expanded ventrolaterally to form an extension which, when the jaws are adducted, overlies the lateral face of the coronoid process (Fig. 4). This wide posterior region of the maxilla is joined to the coronoid process by a medial sheet of connective tissue. The dorsal edge is loosely joined by epidermal tissue to the ventromedial margin of the 1st infraorbital, and the ventral edge is connected firmly to the dorsal edge of the premaxilla.

Lower Jaw

The *dentary* is a long bone and although straight is directed mesad. Its symphysis lies posterior to the median connection of the premaxilla and there is a low symphysial projection on its anteroventral edge.

The dentary divides, posterolaterally, into an upper coronoid and a lower ventral arm. The coronoid region is developed posteriorly into a relatively tall, shallow coronoid process (Fig. 4). The long and narrow dorsal surface anterior to the coronoid process is alveolate and toothbearing. This toothed surface contains 3 rows of caniniform acrodont teeth, those of the outer row being somewhat larger than the inner teeth. The alveolar surface narrows posteriorly and does not extend onto the coronoid process.

The dentary portion of the mandibular sensory canal opens to the surface of the bone through four pores. The posteroventral region of the dentary extends below and beyond the point at which the sensory canal enters the dentary. The dorsal surface of this posteroventral projection (Fig. 4) is grooved and accommodates the ventral edge of the anguloarticular and the anteroventral edge of the retroarticular. The ventral edge of the lower jaw is, therefore, almost entirely formed by the dentary.

The long *anguloarticular* (Fig. 4) is characterised by two unusual features: the presence of a straight dorsal edge with no ascending process, and by the size and dorsal position of the coronomeckelian.

The anterior end of the anguloarticular lies between the coronoid and the ventral limb of the dentary. The posterodorsal edge is capped by a wide, transverse facet that receives the anterior condyle of the quadrate in a euarthroidal joint. On the posteromedial face of the anguloarticular is a small rounded ridge (ectosteal plate). Meckel's cartilage lies between the anterior end of this ridge and the dentary.

The *retroarticular* is a small L-shaped bone connected to the posteromedial face of the anguloarticular. It lies below the dorsal facet on the anguloarticular to which it is connected synchondrally.

The *coronomeckelian* (sesamoid articular) is particularly large and uniquely positioned (Fig. 4) in comparison with its size and position in other teleostean fishes.

It is long, narrow and tapers at both anterior and posterior ends. The anterior end overlaps the dorsomedial margin of the anguloarticular and is connected to its medial face, dorsal to Meckel's cartilage. From this point the coronomeckelian extends posterodorsally across the anterolateral face of the suspensorium. The posterior end lies lateral to the junction of

the ectopterygoid with the quadrate. The anteroventral tendon of part A_3 of the *adductor mandibulae* muscle inserts on to the posterior end of the coronomeckelian and the *ramus mandibularis trigeminus* (part of the Vth cranial nerve) passes downwards, along its ventral edge (Fig. 4), to extend anteriorly into the dentary.

Hyopalatine arch

The stout *hyomandibula* has its dorsal surface produced into two articular heads separated by a shallow depression (Fig. 5). The anterior condyle has a synchondral articulation (*via* a cartilaginous meniscus) with the anterior, prootic-sphenotic fossa on the lateral wall of the neurocranium. The larger, posterior condyle is ellipsoidal and fits into the channel-like pterotic fossa with which it articulates synchondrally.

The ventral part of the hyomandibula is a broad shaft; its tip is cartilage-capped and joined syndesmotically with the posterior end of the symplectic. The anterior edge of this shaft bears a small descending spur (Fig. 5). The *truncus hyomandibularis* (principally composed of fibres from the VIIth cranial nerve) enters the hyomandibula through a dorsomedial foramen and passes down through its shaft to emerge from a ventrolateral foramen.

The posterior edge of the shaft is deeply grooved and accommodates the upper arm of the preoperculum. Dorsal to this groove the posterior edge is produced into a rounded condyle which articulates synchondrally with the operculum. A shallow vertical channel runs across the base of the posteroventral condyle. This channel houses the sensory canal between the preoperculum and pterotic canals.

The *metapterygoid* is widely separated from the hyomandibula (Fig. 5). Anteriorly, it is connected to the quadrate by a narrow cartilage interface and below the cartilage by a prominent dentate suture. The ventral edge contacts the dorsal edge of the symplectic, and the endopterygoid overlies the anterodorsal edge.

The *symplectic* is large (relative to the other suspensorial bones) and lies along the posteroventral arm of the quadrate (Fig. 5). The posterior end is cartilage-capped and connected by a fibrous band of tissue to the hyomandibula. Anteriorly, the symplectic tapers and lies in a recess in the posteromedial wall of the quadrate. The upper surface is produced into a thin lamina with an irregular dorsal edge.

The *quadrate* is fan-shaped (Fig. 5), its anteroventral angle bears a condyle which articulates, *via* a euarthroidal joint with the corresponding anguloarticular facet. The condyle is strengthened by the thickened ventral margin that is bound by connective tissue to the dorsal edge of the preoperculum. A deep recess in the medial face of the quadrate parallel to its ventral edge accommodates the anterior end of the symplectic. A further recess in the anteromedial wall, dorsal to the condyle, accommodates the large posterior ectopterygoid process.

The dorsal and posterodorsal edges of the quadrate are connected by a cartilaginous interface to the endopterygoid and metapterygoid, respectively.

The *endopterygoid* is boomerang-shaped (Fig. 5); its anterior arm lies in a shallow groove along the dorsal surface of the ectopterygoid. The short posterior arm is connected by its ventral edge to the quadrate and to the anterodorsal edge of the metapterygoid. The longer (anterior) arm extends below and beyond the anterodorsal connection of the ectopterygoid to the lateral ethmoid (discussed below; see Fig. 49).

The anterior edge of the *ectopterygoid* is sinusoidal (Fig. 5). A medial facet on the anterodorsal surface connects it directly with the lateral ethmoid. A groove extends for a short distance along the posterodorsal edge and accommodates the anterodorsal margin of the quadrate. Posteriorly, a horn-shaped process extends from the ectopterygoid to lie within a recess in the medial face of the quadrate.

The *palatine* is a long, flake-like element curved around the lateral face of the vomerine shaft (dermal and endochondral components cannot be distinguished in *M. mastacembelus*). A weak spur ascends dorsally to connect the palatine with the lateral ethmoid (Fig. 5). Posterior to the small spur the bone becomes dorsoventrally flattened beneath the anterior orbital region. There are no palatine teeth in this species.

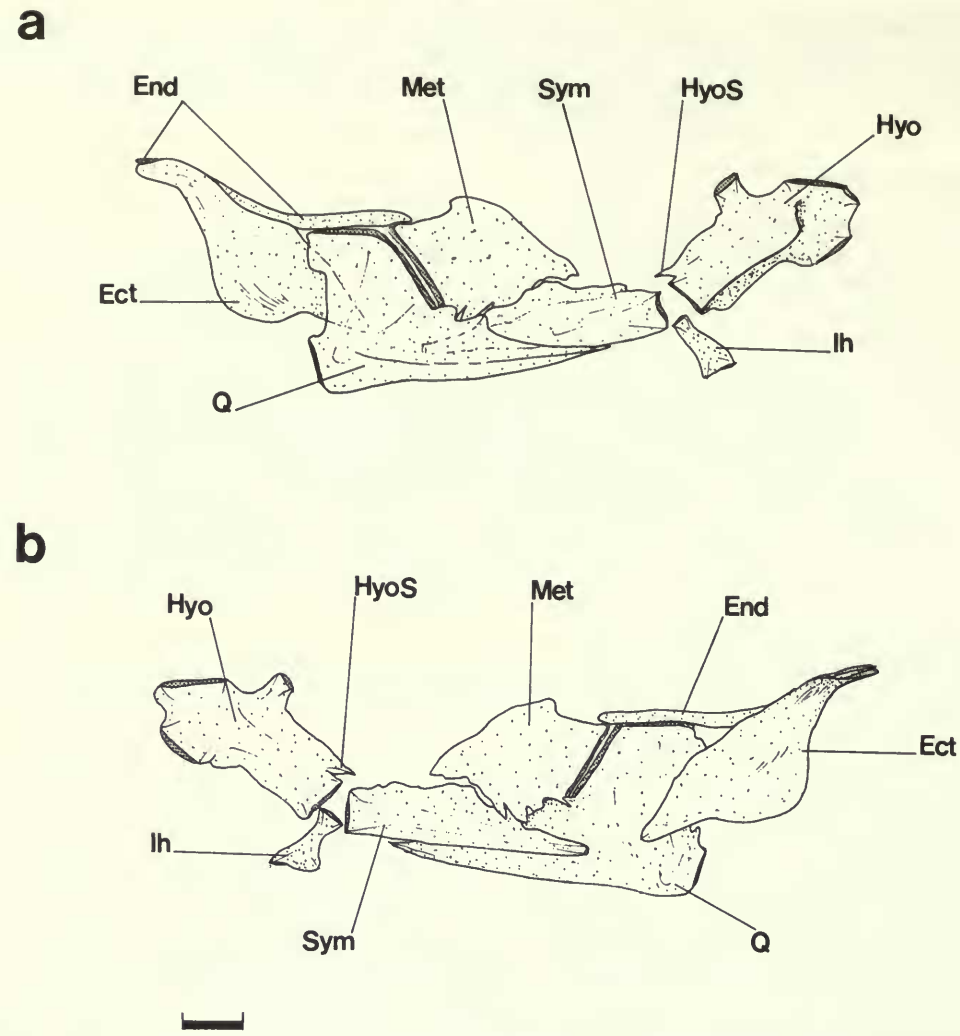

Fig. 5 *Mastacembelus mastacembelus,* left hyo-pterygoid arch in (a) lateral view, (b) medial view.

Opercular series

The *operculum* is characterised by a deeply concave dorsal edge (Fig. 6) which together with the weak, poorly ossified posterolateral flap is tightly sealed to the body-wall by the integument and underlying musculature (see p. 121). Thus, the branchial aperture lies below the suboperculum.

The ventral margin of the operculum overlaps the dorsal part of the suboperculum. A large facet on the anterodorsal edge articulates with a hyomandibular condyle and serves as a fulcrum for opercular dilatation, albeit only slight due to its restriction dorsally. A ridge crosses the lateral face and terminates in the dilatator process ventral to the opercular socket. The *levator operculi* muscle inserts along the dorsal surface of the ridge, and the *'musculus intraoperculi'* (which is unique to the mastacembeloids, see below p. 120) inserts along its ventral surface. The base of the opercular socket is pierced by a foramen which carries a ramus of the *truncus hyomandibularis* (*ramus opercularis superficialis facialis*). This nerve passes along a short enclosed canal to emerge on the anterolateral face of the operculum.

The *preoperculum* is L-shaped (Fig. 6). Its long, lower arm lies along the curved ventral

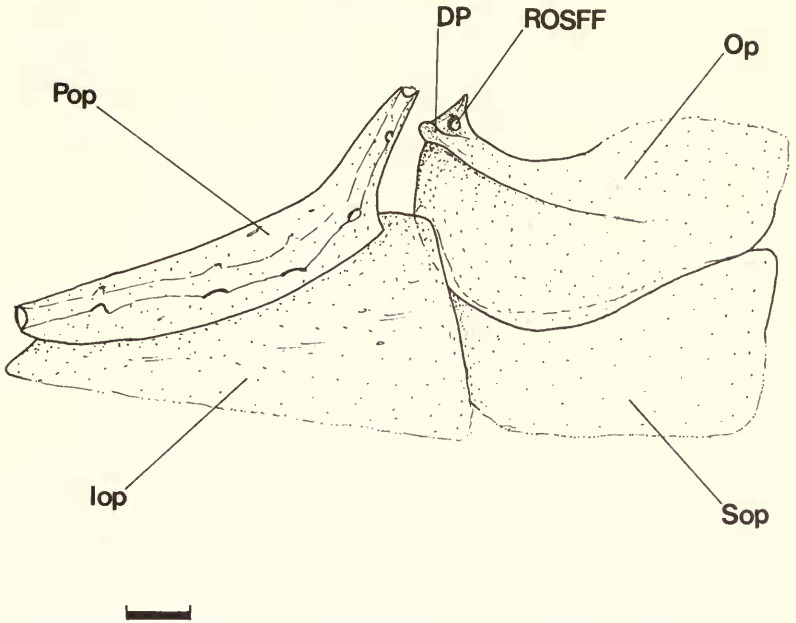

Fig. 6 Opercular series of *Mastacembelus mastacembelus*.

edge of the symplectic and quadrate, connecting them by its vertical arm to the hyomandibula. Anteriorly, the preoperculum is joined to the posterolateral wall of the angulo-articular by a short ligament. Preopercular spines are absent. The ventral edge overlaps the dorsolateral margin of the interoperculum, to which it is loosely joined by connective tissue. The upper arm of the preoperculum is narrow and lies along a deep lateral hyomandibular groove. The lateral face is pierced by 5 pores that open from its sensory canal (3 pores are present on the horizontal and 2 on the vertical limb).

The *interoperculum* is triangular, its broad posterolateral face bevelled anteriorly to a point just posterior to the mandible (Fig. 6); the interopercular ligament connects the anterior tip of the bone to the small retroarticular. Posteriorly, the interoperculum is sloped, dorsomedially, below the ventral edge of the preoperculum to which it is loosely joined by connective tissue.

The *suboperculum* is weak, its shorter, vertical arm hidden in lateral view by the anterior edge of the operculum and the posterior edge of the interoperculum (Fig. 6). The horizontal arm is broader than the vertical arm and the dorsolateral margin is overlapped by the ventral edge of the operculum. The ventral border is poorly ossified and, since it is not connected to the ventral body wall, it contributes to the posterior opening of the branchial chamber.

Hyoid and branchial arches

The *basihyal* is long and spatulate; a low ventral ridge runs along almost the entire length of the bone (Fig. 7). Posteriorly, the ridge lies in a groove along the anterior edge of the basibranchial 1 'keel' and forms a hinge joint.

The paired dorsal and ventral hypohyal bones are joined to basibranchial 1 by fibrous connective tissue. The *dorsal hypohyal* is small and caps the anterodorsal edge of the anterior ceratohyal, to which it is sutured by a number of tongue-like bony flanges (Fig. 7). The medial wall of the dorsal hypohyal is faceted and connects the anterolateral face of basibranchial 1.

Below this facet there is a large central foramen for passage of the hyoidean artery. Ventrally, the dorsal hypohyal is separated from the ventral hypohyal by a cartilaginous interface (Fig. 7).

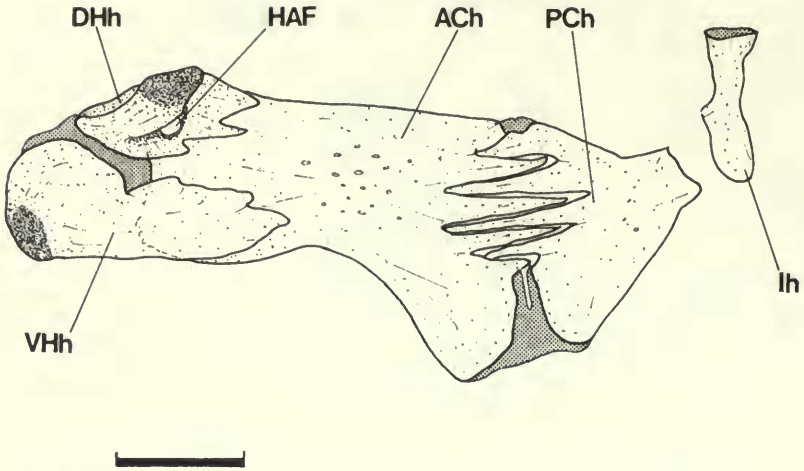

Fig. 7 *Mastacembelus mastacembelus,* right hyoid arch; medial aspect.

The *ventral hypohyal* is connected to the anterior ceratohyal by an interdigitating suture and a short band of cartilage (Fig. 7). Its anterior region is laterally compressed and a facet occurs on the medial face articulating with its partner in a median symphysis, anterior to the front edge of the keel on basibranchial 1. Below this facet is a shallow fossa, which accommodates the anterior end of a large ligament from the urohyal.

The *anterior ceratohyal* is compressed. Its posterior edge is joined to the anterior edge of the posterior ceratohyal by a large tripartite interdigitating suture, above and below which is a short connecting band of cartilage (Fig. 7).

Two branchiostegal rays (3rd and 4th) articulate with the lateral face of the anterior ceratohyal. The 5th branchiostegal is loosely connected to the medial face and the 6th (the weakest) attaches to the anteroventral margin of this bone. A 'berycoid' foramen (McAllister, 1968: 6) is absent.

The *posterior ceratohyal* is also compressed and is approximately triangular in outline (Fig. 7). The 1st and 2nd branchiostegal rays are loosely attached to its lateral face. The distal end is ligamentously connected to the ventral end of the interhyal.

The short, hour-glass shaped *interhyal* connects the posterior end of the hyoid arch (posterior ceratohyal) with the suspensorium, at a point between the symplectic and hyomandibula. The cartilaginous anterior and posterior ends of this bone have their long axes at right angles to each other.

The *urohyal* is extremely elongated and extends posteriorly from below basibranchial 1 to a point midway along ceratobranchial 5. The anterior end is bifurcated and from each head a large ligament extends forward to the ventral hypohyal. On its dorsal surface immediately posterior to its forked anterior end, is a small ascending process (directed posterodorsally), the tip of which lies below the keel on basibranchial I, and is loosely attached by connective tissue (Fig. 9). Posteriorly, the urohyal divides into four weakly ossified membranous prongs; a short dorsal and ventral prong with two large lateral prongs. The latter are subdivided into three small, posteriorly pointed processes (Fig. 9).

There are three ossified and a single cartilaginous basibranchial among the ventral gill arch elements.

Basibranchial 1 is cylindical with a deep ventral 'keel' which tapers to a knife-edge and lies partly below basibranchial 2 and the basihyal (Fig. 9). A round facet on the anterolateral surface lies across its junction with the basihyal, and articulates with the medial face of the dorsal hypohyal.

Basibranchial 2 is narrow-waisted (Fig. 8). The proximal end of hypobranchial 1 lies in the anterolateral, 'waisted' region. Posteroventrally, basibranchial 2 is united by fibrous tis-

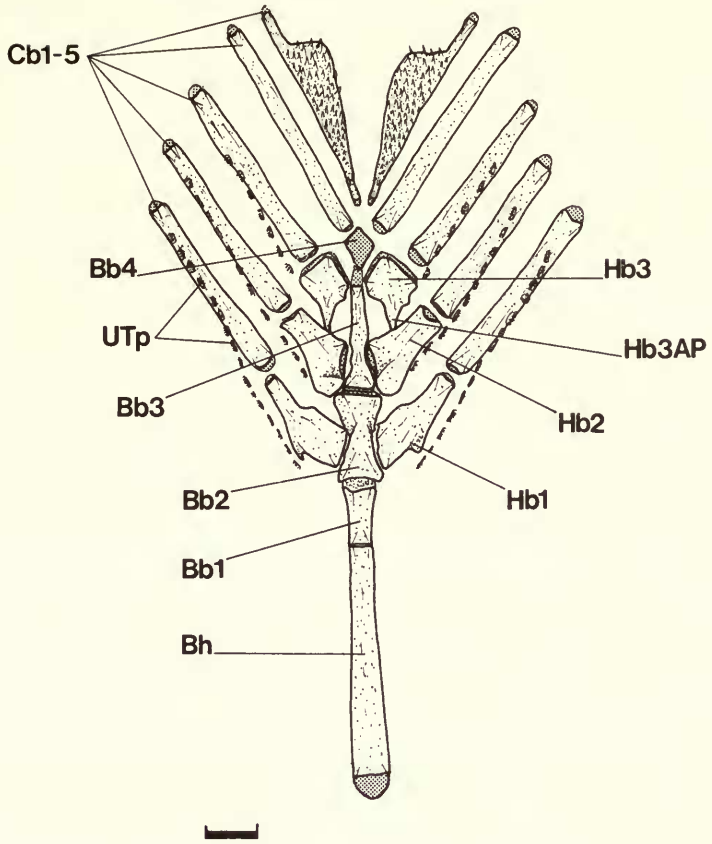

Fig. 8 *Mastacembelus mastacembelus,* lower gill arch elements; dorsal view.

sue to the anterior end of basibranchial 3. A prominent descending process extends from the median anteroventral surface and contacts the posterior edge of the 'keel' on basibranchial 1 (Fig. 9). A pair of descending processes also extend from each posterolateral corner of basibranchial 2. The tips of these processes are connected, by a pair of converging ligaments, to the posteroventral edge of the 'keel' on basibranchial 1 (the ventral aorta lies in the midline between these posteroventral processes).

Basibranchial 3 is long and relatively narrow; the medial end of hypobranchial 2 contacts the notched anterolateral wall. The posterior end is unossified and forms a rod-like length of cartilage capable of sliding below basibranchial 4 when the branchial arches contract (Fig. 8).

Basibranchial 4 is a rhomboid, cartilaginous element (Fig. 8). Its anterolateral face contacts the posteromedial edge of hypobranchial 3, and its posterolateral edges the ends of the 4th and 5th ceratobranchials.

Hypobranchials 1 & 2 each have a broad proximal (anteromedial) face faceted for articulation with their corresponding basibranchial elements. Hypobranchial 2 is also connected, by a medial flange, to the posterolateral descending process on basibranchial 2.

Hypobranchial 3 is characterised by a large anteroventral process extending forward below the 2nd hypobranchial. The anterior tip of this process is ligamentously attached to the posterior descending process on basibranchial 2; the ligament merges in the midline with its opposite number to produce a wide, ventral sheet of collagenous tissue. The ventral aorta runs along the dorsal surface of this medial aponeurosis, between it and the basibranchial elements.

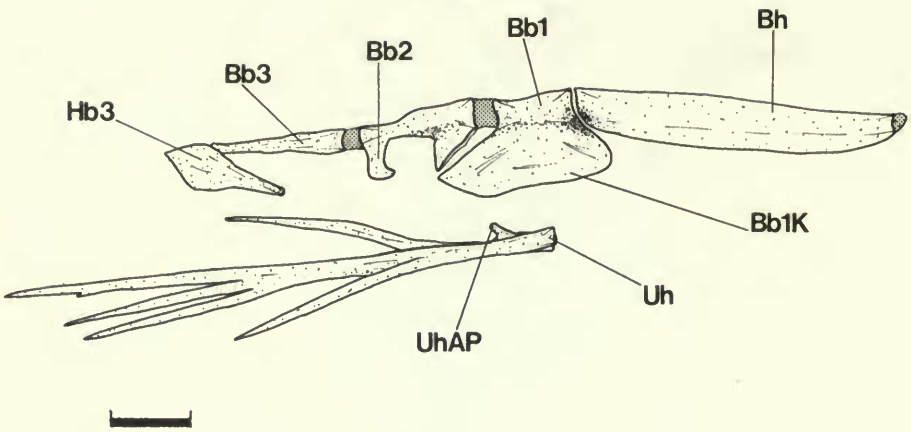

Fig. 9 *Mastacembelus mastacembelus*, basihyal and branchial bones in lateral view, right side.

The posterior end of each hypobranchial is connected by fibrous tissue to its corresponding ceratobranchial. Small, irregularly positioned dermal toothpatches are supported along the anterior margin of hypobranchial 1 and 2. No toothplate is associated with the dorsal surface of hypobranchial 3.

Ceratobranchials 1–5 are rod-like elements; with the exception of the 5th, are all essentially alike. The distal ends of ceratobranchials 1–4 are each joined by connective tissue to a corresponding epibranchial bone. Along the ventral face of ceratobranchials 1–4 is a hollow channel that accommodates the efferent blood vessels and the bases of the gill filaments. Numerous small, round, dermal toothpatches are supported along the anterior face of ceratobranchials 1–4.

The 5th ceratobranchial bears a large fused toothplate ('lower pharyngeal jaw'). This toothplate is expanded posteromedially, but does not contact its partner in the midline. The medial edge of the expanded toothplates and the posteromedial margin of the bone are joined to the oesophagus. The toothplate bears acrodont caniniform teeth graded in size, with the largest along the medial edge. The posterior end of ceratobranchial 5 forms a relatively short 'muscular process' (Liem, 1974). A broad sheet of fibrous tissue connects the posterolateral edge to the lateral face of the cleithrum.

The dorsal gill arch elements lie posterior to the cranium.

Epibranchials 1 and 2 are each characterised by wide anterior edges; a round dermal toothplate is supported on the anteroventral face of each (Fig. 10).

Epibranchials 3 and 4 both bear an ascending uncinate process. The dorsal tips of these processes are connected by a short collagenous strand of tissue.

Apart from a short lateral region, the dorsal edge of each epibranchial is free of gill filaments.

Pharyngobranchials 2 and 3 are the only ossified pharyngobranchial (infrapharyngobranchial) elements present. The posterior end of pharyngobranchial 2 is attached by a collagenous strand to the medial end of epibranchial 2. This collagenous strand is also connected to the tip of a short process on the lateral margin of pharyngobranchial 3. Pharyngobranchial 3 extends anteriorly from this process to lie parallel with the anterior end of pharynobranchial 2. A collagenous strand of tissue connects their anterior tips with the medial end of epibranchial 1 (Fig. 10). There is no trace of an interarcual cartilage (Travers, 1981) between epibranchial 1 and pharyngobranchial 2.

The posterior end of pharyngobranchial 3 is broad and connected to the medial end of epibranchial 3.

A small cartilaginous element lying posterior to pharyngobranchial 3 (between it and the medial end of epibranchial 4) is interpreted as a cartilaginous 4th pharyngobranchial. The

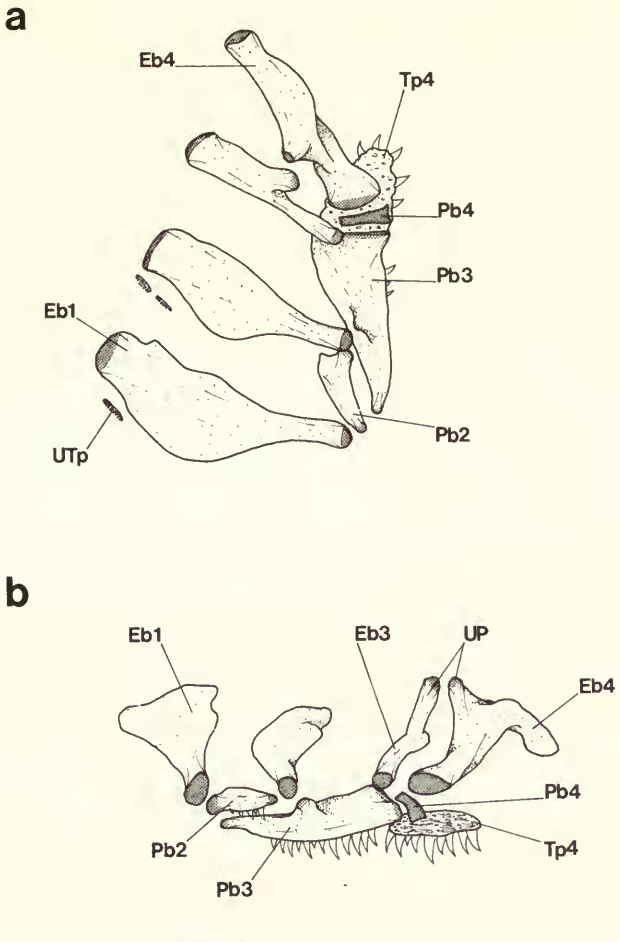

Fig. 10 *Mastacembelus mastacembelus,* right upper gill arch elements in (a) dorsal view, (b) medial view.

largest toothplate of the dorsal gill arch elements is fused to the ventral face of pharyngobranchial 3. A smaller toothplate is fused to the ventral face of pharyngobranchial 2. A further toothplate lies ventral to the cartilaginous pharyngobranchial 4.

The toothplates on the pharyngobranchial bones, together with the free 4th pharyngobranchial toothplate, constitute the 'upper pharyngeal jaws'. The dentition of these elements is similar to that found on ceratobranchial 5 which they oppose.

There are no *gill rakers* on the branchial arches.

Pectoral girdle

The pectoral girdle lacks a bony connection to the neurocranium and lies posterior to it adjacent to the 3rd and 4th abdominal vertebrae.

The thin *supracleithrum* is relatively long and narrow (Fig. 11). The ventral end overlaps the dorsolateral wall of the cleithrum to which it is loosely attached. A portion of the postcranial sensory canal system passes longitudinally through its dorsal tip.

The *cleithrum* is the largest bone of the pectoral girdle. It has a vertical dorsolateral shaft and a ventral limb which curves anteromedially to contact its partner in a median symphysis. The scapula and coracoid lie just distal to a trough-like region in the lateral face (Fig. 11).

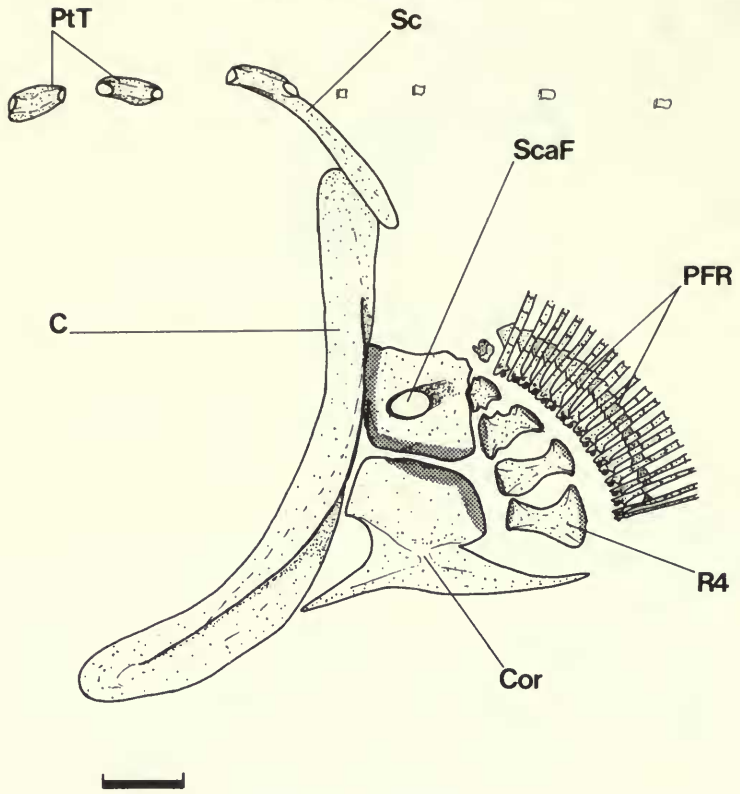

Fig. 11 *Mastacembelus mastacembelus,* lateral view of pectoral girdle; left side, with two post-temporal tubules.

Baudelot's ligament extends between the basicranium and dorsomedial face of the cleithrum and the ventromedial face of the supracleithrum.

The *scapula* is almost square in lateral outline. A large foramen pierces its anterolateral face; the nerve trunk to the pectoral fin rays passes through this opening. The cartilaginous anterior edge lies within the dorsal region of the cleithral trough. The posterior edge supports the 1st and 2nd radials and dorsal to these a slight posterior projection of the scapula articulates directly with the base of the primary fin ray (Fig. 11). The scapula and coracoid are separated by a narrow cartilage interface.

The *coracoid* is a narrow-waisted, flat bone; the lower region drawn out both anteriorly and posteriorly into pointed processes. The posterior process extends to a point below the posterior edge of the radials. The dorsal cartilage interface extends along the posterodorsal edge and supports the 3rd and 4th radials.

The four *radials* (actinosts) are short, spool-like, independent elements; the smallest lying dorsally (1st). The ends of each radial are cartilaginous and form a shallow facet for articulation anteriorly with the scapula and coracoid (as described above) and posteriorly with the base of each fin ray.

The pectoral fin has 22 segmented *fin rays*; each composed of independent halves and branched distally. The innermost halfrays (posterior) each have a ventral proximal process that overlaps the lower neighbouring halfray (Fig. 11). Distal to this process is a 2nd triangular flange that overlaps the upper neighbouring element. The outer (anterior) halfrays also have a ventral bony lip overlapping the lower neighbouring element. Fin movement results in a complex interlocking of these flanges.

Vertebral column

The total vertebral count is 86, *viz.*, 38 abdominal (precaudal vertebrae), 47 caudal and the fused ural and first preural centra. Following the method of Greenwood (1976: 65) the first caudal vertebra is identified as that with which the first anal pterygiophore articulates.

The first four *abdominal vertebrae* are the most distinctive of the entire series (Fig. 12). Their broad neural arches are pierced by numerous perforations. The anterior half of the 1st centrum is rounded to form a hemispherical condyle. This condyle articulates with the tripartite occipital socket in a 'ball and socket' joint. The first neural arch contains a distinctly large foramen just above its point of fusion with the centrum.

The neural spines of the first four abdominal vertebrae are laterally compressed and elongated. The 1st abdominal vertebra has the largest neural spine (4–5 times wider than the spine on the 5th vertebra); the anterior and posterior edges are approximately parallel and the dorsal edge produced into 3 separate peaks. The 2nd, 3rd and 4th neural spines have 2 dorsal peak-like processes, and the posterior edge of the 2nd is deeply notched. Pre- and postzygapophyses are well developed on all but the 1st abdominal vertebra.

Along the abdominal vertebrae there are a total of 3 pairs of epicentral and 1 pair of epipleural ribs. The *epicentral ribs* occur on the 1st to 4th vertebrae and *epipleural ribs* on the 4th only. The 1st epicentral is lodged in a recess on the lateral wall of the 1st centrum; all other epicentral ribs are supported by their anterior ends lying in a shallow channel along the dorsal surface of the lateral parapophyses.

Lateral parapophyses are present on all abdominal vertebrae except the 1st, and decrease in size posteriorly.

The *Pleural ribs* are all supported in a groove along a ventral arm of the lateral parapophyses (Fig. 12).

By the 10th abdominal vertebra the lateral parapophysis is reduced to a low notch and the ventral arm developed into a prominent, ventromedially curved parapopyhysis that sup-

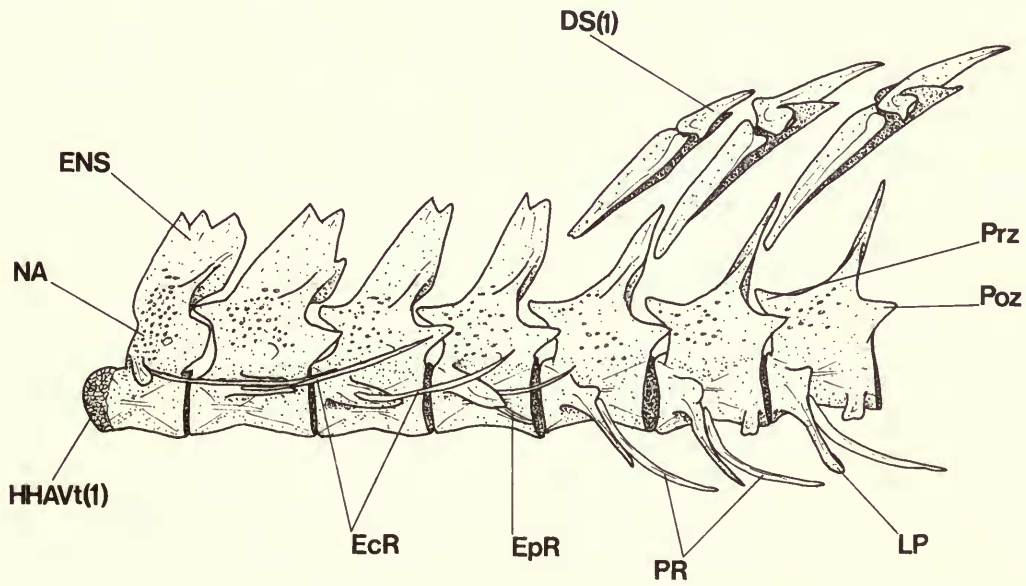

Fig. 12 *Mastacembelus mastacembelus,* anterior abdominal vertebrae with first three dorsal spines; lateral aspect, left side.

ports a large (posteriorly tapered) pleural rib. By the 13th abdominal vertebra the pleural ribs are no longer medially curved. On the 6th and all succeeding abdominal vertebrae there is also a short descending process on the ventral face of the centrum (posterior half).

The abdominal centra are characterised by their asymmetry as the posterior region of each appears to have been drawn out. However, the asymmetry of the centra is gradually lost posteriorly and the last 10 *caudal vertebrae* are symmetrical.

The parapophyses on the 1st caudal vertebra (Fig. 13) are connected in the midline by a short band of fibrous tissue (forming a rudimentary haemal arch). These parapophyses are also branched and support the massive pterygiophore carrying the 1st and 2nd anal spines.

Dorsal and anal fins

There is a total of 35 *dorsal spines* and supporting pterygiophores associated with the 4th to 38th abdominal vertebrae (excluding the 31st and 35th) and the 2nd and 3rd caudal vertebrae. The spines are relatively short, stout structures, curved posterodorsally. Anteriorly, each spine is held in position by the distal end of the supporting pterygiophores, which are fused and form a stout bone that tapers to a point anteroventrally. The distal region of these pterygiophores bears a pair of prominent hooks that lie (laterally) on either side of the spine and hold its base firmly in position (Fig. 13). The proximal end of each spine bears a pair of small anterolateral processes around which the distal pterygiophore is hooked; a pair of lateral ridges present along the pterygiophore, separate the erector from the depressor

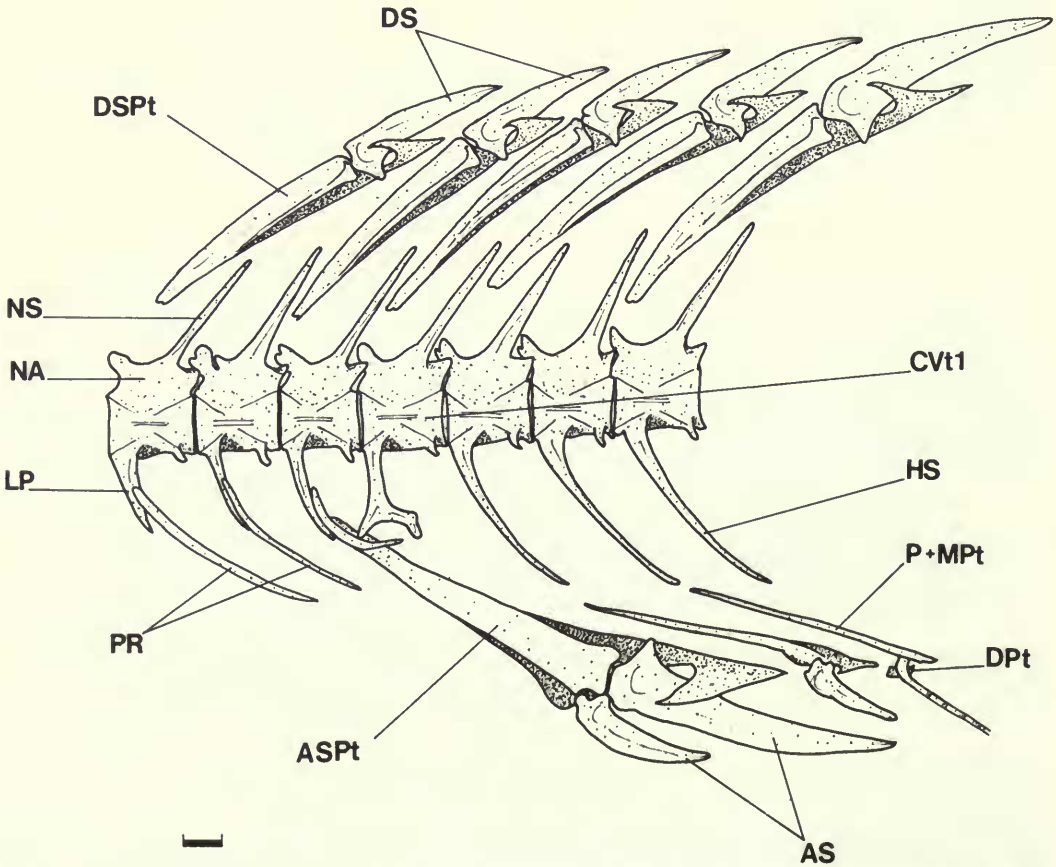

Fig. 13 *Mastacembelus mastacembelus*, abdominal/caudal vertebral junction and associated dorsal and anal spines; lateral aspect, left side.

muscles. A ligament passes from the base of the spine along the anterior edge of the supporting pterygiophore and contributes to the articulation between these elements.

There are 3 *anal spines* (Fig. 13); all are similar in morphology to the dorsal spines except that the 1st and 2nd share a massive pterygiophore. This pterygiophore is supported by the rudimentary haemal arch of the 1st caudal vertebra.

The non-spinous *dorsal* and *anal fins* are composed of 70–73 and 74–78 segmented rays respectively. They extend from the posterior spinous rays to the dorsal and ventral edge of the caudal fin. Each ray is supported by a pterygiophore system composed of 3 elements. On the whole, most neural and haemal spines are associated with 2 pterygiophores; hence each supports 2 fin rays (by the connection of a proximal pterygiophore to the anterior and posterior edges of each neural and haemal spine).

The *proximal pterygiophore* is a long, ventrally pointed bone much smaller and weaker in comparison with its spine supporting counterpart. The distal end is fused to a cone-shaped medial pterygiophore, the two forming a single unit (Fig. 13). The dorsal surface of the *medial pterygiophore* is flat and the small, independent distal pterygiophore of the preceeding fin ray articulates with it. The posterior end of the medial pterygiophore is collagenously joined to the distal pterygiophore of the same ray.

The *distal pterygiophore* is a small saddle-shaped independent structure, composed of separate halves. It lies between the base of the fin ray and the supporting medial pterygiophore element.

Caudal fin

The caudal fin rays lie posterior to the last ray of the dorsal and anal fins, to which they are joined by a thin membrane.

The *hypural* bones fan out from the fused ural and first preural centra and are composed of 4 relatively large, autogenous elements (2 above and 2 below the lateral line), and an extremely small splint of bone along the dorsal edge of the upper hypural (Fig. 14). Ventral to these lies an independent *parhypural.* A large vascular canal passes through the head of this bone (Fig. 14).

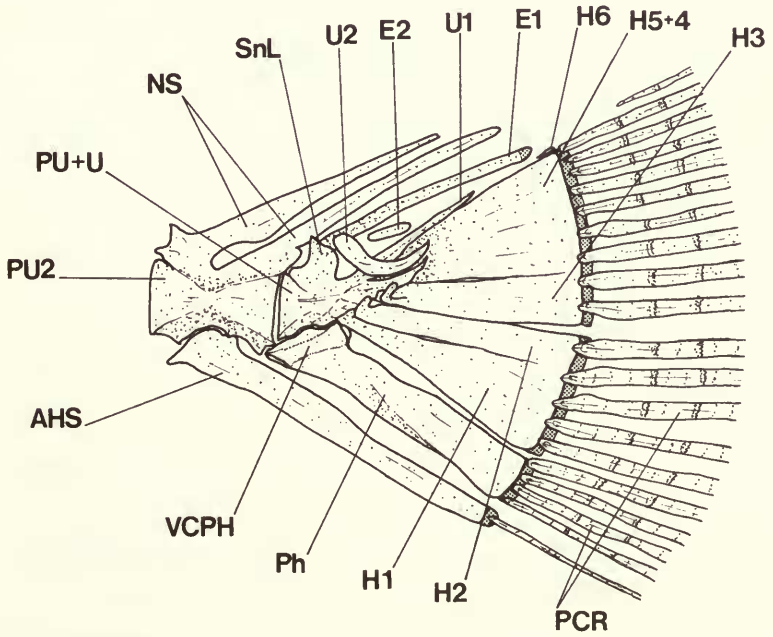

Fig. 14 *Mastacembelus mastacembelus*, caudal fin skeleton; lateral aspect, left side.

A *uroneural* (1) is fused along the dorsal edge of the fused ural and preural vertebra and is tapered to a fine point posteriorly. A second, sickle-shaped uroneural bone (2) lies lateral to the first and the base of the dorsal hypural.

A long *epural* extends posteriorly from the reduced neural arch on the fused ural and preural centra to the anterior region of the fin rays. Between this long epural and the fused ural and preural vertebra is a second, smaller epural element.

The 2nd preural vertebra bears an autogenous haemal arch from a deep V-shaped notch in the lateral wall of the centrum. The haemal spine on this arch is long and directly supports the ventral caudal fin ray. The neural arch is large and fused to the centrum. Two spines extend from this arch and may indicate that intervertebral fusion has occurred. These neural spines are long but do not contribute to the support of caudal fin rays.

There are 19 segmented, unbranched caudal fin rays (9 forming the upper lobe and 10 the lower lobe of the caudal fin).

Squamation

Small *cycloid scales* cover the body and head, except for its dorsal surface, i.e. the nasals, frontals & parietals.

Osteology of *Chaudhuria caudata*

This description is based on three specimens (see Table 3). Two individuals (38 mm. and 42 mm. standard length) from the collections at the BM(NH) are alizarin stained only. A third specimen (on loan from the MCZ) was double stained and is 43 mm. long. In this alizarin/alcian blue transparency numerous mature eggs (approx. 30) are visible in the posterior region of the body cavity, indicating that specimens of *Chaudhuria* at this size are adult.

Neurocranium

Ethmovomerine region

The *supraethmoid* is a particularly elongate bone; it consists of a laterally compressed region separating the olfactory sacs, and a short posterodorsal process lying between the anterior tips of the frontal (Fig. 15ai). The anterodorsal edge is indented and supports a relatively large tapered rostral cartilage. The anterior tip is divided into two short, blunt processes. Ventrally this region is fused to the anterodorsal edge of the vomer; posteroventrally it remains cartilaginous and extends along the anterodorsal surface of the parasphenoid and into the orbital cavity as a septal cartilage.

The *vomer* is developed anteriorly into a facet which extends around the tip of the bone. The anterolateral region of this facet articulates with the medial face of the ascending process of the premaxilla. The vomerine shaft lies in a ventral groove in the parasphenoid and extends posteriorly to a point adjacent to the anterior end of the prootic.

Each *lateral ethmoid* is a vertical, plate-like bone pierced by a large central opening. The medial edge contacts its partner in the midline dorsal to a cartilaginous septal region of the supraethmoid. Short anterior and posterior processes extend from the dorsal edge of the lateral ethmoid and are covered by the nasal and frontal respectively. The narrow ventrolateral face is joined syndesmotically to the posterodorsal tip of the 1st infraorbital.

The flattened *nasal* slopes ventrolaterally and covers the olfactory cavity; it is poorly ossified (especially anteriorly). The medial edge is loosely connected to the dorsal margin of the supraethmoid, and the lateral edge to the 1st infraorbital bone (Fig. 15aiii). Posteriorly it extends as a flattened projection above the lateral ethmoid and anterior surface of the frontal.

Orbital region

The *pterosphenoid* and *basisphenoid* are absent. The *parasphenoid* has a long, narrow

anterior process which terminates ventral to the lateral ethmoids (Fig. 15aii). It lacks a distinct ascending arm and has only a low lateral wall contacting the posteroventral edge of the prootic; it is unattached to any other bone. Posteriorly, the lateral wall is reduced to a shaft ventral to the median connection between the prootic bones. From this region the parasphenoid is divided into a pair of long, needle-like processes which extend to the posteroventral edge of the basioccipital. A low ventral ridge on the basioccipital lies between these processes. Adjacent to the lateral commissure the dorsal margin of the parasphenoid is notched for passage of the internal carotid artery.

The *1st infraorbital* bone is the only poorly ossified element of the infraorbital series present. It tapers anteriorly and contacts the ventral edge of the nasal and dorsal surface of the maxilla (Fig. 16a). The posterodorsal edge is indented and surrounds the ventral rim of the posterior olfactory opening. The posterior edge of this opening is formed by an ascending posterodorsal process on the 1st infraorbital. The medial tip of this process articulates synchondrally with the lateral ethmoid.

Otic region

The *prootic* is a particularly long bone and has a wide, tapered, anterior process extending to the orbital cavity. (Fig. 15ai). The dorsal connection with the sphenotic is interrupted by the single foramen in the pars jugularis. A slender lateral commissure arches across the centre of this foramen. Anterior to the trigeminofacialis chamber the prootic tapers into a long rostrodorsally directed process. Its dorsolateral face is pierced by a pair of round foramina which open into a medial groove along the anteromedial face of the process, and extend to its tip.

A shallow fossa in the posterodorsal margin of the prootic combines with a similar one in the sphenotic to accommodate the anterior hyomandibular condyle. Posteriorly, the prootic borders the pterotic, exoccipital and basioccipital bones and houses the anterior third of the sacculus.

The *sphenotic* lies between the dorsal edge of the prootic and the dorsolateral edge of the frontal. It has a long anterior projection extending into the orbital cavity, and terminates as a broad, blunt process, slightly posterior to the tip of the prootic anterior process (Fig. 15ai). The ventral edge forms the anterodorsal rim of the single foramen in the pars jugularis. A postorbital process is absent. The posterior edge borders the pterotic, and a posterodorsal process extends medially below the parietal to connect, synchondrally, the tip of a process apparently originating from the ventral surface of the supraoccipital.

The *pterotic* is an inflated bone, due to a medial cavern that encloses the horizontal semicircular canal, with a grooved ventral surface that accommodates the posterior hyomandibular condyle (Fig. 15aii). The dorsal edge is overlapped by the dorsolateral margin of the parietal. Ventrally it contacts the prootic and exoccipital and forms with these bones a relatively deep lateral recess. The posttemporal fossa is absent and posteriorly the pterotic borders the epioccipital.

The *epioccipital* lies between the exoccipital and pterotic and dorsally contacts the posterolateral edge of the supraoccipital and posterior edge of the parietal.

The inner face of the epioccipital houses the posterior semicircular canal which causes its relatively wide dorsolateral face to be somewhat bullate.

The *exoccipital* has a perforated dorsal surface which is prevented from contacting its partner in the midline by a posterior extension of the supraoccipital. The posterolateral face of the bone has three major foramina, *viz* those of the glossopharyngeus, occipitospinal and vagus nerves. This region is curved ventromedially and contacts its partner in the midline dorsal to the basioccipital.

Below their median connections the ventral surface of each exoccipital is developed into a slightly concave, deltoid facet. These facets, with a similar one from the basioccipital, form the tripartite occipital facet, a concave socket that articulates with the rounded anterior end of the 1st abdominal centrum (Fig. 21aii). The ventral region of the exoccipital bears a small

process which is directed posteriorly and extends beyond the posteroventral edge of the basioccipital.

The *basioccipital* is large, relative to the size of the other basicranial bones, and contacts the exoccipital and prootic (Fig. 15aii). The long ventral processes on the parasphenoid pass across its ventral surface on either side of a low longitudinal ridge. The posterodorsal surface is faceted and contributes to the tripartite occipital socket.

The *supraoccipital* is the major element in the roof of the basicranium (Fig. 15aiii). It is a flattened bone that is transversely convex and bounded on either side by the posterior

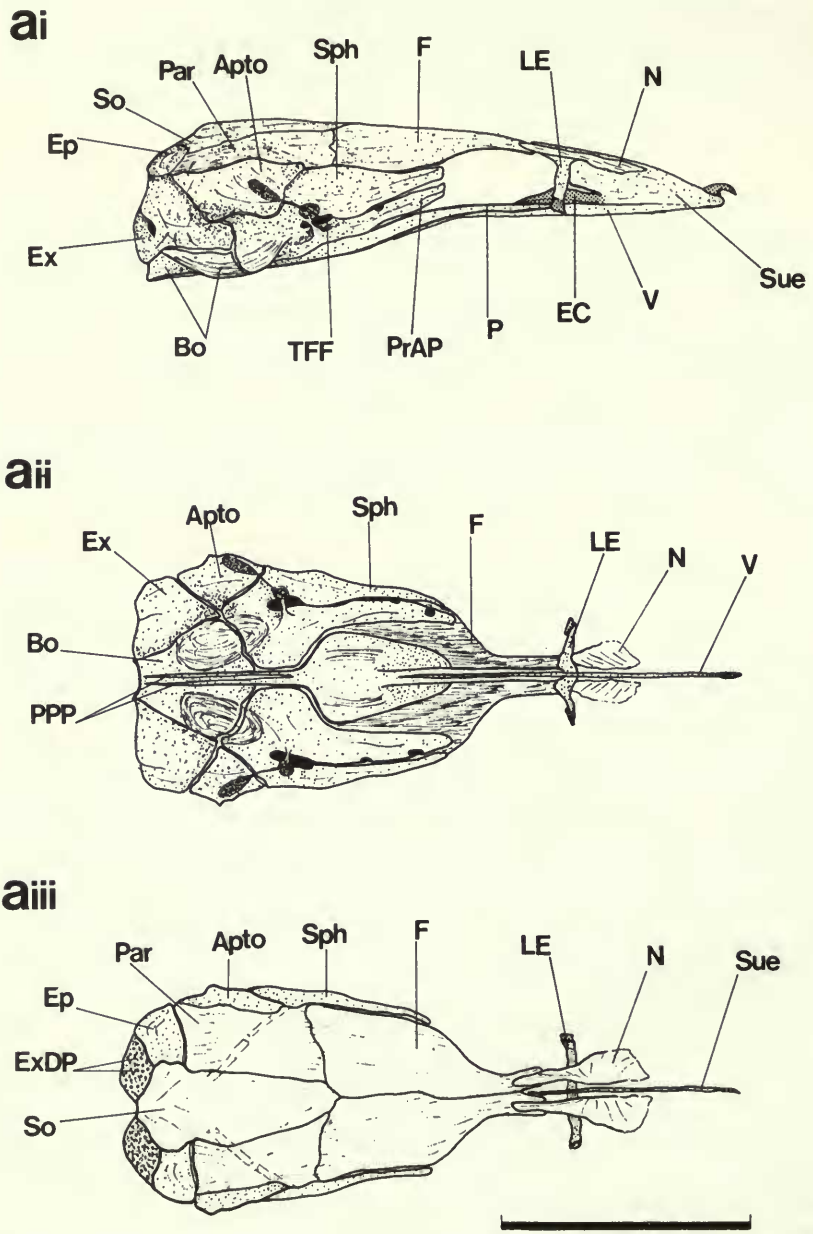

Fig. 15 Neurocranium in (a) *Chaudhuria caudata,* and (b) *Pillaia indica*: right lateral view (ai & bi), ventral view (aii & bii) and dorsal view (aiii & biii).

portion of the frontals, the parietals, epioccipitals and the dorsomedial edge of the exoccipitals. However, none of these surrounding bones overlaps the supraoccipital margin. Its posterior edge contributes to the rim of the foramen magnum.

There is no sign of the *extrascapula* (lateral or medial) or the *posttemporal* bones.

The flattened dorsal surface of the *frontal* narrows anteriorly as a short process that terminates below the posterior end of the nasal (Fig. 15aiii). Posteriorly, the frontal is long and curved ventrolaterally. A descending lamina is absent.

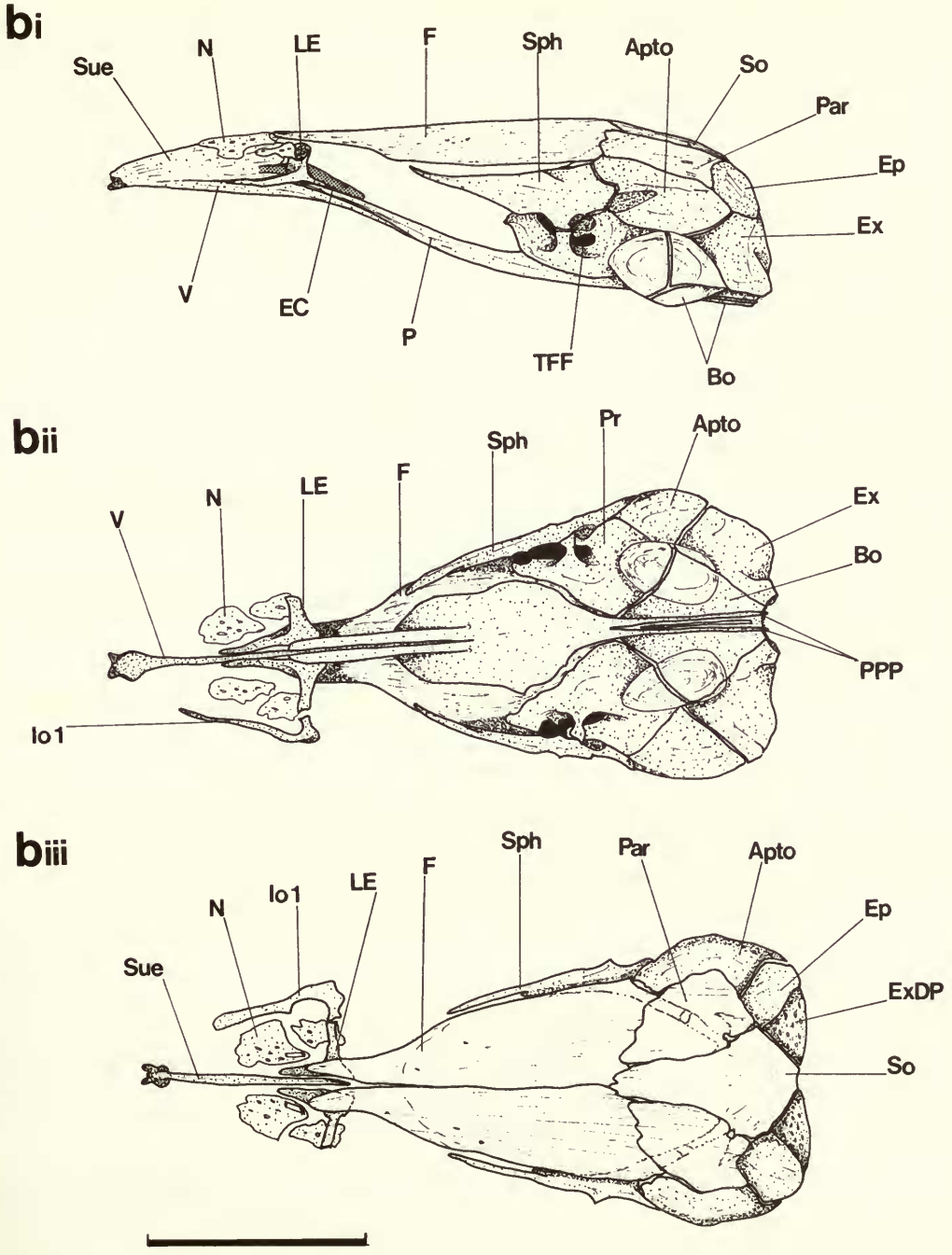

The *parietal* has a flattened, unsculptured dorsal surface that is relatively broad compared with the other roofing bones (Fig. 15aiii). It lacks a posterolateral flange and is surrounded by the supraoccipital, frontal, pterotic and epioccipital bones. A notch along its posteromedial edge forms, with the margin of the supraoccipital, a small dorsal opening.

There is no sign of the *cephalic sensory canal system* in any neurocranial bones. The somatic component passes through the tip of the supracleithrum and appears to terminate just posterior to the cranium.

Jaws

The upper jaw in *Chaudhuria,* based on Annandale's (1918) original description, was assumed by Yazdani (1978: 284) to consist of a single bone; however, this is not the case.

The *premaxilla* is a long, narrow, weakly curved bone, and has a low stump-like ascending process on its anterodorsal surface (Fig. 16a). The ventral surface has a narrow alveolar surface that bears 2 rows of long, weak villiform teeth (decreasing in size posteriorly).

The *maxilla* is a relatively large bone (compared with the size of the premaxilla; Fig. 16a). Its anterior end extends to the posterior edge of the premaxillary symphysis and is connected to the premaxilla ascending process and lateral facet on the head of the vomer. Posteriorly the maxilla overlies the lateral face of the coronoid process on the dentary.

The *dentary* is relatively short. Its symphysis lies in the vertical posterior to the premaxillary symphysis. A prominent symphysial process descends from the anteroventral edge. Posteriorly, the dentary divides into an upper coronoid and lower ventral arm (Fig. 16a). The coronoid region is developed into a tall, narrow process. The dorsal surface anterior to the coronoid process is alveolate and bears 3 rows of villiform teeth, decreasing in number and size posteriorly. The ventral arm of the dentary extends posteriorly as a long pointed process lying below the margin of the anguloarticular. From the ventral edge of this process a further short posteromedially directed process may develop. The region between these processes may be bridged by partly ossified tissue.

The *anguloarticular* is long and pointed (Fig. 16a). Its dorsal edge is straight, apart from a low projection on the anterior edge of the posterodorsal facet. Meckel's cartilage lies along the medial face, and passes into the dentary.

The *retroarticular* is a small, L-shaped bone (its shorter horizontal limb extending anteriorly). The dorsal surface of the vertical limb articulates synchondrally with the posteromedial face of the anguloarticular facet (Fig. 16a). The interopercular ligament is connected to the posterior edge.

The *coronomeckelian* is a short rod of bone that lies on the posterodorsal surface of Meckel's cartilage but does not protrude above the dorsal edge of the anguloarticular (Fig. 16a). The anterior end of the tendon from part A_3 of the *adductor mandibulae* inserts on the coronomeckelian.

Hyopalatine arch

The *hyomandibula* is a short, stout bone, its dorsal surface produced into two condyles which articulate with the lateral face of the neurocranium, and its posterodorsal edge produced into a third condyle which articulates with the operculum (Fig. 17a). The descending hyomandibular shaft is short and is joined to the symplectic and interhyal medial to the preoperculum. A wide flange anterolateral to the shaft is connected anteriorly to the metapterygoid and ventrally to the posterodorsal edge of the symplectic. A large foramen for the *truncus hyomandibularis* pierces the lateral wall of the hyomandibula, ventral to its anterior condyle.

The *symplectic* is a rod-like bone without dorsal lamina, and does not extend forward to the quadrate (Fig. 17a).

Its dorsal edge is connected to the ventral edge of the metapterygoid, and ventrally it lies along the lower limb of the quadrate, passing posteriorly on the medial aspect of the preoperculum.

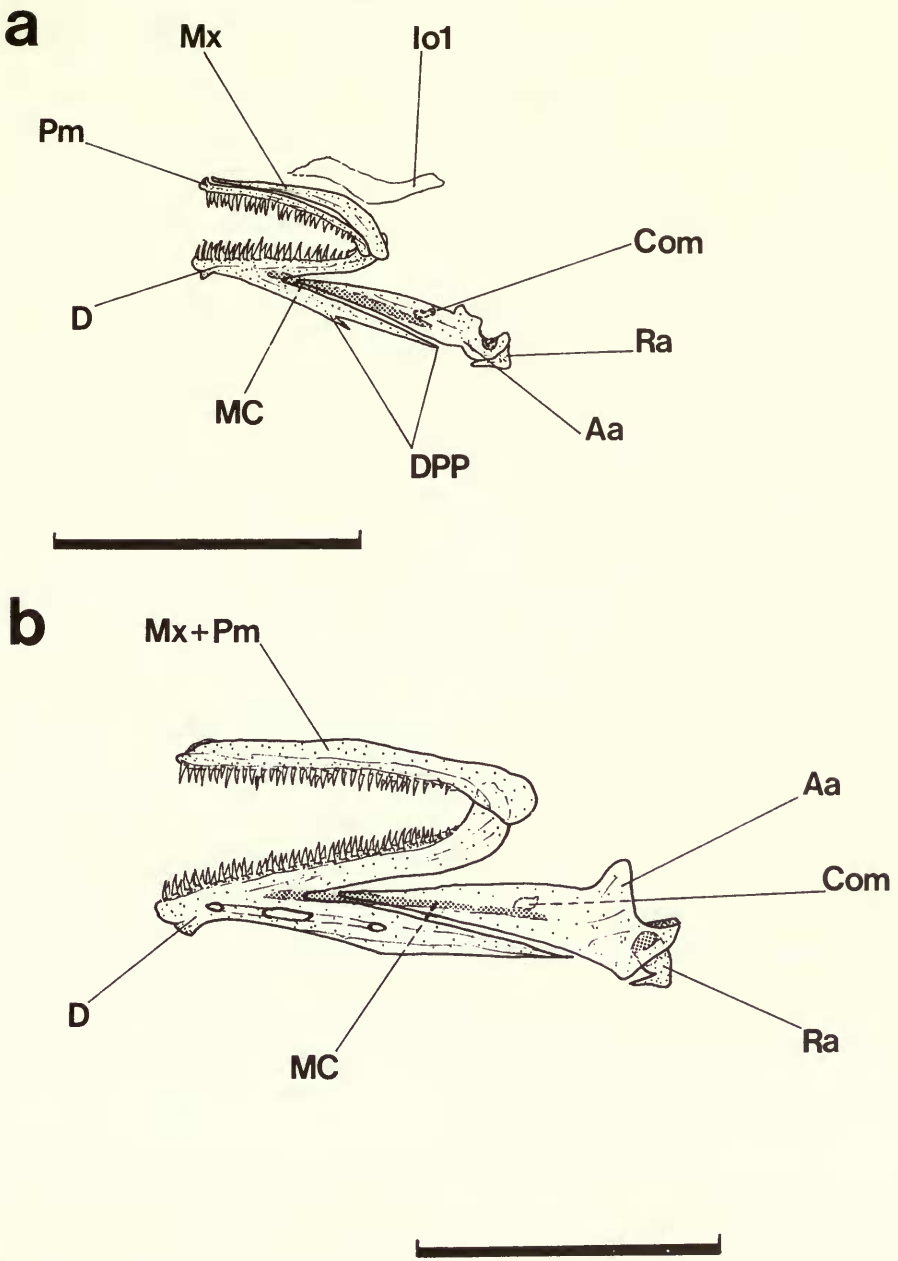

Fig. 16 Upper and lower jaw bones in (a) *Chaudhuria caudata* and (b) *Pillaia indica;* lateral view, left side.

The *metapterygoid* lies close to the anterior edge of the hyomandibula. Its anterior edge is connected by a cartilaginous interface with the quadrate. The anterodorsal corner has a slight projection that overlies the dorsal edge of the quadrate.

The *quadrate* is large in comparison with the other suspensorial bones. Its anterior edge is notched and ventrally forms a stout condyle which articulates with the anguloarticular facet. This condyle is strengthened by the thickened ventral region of the quadrate.

An *endopterygoid* is absent.

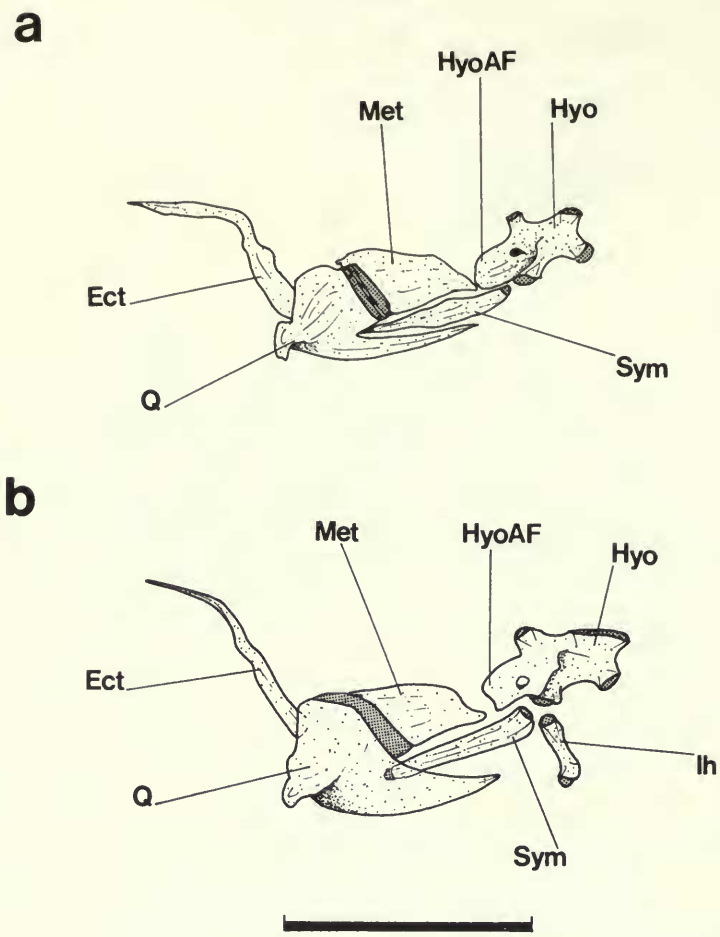

Fig. 17 Hyopalatine arch, in (a) *Chaudhuria caudata* and (b) *Pillaia indica*; lateral view, left side.

The *ectopterygoid* is particularly long with a relatively narrow lateral face whose posterior region lies medial to the anterior edge of the quadrate (Fig. 17a).

The anterior limb is curved medially (ventral to the lateral ethmoid) and has its medial face connected to the vomerine shaft. This is the anterior suspensorial articulation with the neurocranium as there is no connection between the ectopterygoid and lateral ethmoid.

The *palatine* is absent.

Opercular series

The *preoperculum* is crescentic, lacking distinct vertical and horizontal arms; the lateral face is wide (Fig. 18a). Dorsally, it is tucked within a deep groove on the lateral face of the hyomandibula.

The *interoperculum* is connected ligamentously to the retroarticular and has a poorly ossified ventral margin.

The *suboperculum* has a thin dorsal arm that ascends between the interoperculum and operculum, apart from this arm it is poorly ossified.

The *operculum* is developed anterodorsally into a prominent concave facet for articulation with the posterior hyomandibular condyle (Fig. 18a). The ridge on its lateral face extends from the base of the facet and forms a distinct dilatator process. The dorsal edge of the operculum is notched and its posteroventral margin is poorly ossified.

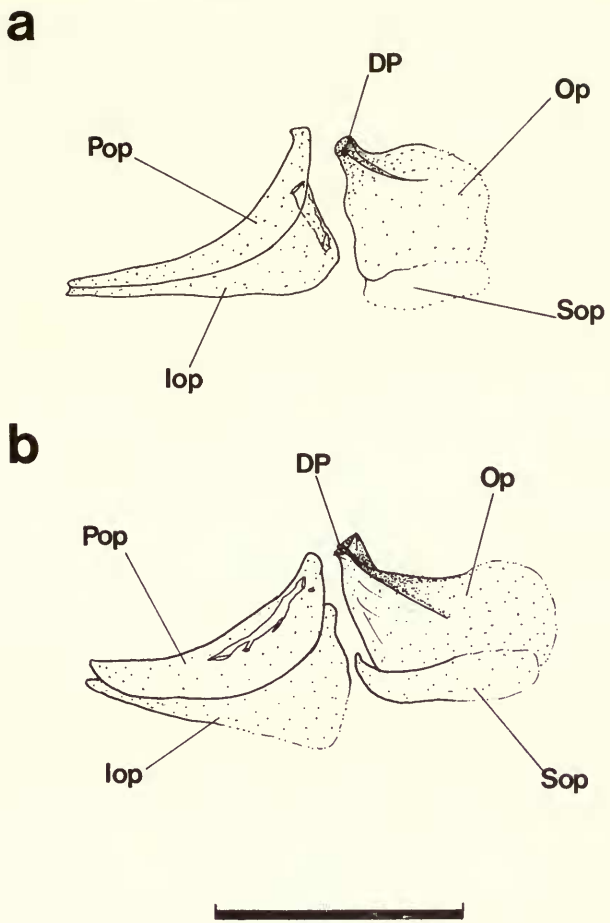

Fig. 18 Opercular series of (a) *Chaudhuria caudata* and (b) *Pillaia indica.*

Hyoid and branchial arches

The *basihyal* is spatulate with a low ventral ridge, and has its posterior end connected to the anterior end of basibranchial 1 (Fig. 20ai).

The *dorsal* and *ventral hypohyal* bones are connected to the posterolateral face of the basihyal across its border with basibranchial 1 (Fig. 20ai). These elements are connected to each other and the proximal end of the anterior ceratohyal by a narrow cartilaginous interface. The dorsal hypohyal is pierced by a large central foramen for the passage of the hyoidean artery. Dorsal to this foramen its medial face is faceted and articulates with the anterolateral face of basibranchial 1. The compressed anterior region of the ventral hypohyal has a medial facet that contacts its partner in the midline ventral to the posterior end of the basihyal.

The *anterior ceratohyal* is hatchet-shaped, in lateral view, and supports the base of the 3rd and 4th branchiostegal rays distally on its wide anterior face. (Fig. 19a). The narrow proximal end supports the 1st and 2nd branchiostegal rays. A single process extends from its lateral end and is housed in a recess on the posterior face of the posterior ceratohyal. Apart from this projection the ceratohyals are connected only by a straight suture incorporating a wide cartilaginous interface.

The *posterior ceratohyal* has a wide ventral lip that supports, on its posterior face, the base of the 1st and 2nd branchiostegal rays. The distal end of this bone is connected by a tough ligament to the interhyal.

The *interhyal* is a short rod-shaped bone that is joined to the fibrous connective tissue between the symplectic and hyomandibula, medial to the preoperculum (Fig. 19a).

The *urohyal* is forked anteriorly with each tip ligamentously connected to the ventral hypohyal. Posteriorly, it increases in depth and is relatively short, terminating at a point ventral to basibranchial 4 without developing into prong-like processes.

Basibranchial 1 is a short, cylindrical element without a ventral keel. Anterolaterally it articulates with the medial face of the dorsal hypohyal, and posteriorly with basibranchial 2 (Fig. 20ai).

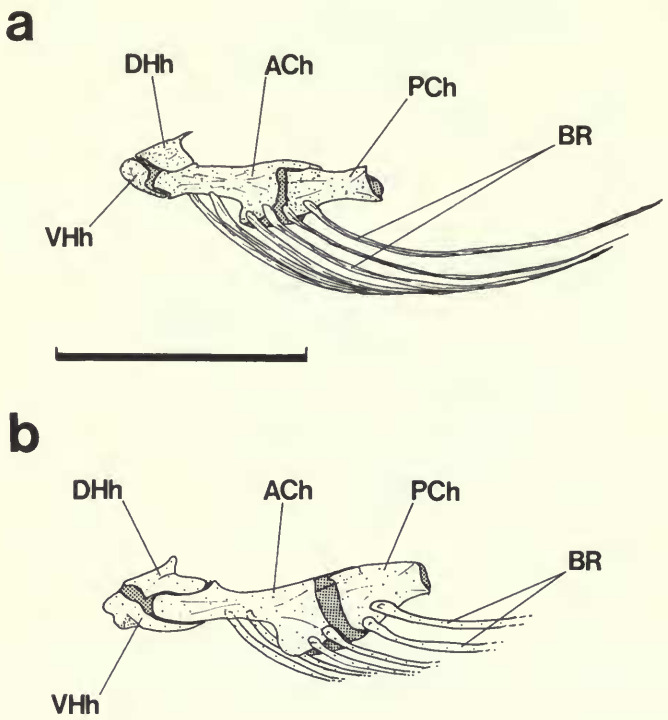

Fig. 19 Hyoid arch, in (a) *Chaudhuria caudata* and (b) *Pillaia indica*; lateral view, left side.

Basibranchial 2 is rod-like and the medial face of hypobranchial 1 connects to its anterolateral face. There are no ventral processes and posteriorly it is joined to basibranchial 3.

Basibranchial 3 is long and its tapered posterior end terminates in a cartilaginous tip (Fig. 20ai). The medial end of hypobranchial 2 is connected to the anterolateral face of basibranchial 3.

Basibranchial 4 is a small cartilaginous element (Fig. 20ai). Its anterolateral face is connected to the medial end of hypobranchial 3, and its posterolateral face to the medial end of ceratobranchial 4.

Hypobranchials 1 and 2 are relatively short rod-like bones distally connected to the anterior (medial) end of their corresponding ceratobranchials (Fig. 20ai).

Hypobranchial 3 is shorter and broader than its anterior counterparts; its anterior process is relatively short and does not extend below hypobranchial 2 (Fig. 20ai). A round toothplate with small caniniform teeth is fused to the dorsal surface.

Ceratobranchials 1–5 are long, rod-like bones, all, apart from the 5th, essentially similar. The distal ends of ceratobranchials 1–4 are joined by connective tissue to the distal ends of the corresponding epibranchial bones. The ventral surface of each ceratobranchial is grooved and accommodates the bases of the gill filaments.

Ceratobranchial 5 carries a fused toothplate which has a slight medial expansion and bears relatively large caniniform teeth (Fig. 20ai). Posterior to its toothplate, ceratobranchial 5 curves dorsolaterally to form a process for muscle attachment. All dorsal gill arch elements lie posterior to the neurocranium, as do some of the ventral elements.

Epibranchials 1 & 2 are but slightly curved, narrow bones (Fig. 20aii). The medial end of epibranchial 1 is connected to the anterior end of the small rod-like pharyngobranchial 1, and epibranchial 2 connects with its posterior end.

Epibranchials 3 and 4 both have an ascending uncinate process (Fig. 20aii). The dorsal tips of these processes are connected by a short strand of collagenous tissue. The medial end of epibranchial 3 is connected to the posterolateral margin of pharyngobranchial 3. The medial end of epibranchial 4 is broad and is joined to the wide posterior end of pharyngobranchial 3.

Pharyngobranchial 2 and 3 are the only pharyngobranchial (infrapharyngobranchial) bones present. Pharyngobranchial 2 is a small, untoothed element that lies between the proximal ends of epibranchials 1 and 2 (Fig. 20aii). Pharyngobranchial 3 is a much larger bone and bears a large toothplate fused to its ventral surface. The proximal end of pharyngobranchial 3 is connected to the distal end of pharyngobranchial 2 and together these are joined to the tip of epibranchial 2. The distal end of pharyngobranchial 3 is broad and connected to the wide proximal face of epibranchial 4. The proximal end of epibranchial 3 is not connected to the distal end of pharyngobranchial 3 but is connected to its posterolateral margin. A large toothplate lies below the proximal end of epibranchial 4 and is the pharyngobranchial 4 toothplate, although there is no sign of its corresponding bone. This toothplate and that on pharyngobranchial 3 have relatively large caniniform teeth with posteriorly directed tips.

Pectoral girdle

The pectoral girdle lies posterior to the neurocranium, adjacent to the 3rd and 4th abdominal vertebrae. It lacks a posttemporal connection to the neurocranium and there are no posttemporal canal tubules surrounding the postcranial sensory canal anterior to the supracleithrum.

The *supracleithrum* is a small sinusoidal element (Fig. 21ai). The postcranial laterosensory canal passes through its dorsolateral face; ventrally it overlaps the dorsolateral face of the cleithrum to which it is loosely connected.

The *cleithrum* is bowed and has a narrow lateral face. Dorsally it contacts the supracleithrum, ventrally it meets its partner in a median symphysis (Fig. 21ai).

Apart from these two bones the pectoral girdle consists only of two indistinct cartilaginous elements that lie posterior to the cleithrum, are partly fused anteriorly and appear to support the fin rays. These rays are indistinct in the specimens examined although Annandale & Hora (1923) described 7 segmented pectoral fin rays in *Chaudhuria.*

Vertebral column

The total vertebral count is 72, *viz.*, 25 abdominal, 46 caudal and the fused ural and first preural centra.

The unusual form of the vertebrae in *Chaudhuria* has been described by Annandale (1918). The first 6 *abdominal vertebrae* have antero-posteriorly expanded neural spines (Fig. 21aii). Those on the subsequent centra are subdivided into an anterior and posterior peak, giving the neural arch on these vertebrae the appearance of having two spines. A short neural projection anterior to the spine occurs on all abdominal vertebrae apart from the 1st–6th. The anterior spine is directed dorsally and less backwards than the posterodorsally directed posterior spine. It decreases in height posteriorly and is absent from the caudal vertebrae apart from a slight projection on the first three or four of these elements.

The neural arches of the anterior abdominal vertebrae have a densely perforated lateral surface. The anterior end of the 1st abdominal centrum is rounded to form a hemispherical condyle that articulates with the tripartite occipital socket in a 'ball and socket' joint.

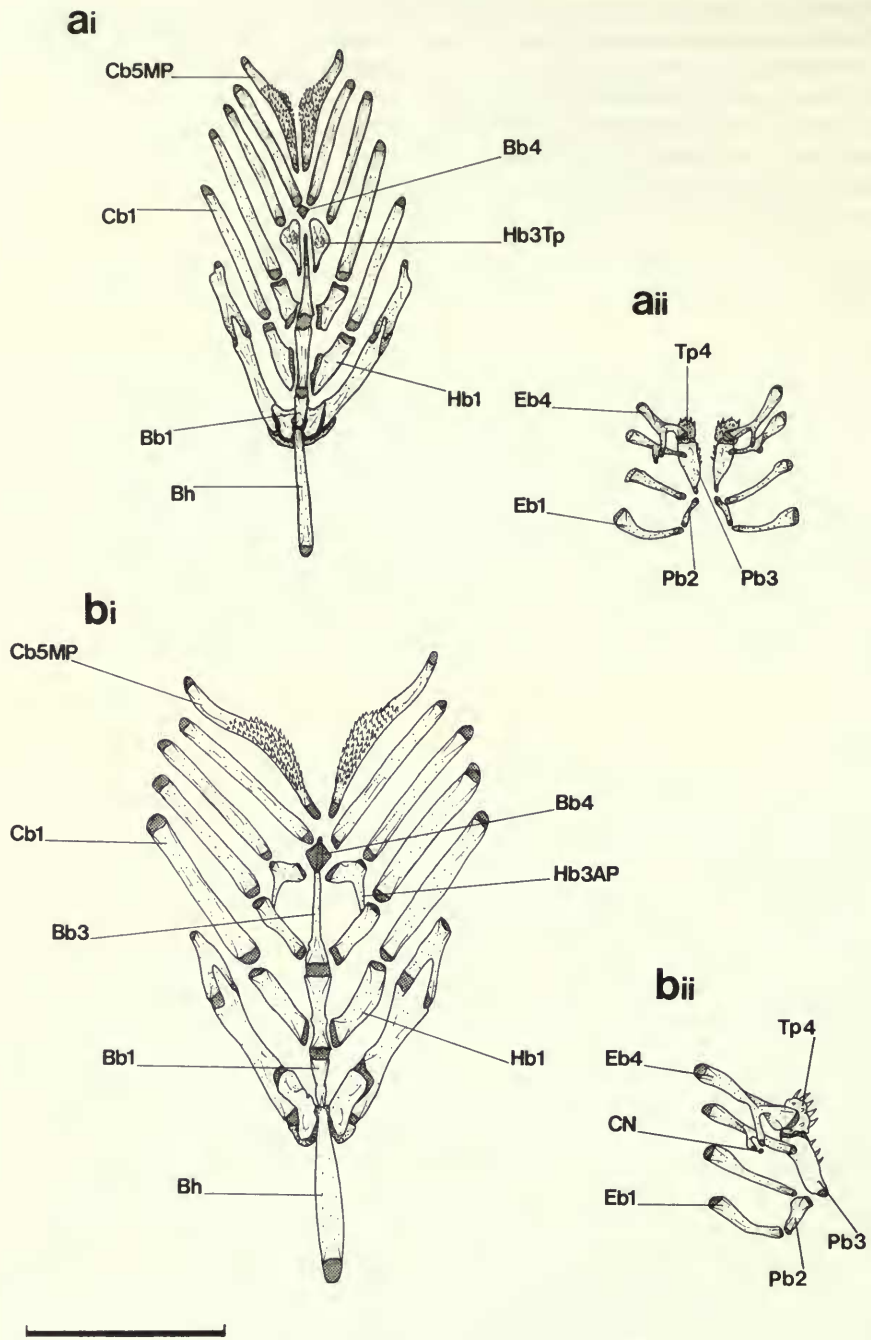

Fig. 20 Hyobranchial arches in (a) *Chaudhuria caudata* and (b) *Pillaia indica*; dorsal view of lower bones (ai & bi), and upper bones (aii & bii).

Pre- and postzygapophyses are well developed on all but the 1st abdominal vertebra. Laterally directed parapophyses occur on this and all subsequent abdominal vertebrae; apart from those on the 1st–3rd vertebrae, their tips curve ventrally.

Epicentral ribs occur on the 1st abdominal vertebra only, and *epipleural ribs* are absent.

Pleural ribs are present on the 4th and all succeeding abdominal vertebrae. They are supported in a groove along the posterior face of the parapophyses. A small bone lies posterior to the tip of the parapophysis on the 3rd abdominal vertebra and may represent a pleural rib. The *caudal vertebrae* have short, narrow neural and haemal spines. The abdominal and caudal centra are characterised by their asymmetry which is gradually lost posteriorly.

Dorsal and anal fins

Dorsal and anal spinous rays and their supporting pterygiophores are absent.

Forty *dorsal* and *anal branched fin rays* extend from a point above and below the abdominal/caudal vertebral junction to the 7th or 8th preural vertebra. Each fin is supported by a pterygiophore system composed of 3 elements; a large well ossified *proximal pterygiophore* fused to a cartilaginous *medial pterygiophore*, and a small independent *distal pterygiophore*. The lack of fin rays (and their supporting pterygiophores) on the posterior 6 or 7 caudal vertebrae is a diagnostic feature of *Chaudhuria* originally described by Whitehouse (1918).

Caudal fin

The caudal fin is distinct from the dorsal and anal fins and is composed of 8 segmented fin rays.

Two *hypural* bones (possibly composed of hypurals 1+2, and 3+4+5+6) fan out from the fused ural and first preural centra (Fig. 23a). These elements are autogenous and each supports 4 fin rays along its cartilaginous posterior margin.

A small *parhypural* is fused along the ventral edge of the hypaxial hypural.

The *uroneural* is small and appears to be fused along the dorsal edge of the fused ural and first preural centra. There is a single *epural* bone. The 2nd preural vertebra has a fused neural and haemal arch with short spines which do not support fin rays.

Squamation

The body is entirely *scaleless*.

Osteology of *Pillaia indica*

This description is based on two specimens (both on loan from the ZSI; see Table 3). The larger specimen (68mm. standard length) is poorly preserved and stained (alizarin only). The second individual is smaller (only 44.5 mm. long) but has responded well to both stains (alizarin & alcian blue), and its internal anatomy is clearly visible.

Neurocranium

Ethmovomerine region

The *supraethmoid* is similar to that described in *Chaudhuria* (p. 32 Fig. 15ai) apart from a notch in the anterodorsal edge which houses a small rostral cartilage (Fig. 15bi).

The *vomer* is curved posteroventrally and extends to a point adjacent to the middle of the ascending lateral walls on the parasphenoid (Fig. 15bi). The long anterior arm of the ectopterygoid lies along the posterolateral face of the shaft (discussed below).

Each *lateral ethmoid* consists of a thin medial wall from which a stout, curved strut arches laterally giving it a somewhat tubular shape (Fig. 15bi). The medial wall contacts its partner in the midline, dorsal to the cartilaginous region of the supraethmoid, and the lateral face articulates syndesmotically with a medial facet on an ascending process on the 1st infraorbital bone. Below this connection the lateral ethmoid is drawn out into a tapered anteroventral process that lies along the dorsolateral margin of the vomerine shaft. The anterior end of the suspensorium lies adjacent to this process, but there is no direct contact.

The *nasal* is a weakly ossified, flattened bone (Fig. 15bi) that slopes ventrolaterally and overlies the olfactory cavity in a manner corresponding closely to that in *Chaudhuria* (Fig. 15ai). A number of small, irregular pores pierce the posterodorsal surface.

Orbital region

The lateral face of the orbital region is open and there is no sign of *pterosphenoid* or *basisphenoid* bones. The *parasphenoid* has a short anterior process, possibly associated with the small orbital cavity, which is bent dorsorostrally and terminates at a point below the lateral ethmoid (Fig. 15bii). A wide lateral wall ascends from the parasphenoid and, apart from contacting the posteroventral edge of the prootic, is unattached to any other bone. Posteriorly, the lateral wall narrows to a reduced shaft and from this region the parasphenoid is divided into a pair of long, needle-like processes which extend across the posteroventral edge of the basioccipital.

The *1st infraorbital* bone is the only element of the infraorbital series. Ventrally it is connected to the dorsal surface of the upper jaw element.

Otic region

The *prootic* lies between the posterolateral wall of the parasphenoid and the sphenotic. The trigeminofacialis chamber is similar to that described in *Chaudhuria* (p. 33), but anterior to it the prootic in *Pillaia* has a short, blunt projection that is unattached to any other bone. The posterior region of the prootic borders the pterotic, exoccipital and basioccipital bones and houses the anterior third of the relatively large sacculus.

The *sphenotic* has a long tapered anterior projection that passes along the dorsolateral edge of the frontal (Fig. 15bi). The tip of this process extends to a point adjacent to the anterior end of the parasphenoid lateral wall. This region of the sphenotic is unconnected to any other bone. The ventral edge contacts the prootic and forms the anterodorsal rim of the single large foramen in the pars jugularis. A low postorbital process dorsal to the lateral commissure in the trigeminofacialis chamber, is just discernible. The posterior position of this process (relative to the orbit) illustrates that the main region of neurocranial elongation in *Pillaia* is precommissural. Posterior to the process the neurocranium is of more typical perciform proportions.

The *pterotic* has an inflated lateral face and the dorsal edge is overlapped by the dorsolateral margin of the parietal. The ventral surface is grooved and accommodates the posterior hyomandibular condyle (Fig. 15bi). Below this groove the pterotic contacts the prootic and exoccipital. There is no posttemporal fossa although the ventral margin forms part of the roof of a recess in the lateral wall of the basicranium.

The *epioccipital* is small and forms, in conjunction with the exoccipital and supraoccipital, the posterodorsal wall of the basicranium (Fig. 15bi & iii).

The dorsomedial process on the *exoccipital* is prevented from contacting its partner in the midline by the posterior end of the supraoccipital. The dorsal surface is pierced by numerous small perforations. Three major foramina pierce the posteroventral face. Below their midline connection each exoccipital has a somewhat concave deltoid facet which contributes to the tripartite occipital facet (a concave socket) that articulates with the rounded anterior half of the first abdominal centrum (Fig. 21bii).

The large *basioccipital* relative, that is, to its size in other mastacembeloids, contacts the prootic anteriorly and the exoccipital dorsally. The tips of the parasphenoid ventral processes extend beyond its posteroventral edge. A facet on the posterior face contributes to the occipital facet.

The *supraoccipital,* which is also relatively large, lacks any form of sculpturing, is transversely convex and bounded on either side by the parietals and by a posterior extension of the frontals. All these surrounding bones overlap its margin. Posteriorly, contact is made with the exoccipitals, and the supraoccipital contributes to the rim of the foramen magnum (Fig. 15biii).

The *extrascapulae* (both lateral and medial) and the *posttemporal* are absent.

The flattened *frontal* lacks a descending lamina, crests, or any form of sculpturing. Anteriorly it has a relatively short, narrow region (dorsal to the small orbit), which overlies the lateral ethmoid; the longer posterior part is curved ventrolaterally.

The *parietal* is small compared with this bone in *Chaudhuria* and other mastacembeloids. It has a narrow dorsal surface and a short posterolateral flange which lies along the dorsal junction between the epioccipital and exoccipital. A distinct notch in the posteromedial edge of the parietal forms, with the supraoccipital, a small opening in the posterior surface of the neurocranium (Fig. 15biii).

Only short branches of the *cephalic sensory canal system* occur in the preoperculum, dentary, frontal, 1st infraorbital and nasal bones, and are presumably inter-connected by dermal branches.

Jaws

The single *upper jaw* element has been described by Yazdani (1976*a* & *b*; 1978). This element appears from its shape to incorporate the premaxilla with the maxilla, and may well have formed during ontogeny by the fusion of these bones (see discussion on p. 37, Fig. 16b). A short flange on the anteromedial face of the upper jaw bone articulates with the faceted anterior end of the vomer. The ventral surface is alveolate and bears an outer row of long caniniform teeth, and 1 to 2 inner rows of small teeth, decreasing in size posteriorly.

Each *dentary* is joined to its partner in a symphysis lying in the vertical below the upper jaw symphysis. A short symphysial process descends from the anteroventral edge of the dentary. The coronoid region is developed into a relatively tall, shallow process and is covered laterally by the posteroventral limb of the upper jaw. The alveolar surface along the dorsal edge (anterior to the coronoid process), bears an outer row of large caniniform teeth, relative to the size of the jaw, and 2 to 3 inner rows of smaller teeth. The posteroventral arm extends as a long pointed process along the ventral edge of the anguloarticular. A short sensory canal lies within the dentary which is pierced by three pores.

The *anguloarticular* is a long tapered bone (Fig. 16b), and has a straight dorsal edge apart from a low projection anterior to the deep facet on the posterodorsal corner. Meckel's cartilage is long, rod-like, and passes along the medial face into the dentary.

The *retroarticular* is small and roughly L-shaped with a very short lower arm (Fig. 16b). Except for its dorsal connection the retroarticular is free from the posteromedial face of the anguloarticular. The interopercular ligament is connected to the free posteroventral edge.

The small *coronomeckelian* is similar to that in *Chaudhuria* (Fig. 16).

Hyopalatine arch

The *hyomandibular* shaft is short; a wide flange situated on its anterolateral face is connected anteriorly to the metapterygoid, and ventrally to the dorsal edge of the symplectic in an arrangement that corresponds closely to that seen in *Chaudhuria* (Fig. 17a & b).

The long *symplectic* has a narrow lateral face and no dorsal lamina. Its anterior end lies below the posteromedial face of the quadrate.

The *metapterygoid* has a small anterodorsal projection which, together with the bone's anterior edge, is separated from the quadrate by a cartilaginous interface.

The *quadrate* has a straight anterior edge which ventrally forms a stout condyle for articulation with the anguloarticular facet.

The *endopterygoid* is absent.

The long *ectopterygoid* has a narrow lateral face and only its posterolateral margin lies medial to the anterodorsal corner of the quadrate (Fig. 17b). The anterior end is curved anteromedially and its medial face is loosely joined by connective tissue to the vomerine shaft. This connection is the anterior point of articulation between the suspensorium and neurocranium.

The *palatine* is absent. It may be incorporated into the anterior arm of the ectopterygoid,

possibly by fusion, during ontogeny. The lack of direct articulation between the ectopterygoid and lateral ethmoid, and the absence of a palatine, were not recognised by Yazdani (1976*b*:168) who described: narrow palatines '... movably united to parasphenoid and vomer' and the '... pterygoid (ectopterygoid) movably united to lateral ethmoid outside the palatine'.

Opercular series

The *preoperculum* lacks distinct vertical and horizontal arms (Fig. 18b), and is thus crescentic in shape. The lateral face of the preoperculum is wide and accommodates a short, indistinct sensory canal (as discussed above).

The *interoperculum, suboperculum* and *operculum* are generally poorly ossified (Fig. 17b) and are arranged as in *Chaudhuria* (p. 38).

Hyoid and branchial arches

The *basihyal* is straight with a low ventral ridge. Posteriorly it overlies the anterior tip of basibranchial I (Fig. 20bi).

The paired *dorsal* and *ventral hypohyal* bones, the *anterior* and *posterior ceratohyals* and the *interhyal*, closely correspond with the same elements in *Chaudhuria* (see above, p. 39 and Fig. 19 a & b).

The *urohyal* is forked anteriorly, posterior to this point a low ridge ascends from the dorsal surface ventral to basibranchial 2. The posterodorsal corner of the ridge is connected by a diverging ligament to the anterior tips of each hypobranchial 3.

Basibranchial 1 lacks a ventral keel.

Basibranchial 2 is narrow-waisted and lacks ventral processes.

Basibranchial 3 is particularly long and tapered posteriorly; its cartilaginous tip lies ventral to basibranchial 4 (Fig. 20bi). This rod-like region is capable of sliding below basibranchial 4 when the branchial arches contract.

Basibranchial 4 is a rhomboidal cartilaginous element (Fig. 20bi). Its anterolateral wall is connected to the medial edge of hypobranchial 3, and its posterolateral wall to the medial end of ceratobranchial 4.

Hypobranchial 1 and 2 are cylindrical apart from a slight prominence along the anterior margin.

Hypobranchial 3 is a small bone with a distinct, long and tapered anterior process which terminates below hypobranchial 2 (Fig. 20bi). The tip of this process is connected ligamentously to the posterior edge of the low ridge on the urohyal. The hypobranchial 3 toothplate is absent.

Ceratobranchials 1–5 are rod-like elements and with the exception of the 5th are essentially alike. The dorsal surface of ceratobranchial 5 supports a narrow, fused toothplate bearing relatively large caniniform teeth. Posterior to its toothplate, ceratobranchial 5 curves dorsally into a relatively long process for muscle attachment (Fig. 20bi).

All the dorsal gill arch elements lie posterior to the neurocranium and are essentially similar to those found in *Chaudhuria* (Fig. 20aii).

Pectoral girdle

The pectoral girdle lacks a bony connection to the neurocranium and lies posterior to the skull, adjacent to the 3rd and 4th abdominal vertebrae. Posttemporal sensory canal tubules are absent.

The *supracleithrum* is small (Fig. 21bi) and accommodates a section of the postcranial sensory canal in its dorsolateral face.

The *cleithrum* is a stout bone relative to the size of the other pectoral elements, is bowed and meets its partner in a ventral symphysis. The dorsal end is pointed and its posterior edge deeply grooved (Fig. 21bi).

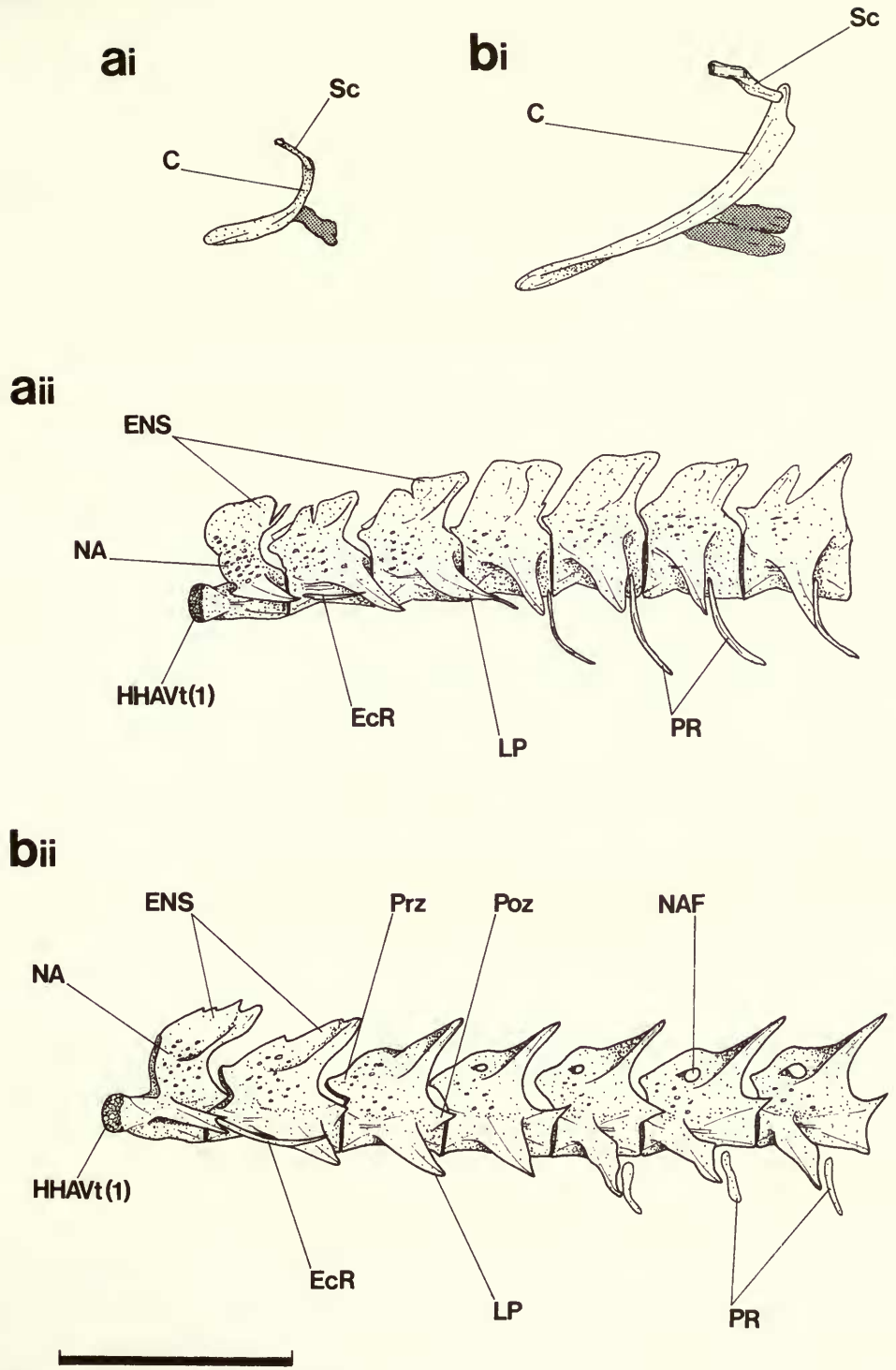

Fig. 21 Postcranial skeleton in (a) *Chaudhuria caudata* and (b) *Pillaia indica*; lateral view (left side) of pectoral girdle (ai & bi) and anterior abdominal vertebrae (aii & bii).

The remaining pectoral elements are small, ill-defined and cartilaginous. The fin rays do not appear to have differentiated in the specimens I examined, but Yazdani (1978) records 6 rays in the pectoral fin.

Vertebral column

The total vertebral count is 66, *viz.*, 28 abdominal, 37 caudal and the fused ural and first preural centra.

The first two *abdominal vertebrae* have compressed neural spines; that on the 1st has a serrated dorsal peak. The neural arches of these vertebrae have a perforated dorsolateral surface; anteroventral to the neural spine, a large foramen pierces the lateral face of the neural arch on all but the first 3 abdominal vertebrae. The anterior end of the 1st abdominal centrum is rounded to form a hemispherical condyle that articulates with the tripartite occipital socket in a 'ball and socket' joint.

Pre- and postzygapophyses are well developed on all but the 1st abdominal vertebra which also lacks a well developed parapophysis. Laterally directed parapophyses occur on the 2nd, 3rd and 4th vertebrae but on the 5th they are curved ventrally, becoming increasingly so on all succeeding abdominal vertebrae.

Along the abdominal vertebrae there is a total of 1 pair of epicentral and 24 pairs of pleural ribs.

The pair of *epicentral ribs* occurs on the 1st vertebra (Fig. 21bii). This vertebra lacks lateral parapophyses and the anterior end of each rib is lodged in a recess within the posterolateral margin of the centrum, ventral to the postzygapophysis. The rib extends posteriorly to a point beyond the 2nd vertebra and its tip is connected by a short ligament to the dorsomedial face of the cleithrum.

Pleural ribs are present on the 5th and all succeeding abdominal vertebrae. They are supported in a groove along the posterior face of the lateral parapophyses (Fig. 21bii).

The *caudal vertebrae* have short, narrow neural and haemal spines and on some of the posterior vertebrae the spines have forked tips. A deep notch in the dorsolateral margin of the neural arches (Fig. 22, anterolateral to the neural spines) appears to have developed by the expansion of a foramen seen in the neural arches from the more posterior abdominal vertebrae.

The asymmetry of the abdominal and caudal centra is gradually lost posteriorly.

Dorsal and anal fins

Dorsal and *anal spinous rays* and their supporting pterygiophores are absent.

The *dorsal* and *anal branched fin rays* are composed of 35 and 36 segmented elements respectively. They extend, from a point above and below the abdominal/caudal vertebral junction, to the dorsal and ventral edge of the caudal fin, with which they are confluent. Each ray is supported by a pterygiophore system composed of 3 elements (Fig. 22).

The *proximal pterygiophore* is a long, well-ossified element. Its distal end is fused to a medial pterygiophore. The rod-like *medial pterygiophore* is cartilaginous and lies anterior to the small, independent and ossified *distal pterygiophore.*

Caudal fin

The caudal fin is composed of 10 segmented fin rays which, although confluent with the posterior rays of the dorsal and anal fins, extend posteriorly well beyond their tips.

Two *hypural* bones fan out from the fused ural and first preural centrum (Fig. 23b), these probably represent the fused 1st+2nd & 3rd+4th+5th+6th hypurals found in more primitive teleosts. The elements each support 5 fin rays along their cartilaginous posterior margin. A small *parhypural* is sutured along the ventral edge of the hypaxial hypural. The epaxial hypural, the ural and first preural centra are fused into a single element (Fig. 23b).

The *uroneural* is fused along the dorsal edge of the fused ural and first preural centra. There is only a single short *epural* which has a barbed, leading edge.

The 2nd preural vertebra has fused neural and haemal arches. The corresponding spines are short and do not support fin rays. The tip of the haemal spine is forked as it is on the 3rd, 4th and 6th preural vertebrae. The neural spines are forked on the 5th and 6th preural vertebrae.

Squamation

The body is entirely *scaleless.*

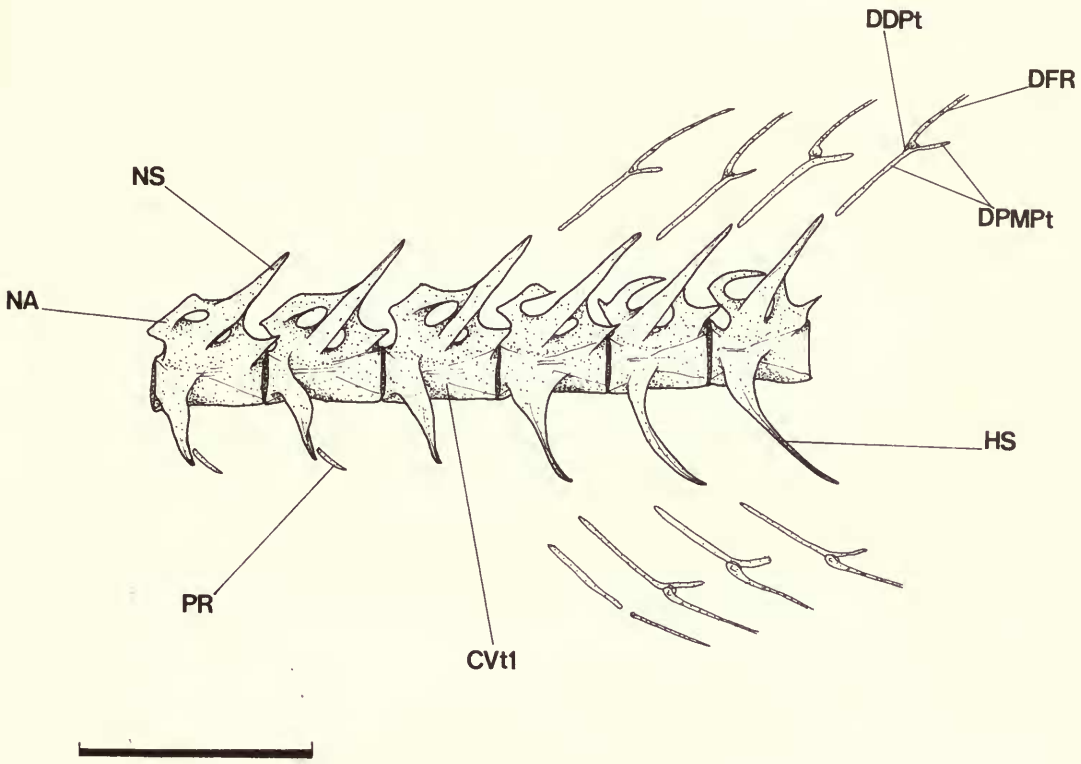

Fig. 22 *Pillaia indica,* abdominal/caudal vertebral junction and associated dorsal and anal fin rays: lateral aspect, left side.

Comparative osteology of the Mastacembeloidei

The osteological descriptions of *Mastacembelus mastacembelus, Chaudhuria caudata* and *Pillaia indica* are used here as the basis for a comparative osteological study of all available mastacembeloid species (see list of study material, Table 3). Each major osteological functional unit within a species is compared with its condition in *M. mastacembelus* in order to identify interspecific differences and similarities. Whether these character states are apomorphic or plesiomorphic for the group as a whole, or for any sublineage, and thus their value as indicators of phylogenetic relationships is considered in the sequal to this study (Travers, 1984).

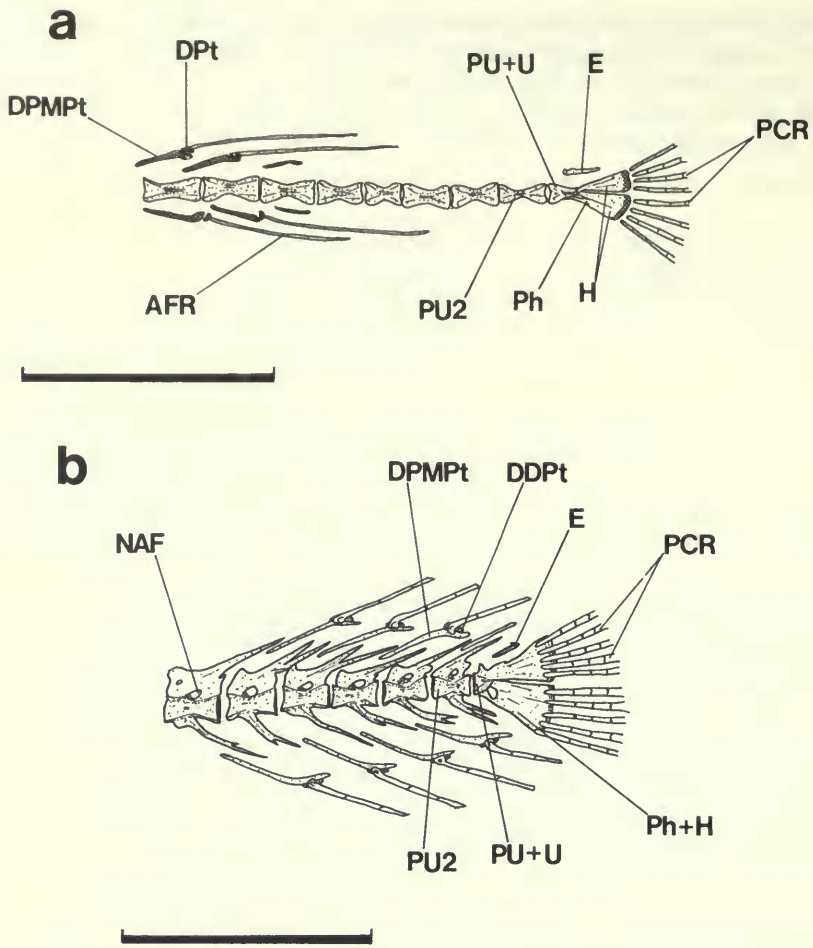

Fig. 23 Posterior caudal vertebrae, associated fin rays and caudal fin skeleton in (a) *Chaudhuria caudata* and (b) *Pillaia indica*; lateral view, left side.

Neurocranium

Ethmovomerine region

The condition of the ethmovomerine region in *Mastacembelus mastacembelus* (Fig. 1a) is typical of that found in most mastacembeloids.

The posterolateral face of the *supraethmoid* septum is pierced by a fenestra in *M. longicauda* and *M. reticulatus* from West Africa (Fig. 33). A similar fenestra is also found in *M. sclateri* (Fig. 33d), although in this species it notches the posterodorsal edge of the supraethmoid. The fenestra is generally covered by a membrane and serves as the site of origin for the oblique eye muscles.

Vomerine teeth were recorded by Regan (1912) although they are absent in all specimens I examined; Regan may well have misidentified the small toothplate that sometimes occurs on the anteroventral surface of the palatine.

The near tubular *lateral ethmoid* is characteristic of both Asian, including the Middle Eastern, and African species. The centre of the lateral ethmoid in *Mastacembelus marchii* is subdivided by a median partition into two distinct tube-like canals.

The ventral edge of the posterior opening in the lateral ethmoid in *M. maculatus* (Fig. 26a) is curved posteroventrally as it is in the West African species *M. goro, M. greshoffi,*

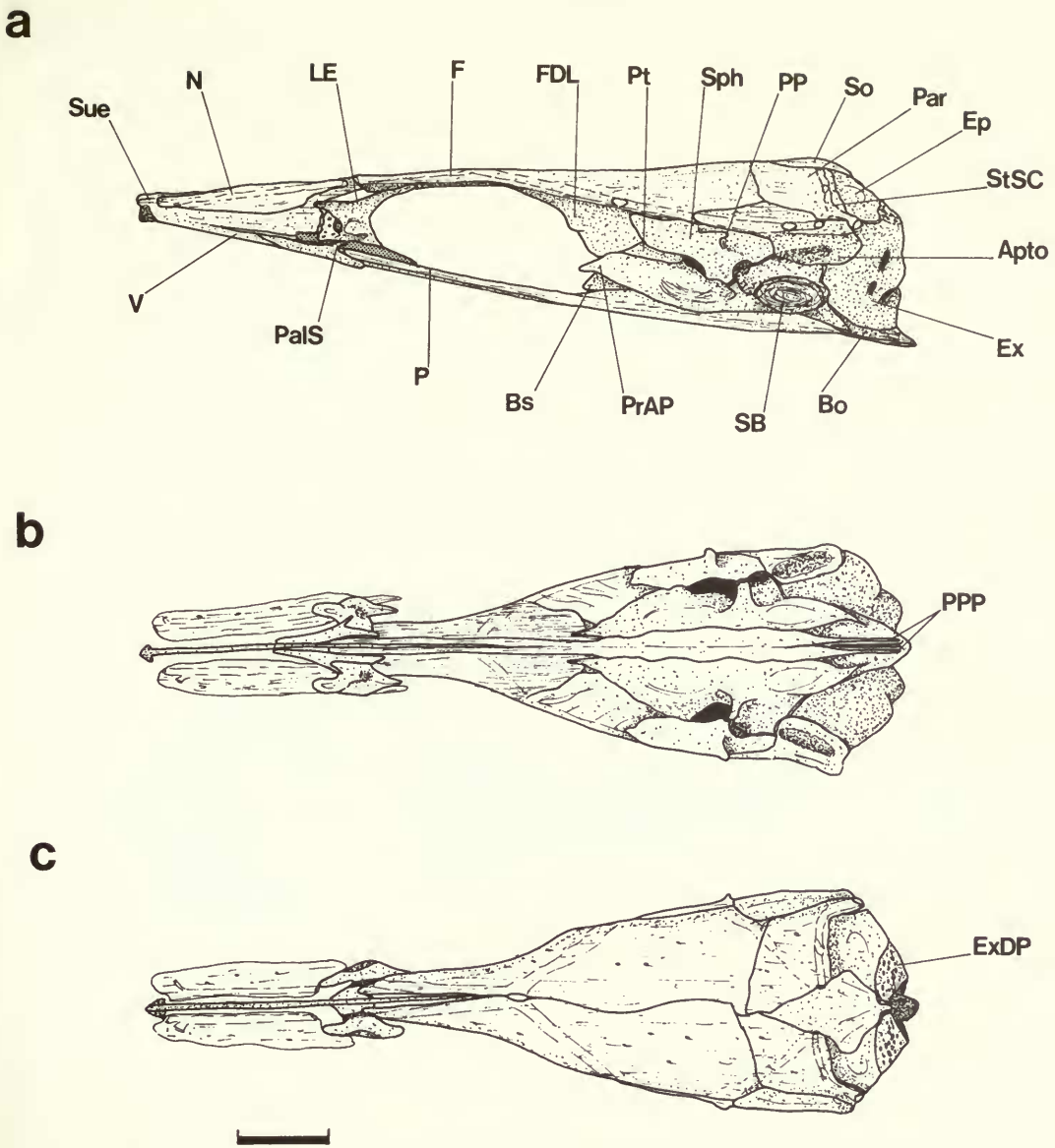

Fig. 24 *Mastacembelus sinensis,* neurocranium in (a) lateral view, left side, (b) ventral view and (c) dorsal view.

M. longicauda, M. loennbergii and *M. niger.* This ventral projection lies along the dorsal edge of the cartilaginous posterior end of the supraethmoid. The dorsal surface is grooved longitudinally to accommodate the anterior end of the large *nervus olfactorius* (p. 13) and the tip may contact the pterosphenoid (e.g. *M. maculatus* Fig. 26a).

Orbital region

In a number of taxa the morphology of the orbital region departs considerably from that of *M. mastacembelus.*

The *pterosphenoid,* which generally forms a part of the anterolateral wall to the cranial cavity, is absent in *Chaudhuria* (Fig. 15ai) and *Pillaia* (Fig. 15bi). It is small in

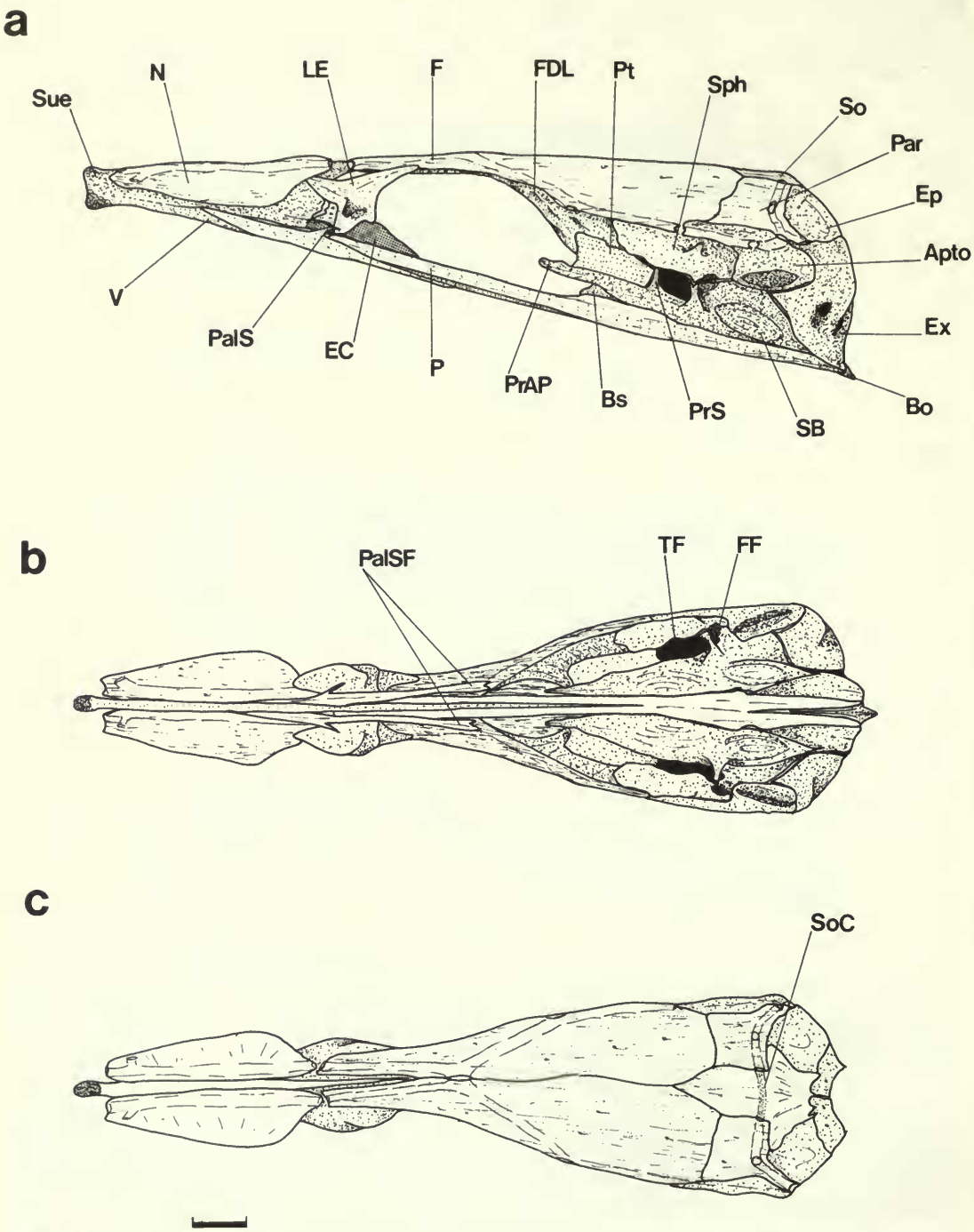

Fig. 25 *Mastacembelus erythrotaenia,* neurocranium in (a) lateral view, left side, (b) ventral view and (c) dorsal view.

Mastacembelus aviceps (Fig. 40 a & b), a microphthalmic species from the lower Zairean rapids (Roberts & Stewart, 1976), and is discernible only as a splint-like bone sutured to the ventrolateral edge of the frontal.

The posterior and anterior connections of the pterosphenoid may also differ from those in *M. mastacembelus* (p. 14). Posteriorly, it does not contribute to the rim of the trigeminal foramen in a number of species both among the Asian (e.g. *M. erythrotaenia,* Fig. 25a) and African (e.g. *M. frenatus,* Fig. 31a) taxa; in these the anterior rim of the trigeminal foramen is formed by the prootic and sphenotic.

The anterior edge of the pterosphenoid is partly restricted from bordering the postorbital edge of the neurocranium in four African species; *M. micropectus* (from Lake Tanganyika), *M. stappersii* (from Zaire), *M. goro* and *M. batesii* (from Cameroon). In these species the descending frontal lamina is particularly large and curves ventromedially, contacting its partner in the midline. The optic foramen in these species is predominantly enclosed by the frontals.

A *basisphenoid* is present in almost all mastacembeloids, (*pace* Regan, 1912; Bhargava, 1963*a*; and Maheshwari, 1965*a*), although it may be obscured in lateral view by the prootic, pterosphenoid and parasphenoid (Taverne, 1980). A large basisphenoid (relative to that in *M. mastacembelus*) occurs in *Macrognathus* species (*M. siamensis, M. aral,* and *M. aculeatus*), and to a lesser extent in *Mastacembelus zebrinus* among the Asian species and *M. shiranus, M. congicus, M. liberiensis, M. longicauda* and *M. loennbergii* among the African species. In these fishes the dorsal tip of the basisphenoid bridges the ventromedial edge of each pterosphenoid, which is incompletely sutured in the midline. A relatively large basisphenoid is associated with a greater distance between the pterosphenoid and parasphenoid bones, and consequently with a less depressed orbital region than that in *M. mastacembelus* (Fig. 1a) or in other species with a small basisphenoid.

The posterior edge of the large basisphenoid in *M. shiranus, M. congicus, M. liberiensis, M. longicauda* and *M. loennbergii* contributes, with the pterosphenoid, parasphenoid and anterior process of the prootic, to the formation of a large lateral foramen in the anteroventral wall of the neurocranium (Figs. 32a & 33a). This forms an unusually wide opening to the posterior myodome which in other species is generally a small foramen obscured, in lateral view, by the prootic. In *Macrognathus aculeatus* (Fig. 30a) and *Mastacembelus zebrinus* (Fig. 27a) the basisphenoid is particularly large and consequently there is a characteristically wide opening to the posterior myodome.

The basisphenoid is absent only in *Chaudhuria* and *Pillaia* among the Asian, and *Mastacembelus brichardi, M. crassus* and *M. aviceps* among the African taxa (Figs. 39a & 40a: possibly *M. latens* should be included here as well).

The general arrangement of the *parasphenoid* described in *Mastacembelus mastacembelus* (p. 14) is found in the majority of mastacembeloid taxa. However, there is interspecific variation in the posterior region of this bone. In *Chaudhuria* and *Pillaia,* and to a lesser extent in *Mastacembelus sinensis* (Fig. 24b), the posterior parasphenoid processes are particularly long and narrow. They are distinguished in *Chaudhuria* and *Pillaia* at a point below the medial connection between the prootics (slightly posterior to this point in *M. sinensis*), and extend posteriorly as long, pointed processes to the posterior edge of the basioccipital.

The posterior region of the parasphenoid in the *Macrognathus* species, and in *Mastacembelus pancalus* and *M. zebrinus* (Figs 27 & 28) stands in marked contrast to that in *Chaudhuria* and *Pillaia.* Except for its posterior tip, the parasphenoid is undivided, and its ventral surface is excavated into the form of a 'blind' pit from which the posterior portion of the large *adductor hyomandibulae* muscles originate. The cavity is particularly deep in *M. zebrinus* and *M. pancalus.* These species also differ in having a deep ventral ridge on the parasphenoid. This ridge lies medially along the posteroventral surface of the bone and divides the pit-like cavity; it is deepest in *M. zebrinus.*

The two ascending processes on the posterodorsal edge of the *1st infraorbital* bone (Fig. 3) are generally well-developed in all species. The posterior process articulates syndesmotically with the lateral ethmoid and may protrude posterodorsally in some species (Fig. 41a)

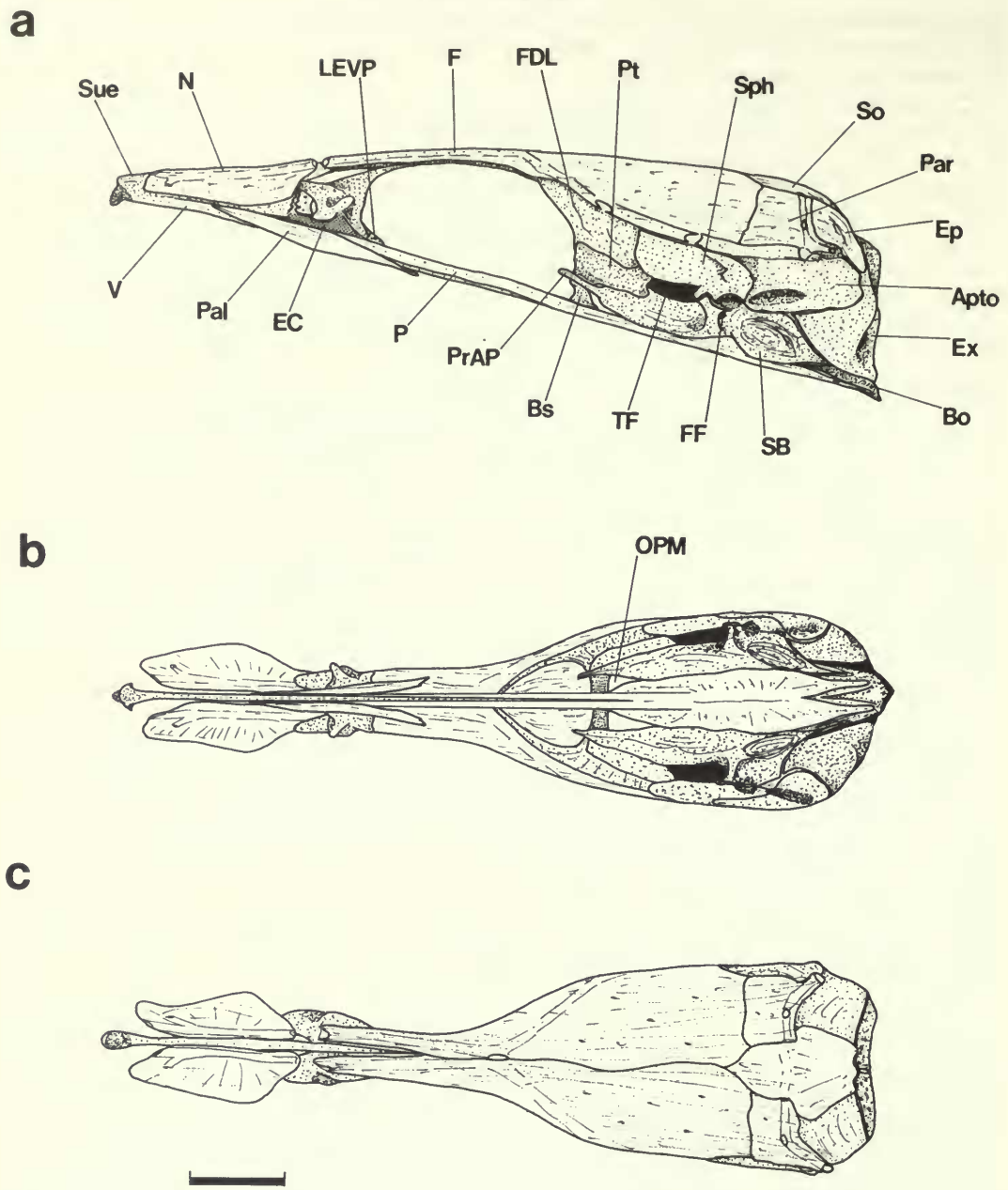

Fig. 26 *Mastacembelus maculatus* neurocranium in (a) lateral view left side, (b) ventral view and (c) dorsal view.

in association with the anterior expansion of the *adductor arcus palatini* muscle (discussed below p. 126). The shorter, anterior ascending process is absent in *Mastacembelus sinensis, Chaudhuria* and *Pillaia.* In these taxa, anterior to the posterior nasal opening the dorsal edge of the 1st infraorbital is straight and is connected by the integument to the nasal.

The posteroventral process or preorbital spine on the 1st infraorbital varies in its degree of development.

A preorbital spine (similar to that described in *M. mastacembelus* p. 16), occurs in the

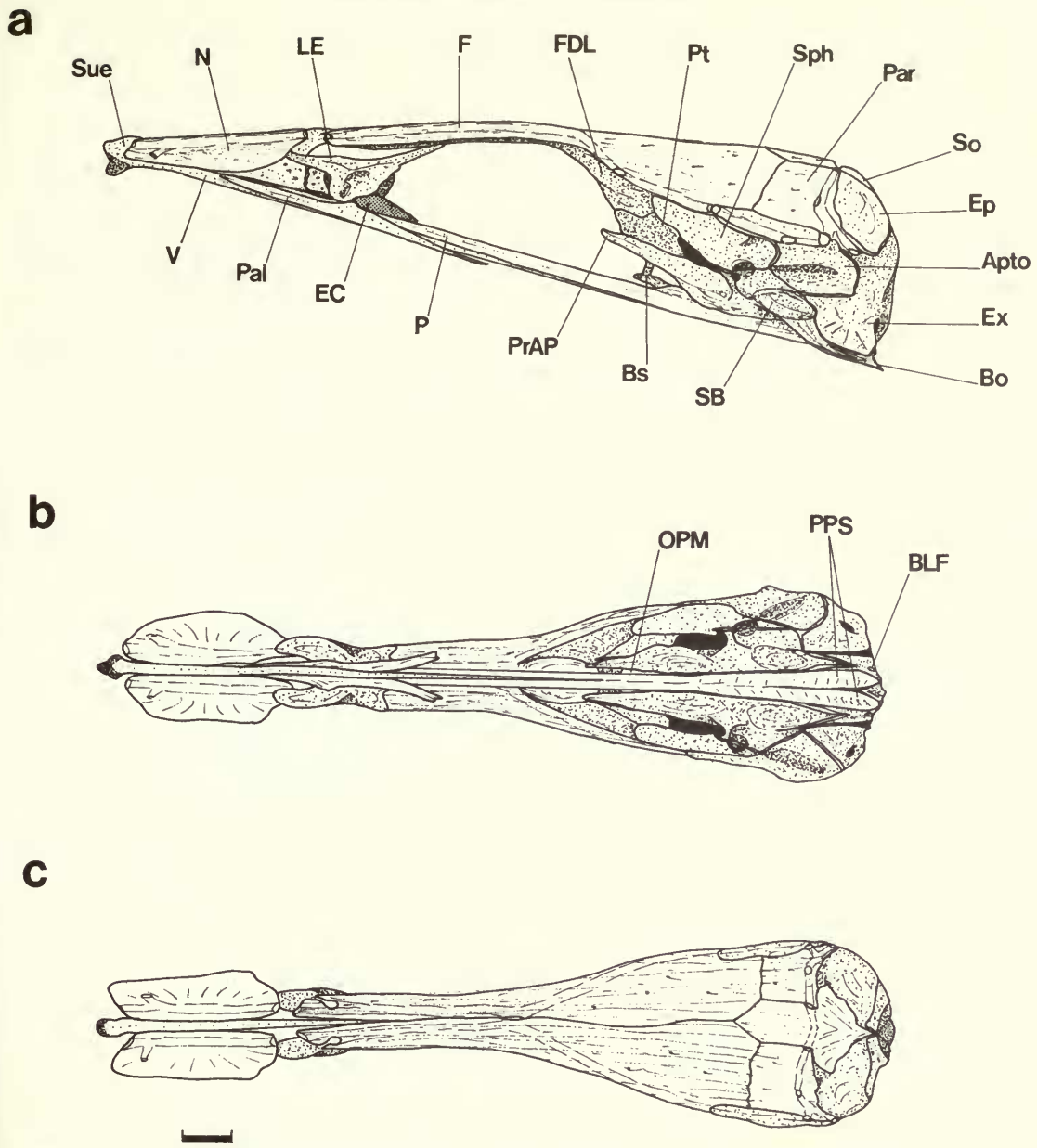

Fig. 27 *Mastacembelus zebrinus,* neurocranium in (a) lateral view, left side, (b) ventral view and (c) dorsal view.

majority of Asian species, it is absent in *Chaudhuria* (Fig. 15aiii) and *Pillaia* (Fig. 15biii) and is represented by a short posterior projection in *Macrognathus* (Fig. 41a). A spine is also well-developed in the majority of African mastacembeloids. In a number of species, however, (e.g. *Mastacembelus albomaculatus,* Fig. 41b) the spine is present only as a slight projection on the posteroventral edge of the 1st infraorbital and in others it is absent (e.g. *Mastacembelus aviceps* and *M. ophidium,* Fig. 41c & d). Intraspecific variation in the morphology of the preorbital spine in *Mastacembelus moorii* has been discussed by Matthes (1962: 73). He found a sequential development from a prominent spine in a juvenile

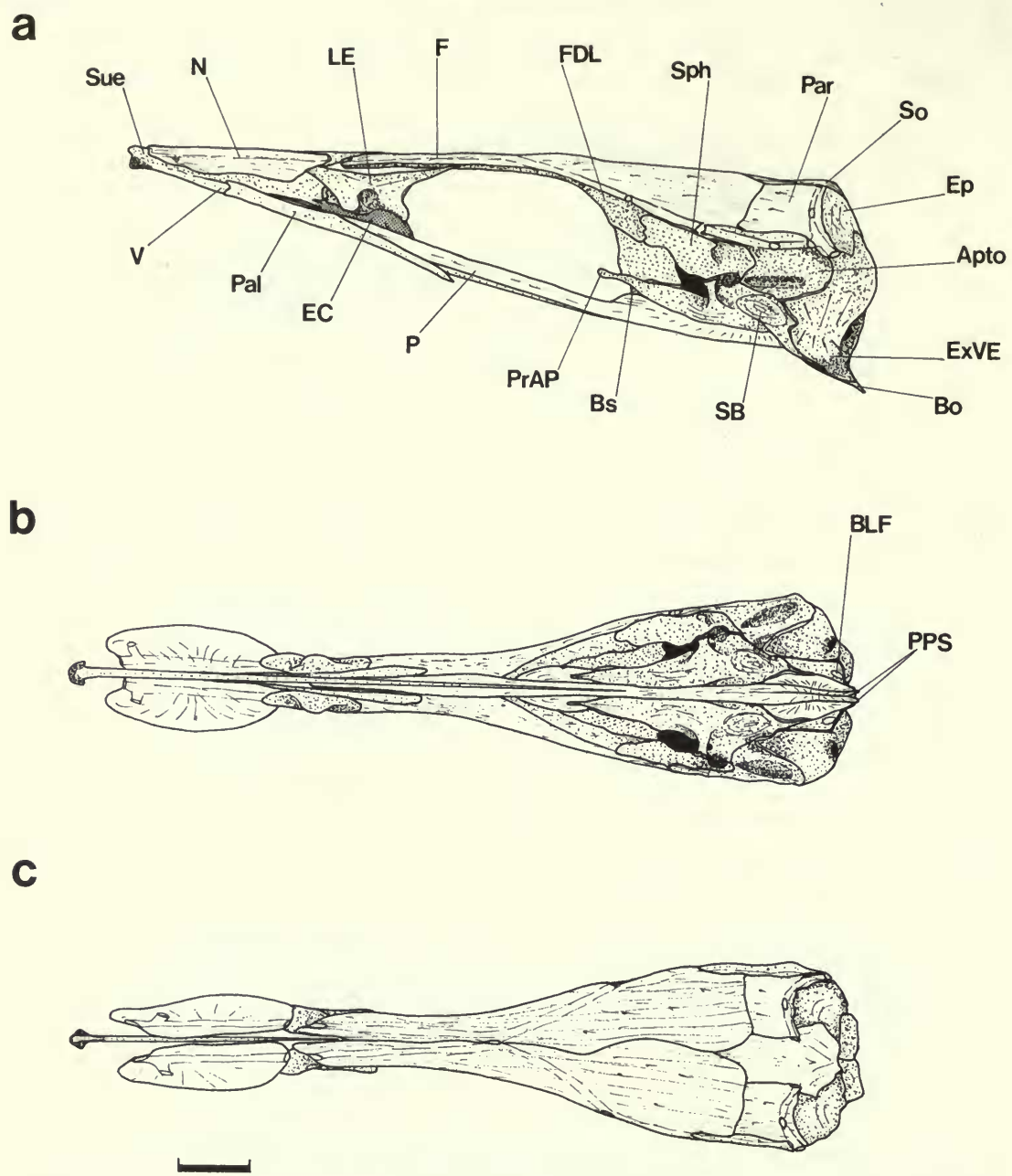

Fig. 28 *Mastacembelus pancalus,* neurocranium in (a) lateral view, left side, (b) ventral view and (c) dorsal view.

specimen (100 mm. long) to a much broader flange with only a slight projection on the posterodorsal corner in an adult specimen (410 mm. long).

If a prominent 1st infraorbital spine is absent in the adult, it was not found in pre-adult specimens of any species examined.

The remaining infraorbital bones are reduced to ossifications around the sensory canal. The extent to which the canal is ossified shows interspecific variation. In some African species

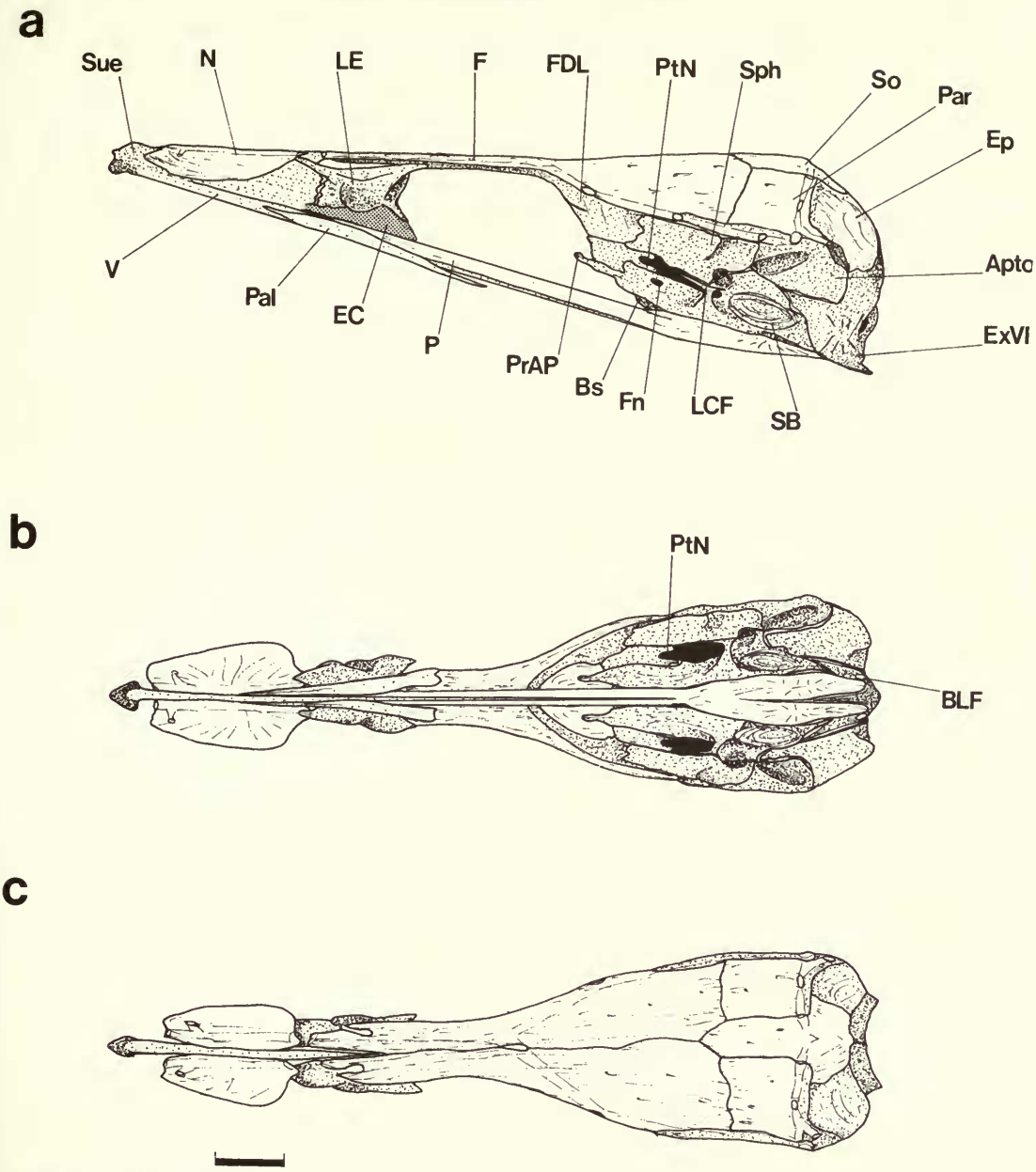

Fig. 29 *Macrognathus siamensis*, neurocranium in (a) lateral view, left side, (b) ventral view and (c) dorsal view.

(e.g. *Mastacembelus cunningtoni,* and *M. frenatus*) the canal is ossified along its entire length, and there are five infraorbital tubules, as in *M. mastacembelus* (p. 16). In contrast some taxa from Asia (e.g. *Chaudhuria* and *Pillaia*) and from Africa (*e.g. Mastacembelus brichardi*) have only the 1st element ossified. Between these extremes there is a series, incorporating the majority of mastacembeloid taxa, in which 1, 2, 3 or 4 tubules are ossified.

Otic region

The bones of the otic region show considerable interspecific variation in their morphology and will be considered individually.

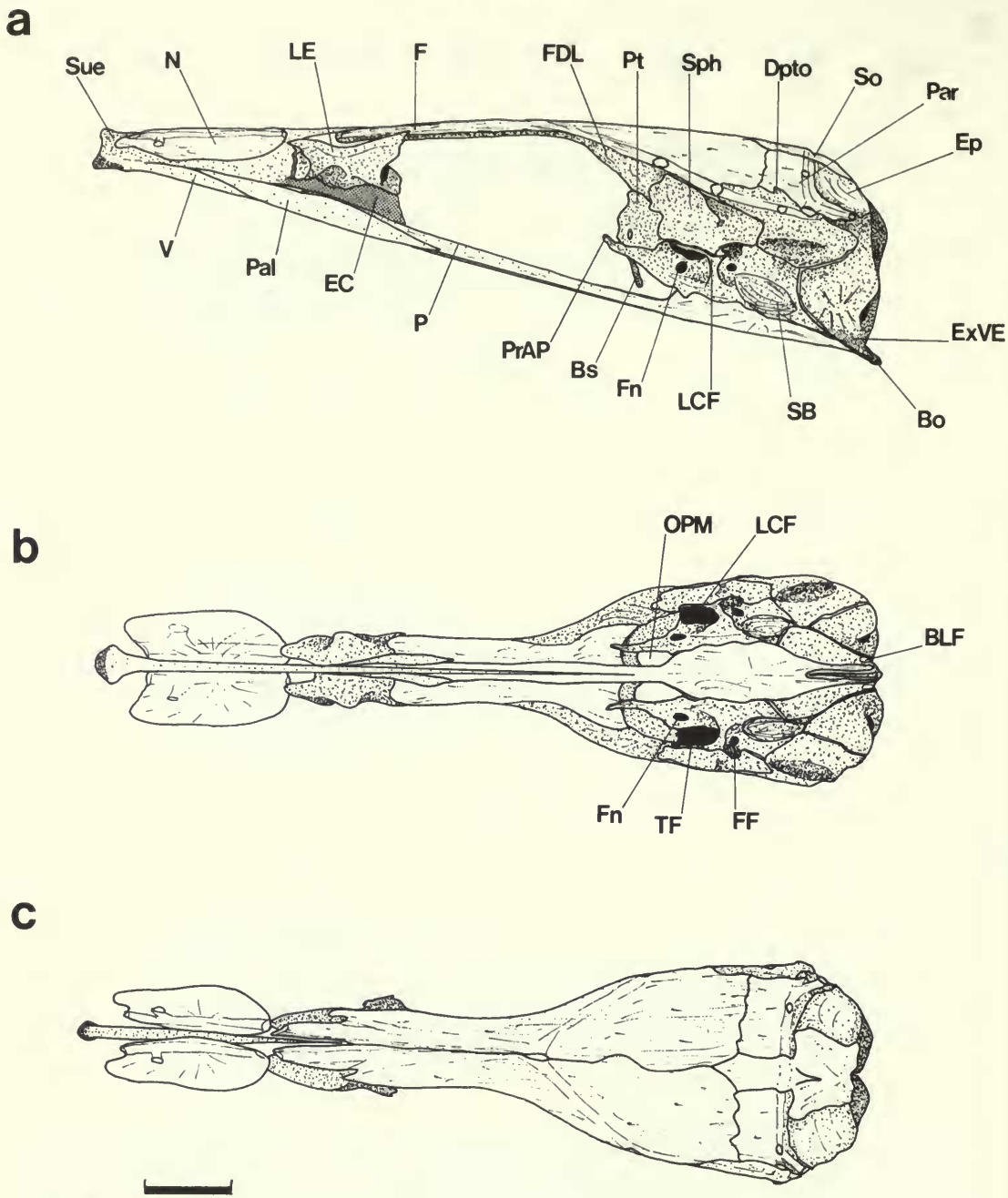

Fig. 30 *Macrognathus aculeatus,* neurocranium in (a) lateral view, left side, (b) ventral view and (c) dorsal view.

The otic region in all mastacembeloids is dominated by a particularly large *prootic* which, together with the sphenotic, pterosphenoid and descending frontal lamina forms the exceptionally long precommissural lateral wall of the neurocranium. The prootic is a long bone with a prominent anterior process in Asian and African species, although among the latter, there are 5 species which do not have the prootic developed to an extent comparable with

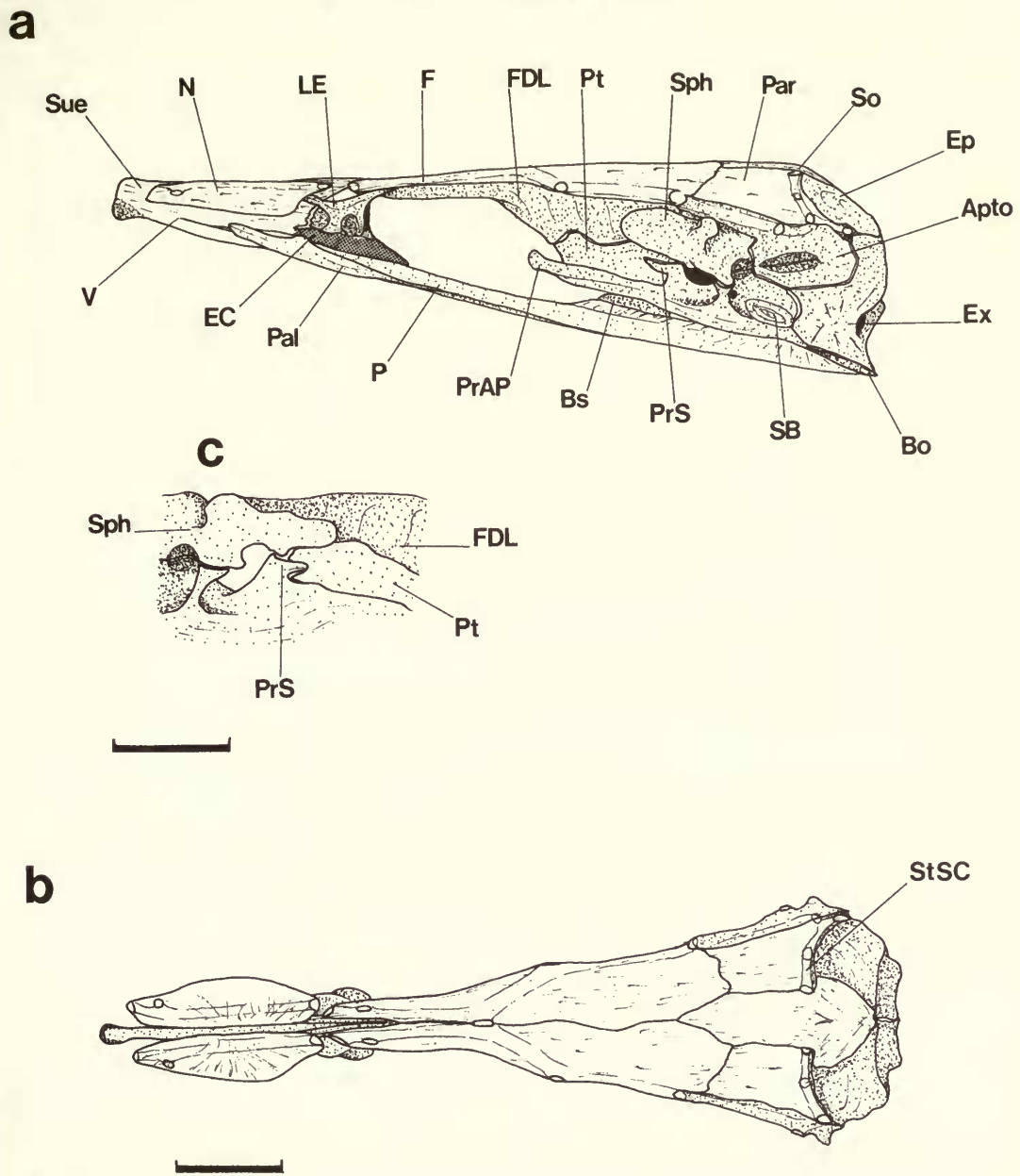

Fig. 31 *Mastacembelus frenatus,* neurocranium in (a) lateral view, left side and (b) dorsal view, and *Mastacembelus shiranus,* otic region (c) in lateral view, right side.

that of *M. mastacembelus.* In *Mastacembelus micropectus, M. brichardi* (Fig. 38a) and *M. longicauda* (Fig. 33a) the anterior prootic process extends only halfway across the lateral face of the pterosphenoid.

The condition in *Mastacembelus crassus* and *M. aviceps* (Figs 38a & 40a) is even more extremely modified. In these two crypto- and microphthalmic species the prootic anterior process is poorly developed, particularly in *Mastacembelus aviceps,* and extends only slightly anterior to the trigeminal foramen, this region of the neurocranium having a tubular shape.

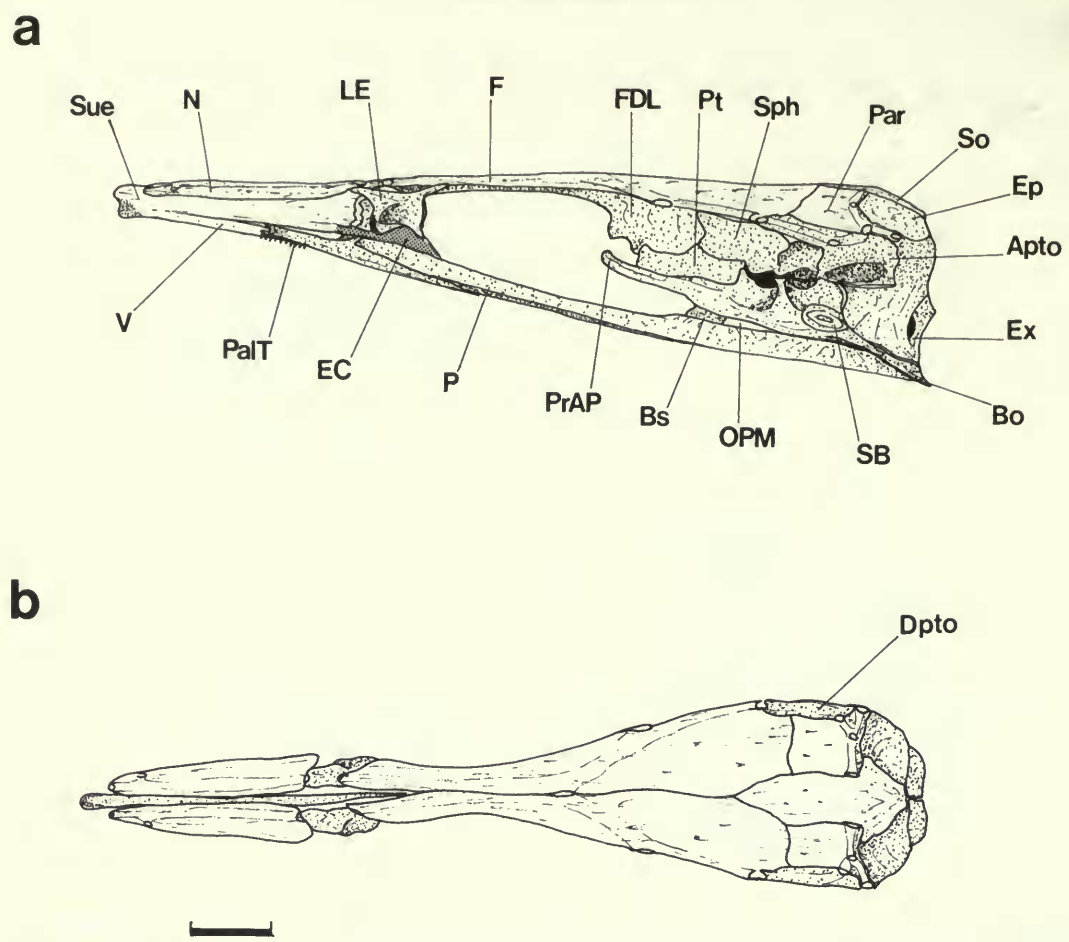

Fig. 32 *Mastacembelus congicus,* neurocranium in (a) lateral view, left side and (b) dorsal view.

Tubular neurocrania have been associated by Rosen & Greenwood (1976: 45) with eye reduction.

Among the Asian mastacembeloids, including those of the Middle East, *Pillaia* is the only taxon lacking a distinct anterior process on the prootic (Fig. 15bi). In *Pillaia,* as in *Mastacembelus aviceps,* the prootic does not extend anteriorly beyond the trigeminal foramen, and its overall tubular neurocranium can probably be correlated with its eye reduction.

In contrast to the arrangement in *M. mastacembelus* (Fig. 1a), the tip of the anterior process on the prootic in some species is curved anterodorsally and contacts a pedicel on the frontal and/or pterosphenoid. In these species the prootic bridges the nerves and blood vessels that emerge from the trigeminal foramen. A prootic bridge of this type was only found in 6 African taxa, *viz., Mastacembelus albomaculatus, M. moorii, M. plagiostomus* and *M. tanganicae,* all endemic to Lake Tanganyika, in *M. paucispinis* from the lower Zairean rapids, and in an undescribed *Mastacembelus* species recently collected by T. Roberts (pers. comm.) from the Cross River rapids in Cameroon.

The tip of the anterior process on the prootic is curved dorsally in *M. paucispinis* and *M. moorii* (Fig. 35 a & d) and contacts a wide pedicel on the lateral face of the descending frontal lamina. The *truncus supraorbitalis* and the internal jugular vein pass medial to the connection between these elements. A similar arrangement occurs in the undescribed species

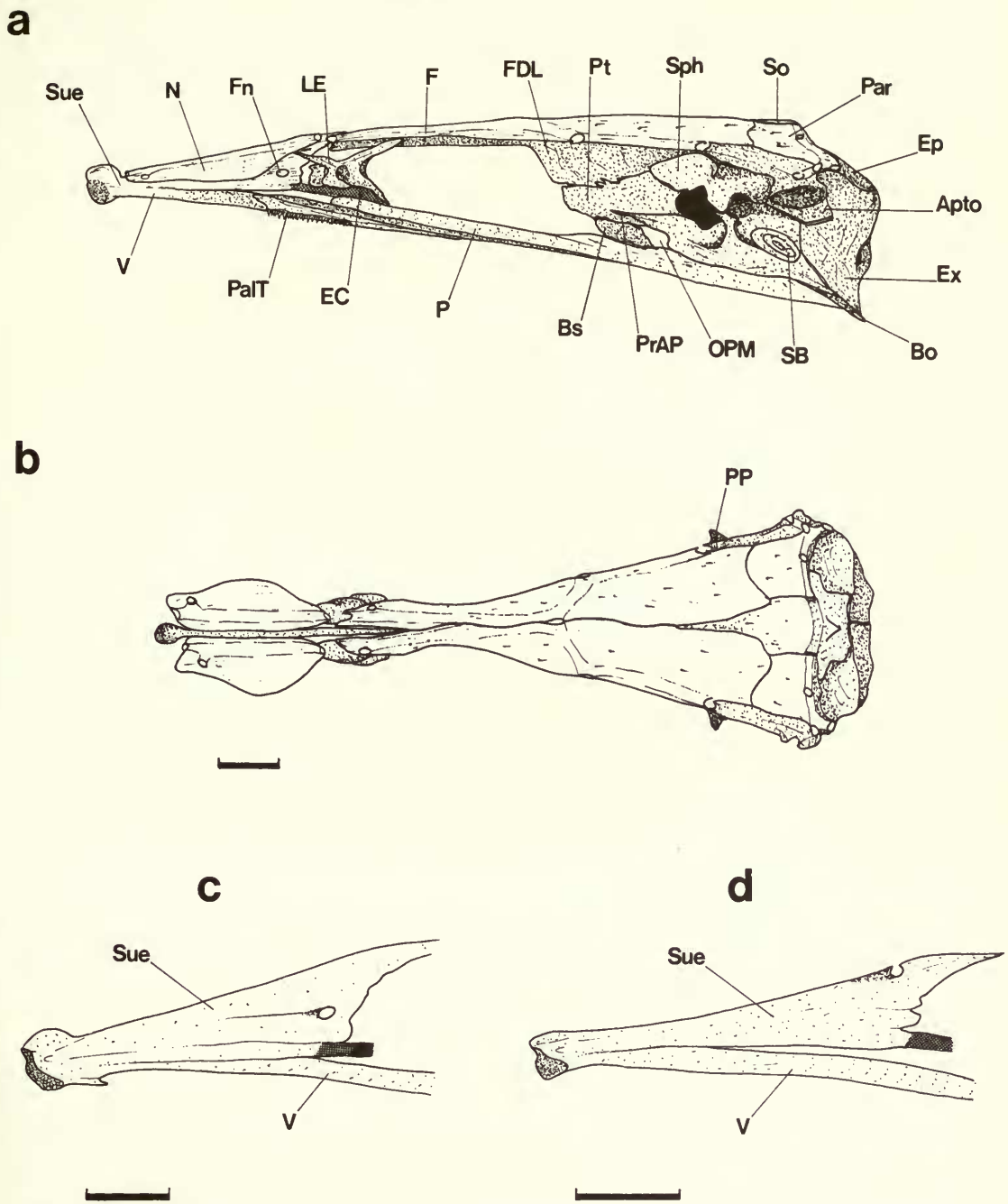

Fig. 33 *Mastacembelus longicauda,* neurocranium in (a) lateral view, left side, and (b) dorsal view, and *Mastacembelus reticulatus* (c), and *Mastacembelus sclateri* (d), ethmoid region in lateral view, left side.

(Fig. 36a). In that species the elements are not in direct contact but are joined by a short ligament. The tip of the anterior process on the prootic in *M. albomaculatus* and *M. plagiostomus* (Fig. 35c & f) forms a similar bridge across the anterolateral wall of the neurocranium by contacting a small pedicel on the pterosphenoid. In *M. tanganicae* (Fig.

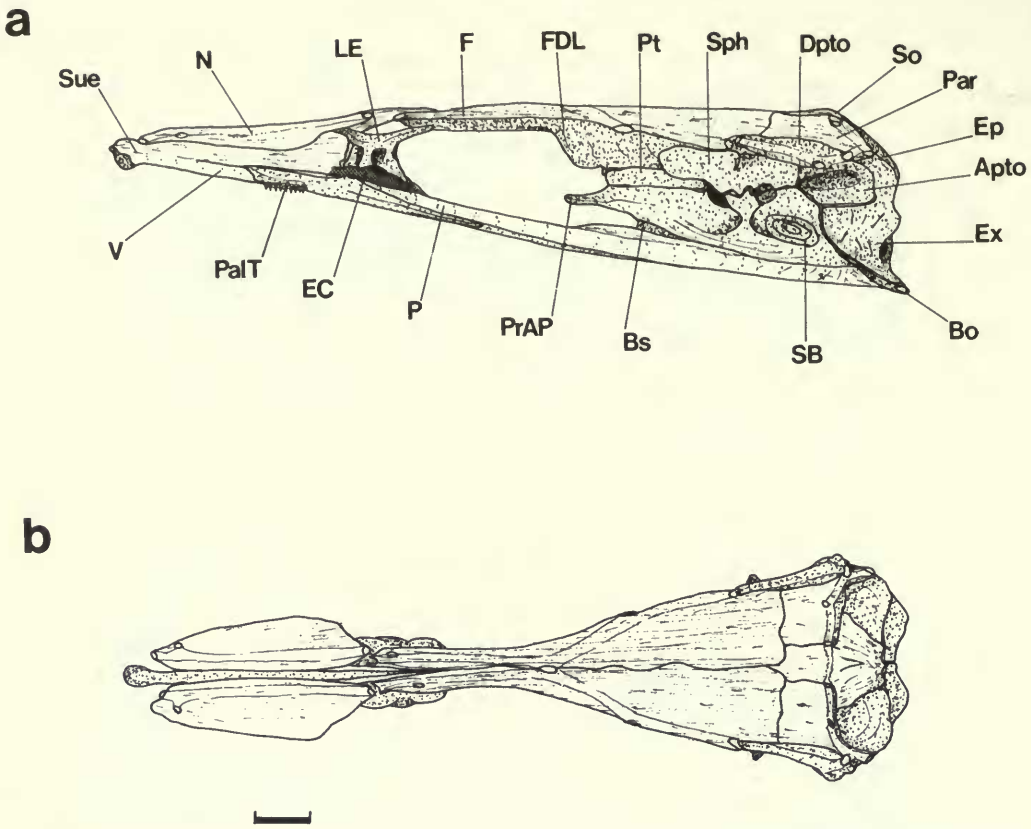

Fig. 34 *Mastacembelus nigromarginatus,* neurocranium in (a) lateral view, left side and (b) dorsal view.

35g) a bridge is present but results from the tip of the anterior process on the prootic curving posterodorsally to lie across the frontal/pterosphenoid lateral border.

Some variability found in the bridge of one specimen of *M. moorii* and one of *M. paucispinis* is not thought to represent significant intraspecific variation since the incomplete bridge on one side of the neurocranium in both these specimens appears to be the result of incomplete ossification at the tip of the anterior prootic process.

The tip of the anterior process is shaped like a hockey stick in the Zairean species *Mastacembelus ubangensis,* in *M. congicus* (Fig. 32a), and in the widely distributed *M. frenatus* (Fig. 31a). In these species the broad, slightly upturned tip of the prootic lies below a horizontal region on the ventral edge of the descending frontal lamina. A long ligament connecting the elements to form a bridge across the *truncus supraorbitalis* and the internal jugular vein, may be interpreted as an intermediate stage in the development of the bridge found, for example, in *M. paucispinis.*

A horizontal shelf-like ridge lies, longitudinally along the prootic, with its dorsal surface sloping ventrally, in 5 African species; *Mastacembelus moorii* and *M. zebratus* from Lake Tanganyika, *M. stappersii* from Zaire, *M. vanderwaali* from southern Africa (Skelton, 1976), and *M. sclateri* from Equatorial Guinea. A prootic 'shelf' is best developed in *M. sclateri* (Fig. 42a).

Here, and to a lesser extent in *M. stappersii* (Fig. 42b), it is continuous with the lower edge of a groove in the ventrolateral face of the pterosphenoid.

In *M. vanderwaali* the 'shelf' is in the form of a narrow ridge on the anterolateral face of the prootic and may represent a less derived condition than that described above. It

resembles the ridge on the anterolateral face of the prootic in *M. mastacembelus* (Fig. 1a, p. 17). *Mastacembelus moorii* has a short, horizontal 'shelf' on the midlateral face of the prootic. The lateral edge of this 'shelf' is inclined dorsally, giving it an up-turned edge affording greater support for the *truncus supraorbitalis* nerve and the internal jugular vein which pass longitudinally along its dorsal surface.

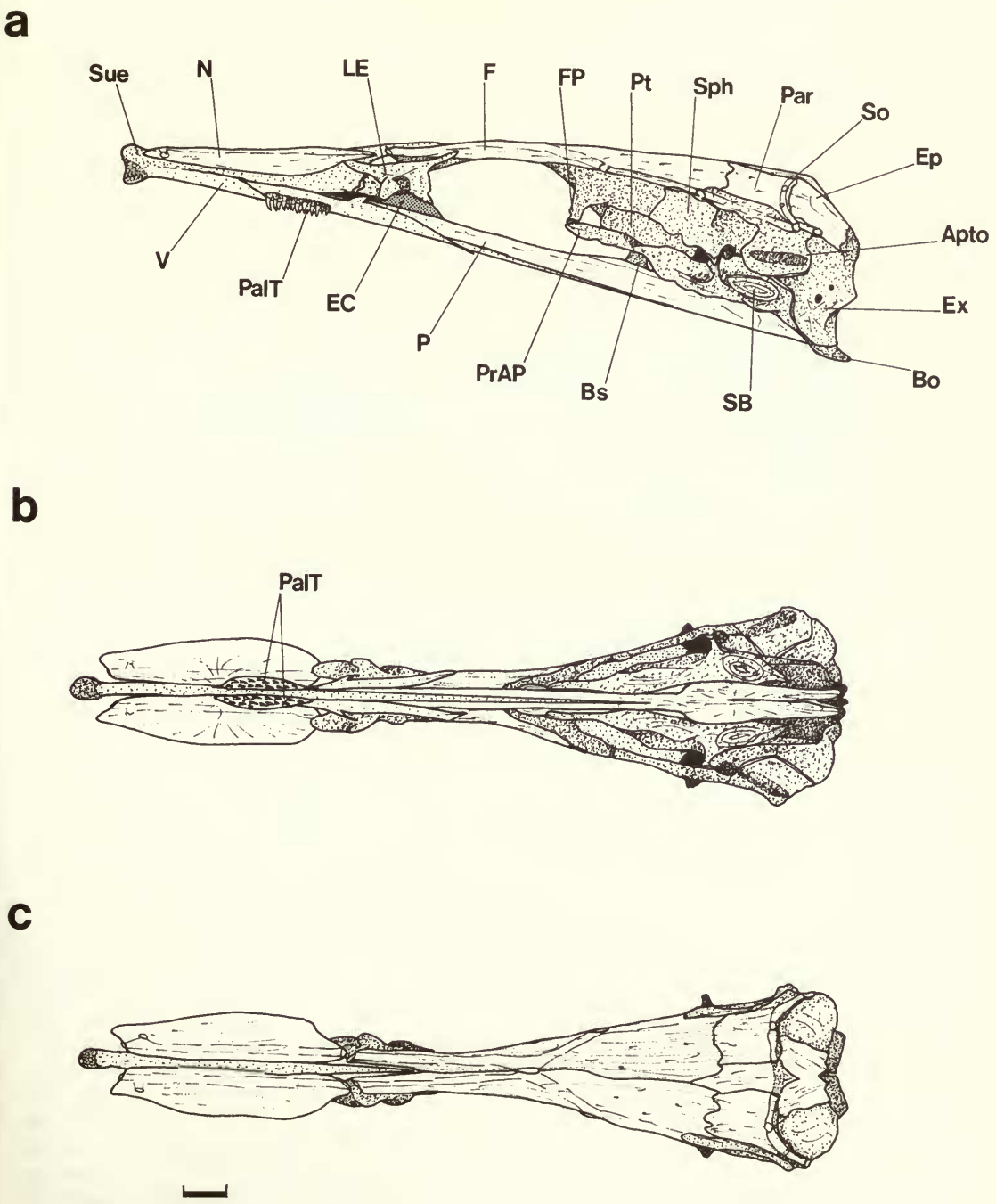

Fig. 35 a–c *Mastacembelus paucispinis* neurocranium. See p. 64 for full caption.

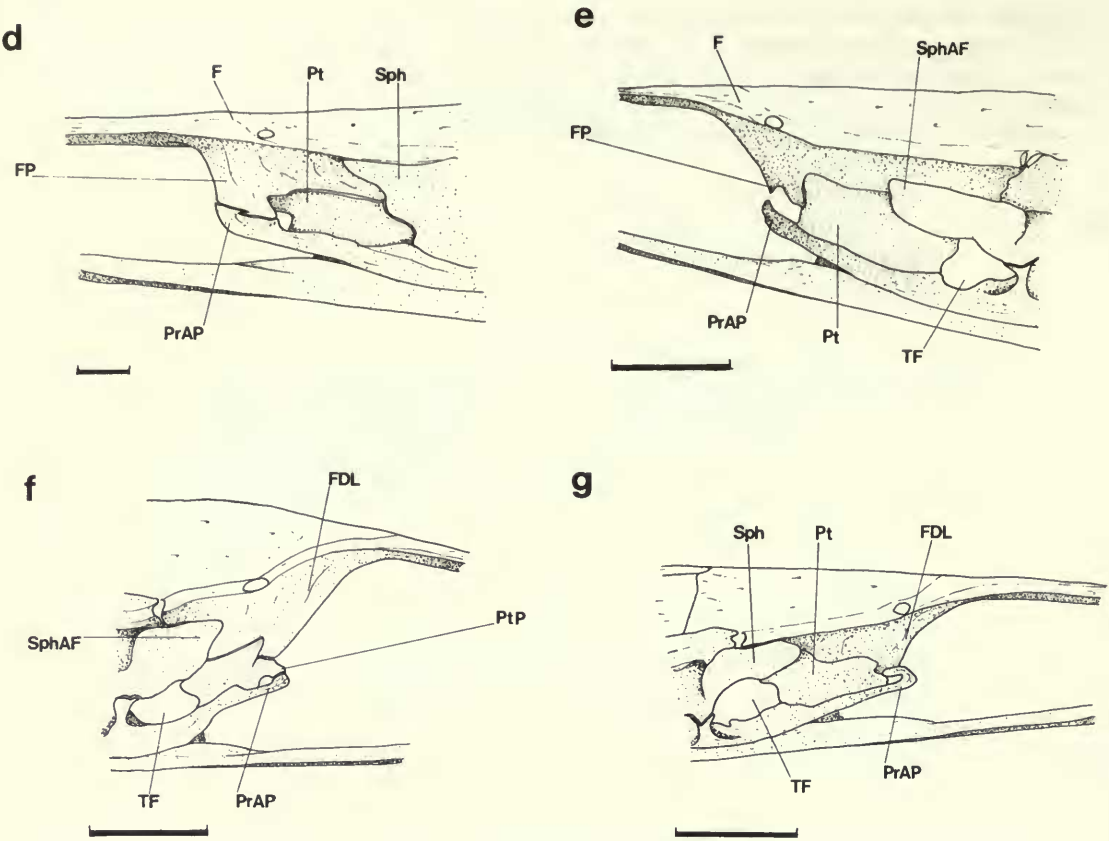

Fig. 35 *Mastacembelus paucispinis,* neurocranium in (a) lateral view, left side, (b) ventral view and (c) dorsal view. Also shown in lateral view is the pre-otic region in (d) *Mastacembelus moorii* and (e) *Mastacembelus albomaculatus* (left side), and (f) *Mastacembelus plagiostomus* and (g) *Mastacembelus tanganicae* (right side). See p. 63 for a–c.

A fenestra between the anterior process and the trigeminofacialis chamber pierces the lateral face of the prootic in the *Macrognathus* species (Figs 29a & 30a) and appears to be covered by a thin membrane.

The trigeminal foramen shows little interspecific variation in either its overall size or its position in the lateral wall of the neurocranium. However, the prootic spur which forms the anterior rim of the trigeminal foramen in *M. mastacembelus* (Fig. 1a) varies interspecifically in size and shape. When present, the tip of this spur may contact the ventral tip of a similar descending sphenotic spur in some Asian (e.g. *Mastacembelus armatus*) and African, (e.g. *Mastacembelus moorii*) mastacembeloids. In this condition, the posterior edge of the spur forms the anterior rim of the trigeminal foramen. The tips of the prootic and sphenotic spurs in other species (e.g. *Mastacembelus mastacembelus* and *M. vanderwaali*) do not always contact each other; instead, the posterior edge of the pterosphenoid is intercalated between their tips and thus contributes to the rim of the trigeminal foramen.

The ascending prootic spur in *Mastacembelus frenatus* (Fig. 31a) and in *M. shiranus* (from Lake Malawi, Fig. 31c) is particularly well-developed. In these species the tip is expanded, giving it in lateral view the shape of a cobbler's last. Apart from *M. frenatus, M. moorii* and *M. ophidium,* all Tanganyikan species lack a prootic ascending spur. This is also true of *M. brichardi, M. aviceps* and *M. brachyrhinus* from the Zairean rapids and *M. liberiensis, M. loennbergii, M. longicauda* and *M. sclateri* from Western Africa. In all African and Asian

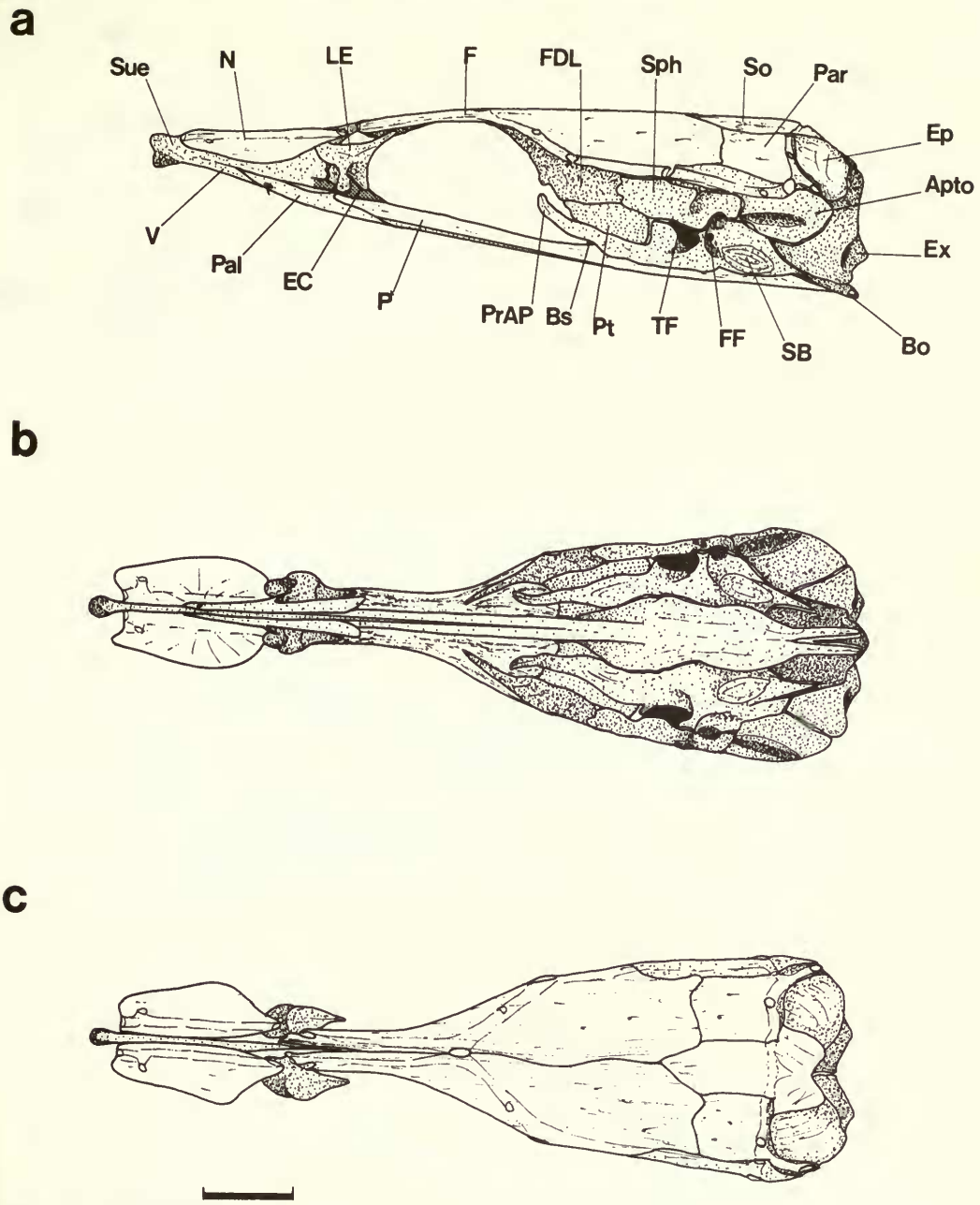

Fig. 36 Neurocranium of an undescribed *Mastacembelus* species in (a) lateral view, left side, (b) ventral view and (c) dorsal view.

species lacking a prootic ascending spur, the posterior edge of the pterosphenoid forms the anterior margin of the trigeminal foramen.

The prootic spur in *Macrognathus siamensis* (Fig. 29a) and *Macrognathus aral* is small. The posterolateral margin of the pterosphenoid is deeply notched in these species, and forms the anterior region of the trigeminal foramen.

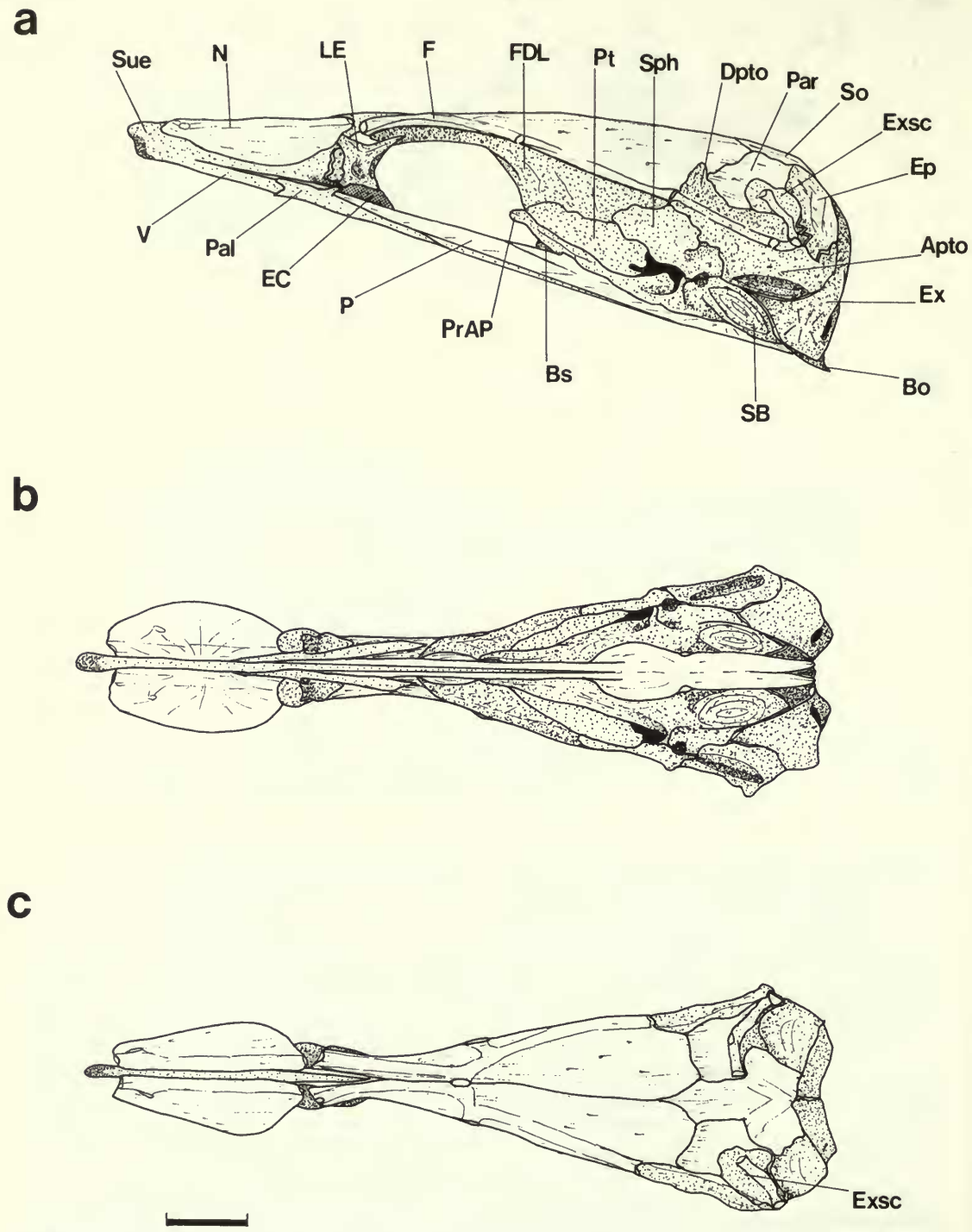

Fig. 37 *Mastacembelus brachyrhinus*, neurocranium in (a) lateral view, left side, (b) ventral view and (c) dorsal view.

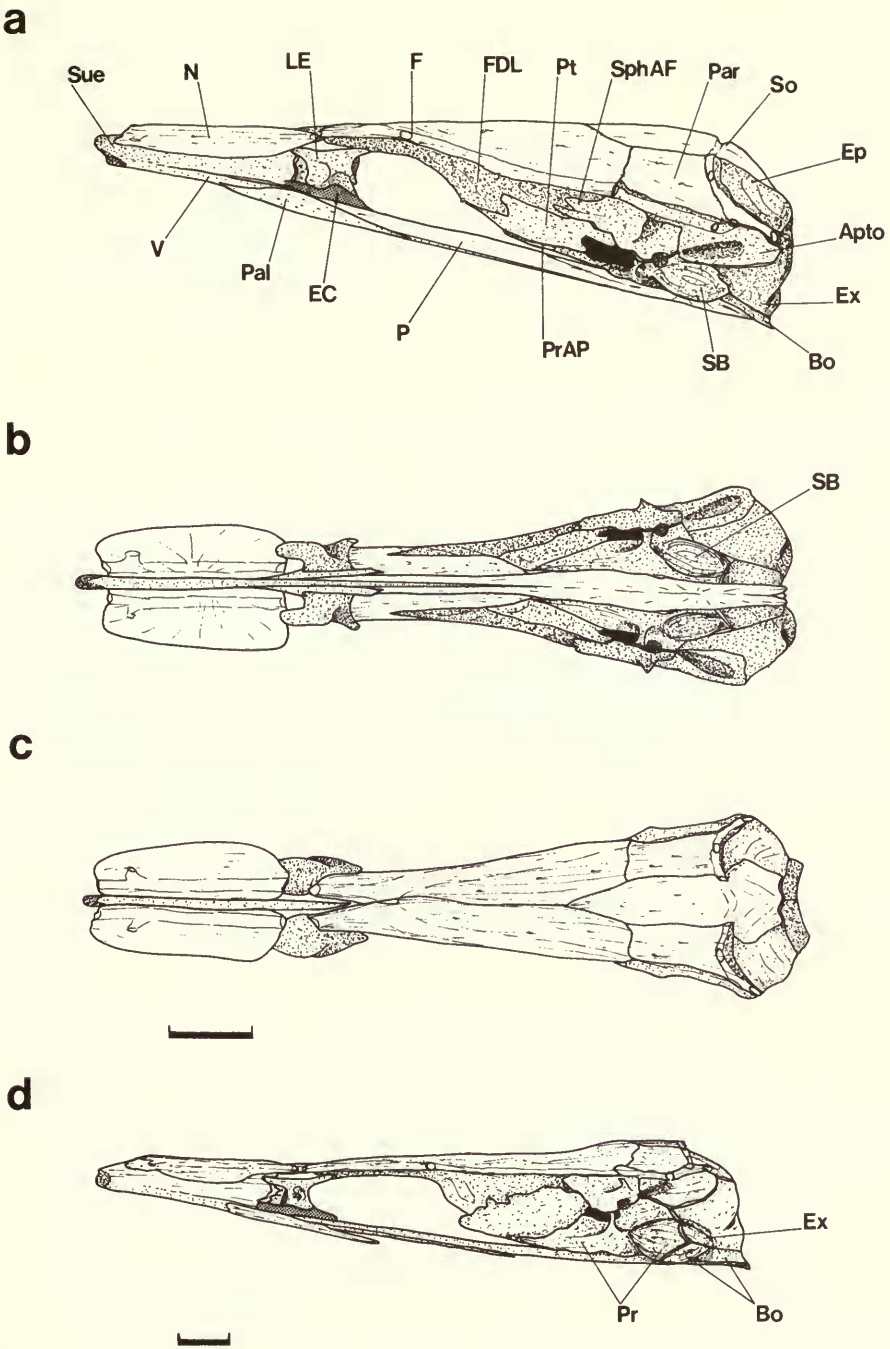

Fig. 38 Neurocranium of *Mastacembelus brichardi* in (a) lateral view, left side, (b) ventral view, (c) dorsal view; and of *Mastacembelus micropectus* (d) lateral view, left side.

The facial foramen in *Mastacembelus longicauda* (Fig. 33a) is unusually large and is connected, *via* a narrow opening, to the posterior margin of the trigeminal foramen. *Chaudhuria,* (Fig. 15ai), *Pillaia* (Fig. 15bi) and *Mastacembelus crassus* (Fig. 39a) lack separate trigeminal and facial foramina, and have a single large foramen in the trigeminofacialis chamber. An

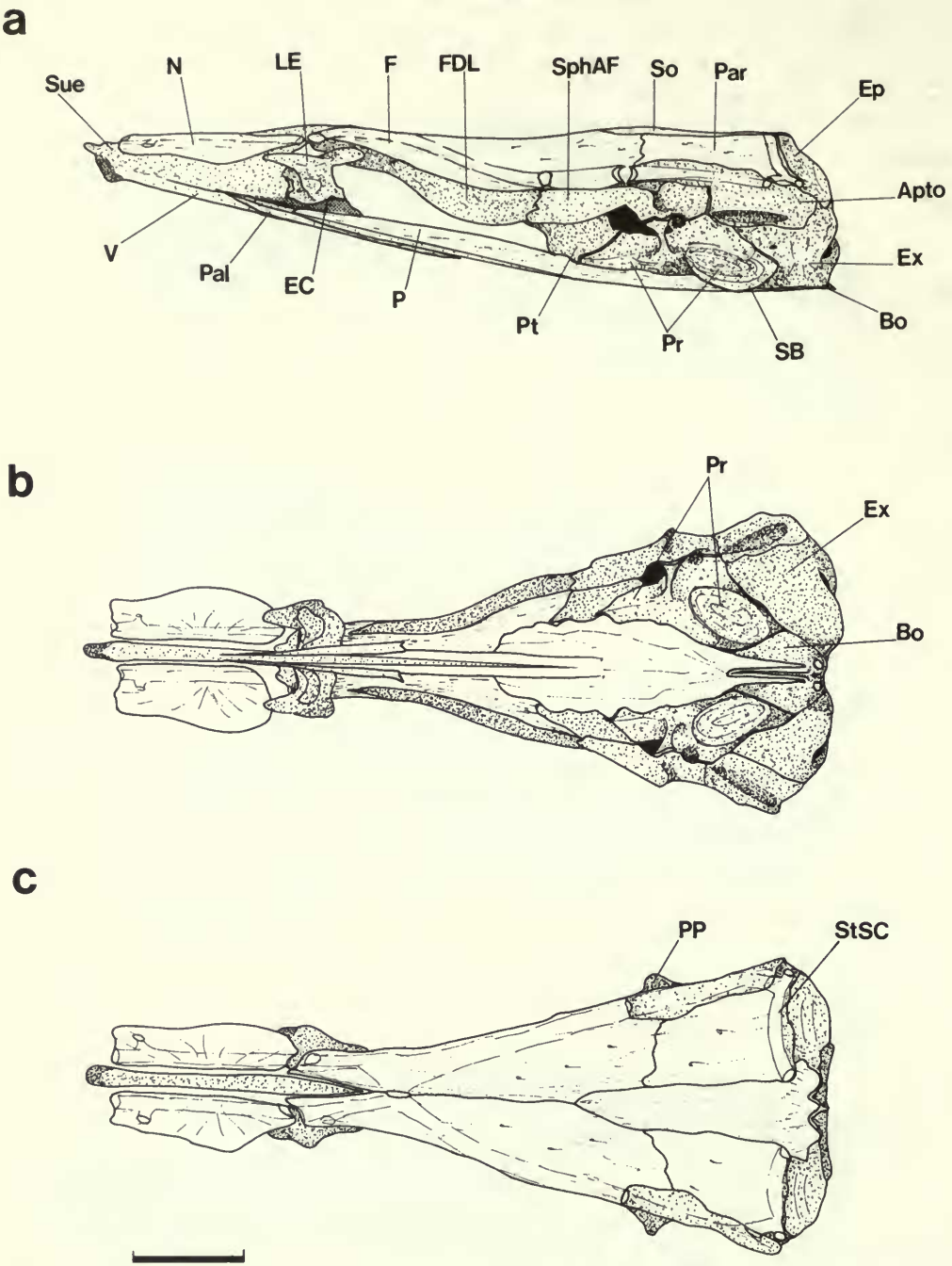

Fig. 39 *Mastacembelus crassus,* neurocranium in (a) lateral view, left side, (b) ventral view and (c) dorsal view.

even more extreme condition is found in *M. aviceps* where, due to the open postorbital lateral wall of the neurocranium, there are no foramina (Fig. 40a).

Interspecific variation in the size and position of the lateral commissure is slight apart from the development of an anterodorsal flange in some taxa. A flange on the anterodorsal face of the lateral commissure in *Macrognathus* is developed to an increasing degree in *M.*

siamensis (Fig. 29a), *M. aral* and *M. aculeatus*. In *M. aral* and *M. aculeatus* it extends anterolaterally to such an extent that in its most extreme condition (i.e. *M. aculeatus* Fig. 30a) it lies above the upper edge of the trigeminal foramen, and is sutured to the entire, precommissural ventral edge of the sphenotic.

A small sacculus lodged in the posteromedial face of the prootic (Fig. 1 a & b) is characteristic of most taxa. The bulla accommodating the sacculus in *M. brichardi* (Fig. 38 a & b), *M. crassus* (Fig. 39a & b) and *M. aviceps* (Fig. 40 a & b) is particularly large relative to the recess in *M. mastacembelus*. However, this otolith recess, regardless of its size, is accommodated entirely within the prootic in these species, as it is in the majority of mastacembeloids examined. A large bulla also occurs in *Mastacembelus micropectus* (Fig. 38d), *Chaudhuria* (Fig. 15ai & ii) and *Pillaia* (Fig. 15bi & ii). In these taxa, however, it is not lodged entirely in the prootic, but lies partly in the prootic, exoccipital and basioccipital bones.

There is little interspecific variation in the morphology of the *sphenotic*. A prominent anterolateral flange occurs in all taxa. This extension of the sphenotic, and the posterior position of its postorbital process, may be correlated with the long precommissural region of the neurocranium. The anterior edge of the sphenotic is sutured to the posterior edge of the frontal lamina (by which it is excluded from the postorbital border of the orbit) in most mastacembeloids. In *Chaudhuria* (Fig. 15ai) and *Pillaia* (Fig. 15bi) the anterior region is attenuated and, since the descending frontal lamina is absent, the tip passes to the posterior margin of the orbit. A similar condition occurs in *M. aviceps* (Fig. 40a) which also lacks a descending frontal lamina although in this species the sphenotic is shorter and does not extend anteriorly to the margin of the orbit. This arrangement is associated with the extreme precommissural attenuation of other neurocranial bones and a reduction in eye size.

The postorbital process on the sphenotic is developed to a varying extent. It is particularly large in the Tanganyikan species *Mastacembelus moorii* and *M. ophidium*, and in the west African species *M. goro* and *M. longicauda* (Fig. 33). In *Mastacembelus shiranus* the process is short, and it is absent in *M. vanderwaali*. When present this process serves as a point of insertion for the *levator arcus palatini* muscle (p. 119).

A ventrolateral 'wing' of the sphenotic occurs in *Mastacembelus congicus, M. niger, M. marmoratus, M. ubangensis, M. vanderwaali, M. goro, M. sclateri* and *M. nigromarginatus* (from Ghana; Fig. 34) and *M. reticulatus* (from Sierra Leone). It is particularly well developed in *M. congicus* (Fig. 32a) and overlies the trigeminal foramen to a greater extent than in any other species.

A small descending spur, like the prootic spur described above, on the ventral edge of the sphenotic occurs mosaically among the Asian and African species.

The most significant interspecific variation in the morphology of the *pterotic* occurs in a single Zairean species—*Mastacembelus brachyrhinus* (Fig. 37a & c). The dorsal (dermopterotic) part of the pterotic in this species is enlarged in comparison with its condition in *M. mastacembelus* (Fig. 1a & c), which latter condition represents the more usual mastacembeloid arrangement. The enlarged dorsal region of the pterotic in *M. brachyrhinus* is combined with a posterodorsal expansion of the frontal.

The condition of the *epioccipital* in *M. mastacembelus* (Fig. 1c) reflects the arrangement of this bone in both Asian and African mastacembeloids.

The *exoccipital* varies interspecifically in a number of features. Its dorsomedial process, as described in *M. mastacembelus* (p. 18), is not connected to its partner in *Mastacembelus sinensis* (Fig. 24c), *Chaudhuria* (Fig. 15aiii) or in *Pillaia* (Fig. 15biii). In these species the posterodorsal edge of the supraoccipital lies between the dorsomedial face of each exoccipital. The foramen magnum is not, therefore, surrounded by the exoccipitals alone but by the posterior edge of the supraoccipital as well. A further characteristic of the exoccipital in these three taxa is its perforated dorsal surface.

The ventrolateral face of the exoccipital is expanded in taxa with a deep basicranium (p. 53). In these, which include *Mastacembelus pancalus* (most extreme basicranial expansion), *Mastacembelus zebrinus* and to a lesser extent *Macrognathus*, the lateral wall of the

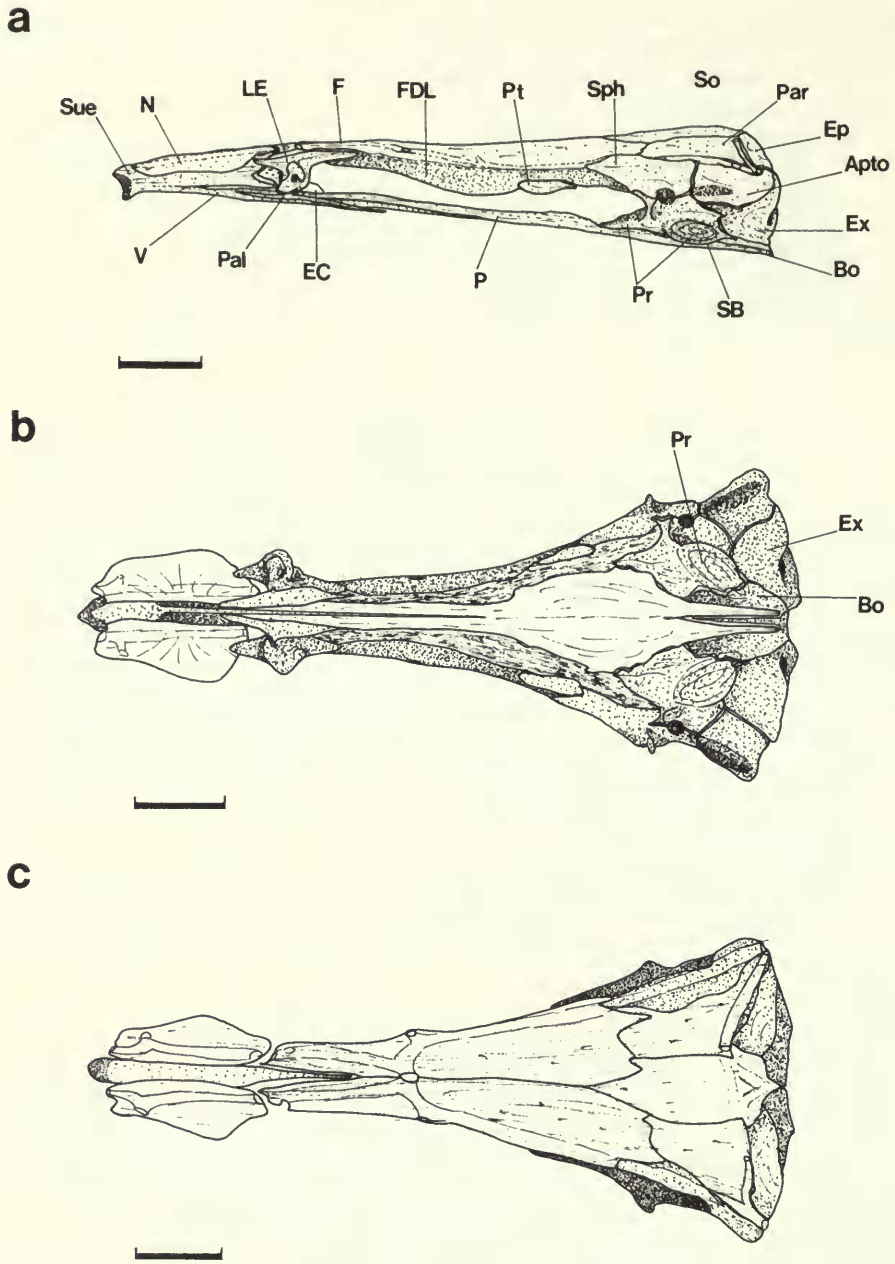

Fig. 40 *Mastacembelus aviceps,* neurocranium in (a) lateral view, left side, (b) ventral view and (c) dorsal view.

exoccipital is expanded ventrally and thus contributes to the deepening of the basicranium. The *basioccipital* also contributes to the overall increase in depth of the basicranium in *M. pancalus, M. zebrinus* and in *Macrognathus* species.

The expanded *basioccipital* in *M. pancalus* extends posteroventrally below the craniovertebral joint. The fossa for Baudelot's ligament is particularly deep in *M. pancalus* (Fig. 28b), it lies on the posteroventral edge of the basioccipital, and has an ovoid opening. The fossa is in a similar position in *M. zebrinus* and all the *Macrognathus* species.

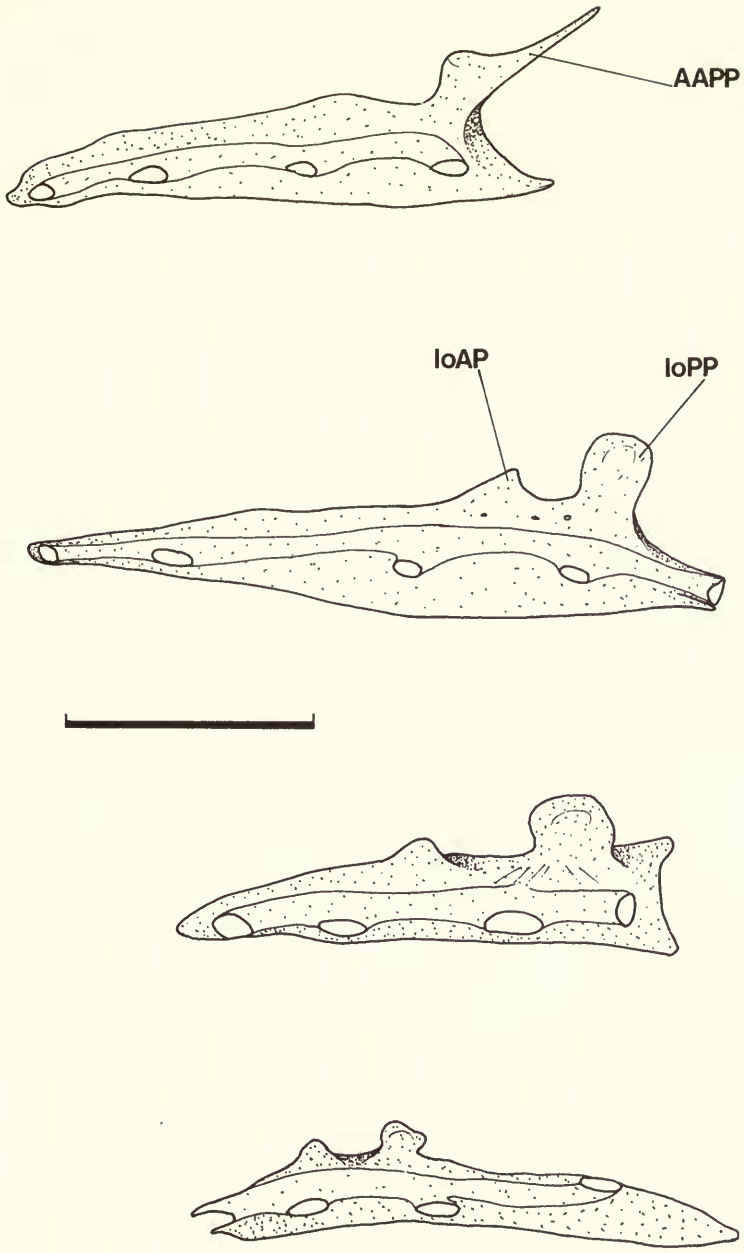

Fig. 41 Lateral view of left 1st infraorbital bone in (a) *Macrognathus aculeatus,* (b) *Mastacembelus albomaculatus,* (c) *Mastacembelus aviceps* and (d) *Mastacembelus ophidium* (right side).

A tripartite occipital facet, (p. 18) occurs in all mastacembeloids.

There is little interspecific variation in the morphology of the *supraoccipital,* apart from the extent to which it contributes to the dorsal rim of the foramen magnum (discussed above).

The supraoccipital is a comparatively small bone in *M. sinensis* (Fig. 24c) and may not contact the frontals anteriorly; as a result the anteromedial edge of the parietals contact medially.

The transverse channel that crosses the posterodorsal surface of the supraoccipital in *M. mastacembelus* (Fig. 1c) is absent in several Asian and African species. Among the Asian taxa, *Mastacembelus pancalus* (Fig. 28c), *M. sinensis* (Fig. 24c), *Chaudhuria* (Fig. 15aiii) and *Pillaia* (Fig. 15biii) all lack a channel; and it is also absent in *Mastacembelus albomaculatus, M. cunningtoni, M. frenatus* (Fig. 31c), *M. plagiostomus, M. tanganicae, M. zebratus, M. shiranus, M. congicus* (Fig. 32c), *M. aviceps* (Fig. 40c) and *M. ubangensis* among the African species. The sensory canal commissure in these African species lies within the integument above the dorsal surface of the supraoccipital.

A dermosupraoccipital, as described in *Mastacembelus congicus* by Taverne (1973), was not distinguished in any mastacembeloids examined, nor could I find any trace of the element Patterson (1977: 98) described as '... a plate-like median extrascapular which overlies the supraoccipital and may fuse with it in full grown individuals'.

The transverse channel across the dorsal surface of the supraoccipital, which accommodates the supratemporal sensory canal commissure, is covered by a thin layer of bone in some species (e.g. *Mastacembelus moorii*) and presumably results from the supraoccipital enclosing this canal during ontogeny.

The *extrascapulae,* both lateral and medial, are absent in all mastacembeloid taxa although my specimen of *Mastacembelus brachyrhinus* (Fig. 37c) is presumably exceptional as a left lateral extrascapula is clearly discernible.

The *frontal* shows interspecific variation in the morphology of its dorsal surface and its vertical lamina. In *M. mastacembelus* (Fig. 1a) and a number of other Asian species (e.g. *Mastacembelus erythrotaenia,* Fig. 25c), and the majority of African species (e.g. *Mastacembelus frenatus,* Fig. 31c) the dorsal surface of the frontal is almost flat, with only the lateral edge curved ventrally. A group of Asian taxa including *Mastacembelus pancalus, M. zebrinus* and the *Macrognathus* species have a frontal with a strongly curved dorsal surface. In *M. pancalus* (Fig. 28a) the lateral edge of the frontal is curved ventrally to such an extent that, in transverse section, the highest point on the dorsal surface of the neurocranium is along the median connection of the frontals. A similar type of frontal morphology occurs in *M. zebrinus* and to a lesser extent in the *Macrognathus* species. Its curvature in these species gives the neurocranium a much deeper appearance than that of *M. mastacembelus.* A further consequence of a steeply sloping frontal is the relatively ventral position of the trigeminofacialis chamber. Such a condition may also be correlated with the marked basicranial expansion in these taxa (as described earlier p. 69).

The dorsal surface of the frontal is curved to a varying degree in a number of other species (e.g. *Mastacembelus brachyrhinus* and *M. brichardi*), but no other Asian or African taxa exhibit the pronounced curvature of the frontal found in *M. pancalus, M. zebrinus* and in all *Macrognathus* species.

The anterior region of the frontal, which roofs the orbit, is short in *Mastacembelus brichardi* (Fig. 38c), *M. crassus* (Fig. 39c) and *M. aviceps* (Fig. 40c), and is apparently associated with the small eyes of these rapids-dwelling species (see also p. 125).

A descending vertical lamina on the frontal, as described in *M. mastacembelus* (p. 19) is a characteristic feature of all mastacembeloids apart from *Chaudhuria* (Fig. 15ai) and *Pillaia* (Fig. 15bi). The lack of a frontal lamina is one of many characters in the neurocranium of *Chaudhuria* and *Pillaia* that are possibly reductional. A comparatively low descending frontal lamina occurs in the highly derived taxa of the Zairean rapids, *Mastacembelus aviceps* (Fig. 40a) and *M. crassus* (Fig. 39a). Variability in the size of the lamina and the presence of a pedicel on its lateral face have been discussed above (p. 60).

There is little interspecific variation in the morphology of the *parietal.* The parietals in all Asian and African species apart from *Chaudhuria* (Fig. 15aiii) and *Pillaia* (Fig. 15biii) accommodate the supratemporal branch of the cephalic sensory canal system (Maheshwari, 1971), normally associated with the extrascapulae. A pore is present in the canal in all taxa except *Chaudhuria* and *Pillaia.* The medial connection between the parietals in *Mastacembelus sinensis* (Fig. 24c) is unique to that species, and is directly related to the small dorsal area of the supraoccipital (p. 71). The relatively small dorsal surface area of the parietal in

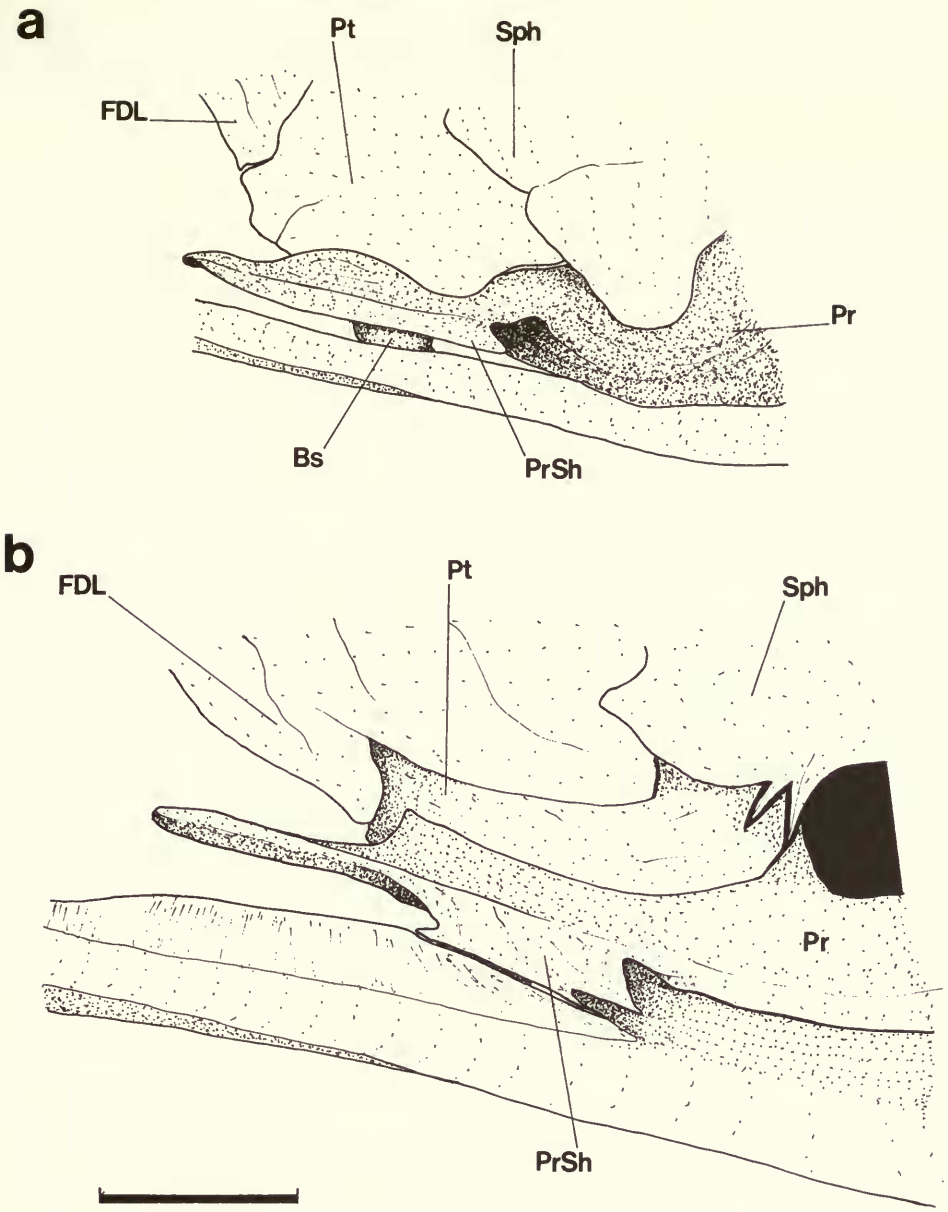

Fig. 42 Pre-otic region of neurocranium in (a) *Mastacembelus sclateri* and (b) *Mastacembelus stappersii*; lateral view, left side.

Mastacembelus brachyrhinus (Fig. 37c), in association with the enlarged pterotic and posterior region of the frontal (p. 69), is a characteristic of the species.

The absence of a *posttemporal* bone is a characteristic feature of all taxa. The only remnant of this bone in *M. mastacembelus* is two ossified tubules which surround two sections of the postcranial sensory canal (p. 19). Interspecific variation in the number of posttemporal tubules among Asian and African species is summarised in Table 4. Tubules are completely absent in some Asian (including *Mastacembelus armatus, M. sinensis, Chaudhuria* and *Pillaia*) and African taxa (including *Mastacembelus shiranus, M. congicus, M. brichardi, M. niger, M. sclateri* and *M. flavomarginatus*). Intraspecific variation in the number of tubules

Table 4 Number of posttemporal tubules in mastacembeloid species.

	Absent	1	2	3
Oriental mastacembeloid taxa				
Mastacembelus armatus	+			
Mastacembelus erythrotaenia			+	
Mastacembelus maculatus		+		
Mastacembelus mastacembelus			+	
Mastacembelus pancalus		+		
Mastacembelus sinensis	+			
Mastacembelus unicolor			+	
Mastacembelus zebrinus		+		
Macrognathus aculeatus		+		
Macrognathus siamensis		+		
Chaudhuria caudata	+			
Pillaia indica	+			
African mastacembeloid taxa				
Mastacembelus albomaculatus			+	
Mastacembelus aviceps			+	
Mastacembelus batesii			+	
Mastacembelus brachyrhinus			+	
Mastacembelus brevicauda			+	
Mastacembelus brichardi	+			
Mastacembelus congicus	+			
Mastacembelus crassus			+	
Mastacembelus cunningtoni			+	
Mastacembelus ellipsifer			+	
Mastacembelus flavomarginatus	+			
Mastacembelus frenatus			+ (L)	+ (R)
Mastacembelus goro		+		
Mastacembelus greshoffi			+	
Mastacembelus liberiensis			+	
Mastacembelus loennbergii			+	
Mastacembelus longicauda			+	
Mastacembelus marmoratus			+	
Mastacembelus micropectus			+	
Mastacembelus moorii			+	
Mastacembelus niger	+			
Mastacembelus nigromarginatus			+	
Mastacembelus ophidium		+ (R)		+ (L)
Mastacembelus paucispinis			+	
Mastacembelus plagiostomus				+
Mastacembelus platysoma			+	
Mastacembelus reticulatus			+ (L)	+ (R)
Mastacembelus sclateri	+			
Mastacembelus shiranus	+			
Mastacembelus stappersii			+	
Mastacembelus tanganicae			+	
Mastacembelus vanderwaali			+	
Mastacembelus zebratus				+
Mastacembelus sp. nov.			+	

may also occur. For example, one side of the head in a specimen of *M. frenatus* and one of *M. reticulatus,* has three and the other side two tubules, while a specimen of *M. ophidium* has three tubules on the left and only one of the right side.

Jaws

Upper jaw

There is little variation in the overall morphology of these bones. The most extreme variation occurs in *Pillaia* (Fig. 16b) where the upper jaw is formed from a single tooth bearing element. This bone was identified by Yazdani (1976*a*) as a *premaxilla*, and he suggested '... the posterior part of the upper jaw bone in *Pillaia indica* represents the maxilla which has fused with the premaxilla in the course of evolution ...'. The jaws in the specimens of *Pillaia* examined confirm that a single bone is present, but, whether this is the result of fusion or the loss of the *maxilla* cannot be determined without ontogenetic evidence.

The upper jaw arrangement in *Mastacembelus aviceps,* from the lower Zairean rapids, may help clarify this problem. The anterior half of the maxilla in *M. aviceps* (Fig. 44a) is reduced to an attentuated bony strand lying within a longitudinal groove on the dorsal surface of the premaxilla. Posteriorly, the maxilla is thickened and expanded ventrolaterally to a level below the premaxilla, with which bone it is tightly connected. These modifications in *M. aviceps* give its upper jaw a marked resemblance to that in *Pillaia.* This may be the result of a similar developmental trend in the two taxa, a trend which in *Pillaia* is at a more advanced stage and has involved the complete loss of the reduced anterior region of the maxilla and a fusion of the broader posterior flange to the premaxilla.

The anterior region of the maxilla is expanded in *Mastacembelus moorii* (Fig. 43a) and *M. ophidium* (Fig. 43b) from Lake Tanganyika. In these species the anterior half of the maxilla is lateromedially compressed, giving it a wide anterolateral face which may function as a support for the exceptionally large and fleshy lips.

The premaxillary dentition exhibits considerable variation in the size and number of teeth. Typically it consists of an outer row of large caniniform teeth followed by three of four inner rows which decrease in number and tooth size posteromedially, e.g. the Asian *Mastacembelus maculatus* and *M. armatus,* and the African *M. frenatus* and *M. goro.* Teeth in the outer row are particularly large in *Mastacembelus moorii* and *M. ophidium* (Fig. 43a & b) and there are numerous inner rows of small teeth. The dentition in these taxa gives the premaxilla a characteristically wide alveolar surface, possibly related to their piscivorous diet.

The alveolar surface on the premaxilla of a third Tanganyikan species, *Mastacembelus cunningtoni* (Fig. 45a) is wide, with up to eighteen irregular rows of small, slender teeth, each with a posteriorly curved tip. A broad alveolar surface on the premaxilla is also a feature of a number of Asian mastacembeloids, including *Mastacembelus zebrinus, M. pancalus* and the *Macrognathus* species (Fig. 46). In these taxa the rostral appendage is larger than in other mastacembeloids, and in *M. pancalus* (and to a lesser extent in *M. zebrinus*) the alveolar surface of the premaxilla is curved ventrorostrally around its buccal face. The under surface bears numerous, small, irregularly spaced caniniform teeth which tend to lie horizontally, their tips directed posteriorly. Anteriorly, the premaxillary alveolar surface contacts its partner in a symphysis anteroventral to the head of the vomer. Furthermore, the anterior tip of this tooth bearing surface has fragmented into a single plate on the right premaxilla in a specimen of *M. pancalus* (Fig. 45b).

The fragmentation of the alveolar surface in *Macrognathus* species appears to represent a more advanced stage in the phylogenetic development of this character from its condition in *Mastacembelus pancalus.* The anterior end of the alveolar surface in *Macrognathus* has fragmented into a long series of laterally expanded, flexible dentigerous bony plates (Fig. 45c) which extend along the ventral surface of the rostral appendage and are tapered anteriorly. The smallest plate lies posteroventral to the anterior nostril and the tip of the rostrum. On the ventral surface of each pair of rostral plates is a transverse row of small caniniform teeth

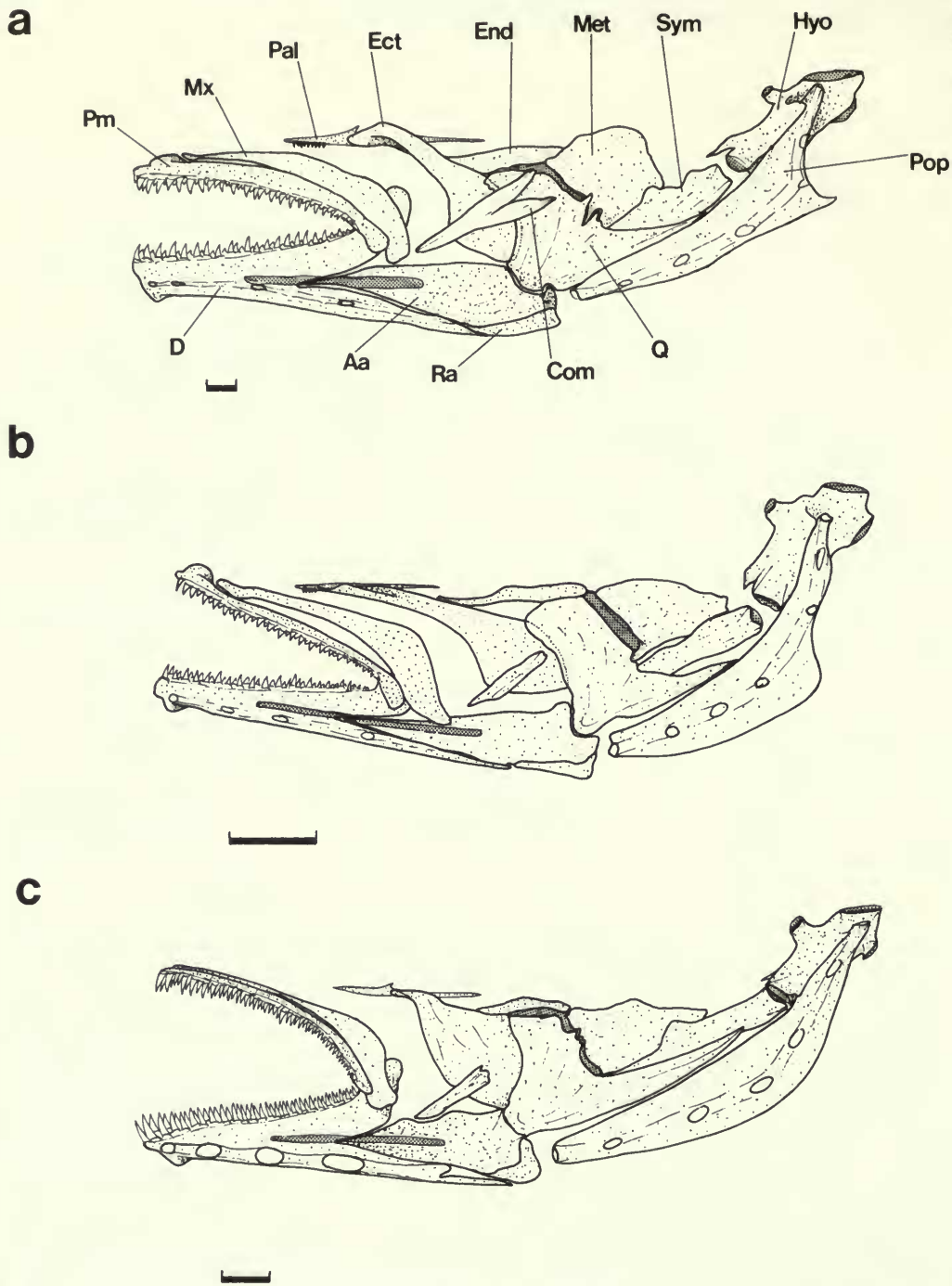

Fig. 43 Hyopalatine arch, preoperculum and jaw bones in (a) *Mastacembelus moorii,* (b) *Mastacembelus ophidium* and (c) *Mastacembelus micropectus;* lateral view, left side.

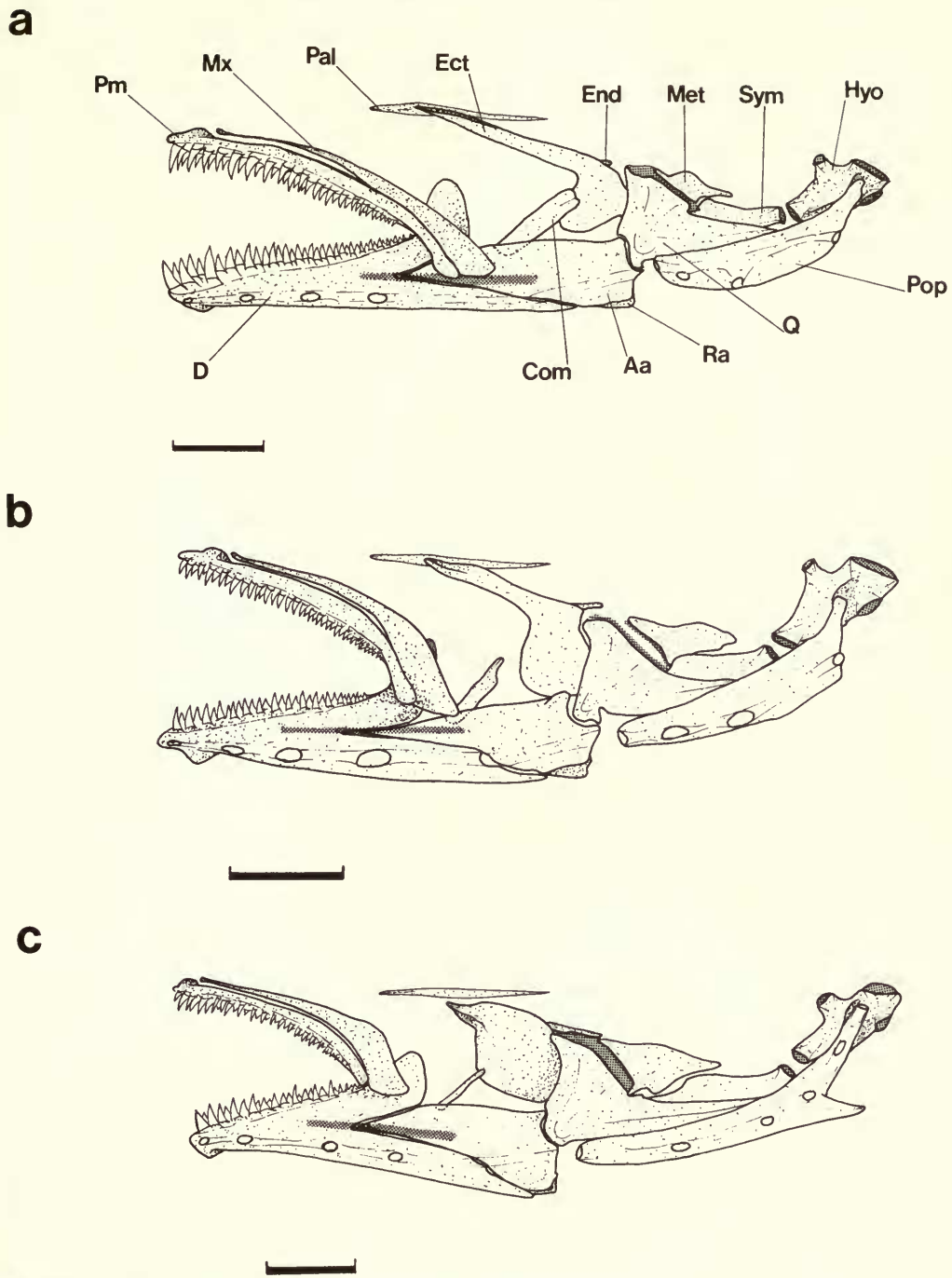

Fig. 44 Hypolatine arch, preoperculum and jaw bones in (a) *Mastacembelus aviceps* (maxilla displaced dorsally), (b) *Mastacembelus crassus,* (c) *Mastacembelus brichardi,* lateral view, left side.

with posteriorly directed tips. The toothed alveolar surface of the premaxillae forms a continuous series with the rostral toothbearing plates.

In the opinion of Roberts (1980: 390) variation in the number of premaxillary rostral plates '... provides perhaps the most important character for distinguishing the species of

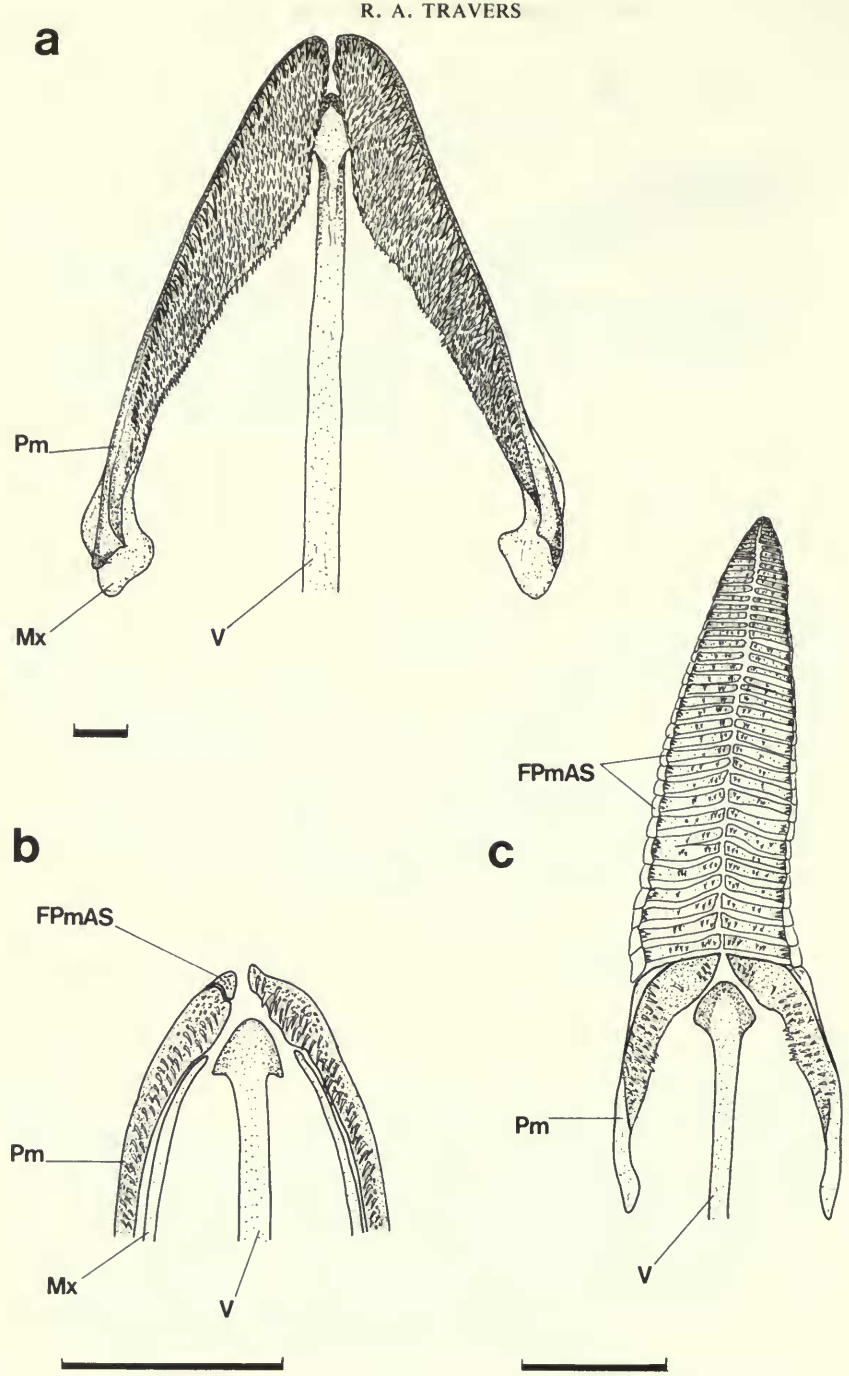

Fig. 45 Upper jaw bones (ventral aspect) in (a) *Mastacembelus cunningtoni*, (b) *Mastacembelus pancalus*, and (c) *Macrognathus aculeatus*.

Macrognathus'. The lowest number occurs in *Macrognathus siamensis* (usually between 9–12 pairs), the highest in *Macrognathus aculeatus* (usually between 38–55 pairs); intermediate between these species are the 14–28 pairs usually found in *Macrognathus aral.* The overall length of the rostral appendage in each of these species is directly proportional to the number of premaxillary plates present.

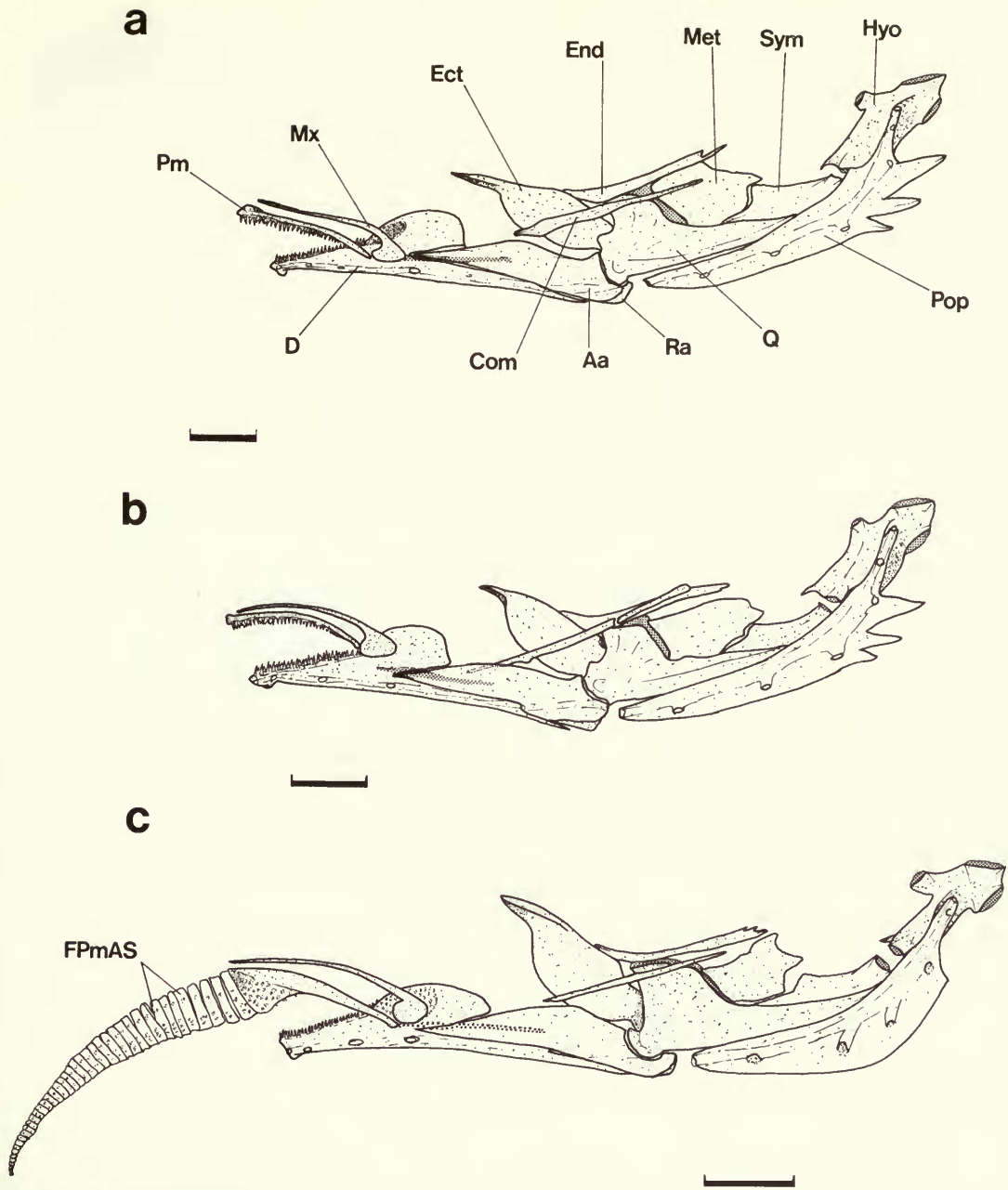

Fig. 46 Hyo-pterygoid arch, preoperculum and jaw bones in (a) *Mastacembelus zebrinus*, (b) *Mastacembelus pancalus* and (c) *Macrognathus aculeatus*; lateral aspect of left side.

Associated with the enlargement and fragmentation of the toothbearing premaxillary alveolar surface in these taxa is the attenuation of the maxilla. In *Mastacembelus zebrinus*, *M. pancalus* and to a greater extent in the *Macrognathus* species, the maxilla has a long, weak anterior process and narrow posteroventral flange (Fig. 46a–c) compared to that of *M. mastacembelus* (Fig. 4) which represents the modal type.

Lower jaw

Interspecific variation in the morphology of the lower jaw is mainly confined to the *dentary* and *coronomeckelian*. The dentary forms almost the entire ventral edge of the mandible in all taxa and in the majority of species its lateral face is pierced by four sensory canal pores. Three pores occur, among the Asian taxa, in *Mastacembelus maculatus, M. pancalus* and in the three *Macrognathus* species; among the African species three pores occur in *Mastacembelus liberiensis, M. greshoffi, M. loennbergii* and *M. ubangensis*.

Dentary pores are reduced to three in *Pillaia* and are absent in *Chaudhuria* (as discussed above p. 36).

The upper or coronoid process of the dentary has two forms, either tall and narrow or low and broad based. The process in *M. mastacembelus* (Fig. 4) is of the tall, narrow type, which also occurs in *Mastacembelus erythrotaenia, M. sinensis, Chaudhuria* and Pillaia among the Asian species examined, as well as in the majority of African species. A low, broad coronoid process occurs in most of the other Asian taxa examined including *Mastacembelus zebrinus, M. pancalus* and the *Macrognathus* species (see Fig. 46a), although the size and shape of the coronoid process in *Mastacembelus armatus* and *M. maculatus* appear to be intermediate between these types.

A low, broad coronoid process also occurs in a number of African species including *Mastacembelus cunningtoni, M. ellipsifer, M. moorii* and *M. platysoma* from Lake Tanganyika, *M. congicus, M. paucispinis* and *M. ubangensis* from Zaire; *M. sclateri* from Sierra Leone, and in *M. goro, M. liberiensis* and *M. niger* from West Africa.

Although the coronoid process in *M. zebrinus, M. pancalus* and the *Macrognathus* species is of a low, broad type similar to that in the African species listed above, it may be distinguished by the posterior expansion of the toothbearing alveolar surface onto its medial face (Fig. 57c). A slight encroachment of the dentary toothplate onto the medial face of the coronoid process was only found in *M. goro* among the African taxa.

The other lower jaw element in which considerable interspecific variation occurs is a sesamoid ossification considered to be the coronomeckelian.

The size and position of the coronomeckelian is a diagnostic feature of all mastacembeloid taxa apart from *Chaudhuria* (Fig. 16a) and *Pillaia* (Fig. 16b). It does not lie dorsal to the anguloarticular in these taxa, but is a small ossicle attached to the posterodorsal edge of Meckel's cartilage, on the medial face of the anguloarticular.

Variation in the overall length of the coronomeckelian is indicated by the position at which its posterior tip lies across the suspensorium. In the Zairean rapids species *Mastacembelus brachyrhinus, M. brichardi, M. crassus* and *M. aviceps* (Fig. 44a–c; and possibly *M. latens*), it is much shorter than the modal condition found, for example, in *M. mastacembelus* (Fig. 4). In species with a tall and narrow coronoid process the coronomeckelian extends dorsocaudally from the dorsomedial margin of the anguloarticular to lie above the anterior face of the ectopterygoid.

Some African taxa have a much larger coronomeckelian in comparison with that of the rapids species described above and *M. mastacembelus*. These include *M. cunningtoni, M. ellipsifer, M. moorii,* and *M. platysoma* from Lake Tanganyika; *M. congicus, M. paucispinis* and *M. ubangensis* from Zaire; *M. sclateri* from Sierra Leone; *M. liberiensis, M. goro* and *M. niger* from West Africa. The coronomeckelian in these species extends well beyond the point occupied by the posterior tip of the bone in *M. mastacembelus*; for example, in *M. cunningtoni* the stout bone extends across the lateral faces of the ectopterygoid and quadrate to the latter's border with the metapterygoid. The coronomeckelian in *M. ellipsifer, M. platysoma* (in which it is barbed) and *M. sclateri* is of approximately equal extent to that in *M. cunningtoni,* while in *M. congicus, M. paucispinis, M. liberiensis, M. goro* (Fig. 50c), *M. niger,* and *M. ubangensis* it is shorter, but only slightly so extending to the posterolateral edge of the ectopterygoid at its border with the quadrate and endopterygoid. The coronomeckelian in *M. moorii* (Fig. 43a) has about the same extent as it does in *M. cunningtoni,* but is distinguished by its prominently forked posterior end.

A feature common to all African species with a long coronomeckelian is the low, broad coronoid dentary process (p. 80). In African species coronomeckelian length is apparently correlated with the type of coronoid process present. Species with a relatively short coronomeckelian (e.g. *M. brichardi* and *M. brachyrhinus*) have, without exception, a tall, narrow coronoid process, whilst those with a relatively long coronomeckelian (e.g. *M. cunningtoni* and *M. liberiensis*) have, again without exception, a low, broad coronoid process. Thus, there is an inverse relationship between coronomeckelian length and coronoid process height.

A low, broad coronoid process occurs (as described above) in *M. zebrinus, M. pancalus* and the *Macrognathus* species. The *Macrognathus* coronomeckelian is a larger bone than that found in *M. mastacembelus*; in *Macrognathus aculeatus* (Fig. 46c) it extends from the dorsomedial margin of the anguloarticular, across the lateral face of the ectopterygoid and quadrate to the latter's border with the metapterygoid.

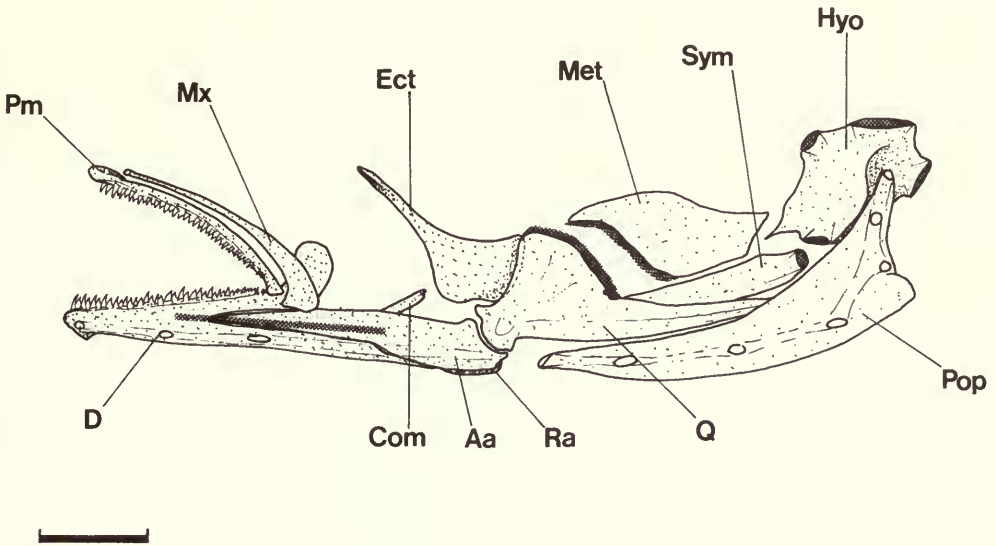

Fig. 47 *Mastacembelus sinensis,* left hyo-pterygoid arch, preoperculum and jaw bones in lateral view.

The length of the coronomeckelian in *M. zebrinus* and *M. pancalus* (which both have a particularly low, broad coronoid process, Fig. 46a & b) also exceeds that in *M. mastacembelus* and even that in *Macrognathus* since it extends posteriorly across the dorsal margin of the anguloarticular to the posterolateral face of the endopterygoid.

A relatively short coronomeckelian occurs in *Mastacembelus sinensis* (Fig. 47) and extends posteriorly from the dorsomedial margin of the anguloarticular but does not reach the anteroventral edge of the ectopterygoid. A relatively tall, narrow coronoid process, described earlier (p. 80) occurs in this species. The type of coronoid process and the condition of the coronomeckelian in Asian mastacembeloids thus appear to have the same relationship as in the African species. The relationship between these bones may be associated with several features of the adductor musculature inserting on them (A_2 & A_3 division); this will be discussed elsewhere (Travers, 1984).

There is little interspecific variation in the morphology of the *anguloarticular*. The lack of an ascending process (coronoid expansion) on the bone in *M. mastacembelus* (Fig. 4) is characteristic of most taxa, but the upper edge of the anguloarticular has a moderately high, broad-based coronoid expansion in *Mastacembelus zebrinus, M. pancalus* and *Macrognathus* species. In these (e.g. see *Macrognathus aculeatus;* Fig. 46c) the dorsal expansion tapers to a low peak which lies just below the anterior end of the coronomeckelian. An

expanded dorsal edge of the anguloarticular is not found in any other Asian or African species. The dorsal edge of the anguloarticular is notched in *Mastacembelus micropectus* (Fig. 43c), the anterior end of the coronomeckelian lying within the notch.

The position of the facet on the anguloarticular (posterodorsal angle) described in *M. mastacembelus* (p. 20) is typical of all taxa apart from the *Macrognathus* species (Fig. 46c) where it notches the dorsal edge anterior to the posterodorsal angle of the bone. Thus, the mandibular joint lies anterior to the posterior end of the anguloarticular.

Hyopalatine arch

The bones of the hyopalatine arch exhibit a number of interspecific differences, but apart from these there are only slight proportional changes in the overall arrangement of the arch.

The anterior edge of the *hyomandibula* shaft in *M. mastacembelus* (Fig. 5) bears a small descending spur. This is an invariable feature of all Asian mastacembeloids with the exception of *Chaudhuria* (Fig. 17a) and *Pillaia* (Fig. 17b), but is not found universally among the African species. For example, among the Tanganyikan species a prominent spur occurs only in *Mastacembelus cunningtoni* and to a lesser extent in *M. micropectus, M. moorii* and *M. ophidium* (Fig. 43 a–c). Other African species with a hyomandibular spur include, *Mastacembelus brachyrhinus, M. marmoratus, M. paucispinis, M. vanderwaali* and the undescribed species.

The hyomandibula and metapterygoid bones are unconnected in the majority of mastacembeloids, a condition typical of almost all species except *Mastacembelus sinensis* (Fig. 47), *Chaudhuria* (Fig. 17a) and *Pillaia* (Fig. 17b). In these taxa the posterolateral edge of the metapterygoid lies in close proximity, attached by connective tissue, to the anteroventral edge of the hyomandibula. The wide gap between these bones in all other mastacembeloids may be related to the particularly large symplectic. Disproportionate growth of this bone, compared to other suspensorial elements, may have resulted in it displacing the metapterygoid and other suspensorial bones away from the hyomandibula (see Figs 43, 44 and 50).

The anterior edge of the *metapterygoid* is connected by a narrow cartilaginous interface to the posterolateral edge of the quadrate in all species examined. The ventral dentate suture, below the cartilage interface, which also connects these elements in *M. mastacembelus* (Fig. 5), is absent in other Asian species and is present in only 4 African species, all from Lake Tanganyika *viz., M. cunningtoni, M. moorii, M. ophidium* and *M. zebratus.*

A small bony spur rises dorsolaterally from the ventral edge of the metapterygoid in *Mastacembelus ubangensis* (Fig. 48). The upper edge of the dorsal lamina on the symplectic in this species is also produced into a short descending process.

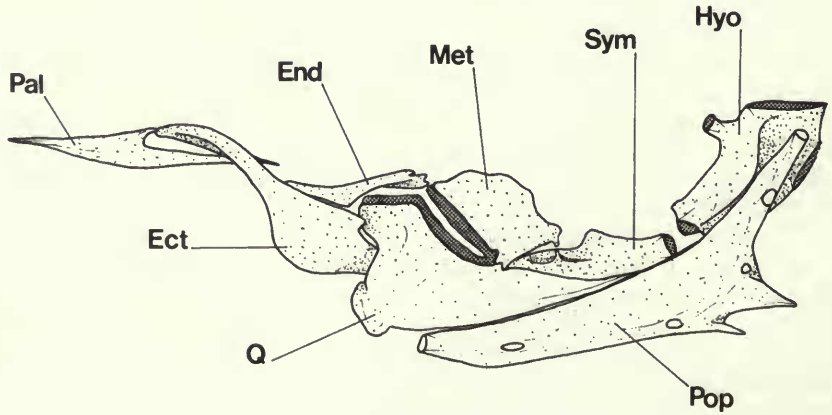

Fig. 48 *Mastacembelus ubangensis,* left hyopalatine arch and preoperculum; lateral aspect.

The *symplectic* (as noted above) is a large element in the hyopalatine arch. Its upper surface, in the majority of species, is produced into a thin lamina with an irregular dorsal edge. Compared with its size in *M. mastacembelus* (Fig. 5), the symplectic is relatively small in *Mastacembelus sinensis* (Fig. 47), *Chaudhuria* (Fig. 17a) and *Pillaia* (Fig. 17b). Associated with its small size in these species is the close contact between the hyomandibula and metapterygoid (discussed above).

The anterior edge of the *quadrate* is indented in *Mastacembelus zebrinus, M. pancalus* and in all *Macrognathus* species (Fig. 46a–c). This curved edge corresponds with the anterior edge of a recess in its anteromedial face, in which lies the large, horn-like ectopterygoid process.

A circular facet on the margin of the quadrate is unique to *Mastacembelus pancalus* (Fig. 46b); the facet articulates with a similar facet on the posterolateral face of the ectopterygoid, dorsal to its horn-like process. Apart from this variation, the form of the quadrate is remarkably constant throughout the group.

Considerable variation occurs in the morphology of the *endopterygoid.* The boomerang-shaped bone in *Mastacembelus mastacembelus* (Fig. 5) also occurs in *M. armatus, M. erythrotaenia, M. oatesii* and *M. unicolor* (see Fig. 49). The anterior process of the endopterygoid in these species extends below and beyond the anterodorsal connection between the ectopterygoid and lateral ethmoid. In no other Asian or African species examined does the endopterygoid contribute to the anterior articulation between the suspensorium (ectopterygoid) and neurocranium (lateral ethmoid). However, in *Mastacembelus maculatus* (Fig. 49c) the anterior tip of the endopterygoid does not lie far from the lateral ethmoid and appears to represent an intermediate condition.

The posterior end of the endopterygoid is distinctly modified in *Macrognathus* (Fig. 46c), *Mastacembelus frenatus* (Fig. 50a), *M. marmoratus, M. niger, M. sclateri* and *M. ubangensis* (Fig. 48). In these taxa the posterior end of the bone is subdivided into 3 prong-like processes whose tips are connected to short tendons running from the *adductor arcus palatini* muscle.

The endopterygoid is less modified in the remaining mastacembeloids examined (e.g. *M. congicus* (Fig. 50b). However, there is a marked tendency for the bone to be reduced in size in three species from the lower Zairean rapids (*Mastacembelus brichardi, M. crassus* and *M. aviceps* Fig. 44a–c: possibly *M. latens* as well). Here the endopterygoid is little more than a small splinter of bone connected to the dorsal end of the quadrate. In *Mastacembelus sinensis, Chaudhuria* and *Pillaia*, however, the bone is entirely absent (see Figs 47 and 17a & b).

The deep anterolateral face of the *ectopterygoid* and its direct articulation with the lateral ethmoid (as described in *M. mastacembelus*, p. 21), are features common to almost all mastacembeloids. The disproportionate anterolateral depth of the ectoptergygoid gives it a sinusoidal shape in most Asian and African taxa. Variation occurs both in the relative depth of the bone in some species, and in the length of its anterodorsal process articulating with the lateral ethmoid.

When compared with other Tanganyikan species, *Mastacembelus moorii* and *M. ophidium* (Fig. 43a & b) have an ectopterygoid with a relatively shallow anterolateral face and a long dorsal process. The bone in Zairean rapids species *M. aviceps* and *M. crassus* (Fig. 44 a & b) is similar to that in *M. moorii* and *M. ophidium.*

The most extreme ectopterygoid variation occurs, however, in *Chaudhuria* (Fig. 17a) and *Pillaia* (Fig. 17b), and to a lesser extent in *Mastacembelus sinensis* (Fig. 47). The bone in *M. sinensis* extends anterodorsally as a long, narrow process, its tip articulating with the lateral ethmoid.

This process is particularly long and anteromedially curved in *Chaudhuria* and *Pillaia;* it does not contact the lateral ethmoid, but extends below it along the lateral face of the vomer.

The depth of the anterolateral face of the ectopterygoid decreases sequentially in *M. sinensis, Chaudhuria* and *Pillaia* (compared Figs 47 and 17a & b), and a progressively smaller region of the bone in these species lies below the quadrate.

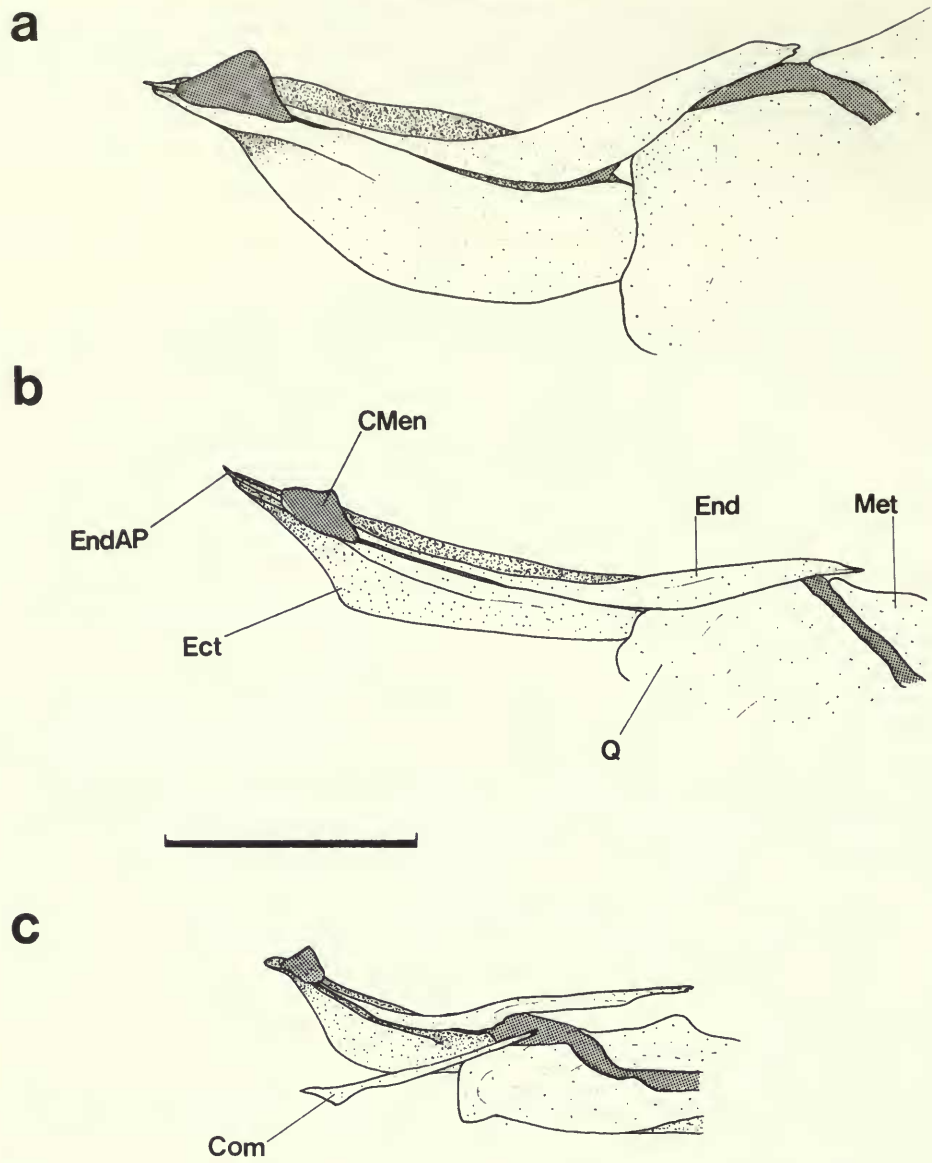

Fig. 49 Endo-ectopterygoid connection, left side, in (a) *Mastacembelus erythrotaenia,* (b) *Mastacembelus armatus* and (c) *Mastacembelus maculatus*; viewed obliquely from a dorso-lateral position.

Modification of the ectopterygoid is associated with the weak, flake-like *palatine* (auto-palatine) in mastacembeloids. The ectopterygoid appears to have replaced the palatine functionally, both with respect to its role as the anterior articulation point of the suspensorium with the neurocranium (discussed in Part II), and with respect to the palatine's contribution to the bony roof of the mouth. The form of the palatine (other than interspecific variation in its dentition and connection to the lateral ethmoid) in *M. mastacembelus* (p. 21 & Fig. 5) is seen in all taxa except *Chaudhuria* and *Pillaia* in which the bone is absent.

All Asian, and the majority of African species lack a palatine, tooth bearing, alveolar surface (dermopalatine). When present, palatine teeth are caniniform with posteriorly directed

tips, arranged in rows, the number of which are interspecifically variable. A single row of teeth occurs in the specimens of *Mastacembelus ophidium* (Fig. 43b) examined, two rows occur in *M. congicus* (Fig. 50b), *M. sclateri, M. loennbergii* and *M. nigromarginatus,* and three rows in *M. longicauda* (Fig. 33a), *M. moorii* (Fig. 43a) and *M. paucispinis* (Fig. 35a

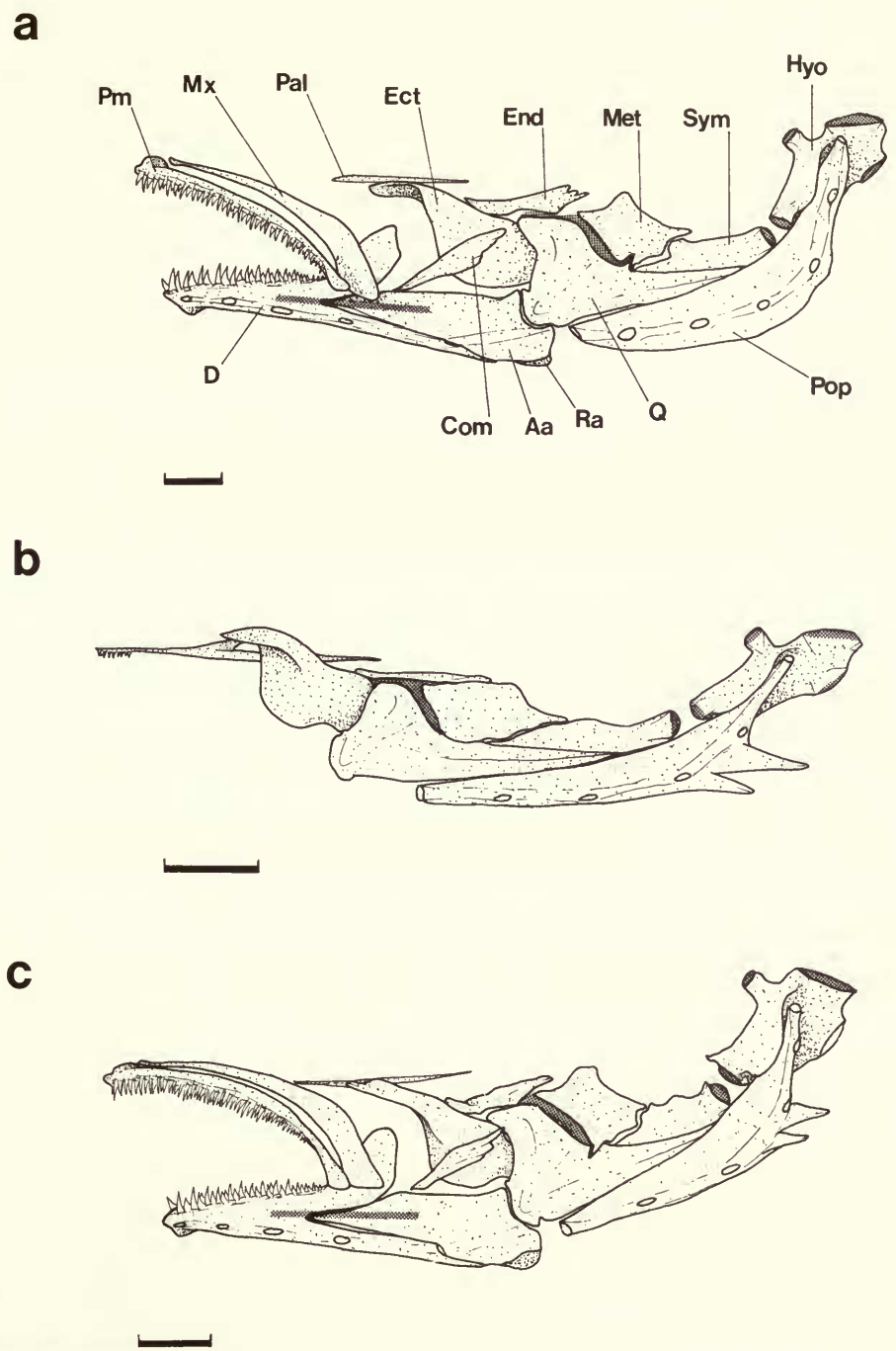

Fig. 50 Left hyopalatine arch, preoperculum and jaw bones in (a) *Mastacembelus frenatus*, (b) *Mastacembelus congicus* (jaw bones not shown) and (c) *Mastacembelus goro*; lateral aspect.

& b). Intraspecific variation in tooth row number is also common; for example a single specimen of *Mastacembelus ellipsifer* has a short toothplate with one row of small caniniform teeth on the left palatine and only a single tooth carried on a very small toothplate, on the right palatine. A specimen of *Mastacembelus vanderwaali* and one of *M. brachyrhinus* have, respectively a single tooth on the left and on the right palatine. Similarly, two teeth are present on the left palatine only of the single specimen of the new *Mastacembelus* species (Fig. 36a & b) from the Cameroonean rapids.

The palatine is connected to the ventrolateral face of the lateral ethmoid in the majority of Asian and in many African species, by a weak, posterodorsally directed spur which ascends from its dorsal edge (see description for *M. mastacembelus,* p. 21). A palatine spur is absent in *Mastacembelus maculatus* (Fig. 26 a & b), *M. pancalus* (Fig. 28 a & b) and the *Macrognathus* species (Figs 29 a & b and 30 a & b) among the Asian mastacembeloids. Among the African species, *Mastacembelus ophidium* (Fig. 43b) is the only East African species lacking a palatine spur, but it is also absent in *Mastacembelus vanderwaali, M. stappersii* and 3 species from the lower Zairean rapids (*M. brichardi, M. aviceps* and *M. crassus;* Fig. 44a–c). Among the West African species a relatively large number, including *Mastacembelus liberiensis, M. goro* (Fig. 50c), *M. longicauda* (Fig. 33a), *M. loennbergii, M. batesii* and *M. brevicauda*, lack the spur.

The palatine spur is thus a relatively constant feature amongst Asian mastacembeloids but has a somewhat mosaic distribution among the African species.

Opercular series

The thinness of the *operculum* (posterior flap), and of the *sub-* and *interopercular* bones are characteristic features of mastacembeloids. Interspecific variation occurs predominantly in the morphology of the *preoperculum*, which shows some intraspecific variability as well. Preopercular features that vary markedly are (1) the number of sensory canal pores, (2) the number of preopercular spines and (3) the relative length of the horizontal limb.

In the Asian and African mastacembeloids the preopercular sensory canal lies within the lateral face of the bone, and opens to the surface *via* a number of circular pores along both the horizontal and vertical limbs.

In most of the Asian species examined there are five sensory canal pores along the ventrolateral face of the bone-enclosed preopercular sensory canal; three on the horizontal limb and two on the vertical limb.

A branched preopercular sensory canal occurs in a number of Asian species. The two posterior pores in the horizontal limb and the ventral pore in the vertical limb of the preoperculum in *Mastacembelus pancalus* and *Macrognathus* species (Fig. 46b & c) lie at the tip of a short descending branch from the main canal. Branched canals are characteristic features of these fishes, associated with the broad, lateral face and relatively short length of the preoperculum. Only two short branches descend from the main canal in *Macrognathus aculeatus* (Fig. 46c) which has a particularly short preoperculum.

The preopercular bones in *Chaudhuria* and *Pillaia* are exceptional amongst mastacembeloids. In *Pillaia* (Fig. 18b) the canal is indistinct and is restricted to the central region of the lateral face of the bone, whereas in *Chaudhuria* (Fig. 18a) there is no canal in the preoperculum.

Based on the number of preopercular canal pores, the African taxa can be divided into two groups *viz.,* those with 5 and those with 4 pores; all the Asian taxa have 5 pores. The African species with 5 pores include half the species found in Lake Tanganyika (*Mastacembelus albomaculatus, M. ellipsifer, M. frenatus, M. moorii, M. ophidium* and *M. platysoma*), as well as *Mastacembelus shiranus, M. stappersii, M. paucispinis, M. reticulatus* and the undescribed species. Almost all the remaining African species have 4 pores, the only exception being 3 species from the lower Zairean rapids, of which *Mastacembelus brachyrhinus,* has 3 and *M. crassus* and *M. aviceps* have 2 pores.

A clearly reductional sequence is manifest in the endemic Zairean rapids species, running from 5 pores in *M. paucispinis*, through 4 in *M. brichardi*, 3 in *M. brachyrhinus*, to 2 pores in the highly derived *M. crassus* and *M. aviceps*. Furthermore, in *M. crassus* and *M. aviceps* the dorsal opening of the preopercular sensory canal does not lie at the tip of the bone but along its posterolateral edge (Fig. 44a & b).

The lack of spines on the preoperculum in *M. mastacembelus* (p. 23) is a feature common to a number of Asian species including *Mastacembelus maculatus*, all *Macrognathus* species, *Mastacembelus sinensis*, *Chaudhuria* and *Pillaia*.

Preopercular spines occur in the other Asian species examined namely *Mastacembelus armatus*, *M. erythrotaenia*, *M. oatesii*, *M. unicolor*, *M. zebrinus* and *M. pancalus*. Although intraspecific variability in the number of spines is common, generally three or four occur in each of these species. This variability may even occur between the number of spines on the left and right preoperculum in the same individual. For example, in a specimen of *M. zebrinus* (Fig. 46a) three spines are present on the left and four on the right side. Considerable variation in preopercular spines also occurs amongst the African mastacembeloids. Many species from east and southern Africa have a single spine, e.g. *Mastacembelus albomaculatus*, *M. moorii*, *M. plagiostomus*, *M. platysoma*, *M. tanganicae* and *M. zebratus*. However, *Mastacembelus cunningtoni* and *M. ellipsifer* are characterised by two spines, while *M. frenatus*, *M. ophidium*, *M. micropectus*, *M. shiranus*, *M. stappersii* and *M. vanderwaali* lack preopercular spines. Spines are absent in the west African *Mastacembelus niger*; a single spine occurs on the left side in one specimen of *M. batesii* and *M. nigromarginatus*. The remaining west African species have two or three spines, as do *Mastacembelus ubangensis* and the undescribed species.

Among the mastacembeloids endemic to the Zairean rapids (Roberts & Stewart, 1976) there appears to be a sequential loss of spines from two in *Mastacembelus paucispinis*, one in *M. brichardi* and *M. brachyrhinus*, to none in the highly derived *Mastacembelus crassus* and *M. aviceps*. Apart from these rapid-dwelling species the number of preopercular spines varying from none to four, appears to have a mosaic distribution among both the Asian and the African mastacembeloid taxa.

The dimensions of the horizontal preopercular limb vary from relatively short and wide (e.g. *Mastacembelus ophidium* and *M. micropectus*, Fig. 43b & c) to long and narrow (e.g. *Mastacembelus vanderwaali* and *M. cunningtoni*) among members of both the Asian and the African mastacembeloids. This variation may be associated with the neurocranial and jaw length.

The vertical limb is generally shorter than the horizontal limb in the majority of mastacembeloids. However, the vertical limb is particularly long in four species from west Africa; *Mastacembelus longicauda*, *M. brevicauda*, *M. nigromarginatus* and *M. reticulatus*.

Hyoid arch

There is remarkably little interspecific variability in the morphology of the hyoid arch. The condition of the arch in *Mastacembelus mastacembelus* (p. 23) is typical of that found generally among both Asian and African members of the suborder.

Variation in the relative length of the *basihyal*, as compared with its condition in *M. mastacembelus* (Fig. 8), occurs in some species. It is relatively short in *Mastacembelus moorii* and *Mastacembelus ophidium* from Lake Tanganyika, having a wide dorsal surface and deep ventral ridge, the former feature giving the bone in *M. moorii* a particularly wide, spatulate surface. The long basihyal in *Mastacembelus erythrotaenia* is distinguished by its relatively narrow dorsal surface and low ventral ridge.

The *anterior* and *posterior ceratohyal* are joined by a series of dentate sutures in all mastacembeloids except *Chaudhuria* (Fig. 20ai) and *Pillaia* (Fig. 20bi). In these taxa a distal flange on the anterior ceratohyal lies in a recess on the posterior face of the posterior ceratohyal; the two elements are connected by a straight suture and a cartilaginous interface.

A variable number of irregular short spikes extend into the cartilaginous interface between

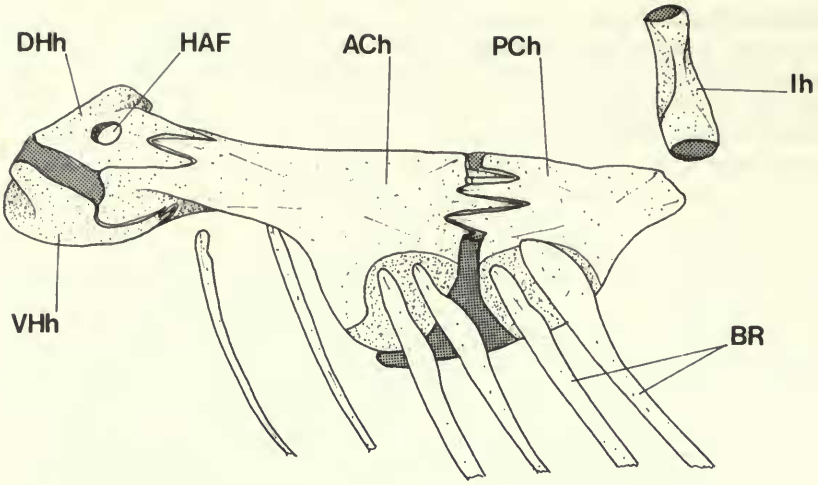

Fig. 51 *Mastacembelus sinensis*, left hyoid arch, in lateral view.

the bones in *Mastacembelus sinensis* (Fig. 51) seemingly a variant of the condition shown by the majority of species.

The *urohyal* shows considerable variation (compared to its condition described in *M. mastacembelus* p. 24), particularly with respect to its length and the arrangement of its posterior, prong-like processes. However, it is in its connection with basibranchial 1 that the most prominent interspecific variation occurs.

A direct connection between the urohyal and basibranchial 1, either by way of an ascending process (or processes) or a synchondral joint (discussed below) occurs in all Asian mastacembeloids except *Mastacembelus sinensis, Chaudhuria* and *Pillaia.* In *M. sinensis* (Fig. 52a) and *Pillaia* the tip of an ascending process on the dorsal surface of the urohyal is connected to the underside of basibranchial 2. In *Chaudhuria* there is neither an ascending urohyal process nor a direct articulation with basibranchial 1.

Since none of the African species has a direct connection between the anterodorsal surface of the urohyal and the ventral edge of basibranchial 1, the process on the urohyal and its connection to basibranchial 1 in the Asian mastacembeloids appears to have resulted in a variety of specific characters.

The urohyal in *Mastacembelus zebrinus* (Fig. 52b) is connected more closely to basibranchial 1 and may represent an intermediate condition between the type of urohyal development seen in *M. mastacembelus* and the direct urohyal–basibranchial 1 articulation in the *Macrognathus* species. The anterodorsal surface of the urohyal in *M. zebrinus* lies directly below the ventral edge of the keel on basibranchial 1 (p. 90). A long, narrow process ascends anterodorsally from the urohyal along the posterior edge of the keel on basibranchial 1. The anterior edge of this process is connected to the posterior edge of the keel, and its tip contacts the ventral surface of basibranchial 2.

Although the urohyal lacks an ascending process in a number of Asian mastacembeloids, these taxa are distinguished by a direct articulation between the anterodorsal surface of the urohyal and the keel on basibranchial 1.

In place of an ascending process in *Mastacembelus pancalus* (Fig. 53a) there is a depression with wide lateral and posterior rims. The ventral edge of basibranchial 1 is cartilaginous and articulates synchondrally with the dorsal surface of this depression in the urohyal.

In *Macrognathus siamensis* (Fig. 53b) the dorsal surface of the urohyal is level but has

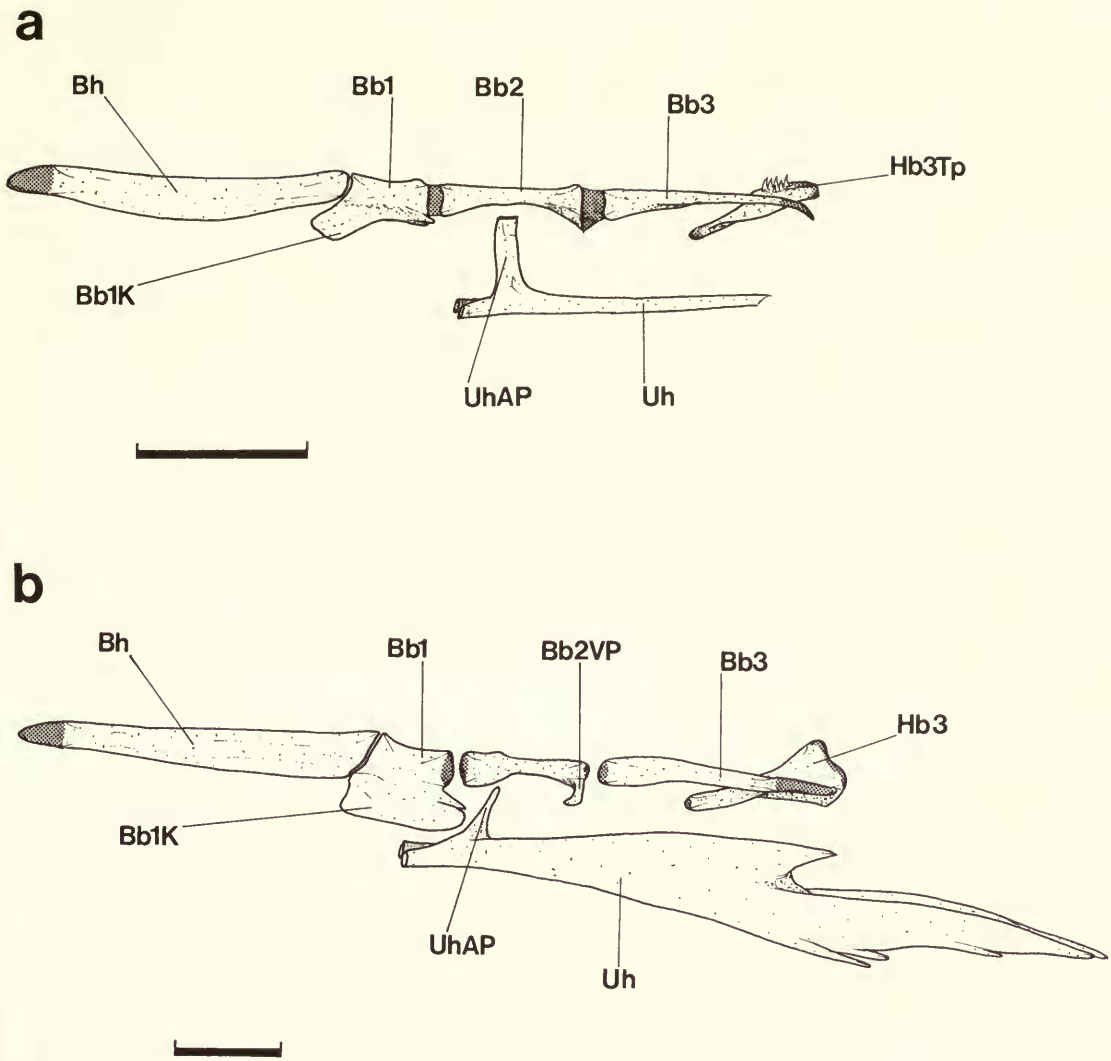

Fig. 52 Basibranchial/urohyal arrangement in (a) *Mastacembelus sinensis* and (b) *Mastacembelus zebrinus*; lateral aspect, left side.

a shallow groove in which the cartilaginous ventral edge of basibranchial 1 articulates. The bifurcated anterior end of the urohyal in *Macrognathus aral* and *Macrognathus aculeatus* (Fig. 53c) forms a shallow longitudinal groove along its dorsal surface in which lies the cartilaginous ventral edge of basibranchial 1. The posterior region of the urohyal in *Mastacembelus pancalus* and the *Macrognathus* species (Fig. 53a–c), generally lacks the prong-like processes that occur in other mastacembeloid taxa. The urohyal in *Mastacembelus oatesii* (Fig. 54) also lacks an ascending process. The anterior tips of the urohyal in this species are particularly deep and form a groove between their medial edges. The ventral edge of basibranchial 1 lies along this groove but it is not cartilaginous, and the elements do not articulate in the manner described for *M. pancalus* and *Macrognathus.* An ascending process (or processes) on the dorsal surface of the urohyal in *Mastacembelus armatus, M. erythrotaenia* and *M. maculatus* is connected to the ventral edge of basibranchial I in an arrangement similar to that in *M. mastacembelus* (p. 24, Fig. 9).

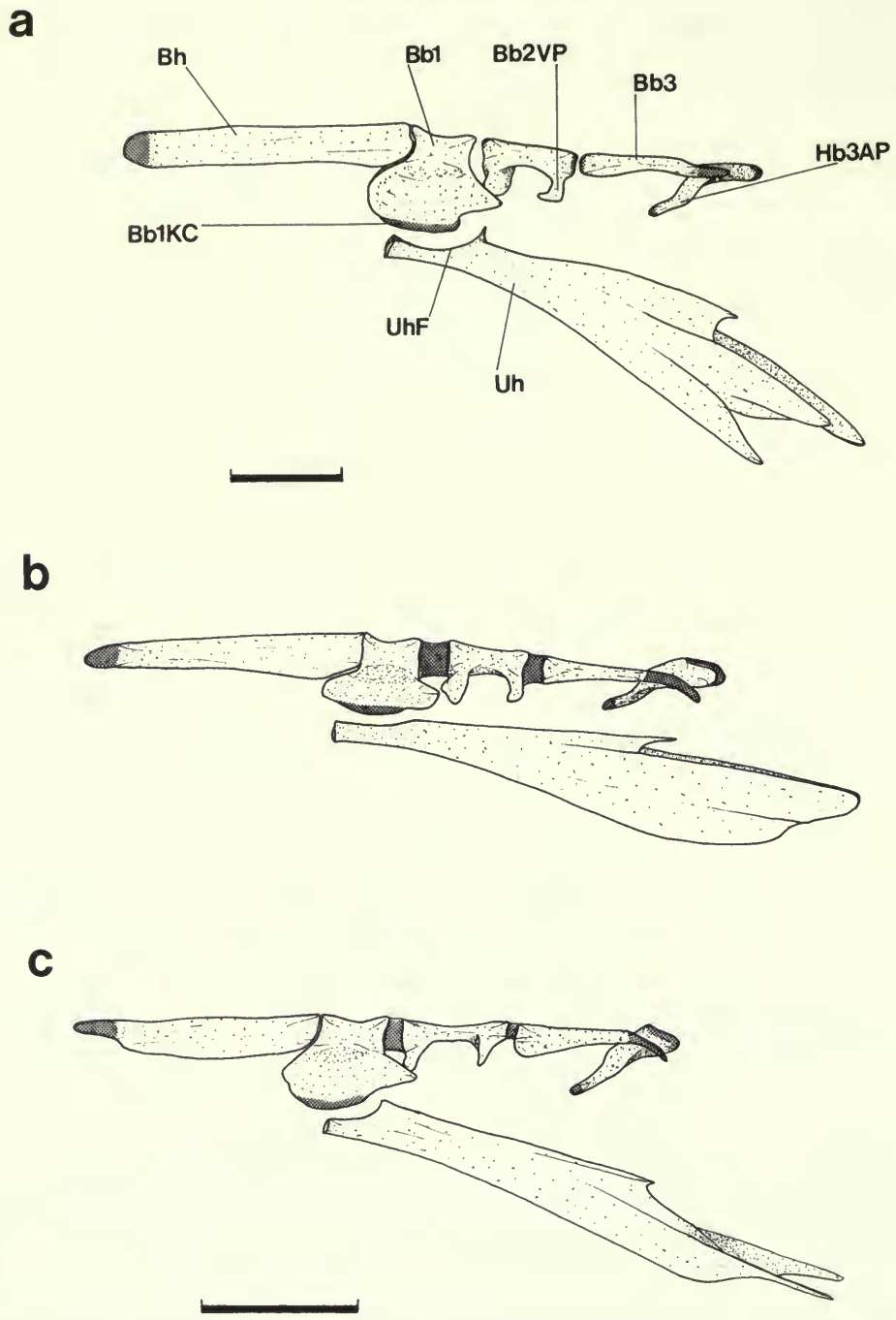

Fig. 53 Basibranchial/urohyal arrangement in (a) *Mastacembelus pancalus,* (b) *Macrognathus siamensis* and (c) *Macrognathus aculeatus*; lateral aspect, left side.

Branchial arches

The basibranchial elements described in *M. mastacembelus* (Fig. 8) are typical of those found throughout the group. The deep ventral 'keel' on *basibranchial 1* is a constant feature of almost all mastacembeloid taxa, but is absent in *Mastacembelus sinensis, Chaudhuria* and

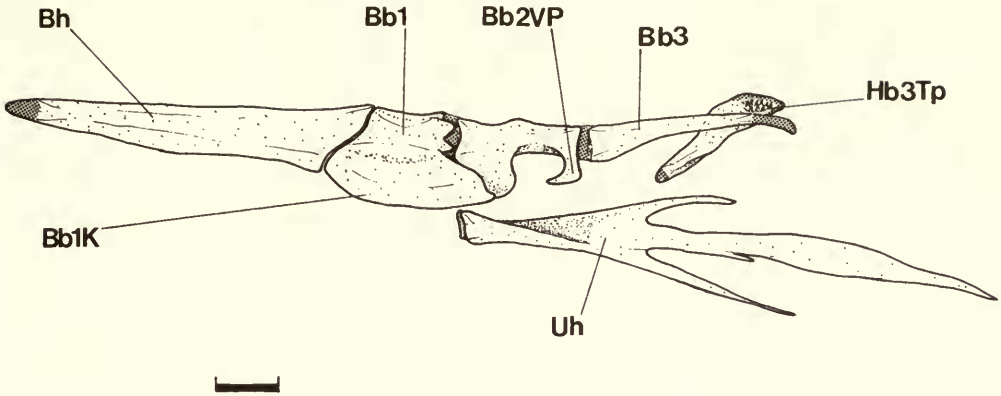

Fig. 54 *Mastacembelus oatesii,* basibranchial/urohyal arrangement; lateral aspect, left side.

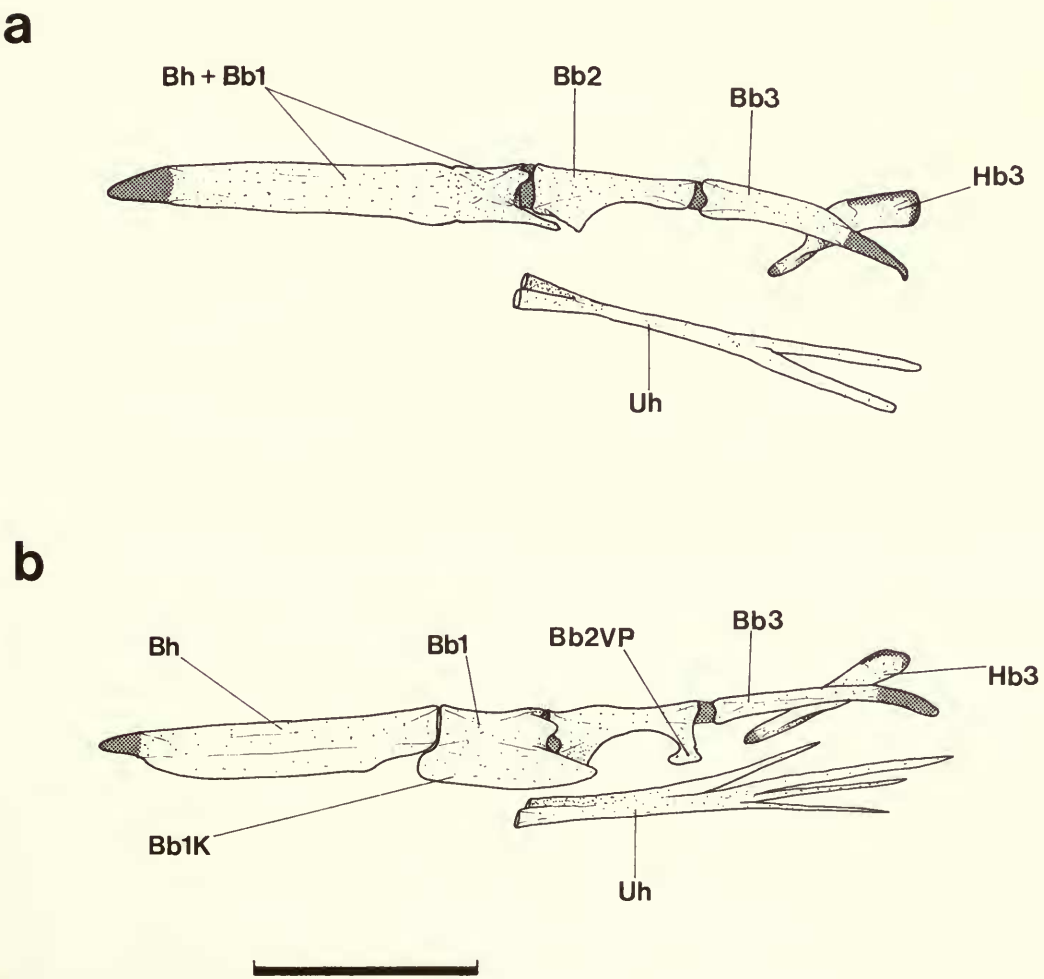

Fig. 55 Basibranchial/urohyal arrangement in (a) *Mastacembelus aviceps* and (b) *Mastacembelus crassus*; lateral aspect, left side.

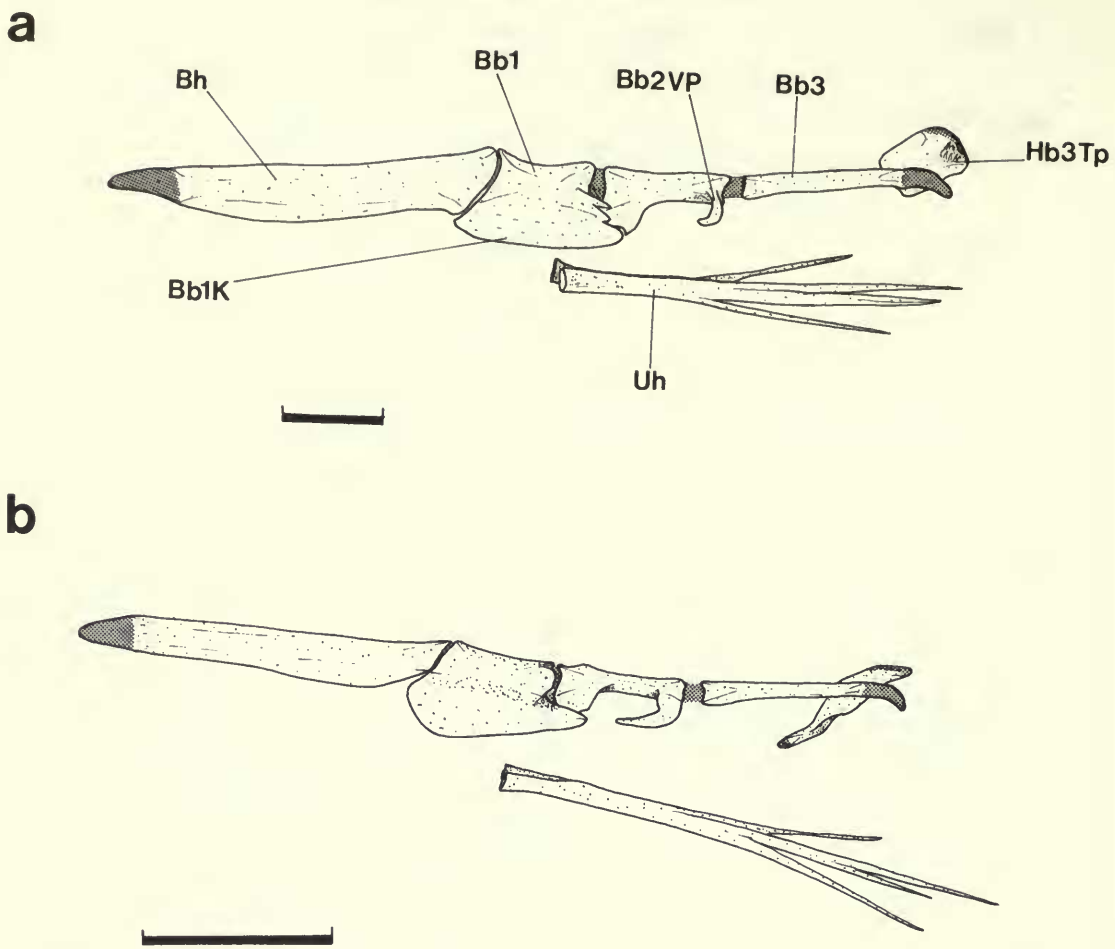

Fig. 56 Basibranchial/urohyal arrangement in (a) *Mastacembelus nigromarginatus* and (b) *Mastacembelus ubangensis*; lateral aspect, left side.

Pillaia (see p. 46). The keel is particularly well-developed in *Mastacembelus pancalus* and *Macrognathus* species (Fig. 53a–c) where the ventral knife-edge is cartilaginous.

The only variation in the 'keel' on basibranchial 1 among the African species is seen in the relatively low 'keel' of *Mastacembelus aviceps* and *M. crassus* (Fig. 55a & b).

A pair of processes, each descending from the posterolateral corner of *basibranchial 2* (as described in *M. mastacembelus* p. 25, Fig. 9), occur in most mastacembeloids. *Mastacembelus sinensis, Chaudhuria* and *Pillaia* among the Asian, and *M. aviceps* among the African species are again exceptional in that they lack these processes.

The tips of the descending processes on basibranchial 2 are connected ligamentously to the posteroventral edge of the keel on basibranchial 1. Part ossification of the ligaments occurs in two African species, *Mastacembelus nigromarginatus* and *Mastacembelus ubangensis* (Fig. 56a & b). Among the west African species each ligament is almost completely replaced by the descending processes arching longitudinally across the ventral surface of basibranchial 2. The anterior tips of the processes in these species contact the keel on basibranchial 1, and a pair of ventral arches of this type are a characteristic feature of *Mastacembelus goro, M. flavomarginatus, M. greshoffi, M. longicauda, M. loennbergii, M. batesii* and *M. brevicauda* (e.g. Fig. 57a–c). The ventral aorta passes longitudinally along the surface of the basibranchial elements and lies between the descending arches on basibranchial 2.

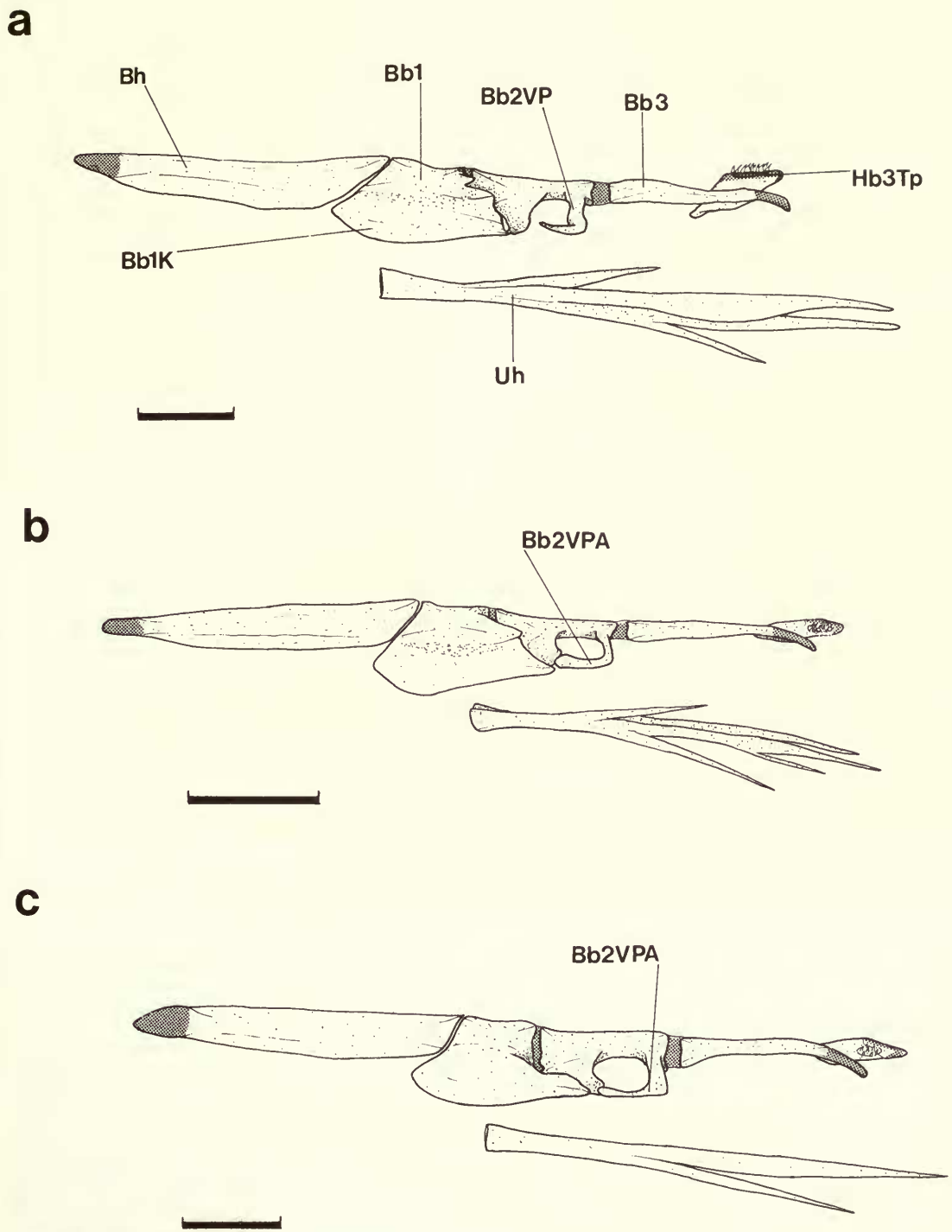

Fig. 57 Basibranchial/urohyal arrangement in (a) *Mastacembelus longicauda,* (b) *Mastacembelus loennbergii* and (c) *Mastacembelus batesii*; lateral aspect, left side.

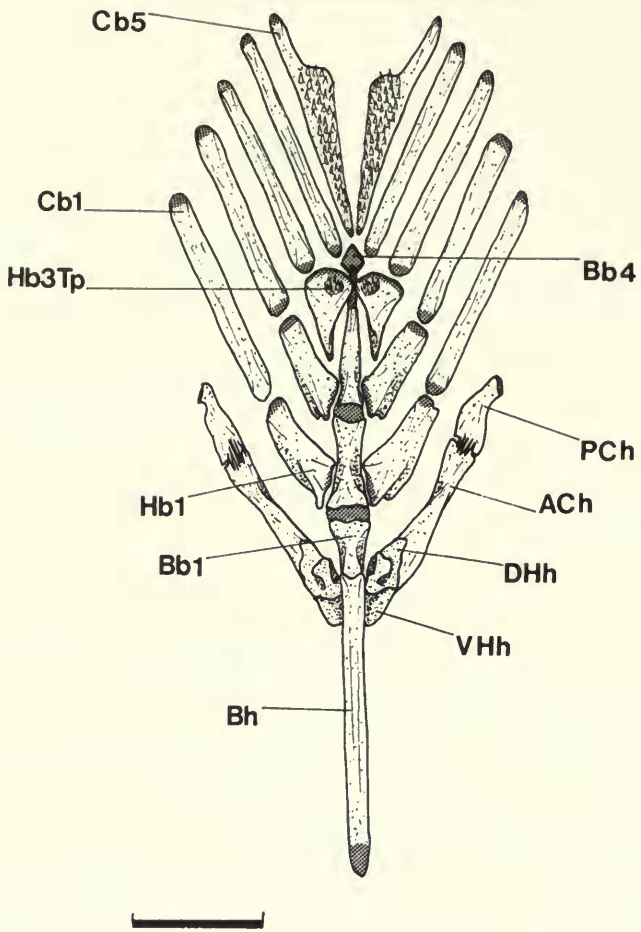

Fig. 58 *Mastacembelus maculatus,* hyoid and lower gill arches in dorsal view.

The first afferent arteries pass between each arch and the ventral surface of basibranchial 2.

There is only slight interspecific variation in the hypobranchial bones, apart from two features of *hypobranchial 3;* the presence of a small toothplate joined to the dorsal surface, and the lack of an anteroventral process extending below hypobranchial 2.

A round toothplate fused to the dorsal surface of hypobranchial 3 (Fig. 58) occurs in the Asian mastacembeloids except *M. mastacembelus* (Fig. 8) and *Pillaia* (Fig. 20bi).

A fused toothplate on hypobranchial 3 is also of frequent occurrence among the African taxa (e.g. Figs 60–63). It is, however, absent in the endemic species from the lower Zairean rapids (i.e. *Mastacembelus paucispinis, M. brachyrhinus, M. brichardi, M. crassus, M. aviceps*), and *Mastacembelus marmoratus, M. niger, M. sclateri, M. ubangensis* and the undescribed species.

The second important feature of hypobranchial 3 is its long anteroventral process. In *M. mastacembelus* this process extends anteriorly below hypobranchial 2 (Fig. 8), with its tip connected ligamentously to basibranchial 2. This process occurs universally among the Asian taxa (e.g. Figs 58 & 59) and in the majority of African species (e.g. Figs 60 & 61). It is absent in a number of species from western Africa, including *Mastacembelus batesii, M. brevicauda, M. flavomarginatus, M. goro, M. greshoffi, M. liberiensis, M. loennbergii, M. longicauda, M. niger, M. nigromarginatus, M. reticulatus* and *M. sclateri* (see Figs 56, 57 & 62). In these species if the anterior edge of hypobranchial 3 is produced at all it is

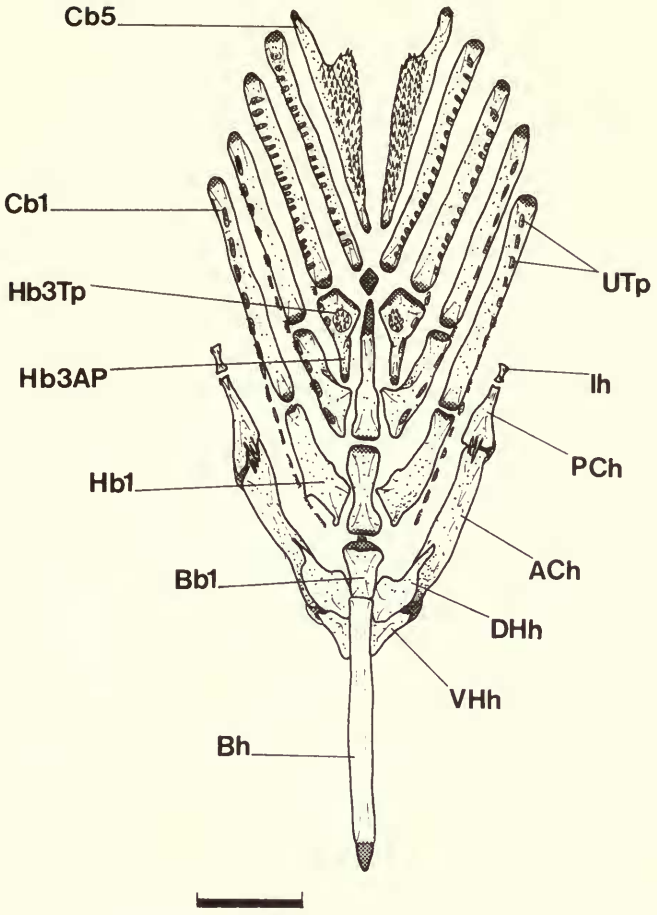

Fig. 59 *Mastacembelus zebrinus,* hyoid and lower gill arches in dorsal view.

in the form of a short stump, (e.g. *M. liberiensis,* Fig. 63); but there is no ligamentous attachment to basibranchial 2.

Ceratobranchial 5 is the only other ventral gill arch element to which a toothplate is fused. Interspecific variation in the dorsal surface area of the toothplate is related to its degree of medial expansion. Compared with *M. mastacembelus* (Fig. 8), it is particularly narrow in *M. maculatus* (Fig. 58), whereas, the Tanganyikan species *Mastacembelus cunningtoni* and *M. tanganicae* (Figs 60 & 61) are distinguished by their wide medial expansion of the toothplate. The toothplate does not contact its partner in the midline in any species.

The dentition of the toothplates fused to the ventral gill arch elements consist of caniniform teeth, tips directed posteriorly, varying interspecifically in size. The small, unfused toothplates irregularly positioned along the length of ceratobranchials 1–4 and hypobranchials 1–3, show considerable inter and intra-specific variation in size and number. When present, the dentition is of small conical teeth (see Figs 59–61).

The dorsal gill arch elements in all taxa lie posterior to the neurocranium, and show a remarkable lack of interspecific variability. The arrangement of the *epibranchial (1–4)* and *pharyngobranchial (2–3)* bones in *M. mastacembelus* (Fig. 10a & b, p. 26) is typical for most mastacembeloids.

Pharyngobranchial 1 is lacking in all mastacembeloids. This may be associated with the posterior position of the dorsal gill arch elements since its absence is a feature common to most eel-shaped fishes (Nelson, 1970). In one specimen of *Pillaia,* pharyngobranchial 2 is

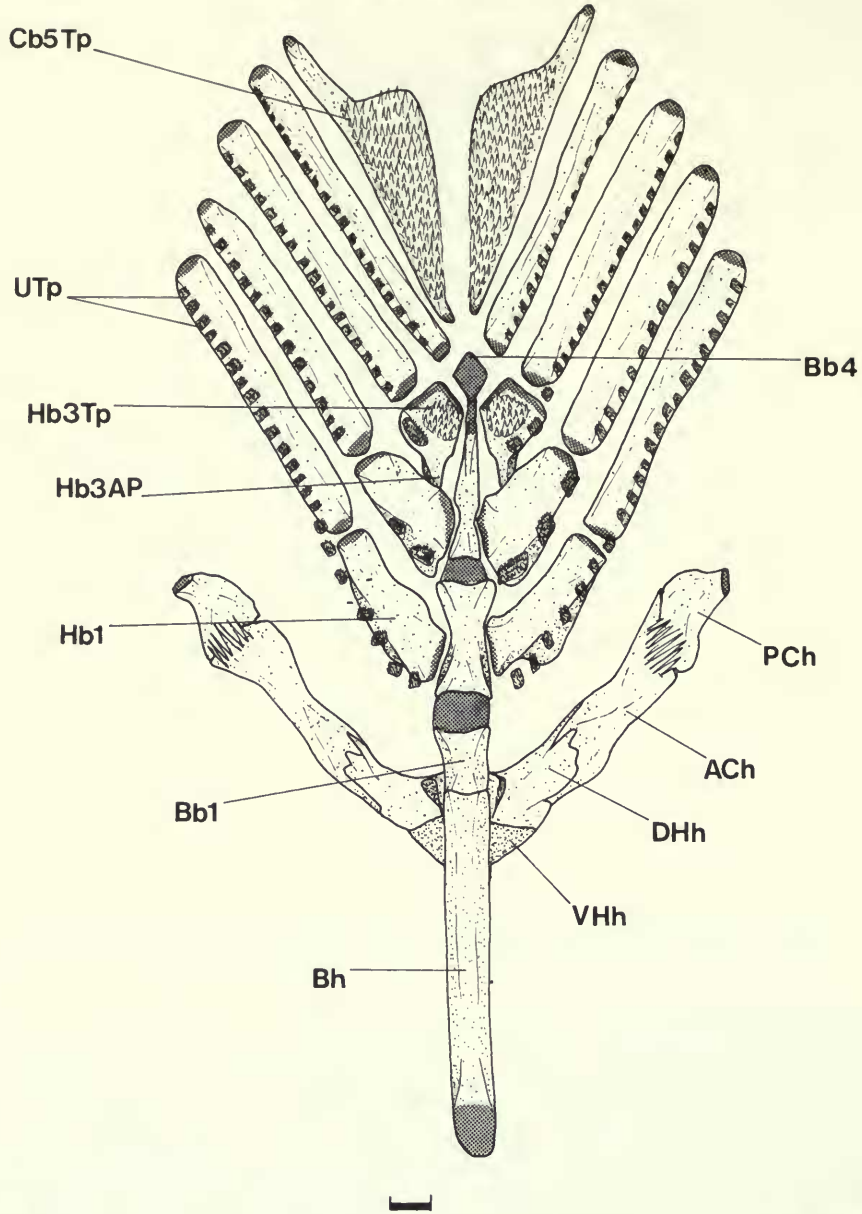

Fig. 60 *Mastacembelus cunningtoni,* hyoid and lower gill arches in dorsal view.

present as a small cartilaginous element within a collagenous strand linking the tips of epibranchials 1 and 2, (a condition generally found only at an early embryonic stage), but in a second specimen a well-developed pharyngobranchial 2 is present (Fig. 20bii).

The anteromedial extension of pharyngobranchial 3, (beyond its point of contact to epibranchial 2) and its connection to the tip of both pharyngobranchial 2 and epibranchial 1, is a feature common to most taxa (as seen in *M. mastacembelus,* Fig. 10a & b). However, pharyngobranchial 3 lacks an anterior extension in *Chaudhuria* (Fig. 20aii) and *Pillaia* (Fig. 20bii); the arrangement of this bone in *M. sinensis* (Fig. 66) appears to be somewhat intermediate between that found in *Chaudhuria* and *Pillaia* and the modal condition. The fourth pharyngobranchial element is invariably cartilaginous in mastacembeloids.

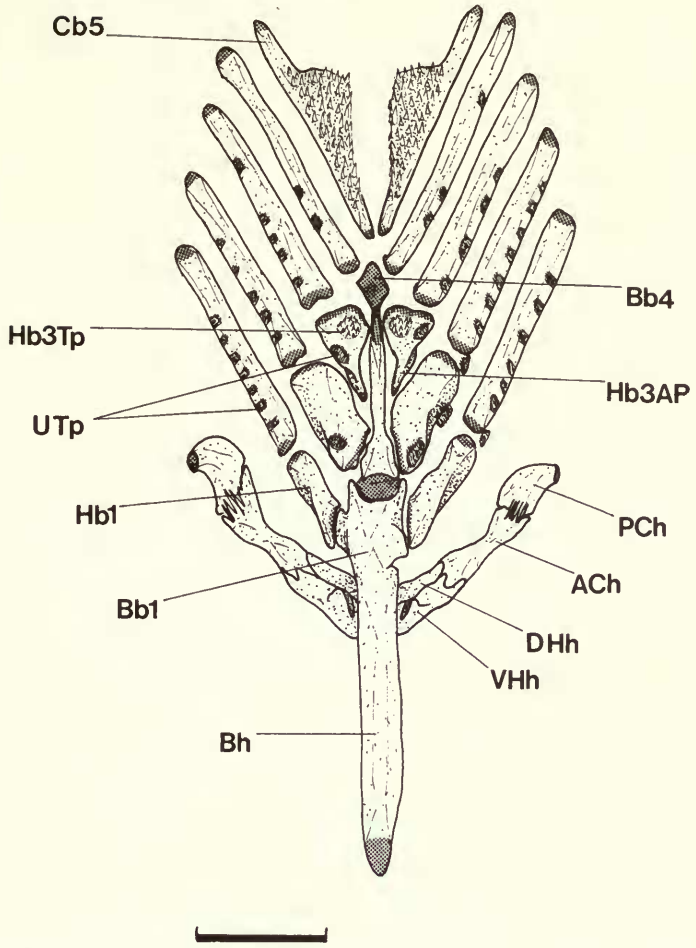

Fig. 61 *Mastacembelus tanganicae,* hyoid and lower gill arches in dorsal view.

The most variable feature of the dorsal gill arch elements is the *unfused toothplates.* Except in *Chaudhuria* and *Pillaia,* small irregularly positioned toothplates lie along the anteroventral face of epibranchials 1 and 2 in all Asian mastacembeloids (Fig. 10a). Amongst the African representatives, Lake Tanganyikan species have similar epibranchial toothplates, (discussed below), but apart from these groups plus *Mastacembelus stappersii* and *Mastacembelus congicus,* plates are absent in African mastacembeloids. The best developed epibranchial dentition occurs in the large, lacustrine, predatory species from Lake Tanganyika (e.g. *M. cunningtoni* and *M. moorii*). In these species the anteroventral edge of epibranchials 1 and 2 is expanded to form a wide bony lip, whose ventral surface supports a series of relatively large toothplates. In a large stained specimen of *M. cunningtoni* (Fig. 64) held at the BM(NH) the toothplate was considered by Nelson (1969: 497) to be fused to epibranchial 1. Close examination of this specimen showed that although the toothplate is indeed tightly connected to epibranchial 1, it can be stripped intact from the overlying bone. In another Tanganyikan species (*Mastacembelus micropectus* Fig. 65) the toothplates are inseparably fused to epibranchial 1.

The pharyngobranchial elements generally support the *fused toothplates* of the dorsal gill arches, and are arranged in a way similar to that described for *M. mastacembelus* (p. 26). A toothplate is generally fused to the ventral surface of pharyngobranchial 2 (as described

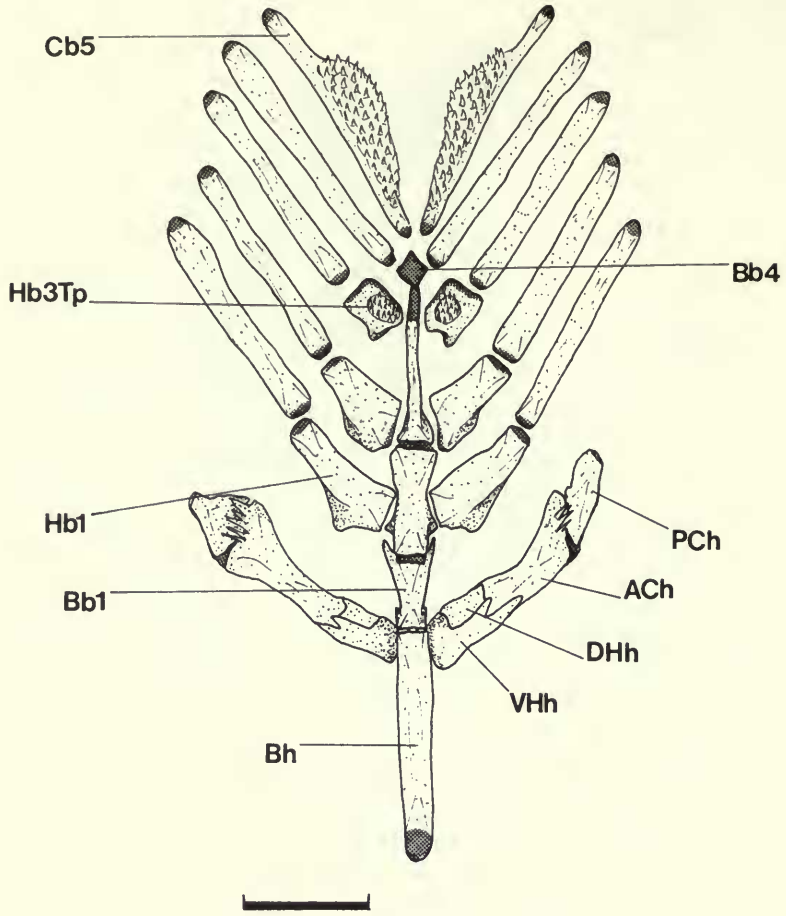

Fig. 62 *Mastacembelus flavomarginatus,* hyoid and lower gill arches in dorsal view.

in *M. mastacembelus* p. 27). Notable exceptions, which lack this toothplate, are the endemic lower Zairean rapids species (*M. paucispinis, M. brachyrhinus, M. brichardi, M. crassus* and *M. aviceps*), *M. marmoratus* and most west African taxa (*M. batesii, M. brevicauda, M. goro, M. greshoffi, M. liberiensis, M. loennbergii, M. longicauda, M. marchii* and *M. niger*). Prominent pharyngobranchial 3 and pharyngobranchial 4 toothplates are features of all mastacembeloids. The dentition on these toothplates, like that on the ventral plates, consists of relatively large caniniform teeth. On the unfused toothplates, the teeth are very much smaller and are usually conical, but are small and caniniform on the large toothplates occurring in the lacustrine species.

Pectoral girdle

The pectoral girdle shows remarkably few interspecific differences, either in overall proportions or in the shape of its constituent bones. The postcranial position of the girdle (adjacent to 3rd and 4th abdominal vertebrae) and the lack of a posttemporal bone connecting it to the neurocranium (as described in *M. mastacembelus* p. 27) are features common to all taxa.

Variation in the ventral limb of the *cleithrum* occurs among the Asian species. The cleithrum has a particularly deep ventrolateral face in *Mastacembelus zebrinus* (Fig. 67). Its ventromedial margin contacts its partner in a median symphysis and gives the pectoral girdle a 'keeled' ventral region. The depth of this keel increases both the surface area

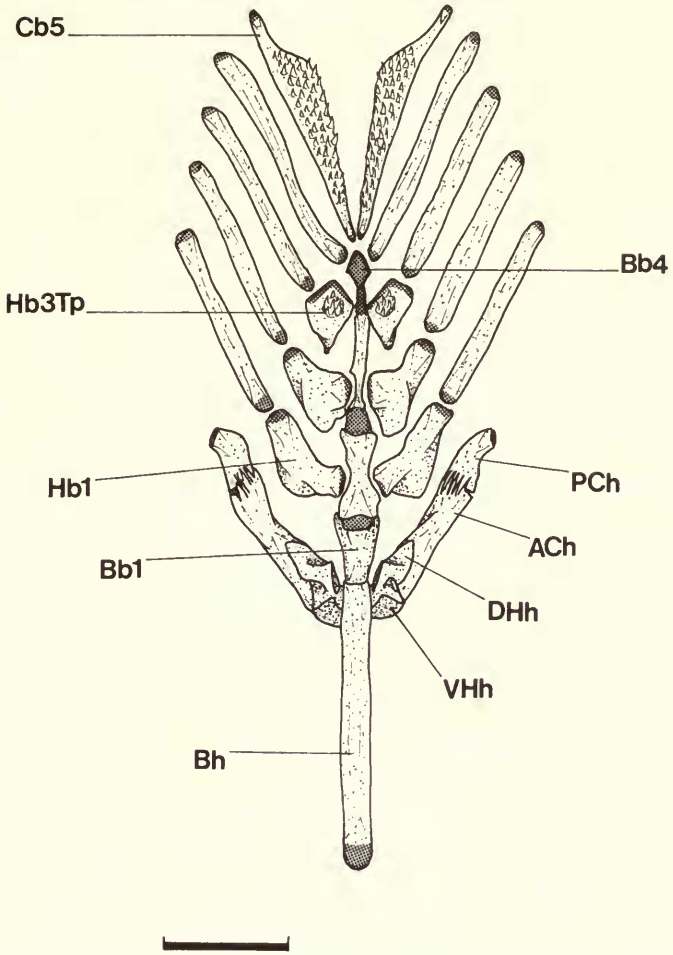

Fig. 63 *Mastacembelus liberiensis,* hyoid and lower gill arches in dorsal view.

available for muscle attachment, laterally, and that of the symphysis between the two halves.

The ventral limb of the cleithrum in *Mastacembelus pancalus* (Fig. 68a) and in the *Macrognathus* species (Fig. 68b) is also deep but proportionally less so than in *M. zebrinus.* The strengthening effect derived from expansion in this region of the girdle may be related to burrowing habits, and in particular the type of burrowing mechanism employed by these taxa (see Part II; Travers, 1984).

A cleithrum with a short, indistinct ventral limb occurs in a number of African taxa including *Mastacembelus brichardi, M. crassus, M. aviceps* (Fig. 69a) from the lower Zairean rapids; *M. micropectus* and *M. plagiostomus* (Fig. 69b) from Lake Tanganyika. In these species the ventral limb of the cleithrum is shallow and this, together with its slight anteroventral curvature, gives the bone a relatively straight overall shape. An accompanying tendency towards reduction of pectoral fin size occurs in these taxa.

The dorsal edge of the cleithrum is serrated in the undescribed *Mastacembelus* species (Fig. 70), *M. nigromarginatus* (Fig. 72) and *M. stappersii*; this contrasts with the smooth edge found in the majority of species.

A postcleithrum is absent in all mastacembeloids.

The *scapula* is pierced by a large foramen which is completely bone enclosed in all Asian taxa as shown for example in *Mastacembelus mastacembelus* (Fig. 11) and the *Macro-*

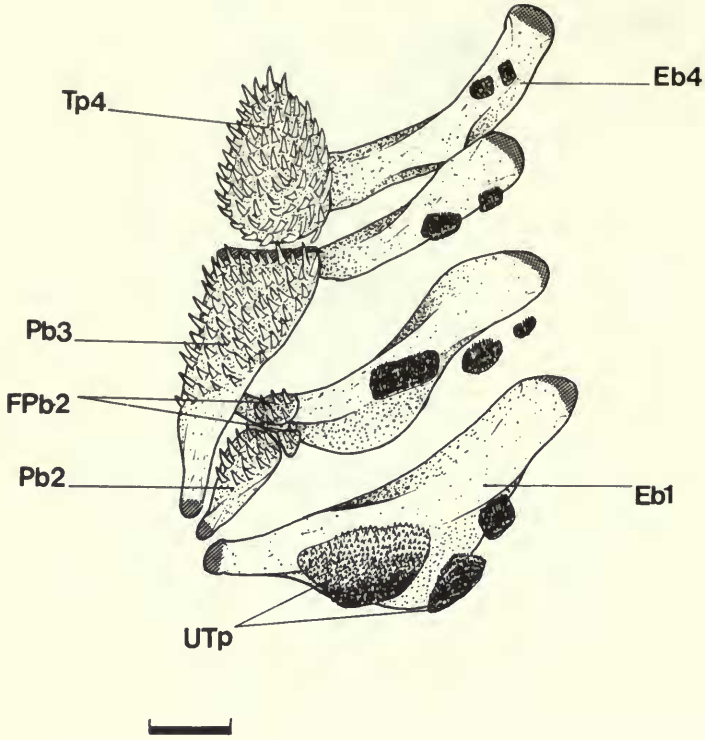

Fig. 64 *Mastacembelus cunningtoni,* upper gill arches; ventral aspect, right side.

gnathus species (Fig. 68b). The anterior edge of the foramen in the majority of African species, however, lies across the anterolateral margin of the bone and is enclosed by cartilage (see Figs 69, 70, 72 & 73).

Four, spool-shaped *radials* occur in all species. The two upper radials articulate with the posterior edge of the scapula, the third with the cartilage interface between it and the *coracoid,* and the fourth with the posterior edge of the coracoid (as described in *M. mastacembelus* p. 28). Radials with bifurcated (or even trifurcated) distal ends occur mosaically. The distal tips of all four radials are bifurcated in *Mastacembelus maculatus* and *M. greshoffi;* the 1st, 2nd and 3rd are bifurcated in *Macrognathus aculeatus* (Fig. 68b); the 2nd and 3rd in *Mastacembelus ophidium;* the 2nd in *M. loennbergii,* while the 2nd and 4th are trifurcated in *M. sinensis* and the 2nd is trifurcated in *M. liberiensis.*

The radials in a juvenile, 4 cm long, specimen of *M. maculatus* (Fig. 71) are cartilaginous and divided along most of their length (apart from the anterior ends), thus giving the appearance of 8 radials (i.e. the primitive teleostean complement: Jarvik, 1980). This suggests that the adult condition of 4 radials results from the fusion of neighbouring pairs of elements during ontogeny. In some cases each pair remains incompletely fused in the adult.

There are interdigiting processes between the radials in *Mastacembelus nigromarginatus* (Fig. 72), whilst in *M. zebrinus, M. brachyrhinus* and the undescribed species the 1st and 2nd radials are coalesced. Such radial fusion also occurs in some *M. tanganicae,* but in other specimens the 1st and 2nd radials are separate, indicating that this feature may be intraspecifically variable. The fusion between radials, the presence of interdigitating processes and, in some specimens, the coalescence of certain radials are all possibly associated with strengthening the pectoral fin base.

The 22 *pectoral fin rays* in *Mastacembelus mastacembelus* (p. 28) are intermediate in number between the highest (26 in *Mastacembelus oatesii*) and lowest (6 in the very small pectoral fin of *Mastacembelus micropectus*; in one individual they are completely lacking).

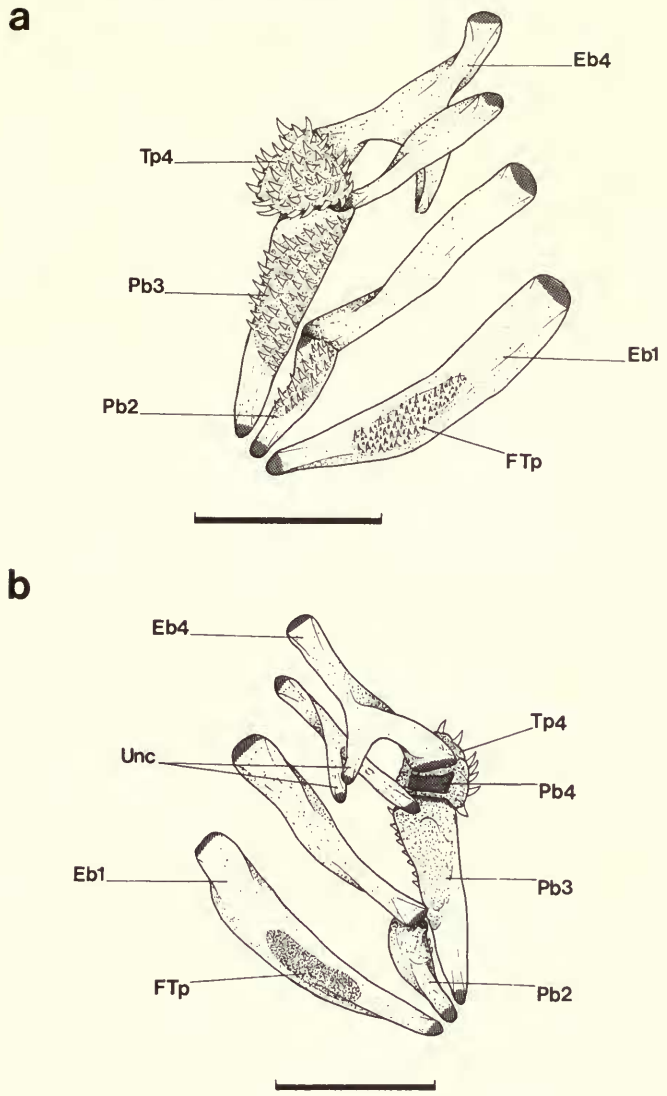

Fig. 65 *Mastacembelus micropectus,* upper gill arches (a) ventral aspect, (b) dorsal aspect; right side.

The pelvic girdle is absent in all mastacembeloids, and apart from *Mastacembelus longicauda* (Fig. 73), no pelvic elements remain. In a specimen of this species a pair of splinter-like bones lie longitudinally between the cleithra and are thought to represent basipterygia.

Vertebral column

There is only slight interspecific variation in the morphology of the *abdominal* and *caudal* vertebrae. The vertebral elements described in *M. mastacembelus* (p. 29) are, in general, typical for most taxa. A hemispherical condyle on the first abdominal centrum (Fig. 12) is present in all mastacembeloids. Wide, laterally compressed neural spines occur on the anterior abdominal vertebrae. These are confined to the first four vertebrae in *M. mastacembelus* (Fig. 12), and in most Asian forms, although the first 6 vertebrae have wide spines in all *Macrognathus* species, and only the first 2 in *Pillaia* (Fig. 21bii).

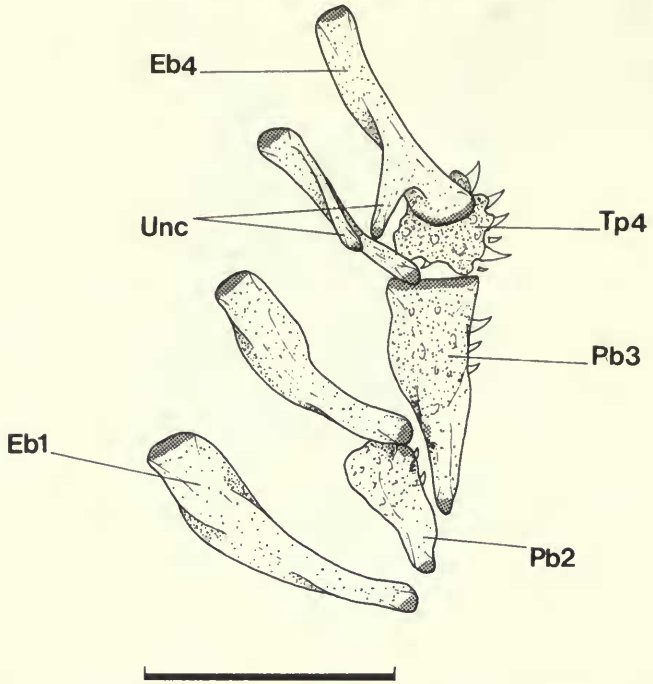

Fig. 66 *Mastacembelus sinensis,* upper gill arches; dorsal aspect, right side.

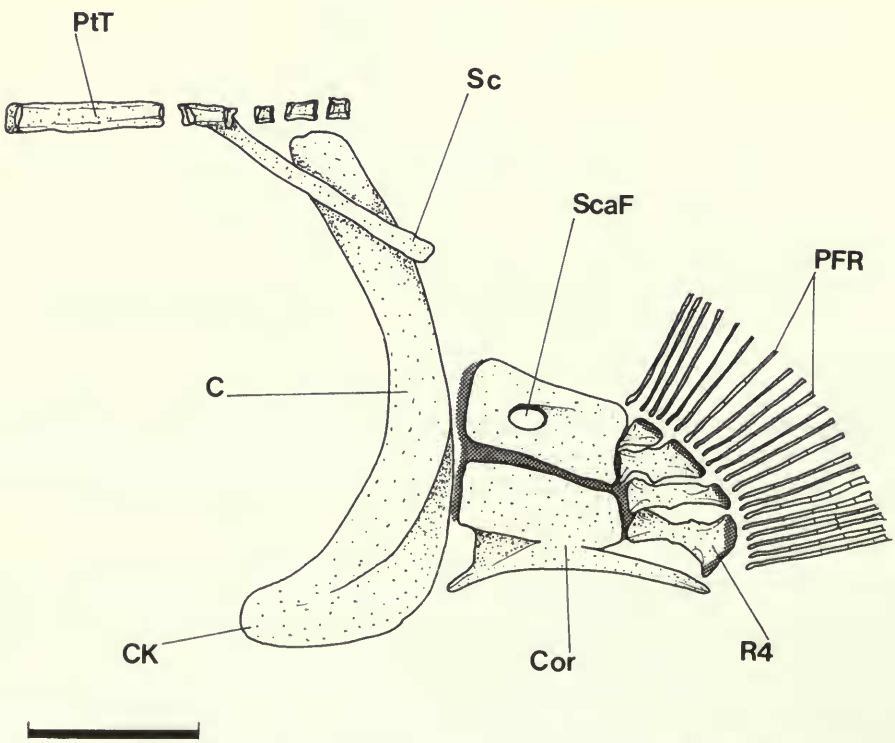

Fig. 67 *Mastacembelus zebrinus,* pectoral girdle; lateral aspect, left side.

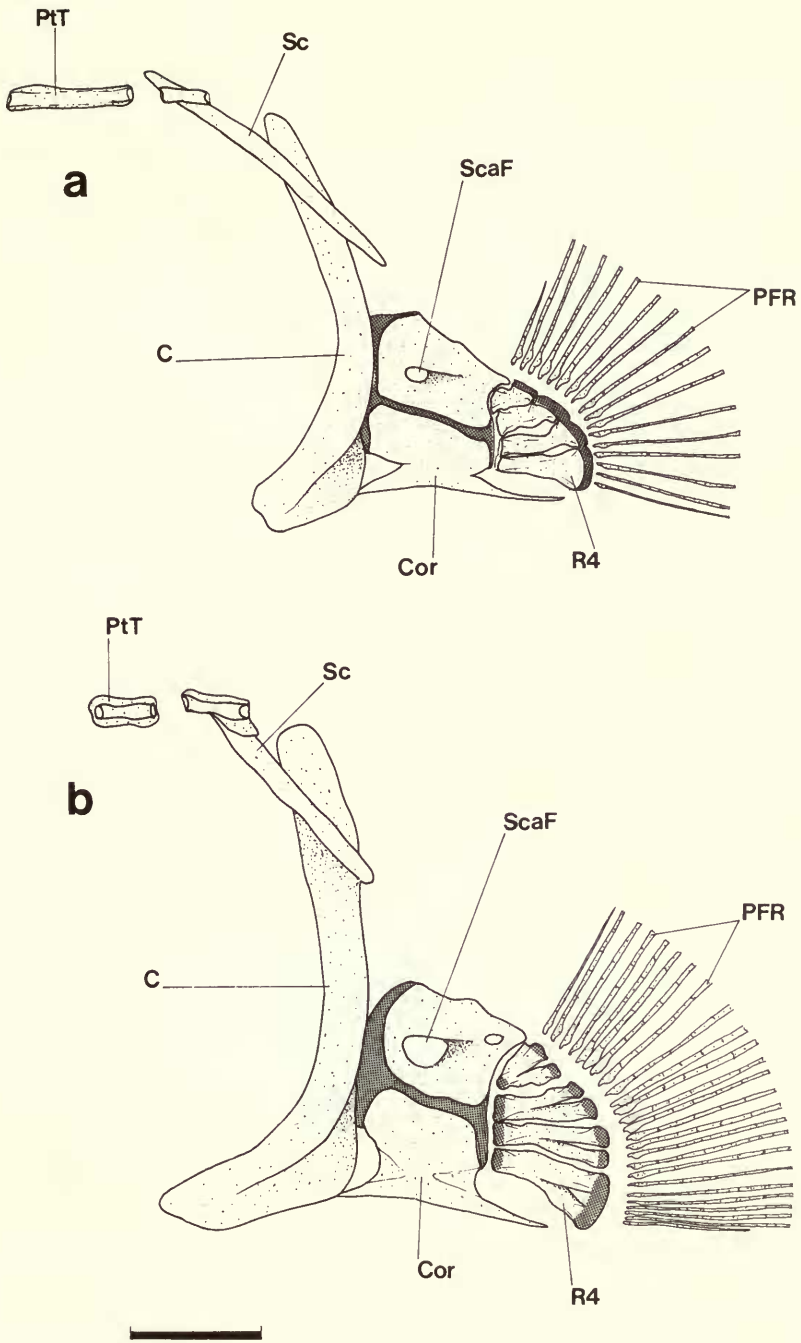

Fig. 68 Pectoral girdle in (a) *Mastacembelus pancalus*, and (b) *Macrognathus aculeatus*; lateral aspect, left side.

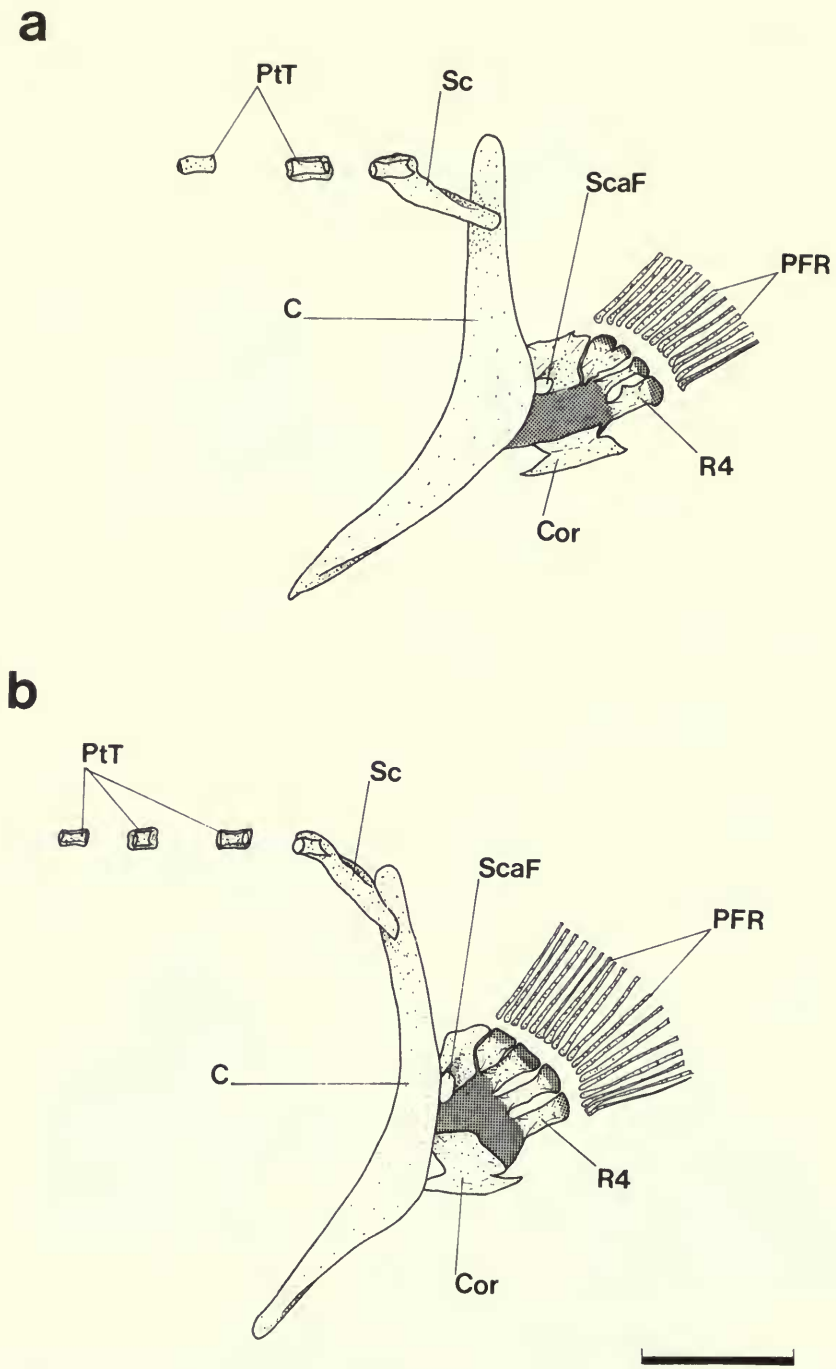

Fig. 69 Pectoral girdle in (a) *Mastacembelus aviceps*, and (b) *Mastacembelus crassus*; lateral view, left side.

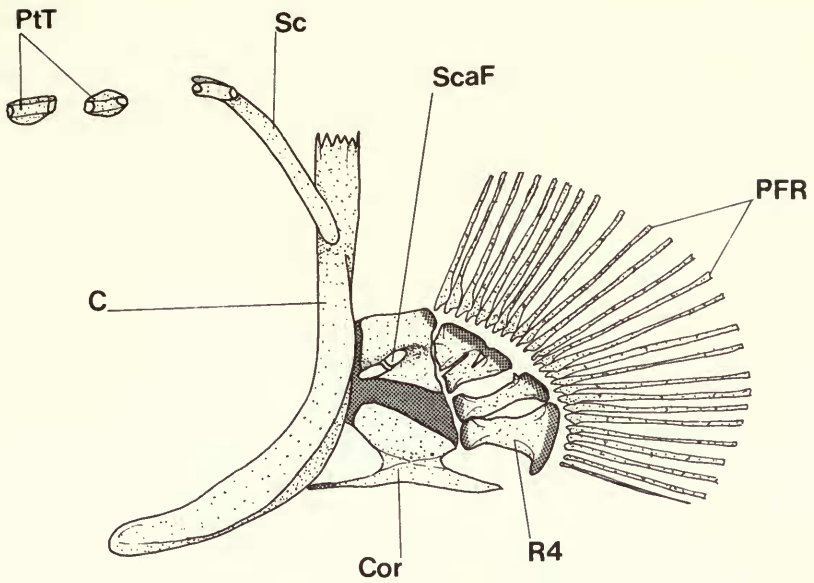

Fig. 70 Pectoral girdle in the undescribed *Mastacembelus* species; lateral aspect, left side.

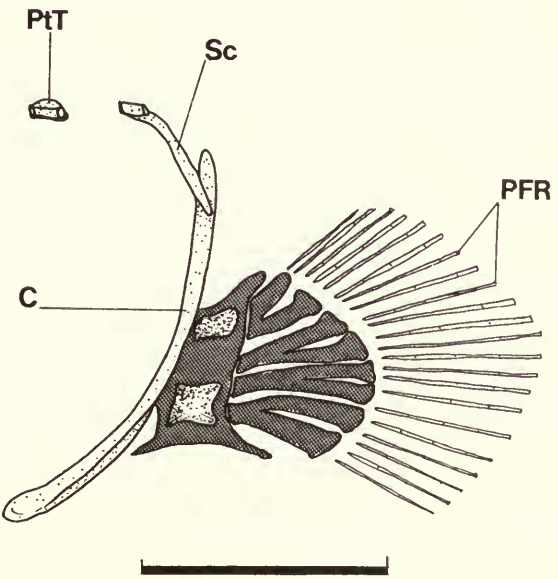

Fig. 71 Juvenile *Mastacembelus maculatus* (S.L.4 cm.) pectoral girdle; lateral aspect, left side.

In the African species wide neural spines are typically developed on the first 5 or 6 abdominal vertebrae. The first 8 vertebrae have wide neural spines in the west African *Mastacembelus loennbergii* and *M. reticulatus* and there are 9 such spines in *M. marmoratus* from Congo.

Anteroposteriorly expanded neural and haemal spines may also occur and are particularly prominent on all posterior caudal vertebrae in the 4 lacustrine species, *Mastacembelus ellipsifer, M. frenatus, M. moorii* and *M. ophidium* (discussed below). Elongated, narrow

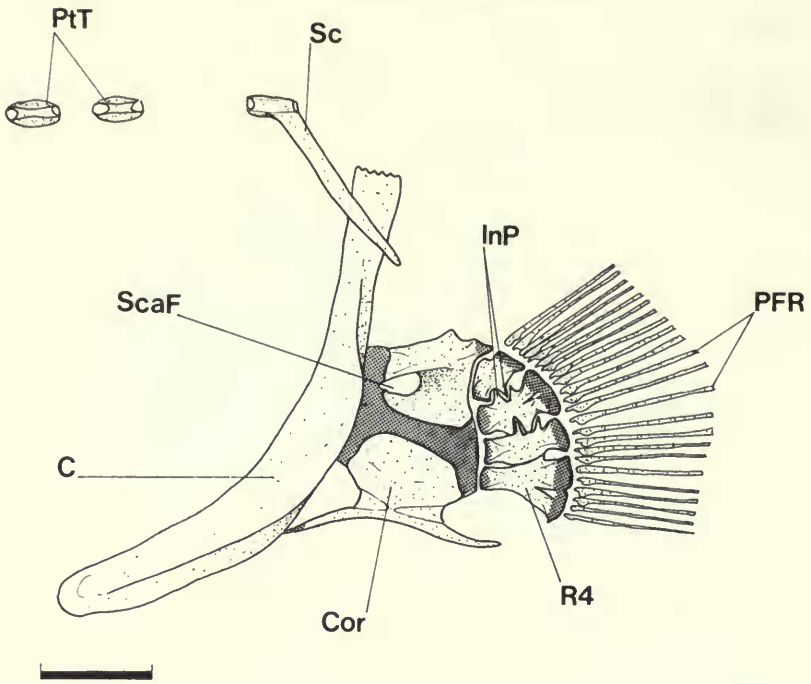

Fig. 72 *Mastacembelus nigromarginatus,* pectoral girdle; lateral view, left side.

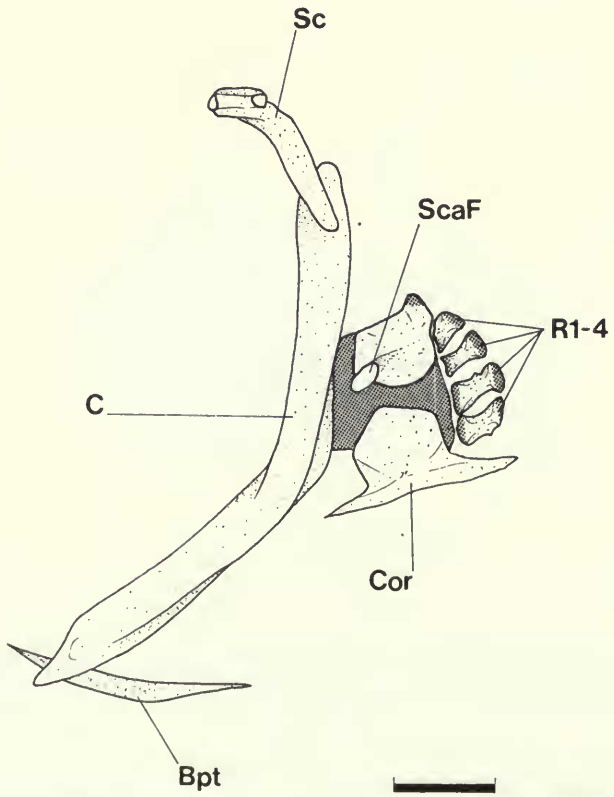

Fig. 73 *Mastacembelus longicauda,* pectoral girdle; lateral aspect, left side.

neural and haemal spines are found in some Asian taxa, including *Mastacembelus pancalus, M. zebrinus, M. keithi, M. caudiocellatus* and *Macrognathus* species (see Part II). The length of their spines gives these taxa a characteristic deep-bodied appearance.

The asymmetry of the centra as described in *M. mastacembelus* (p. 30) is a feature common to all Asian and African taxa examined.

The trend towards elongation, manifest by the skull, is continued postcranially by the relatively high numbers of abdominal and caudal vertebrae. The emphasis on elongation of the body in these taxa, through an increase in the number of vertebrae, is also associated with considerable interspecific variation in the numbers of abdominal and caudal vertebrae (Table 5). The number of abdominal vertebrae in *M. mastacembelus* is 38 (p. 29) and is modal for the majority of Asian and African species.

The lowest number of abdominal vertebrae recorded in any taxon is 25, in *Chaudhuria* and *Mastacembelus aviceps* and the highest 42, in *M. batesii.* The caudal vertebrae show a greater difference between their minimum, (36 in *M. pancalus*) and maximum (70 in *Mastacembelus liberiensis*) numbers. Many Asian taxa are distinguished by their relatively low number of abdominal and caudal vertebrae (see Table 5). These include *Mastacembelus pancalus* and to a lesser extent *M. zebrinus, M. keithi* and *M. caudiocellatus* and the *Macrognathus* species. These species are also outstanding among the mastacembeloids for the relatively greater length of their haemal and neural spines.

A low vertebral count also distinguishes a number of African species including *Mastacembelus albomaculatus, M. micropectus, M. plagiostomus, M. platysoma, M. tanganicae* and *M. zebratus* from Lake Tanganyika, and *M. brachyrhinus, M. brichardi, M. crassus* and *M. aviceps* from the lower Zairean rapids. The low vertebral number in these species is associated with other reductional trends seen in the rapids fishes and the crevice-living Tanganyikan species.

Other Tanganyikan species have a high vertebral count e.g. *Mastacembelus cunningtoni, M. ellipsifer, M. moorii,* and *M. ophidium,* as do many non-Tanganyikan species e.g. *M. liberiensis, M. longicauda, M. loennbergii, M. ansorgii* and *M. cryptacanthus,* and to a lesser degree such forms as *M. paucispinis* and the new species (Table 5). These taxa are distinguished by the marked difference between the number of abdominal and caudal vertebrae, and in having a long and tapered body. In some of these species (*M. moorii, M. ophidium, M. ellipsifer,* and also in *M. frenatus*) the neural and haemal spines on the posterior caudal vertebrae (as many as the last 25) are wide and blade-like.

On several occasions *Mastacembelus moorii* was observed swimming at approximately 10–15 m above the substrate in Lake Tanganyika (pers. obs.) and the unusual condition of the neural and haemal spines on its caudal vertebrae may possibly be a modification related to its habit of midwater swimming.

The endemic Lower Zaire River mastacembeloid fauna shows a reversal of the general trend towards a greater number of caudal vertebrae seen in the African mastacembeloids. Among these Zairean species there is a decrease in numbers of caudal vertebrae from 53 in *M. paucispinis* to 38 in *M. aviceps.*

Epicentral ribs occur on only the first vertebra in *Chaudhuria* (Fig. 21aii) and *Pillaia* (Fig. 21bii), but apart from these taxa are generally found in the arrangement described in *M. mastacembelus* (p. 29).

Epipleural ribs are confined to the fourth abdominal vertebra in *M. mastacembelus* (Fig. 12), an arrangement found in most Asian species although they are present on the third abdominal vertebra in *Mastacembelus sinensis,* and are absent in *Chaudhuria* and *Pillaia.* In the majority of African taxa epipleural ribs are confined to the fourth or fifth abdominal vertebra, but in a number of species from Lake Tanganyika, Zaire and West Africa they are absent.

Interspecific variation in the *pleural ribs,* apart from slight variation in length, is limited to differences in the point at which the ribs first appear. Pleural ribs are absent from the first 3 abdominal vertebrae in *M. mastacembelus* (Fig. 12), and this arrangement is typical for most Asian taxa as well, although in *Mastacembelus sinensis, M. pancalus* and *M.*

Table 5 Number of vertebrae, spinous and branched rays in mastacembeloid taxa.

	Vertebrae		Spinous rays		Branched rays	
	Abdominal	Caudal	Dorsal	Anal	Dorsal	Anal
Oriental mastacembeloid taxa						
Mastacembelus alboguttatus	38	47	37	3	84	83
Mastacembelus armatus	38	50	34	3	78	80
Mastacembelus caudiocellatus	37	44	34	3	68	68
Mastacembelus circumcinctus	30	47	28	3	59	68
Mastacembelus erythrotaenia	38	45	32	3	73	67
Mastacembelus guentheri	38	51	35	3	69	72
Mastacembelus keithi	31	42	32	3	54	59
Mastacembelus maculatus	32	44	26	3	56	61
Mastacembelus mastacembelus	38	47	35	3	73	75
Mastacembelus pancalus	28	36	25	3	36	41
Mastacembelus sinensis	36	44	33	3	68	65
Mastacembelus unicolor	38	48	35	3	74	77
Mastacembelus zebrinus	32	42	31	3	56	58
Macrognathus aculeatus	32	38	14	3	51	51
Macrognathus aral	32	39	21	3	55	54
Macrognathus siamensis	35	40	15	3	60	58
Chaudhuria caudata	25	46	Absent		40	42
Pillaia indica	28	37	Absent		34	36
African mastacembeloid taxa						
Mastacembelus albomaculatus	38	44	37	3	65	64
Mastacembelus ansorgii	37	63	32	3	111	102
Mastacembelus aviceps	25	38	22	2	47	52
Mastacembelus batesii	42	54	33	2	78	78
Mastacembelus brachyrhinus	33	45	31	3	68	72
Mastacembelus brevicauda	40	58	30	2	86	97
Mastacembelus brichardi	32	42	29	3	57	61
Mastacembelus congicus	34	53	29	3	85	91
Mastacembelus crassus	22	44	19	2	52	61
Mastacembelus cryptacanthus	38	65	34	2	118	125
Mastacembelus cunningtoni	33	56	30	3	88	90
Mastacembelus ellipsifer	36	52	33	3	83	86
Mastacembelus flavidus	38	58	37	3	85	75
Mastacembelus flavomarginatus	39	50	27	2	75	85
Mastacembelus frenatus	40	55	35	3	78	77
Mastacembelus goro	40	49	31	3	69	72
Mastacembelus greshoffi	39	56	30	2	130	122
Mastacembelus liberiensis	33	70	28	3	131	124
Mastacembelus loennbergii	38	63	30	2	123	125
Mastacembelus longicauda	38	66	27	3	114	120
Mastacembelus marmoratus	39	50	31	3	70	66
Mastacembelus micropectus	32	50	30	3	72	78
Mastacembelus moorii	33	63	28	3	110	102
Mastacembelus niger	40	51	29	3	74	73
Mastacembelus nigromarginatus	37	56	29	2	91	82
Mastacembelus ophidium	29	66	27	1	104	108
Mastacembelus paucispinis	28	53	9	3	120	85
Mastacembelus plagiostomus	40	48	33	3	59	66
Mastacembelus platysoma	29	42	25	3	66	63
Mastacembelus reticulatus	40	56	30	2	95	92
Mastacembelus sclateri	32	52	26	3	73	75
Mastacembelus shiranus	34	49	29	3	79	86

Table 5 Continued.

	Vertebrae		Spinous rays		Branched rays	
	Abdominal	Caudal	Dorsal	Anal	Dorsal	Anal
Mastacembelus signatus	32	54	29	3	80	82
Mastacembelus stappersii	38	58	33	3	82	87
Mastacembelus tanganicae	39	48	42	3	67	73
Mastacembelus vanderwaali	32	50	24	3	64	65
Mastacembelus zebratus	28	44	26	3	52	56
Mastacembelus sp. nov.	32	56	15	3	112	95

N.B. Numbers shown do not represent statistical samples. For mean number of vertebrae, spinous and branched rays in Oriental *Mastacembelus* species see Sufi, 1956; for frequency distribution of vertebrae and dorsal spinous rays in *Macrognathus* species see Roberts, 1980.

maculatus ribs are only absent on the first 2 vertebrae. In the African taxa pleural ribs tend to be absent from the first 3 or 4 vertebrae, although they are wanting on the first 5 centra in *M. frenatus, M. platysoma, M. vanderwaali* and *M. ubangensis.*

The greatest reduction in the number of pleural ribs, however, is seen in members of the Tanganyikan and Zairean faunas. In these species ribs are absent from as many as the first 20 abdominal vertebrae e.g. *M. albomaculatus* (16), *M. moorii* (16) and *M. micropectus* (14) from Lake Tanganyika, and *M. brachyrhinus* (20), *M. brichardi* (18), *M. crassus* (16) and *M. aviceps* (15) from the lower Zairean rapids.

Dorsal and anal fins

The morphology of the spinous and branched rays, and their supporting pterygiophores is constant in the mastacembeloids but there is considerable inter- and intra-specific variation in the total numbers of these elements (see Table 5 and Sufi, 1956 for morphometric data of Oriental species).

A long row of isolated *dorsal spinous rays* occurs in most mastacembeloids. In *M. mastacembelus* 35 spines extend from the level of the fourth abdominal to the third caudal vertebrae. This posterior extension of the spines across the abdominal/caudal vertebral junction is a common mastacembeloid feature.

Mastacembelus mastacembelus and several other Asian species (including *M. alboguttatus, M. armatus, M. erythrotaenia, M. oatesii* and *M. unicolor*) have high numbers of dorsal spines compared with the number in most Asian taxa (see summary of fin-ray numbers in Sufi, 1956: 108). A low number of spines does not appear to be related to the number of abdominal vertebrae (see below).

The *Macrognathus* species are distinguished from other Asian mastacembeloids by their relatively few dorsal spines; 21 in a specimen of *M. aral,* 15 (plus 1 predorsal; discussed below) in a specimen of *M. siamensis* and 14 in a specimen of *M. aculeatus* (see Roberts, 1980, table 2 for frequency distributions of dorsal spine counts in *Macrognathus*). Although, this number is under half that in *M. mastacembelus,* and although *Macrognathus* does not have significantly fewer abdominal vertebrae or vertebrae of significantly different proportions, the dorsal spines in all *Macrognathus* species also extend across the abdominal/caudal vertebral junction. Consequently, dorsal spines are not present above the anterior abdominal vertebrae, a characteristic feature of *Macrognathus* species. Spines are absent from above the first 18 abdominal vertebrae in the specimens of *M. aculeatus* and *M. siamensis* examined and from above the first 13 abdominal vertebrae in the specimen of *M. aral* (Roberts, 1980 also gives the frequency distributions of predorsal vertebral counts in *Macrognathus*; his table 4).

Dorsal and anal spines are absent in *Chaudhuria* and *Pillaia.*

Twenty-five to 35 dorsal spines are present in the majority of African species (Table 5). Two members of the Tanganyikan fauna (*Mastacembelus albomaculatus* and *M. flavidus*) have 37 dorsal spines, and a third species, *M. tanganicae* has 42, the maximum number found in any mastacembeloid.

The dorsal spines in the African species, regardless of their total number, originate from above the fourth, fifth or sixth abdominal vertebra, and extend across the abdominal/caudal vertebral junction.

Low numbers of dorsal spines are found in several of the rapids dwelling African species (see Table 5). *Mastacembelus paucispinis* (as its name implies), and the undescribed species, have exceptionally few, only 9 (plus 1 predorsal) occurring in *M. paucispinis* and 15 in the single specimen of the new species. Their spines extend posteriorly from above about the fourth or sixth abdominal vertebrae, but do not cross the abdominal/caudal vertebral junction. Associated with this exceptional arrangement of the dorsal spines there is a long rayed dorsal fin extending forward across the abdominal/caudal vertebral junction to a point close behind the last spine.

The low number of dorsal spines in *M. paucispinis* and the undescribed species may be the result of rays not developing into spines or the result of posterior spine loss (i.e. conversion of spines into rays; possibly a response to life in rapids), whereas, the small number in *Macrognathus* (where the spines lie posteriorly and cross the abdominal/caudal vertebral border) appears to be the result of anterior spine loss.

The first dorsal spine in *Mastacembelus ubangensis* and *M. marmoratus,* as well as in some West African species (e.g. *M. batesii, M. brevicauda, M. flavomarginatus, M. goro, M. loennbergii, M. longicauda M. niger* and *M. reticulatus*) is situated relatively far back along the vertebral column, at about the level of the ninth to twelfth vertebrae.

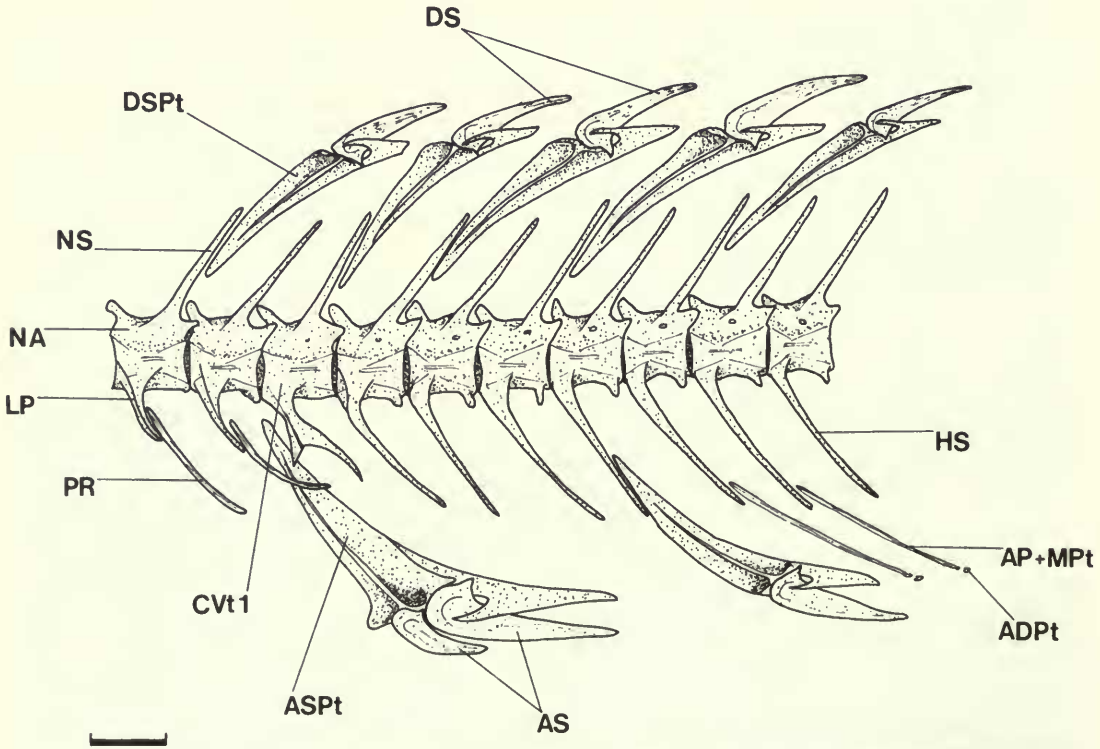

Fig. 74 *Mastacembelus sinensis,* abdominal/caudal vertebral junction and associated dorsal and anal spines; lateral view, left side.

Three *anal spinous rays* occur in all Asian mastacembeloids (apart from *Chaudhuria* and *Pillaia*).

The third anal spine in *M. sinensis* (Fig. 74) is equal in size to the large second anal spine. It is separated from that spine by a gap equal to 4 caudal vertebrae. This arrangement is atypical for the mastacembeloids and is found only in *M. sinensis*.

Three anal spines also occur in the majority of African taxa. However, a single spine is characteristic of *Mastacembelus ophidium,* and 2 anal spines occur in the Zairean rapids' species *M. crassus* and *M. aviceps,* and in a number of west African species including, *M. batesii, M. brevicauda, M. flavomarginatus, M. greshoffi, M. loennbergii, M. nigromarginatus* and *M. reticulatus* (Table 5).

A small bone (predorsal *sensu* Smith & Bailey, 1961), resembling the pterygiophore of a dorsal spine, is present anterior to the pterygiophore of the first dorsal spine in *Macrognathus siamensis* and in some African mastacembeloids includng *M. ophidium* among the Tanganyikan species, and *M. batesii, M. brevicauda, M. flavomarginatus, M. greshoffi, M. loennbergii, M. marmoratus, M. nigromarginatus* and *M. paucispinis* from western Africa.

Interspecific variation in the number of *branched fin rays* and their supporting *pterygiophores* is common. This variation may be directly related to the number of caudal vertebrae, as shown for example by *Mastacembelus liberiensis* which has the highest number of caudal vertebrae (i.e. 70) and also a high number of branched dorsal and anal fin rays (131 & 124, respectively). However, as a general rule, species total number of dorsal fin elements (spines and branched rays) are directly proportional to their total (abdominal and caudal) vertebrae number (see Table 5).

The development of spinous rays may influence the number of branch rays in the dorsal fin in some rapids dwelling species, as shown for example by *M. paucispinis* in which there are 9 dorsal spines, a moderate number of caudal vertebrae (53), but a high number of branched rays (120) which extend anteriorly across the abdominal/caudal vertebral junction. Apart from the undescribed species (p. 110), in no other mastacembeloid taxa were branched rays found to cross the abdominal/caudal vertebral junction.

There are relatively few branched dorsal and anal fin rays (generally not exceeding more than 60 elements) in *Macrognathus* species. *Mastacembelus pancalus* also exhibits a short dorsal and anal fin and has, apart from *Pillaia*, the smallest number of branched rays recorded in any mastacembeloid (36 dorsal and 41 anal) as well as a low number of spinous rays (25). The low number of dorsal fin elements (spines and rays) in these taxa can be directly related to their low total vertebral number (see Table 5) and anterior loss of spines (see p. 109).

Caudal fin

The caudal skeleton shows considerable inter- and intraspecific variation in the topography of its elements. The arrangement found in *M. mastacembelus* (p. 31) is more typical of the Asian than the African taxa.

To obtain an accurate appraisal of the caudal anatomy in a particular species a series of specimens was examined (where possible) in order to assay intraspecific variability. In most cases this had to be done with the aid of radiographs; it was thus not always possible to distinguish finer details (e.g. whether a uroneural is fused to or merely closely associated with the urostyle).

The caudal fin is distinct in the majority of Asian taxa (see Sufi, 1956), a feature distinguishing them from all African species, where the caudal fin is always confluent with the posterior branched rays of the dorsal and anal fins. In those Asian species which have the caudal united with the dorsal and anal fins (e.g. *Mastacembelus erythrotaenia, M. armatus, M. maculatus, M. caudiocellatus* and *M. circumcinctus*) the caudal rays are longer than, and extend beyond the tips of, the last dorsal and anal fin rays. Thus, in effect, a distinct caudal fin is discernible.

Associated with the distinct caudal fin of the Asian species is a relatively high number of principal *caudal rays* (usually about 16–20). *Mastacembelus pancalus* (Fig. 75a) is exceptional in having only 12 fin rays despite its having a distinct caudal fin.

The caudal in *M. sinensis, Chaudhuria* (Fig. 23a) and *Pillaia* (Fig. 23b) is also exceptional among Asian mastacembeloids since it is confluent with the dorsal and anal fins, and has only 8 or 9 rays. This arrangement is similar to that in the African taxa, all of which have a confluent caudal composed, in the majority of species, of 8–10 principal rays (see Figs 76, 77a & 78). Six principal caudal fin rays occur, however, in *Mastacembelus batesii, M. ophidium* and *M. aviceps,* whilst in *M. zebratus* there are only 4.

The number of *hypurals* varies from 5 autogenous elements to a single autogenous fan-shaped hypural plate. The size of the hypurals in taxa with 3 or 4 elements is proportionally smaller than in those with only 2 elements, and is probably the result of hypural fusion (faint suture lines can be seen in some cases e.g. *Mastacembelus congicus* Fig. 76b).

In the Asian species there are usually 4 or 5 hypural elements. This number is associated with the more distinct caudal fin and higher number of rays characterizing these taxa (see Figs 14, 75b & c). *Mastacembelus pancalus* (Fig. 75a) is exceptional in having only 2 large hypural elements (which may be correlated with the relatively low fin ray number i.e. 12) even though its caudal is distinct. Two hypural elements are otherwise found only in *M. sinensis, Chaudhuria* and *Pillaia.*

The majority of African mastacembeloids have only 2 distinct hypurals (Fig. 76a & b). Three hypurals are found only in *M. moorii* and in the undescribed species. A single fan-shaped hypural plate distinguishes *M. ellipsifer* (Fig. 77a) and *M. aviceps* (Fig. 77b) from all other African species.

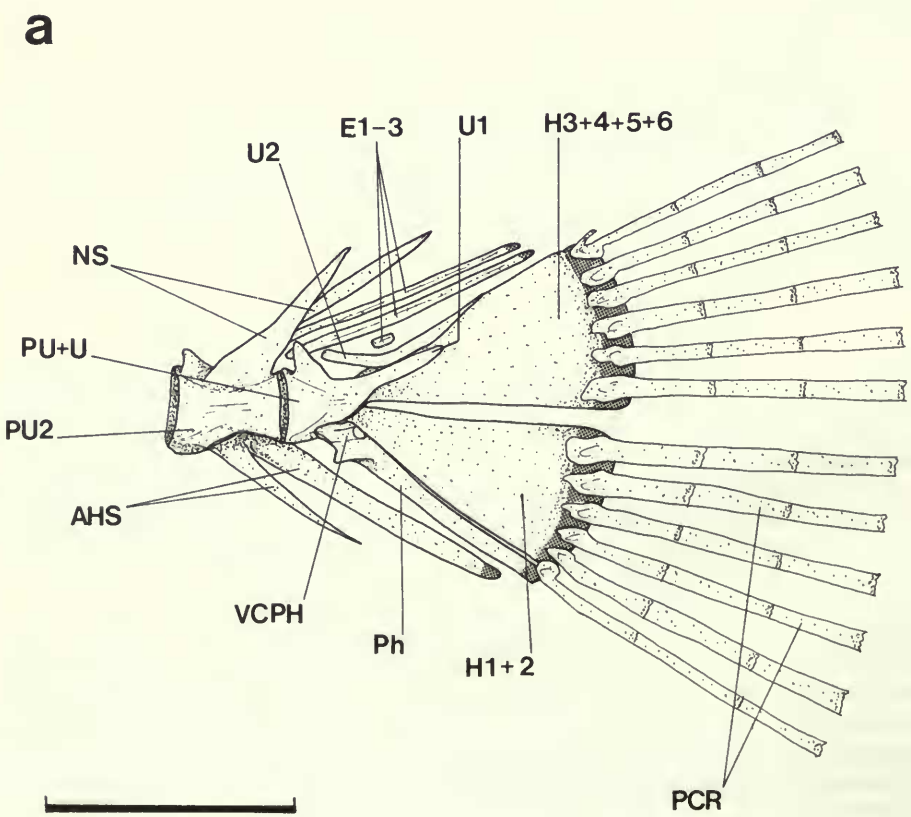

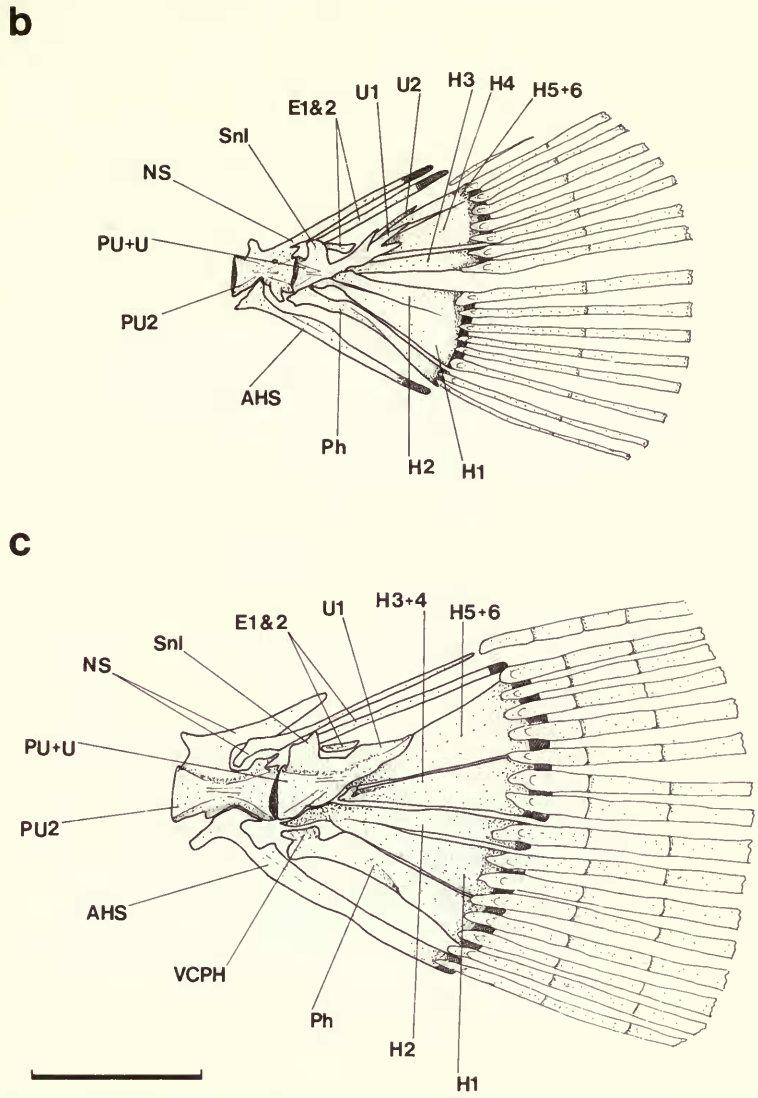

Fig. 75 Caudal fin skeleton in (a) *Mastacembelus pancalus,* (b) *Macrognathus aculeatus* and (c) *Mastacembelus erythrotaenia*; lateral aspect, left side.

The *parhypural* is autogenous and relatively large, compared with its condition in *M. mastacembelus*, in most taxa. It may become fused to the anterior edge of the first hypural in a number of African species (Fig. 78a & b).

Generally, there is only a single *uroneural* apparently fused along the dorsal edge of urostylar centrum, but it is not always possible to establish whether the uroneural is fused or merely closely associated with this centrum. In addition to this element, a single unfused uroneural (uroneural 2) occurs in *Macrognathus aculeatus* (Fig. 75b) and *Mastacembelus pancalus* (Fig. 75a), as well as in a variety of African species, including most of those in Lake Tanganyika. Two uroneurals were also found in two other species, *M. nigromarginatus* and *M. reticulatus,* both from West Africa. In many Asian and African taxa (including *M. maculatus, M. stappersii, M. niger* and *M. vanderwaali,* Fig. 76a), the uroneural has a bony extension developed from its upper margin, this is equivalent to the supraneural lamina discussed by Greenwood & Rosen (1971: 14).

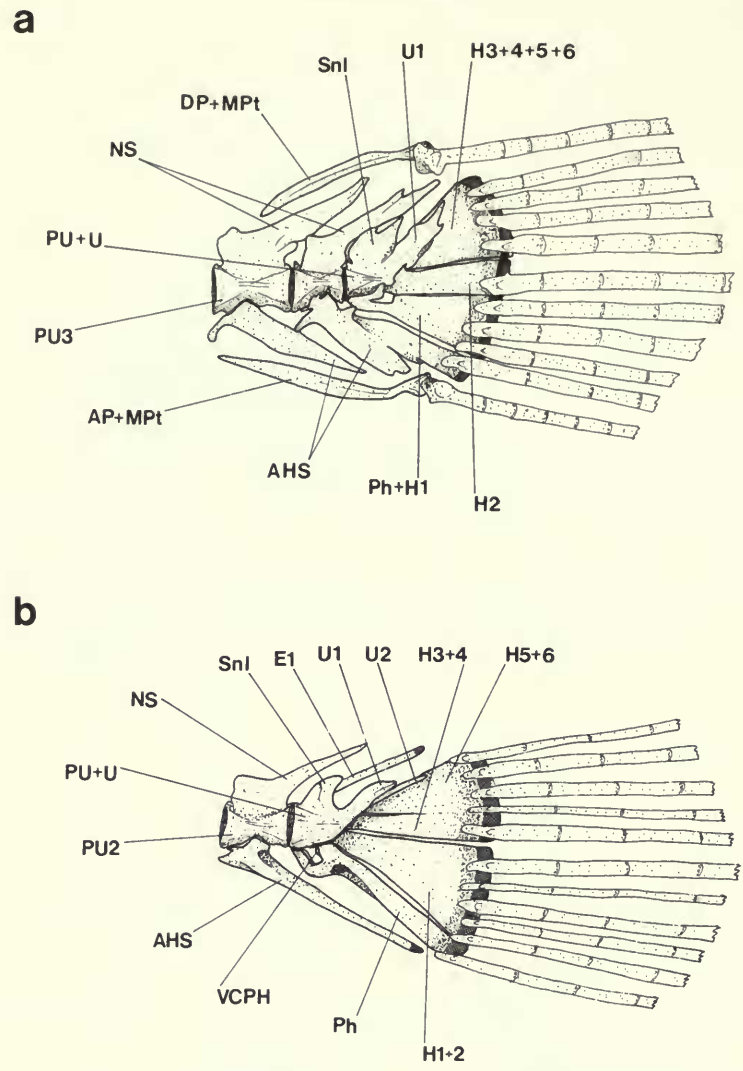

Fig. 76 Caudal fin skeleton in (a) *Mastacembelus vanderwaali* and (b) *Mastacembelus congicus*; lateral view, left side.

The number of *epurals* is also variable and ranges from a maximum of 3 to their total absence. Three epurals are found in *M. pancalus* (Fig. 75a) and *M. unicolor* but in no other species; 2 epurals occur in *M. erythrotaenia, M. guentheri* and *Macrognathus aculeatus* (Fig. 75b), with 1 in most of the remaining Asian taxa. The majority of African species have one or no epural, although *M. moorii,* and *M. nigromarginatus* have 2.

The *second preural vertebra* contributes to the caudal skeleton in a number of mastacembeloids. The haemal arch of this vertebra is autogenous in the majority of Asian taxa (*M. mastacembelus,* Fig. 14; *M. erythrotaenia,* Fig. 75c; and *Macrognathus* species, Fig. 75b). Its long haemal spine extends posteriorly to lie along the anterior edge of the parhypural, and its tip contributes to the support of the ventral caudal fin rays. In *Chaudhuria* (Fig. 23a) and *Pillaia* (Fig. 23b) the haemal arch is fused to the second preural vertebra and has a short haemal spine which does not contribute to the support of the caudal fin rays.

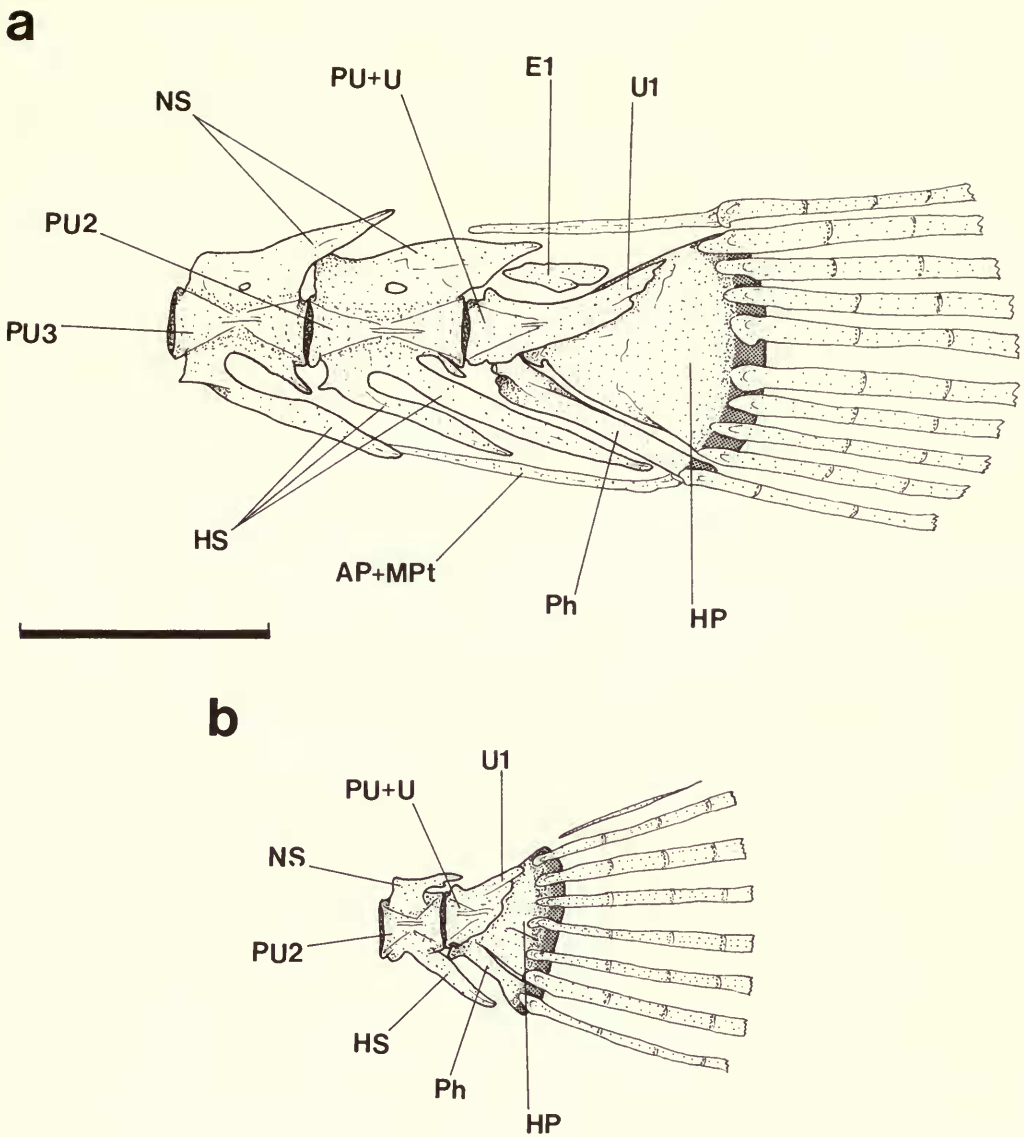

Fig. 77 Caudal fin skeleton in (a) *Mastacembelus ellipsifer,* and (b) *Mastacembelus aviceps*; lateral view, left side.

The haemal spine is short, non-ray supporting, and its arch fused to the second preural vertebra in the majority of African taxa (see Figs 76a, 77 & 78). In *Mastacembelus congicus* (Fig. 76b) however, the haemal spine is ray-supporting, and extends from an autogenous haemal arch in a manner similar to that of most Asian taxa.

Squamation

Small, *cycloid scales* cover the body, apart from the dorsal surface of the head in the majority of mastacembeloids. In some Asian taxa (e.g. *Mastacembelus pancalus*) the dorsal surface of the head is also covered in scales.

Chaudhuria and *Pillaia* among the Asian species, and *Mastacembelus latens,* (Roberts & Stewart, 1976: 307), *M. crassus,* and *M. aviceps* among the African taxa are completely scale-

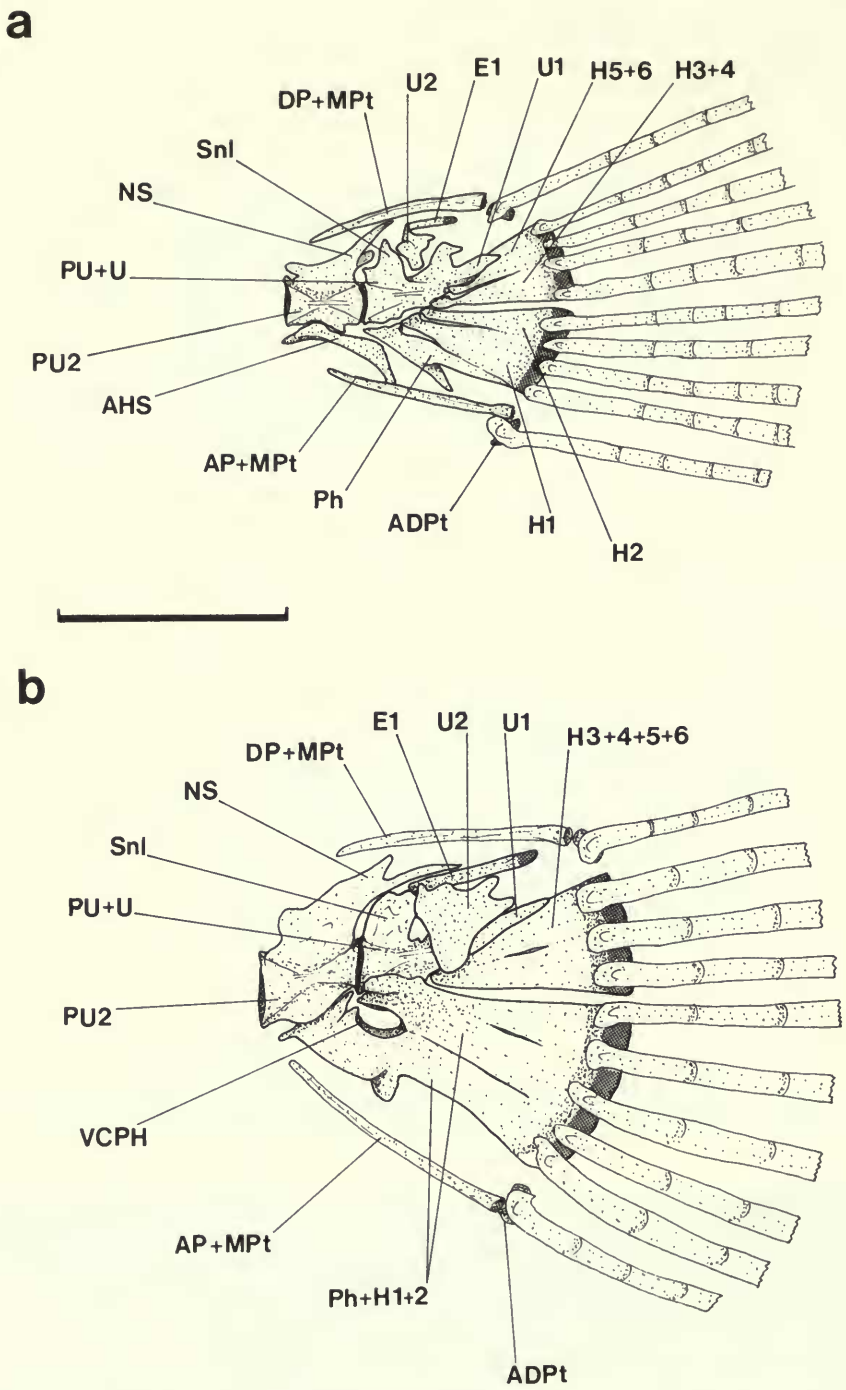

Fig. 78 Caudal fin skeleton in (a) *Mastacembelus shiranus* and (b) *Mastacembelus frenatus*; lateral aspect, left side.

less. An intermediate state between the modal condition and that found in these taxa occurs in *Mastacembelus micropectus.* Here, only the posterior third of the body is scaled.

Myology of *Mastacembelus mastacembelus*

Cephalic muscles

Group one muscles

The massive size of the adductor musculature, in comparison with the relatively small neurocranial, jaw and hyopalatine bones, is probably an indication that the mastacembeloid jaws are capable of powerful biting actions.

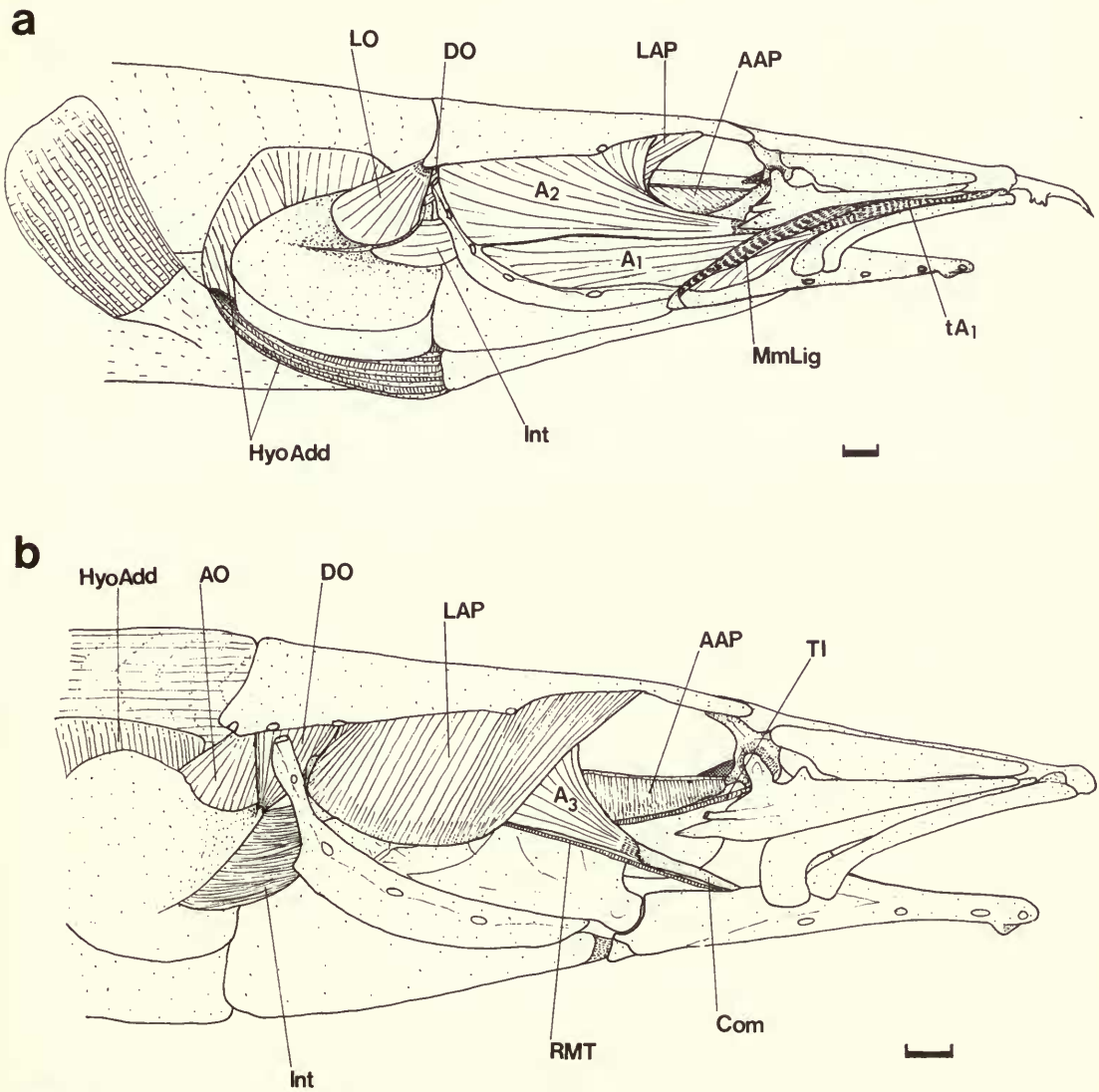

Fig. 79 *Mastacembelus mastacembelus,* (a) superficial cephalic muscles, tendons and ligament after removal of the skin and eyeball, and (b) deep cephalic muscles and tendons after removal of parts A_1 and A_2 of the *adductor mandibulae* muscle and the *levator operculi* muscle; lateral view, right side.

Four subdivisions of the *adductor mandibulae* (A_1; A_2; A_3 & A_w) are present in *Mastacembelus mastacembelus*. A ligament (Fig. 79a) passes superficially across the anterior region of the *adductor mandibulae,* from the lateral edge of the anguloarticular facet to the ventromedial face of the large 1st infraorbital bone. A small subdivision of this ligament passes from its ventral end below the adductor anterior tendon (tA_1) to attach to the mass of connective tissue on the posteromedial face of the maxilla (between it and the lateral face of the coronoid process). Although somewhat displaced, this ligament is thought to be homologous with the maxillo-mandibular ligament recently discussed by Stiassny (1981: 283).

Part A_1 of the *adductor mandibulae* (Fig. 79a) originates from the lateral face of the preoperculum (horizontal arm), symplectic, quadrate and posterolateral face of the anguloarticular. It is the smaller of the superficial adductor elements, and lies ventral to part A_2. A wide tendon (tA_1) extends anteriorly from the lateral face of A_1 and inserts along the ventrolateral margin of the maxilla and dorsal surface of the premaxilla. An inner slip of muscle fibres from the anteromedial face of A_1 insert musculously on the lateral face of the tendinous anterior end of the A_2 division.

Part A_2 forms the main mass of the superficial adductor musculature in *M. mastacembelus* (Fig. 79a). It lies dorsal to A_1 and curves anteriorly around the posteroventral edge of the orbit. The medial fibres of A_2 originate ventrally from the lateral face of the preoperculum (vertical arm), hyomandibula, symplectic, quadrate and coronomeckelian, and dorsally from the dorsolateral edge of the parietal, pterotic and frontal. A_2 is composed of two sections distinguished anteriorly by their separate tendons and sites of insertion. The upper section $A_{2\beta}$ (Fig. 79a) constitutes the bulk of the muscle, its fibres merging anteriorly onto a short, broad tendon that inserts on the posterodorsal edge of the coronoid process. The smaller lower section, $A_{2\alpha}$ (Fig. 80) has a narrow tendon which passes medially to merge with a wide aponeurosis on part A_w of the adductor complex.

The *truncus hyomandibularis* part of the VIIth cranial nerve emerges from the ventral hyomandibular foramen below the level of the dorsal margin of A_2 and runs anteriorly across its medial face before passing below the quadrate. A_2 is separated from the deeper part (A_3) of the *adductor mandibulae* by the *levator arcus palatini* muscle.

Part A_3 lies medial to the *levator arcus palatini* and is separated from it by a thin sheet of connective tissue. This broad muscle originates, ventrally, from the dorsolateral face of

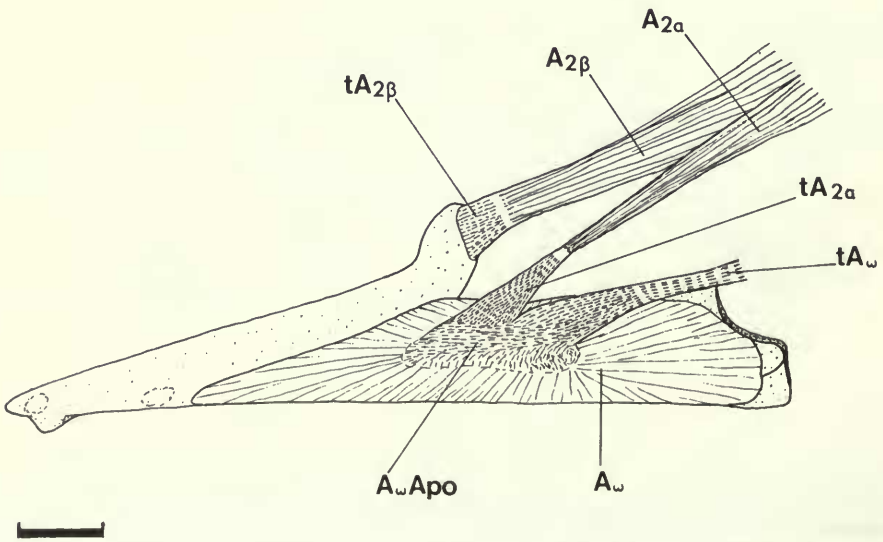

Fig. 80 *Mastacembelus mastacembelus,* lower jaw and associated musculature; medial aspect, right side.

the suspensorium (including the lateral face of the hyomandibula, quadrate, metapterygoid and endopterygoid) and dorsally from the precommissural lateral wall of the neurocranium (including the sphenotic, prootic, pterosphenoid and descending frontal lamina). The fibres course ventrorostrally, merging into a strong tendon (tA_3) that runs across the somewhat bulbous anterolateral face of the ectopterygoid (Fig. 79b). The tendon appears to have ossified in this region, possibly contributing to the unusually large coronomeckelian (Travers, 1984).

The anterior tip of the coronomeckelian is connected tendinously (tA_3) to the medial face of the meckelian fossa—along the posterodorsal edge of Meckel's cartilage. The *ramus mandibularis* of the trigeminal nerve branches from the *truncus infraorbitalis* medial to A_3, and passes ventrorostrally along the ventral edge of tA_3 and the long coronomeckelian.

Part A_w (Fig. 80) originates from the medial face of the mandible (including the anguloarticular, retroarticular and ventromedial margin of the dentary). Its fibres converge on a medial tendinous aponeurosis which is consolidated adjacent to the anguloarticular facet. This aponeurosis inserts on the anteromedial margin of the quadrate, just below the posteromedial process of the ectopterygoid.

The *levator arcus palatini* (Fig. 79b) is a thin sheet compressed between the dorsal region of A_2 and A_3; it originates along the dorsolateral edge of the neurocranium (pterotic and frontal), with its posterior fibres stemming from the postorbital process of the sphenotic.

The muscle runs vertically to insert musculously on the lateral face of the suspensorium, including the ventrolateral face of the hyomandibula and metapterygoid, and the dorsolateral face of the symplectic. It narrows posteriorly and its fibres intermix with the anterior fibres of the *dilatator operculi.*

The *dilatator operculi* (Fig. 79a) lies posterior to the *levator arcus palatini.* The lateral face of the dilatator is partly covered by the posterodorsal edge of *adductor mandibulae* A_2 and the upper arm of the preoperculum. It originates from the lateral face of the pterotic (above its hyomandibular fossa) and from the posterolateral margin of the sphenotic ventral to the postorbital process. Its fibres converge across the lateral face of the posterior hyomandibular condyle, and merge into a short tendon inserting firmly on the dorsal surface of a prominent dilatator process of the operculum.

Group two muscles

The *levator operculi* (Fig. 79a) is a comparatively large and ovoid muscle originating from the posterolateral face of the pterotic dorsal to the posterior end of the hyomandibular condyle. The dorsomedial face overlies the upper region of the *adductor operculi.* Ventral to this the medial face overlies the notched dorsal edge of the operculum, posterior to the opercular facet, and inserts musculously on the dorsolateral face of this bone. The ventral edge of the levator inserts along the narrow dorsal surface of the opercular ridge. This prominence separates it from a distinct muscle–the '*musculus intraoperculi*' (discussed below)–on the ventrolateral face of the operculum. The latter muscle originates on the posterolateral edge of the preoperculum, and inserts musculously on the adjacent lateral face of the operculum, ventral to the operculum ridge (Fig. 79a). There is no connection between this muscle and the *levator operculi* in *M. mastacembelus* (see p. 120).

The *adductor operculi* (Fig. 81) is a relatively small muscle covered, in lateral view, by the *levator operculi* and the operculum. It originates tendinously from the dorsolateral face of the exoccipital at a point below the posterior end of the pterotic facet for the hyomandibula. Its fibres expand ventrocaudally from a dorsal apex to insert musculously on the medial face of the operculum. The fibres along the posterior margin of the adductor intermingle with those from the dorsolateral region of the *hyohyoidei adductores* (discussed below). Between the anteromedial margin of the *adductor operculi* and the posterior edge of the *adductor hyomandibulae* is a pseudobranch (Bhargava, 1953). The buccal face of the pseudobranch lies just above the integumentary lining of the pharynx in a lateral recess in the dorsomedial face of the hyomandibula (Fig. 81).

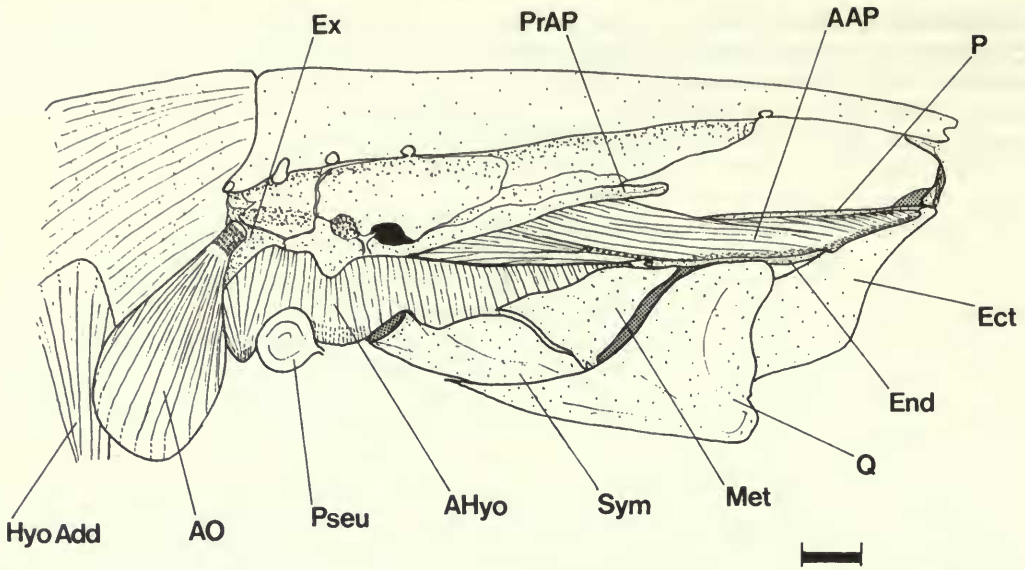

Fig. 81 *Mastacembelus mastacembelus,* deep cephalic adductor musculature after removal of the jaws, opercular series, hyomandibula and associated superficial cranial muscles; lateral view, right side.

The *adductor hyomandibulae* (Fig. 81) is well developed. Since it is apparently formed from the anterior fibres of either the *adductor operculi* or the *adductor arcus palatini* (Winterbottom, 1974), it is considered as a group two derivative.

The *adductor hyomandibulae* originates from the surface of the parasphenoid posterior to the lateral commissure. Fibres also originate from the border of the parasphenoid with the prootic in this region, and from the ventral surface of the small otic bulla in the prootic. The internal carotid foramen ventral to this bulla is covered by the *adductor hyomandibulae.* The muscle expands ventrally, and its lateral fibres insert on the ventromedial face of the hyomandibula. An anteroventral muscle slip extends below the posterior end of the *adductor arcus palatini* to insert musculously on the dorsomedial margin of the symplectic.

The *adductor arcus palatini* (Fig. 81) is an enlarged muscle extending along the side of the neurocranium from below the trigeminofacialis chamber to the lateral ethmoid. It originates mainly along the lateral face of the parasphenoid, from its anterior end (below the lateral ethmoid) to a point ventral to the lateral commissure. Fibres of the adductor also originate from the narrow lateral face of the basisphenoid and the ventrolateral face of the prootic, between the lateral commissure and the tip of its anterior process. The ventral surface of this process is trough-like, thus increasing the area available for muscle attachment.

The *adductor arcus palatini* extends between its area of origin and the dorsomedial face of the suspensorium. A series of small tendons from within the muscle merge into an aponeurosis that inserts on the posterior end of the endopterygoid. Apart from these tendons, the adductor inserts musculously on the dorsomedial face of the metapterygoid, the dorsal edge of the endopterygoid and ectopterygoid, and anteriorly, on the dorsal surface of the flattened suborbital region of the palatine.

A number of other myological features warrant description; not least of these is the distinct muscle (already noted; p. 119) originating from the posterior edge of the preoperculum and inserting on the lateral face of the operculum, ventral to the operculum ridge (Fig. 79b). The fibres of this muscle do not appear to intermingle with those of any other muscles in this region. It is innervated by a branch of the *truncus hyomandibularis* (VIIth.). Winterbottom's

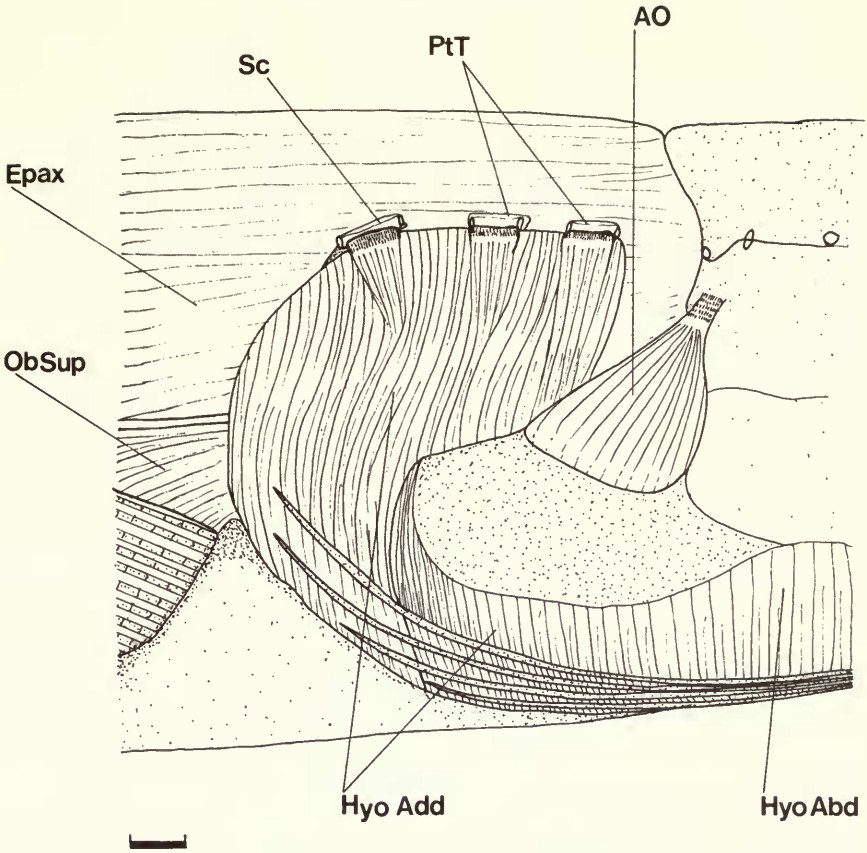

Fig. 82 *Mastacembelus mastacembelus, hyohyoidei adductores* muscle after removal of the opercular series; lateral view, right side.

(1974) synonymy gives no clue to the identity of this muscle. In view of its position within the opercular series I have named it the '*musculus intraoperculi*'. The presence of this muscle (possibly derived from the *hyohyoidei adductores;* see Travers, 1984) may be correlated with the restricted opercular opening in *M. mastacembelus,* and thus the need for an atypical method of expanding the branchial chamber.

The *hyohyoidei adductores* (Fig. 82) are large in *M. mastacembelus.* This muscle is innervated by the *ramus hyoideus* (part of the *truncus hyomandibularis* of VII), and lies anteriorly as a sheet of fibres between the distal parts of the branchiostegal rays. From there it extends dorsally above the last branchiostegal ray and continues around the dorsal margin of the operculum. The operculum partly overlies this dorsolateral expansion of the *hyohyoidei adductores,* whose lateral fibres are loosely connected to the medial face of the bone by a thin fascia. The dorsomedial face of the *hyohyoidei adductores* (above the operculum) inserts musculously along the lateral *epaxialis* musculature. The anterior edge of the muscle borders the *adductor operculi,* and there is some intermingling of their fibres. Posteriorly, the *hyoidei* inserts along the dorsolateral face of the cleithrum, the lateral face of the supracleithrum and the ventral margin of the posttemporal tubules (Fig. 82). The insertion of the muscle along the postcranial sensory canal marks its upper edge. This dorsal encroachment of the *hyohyoidei adductores* is responsible for the restricted opercular opening in *M. mastacembelus.*

The hypaxial musculature is considered to be composed of the dorsal *obliquus superioris* and the ventral *obliquus inferioris* by Winterbottom (1974).

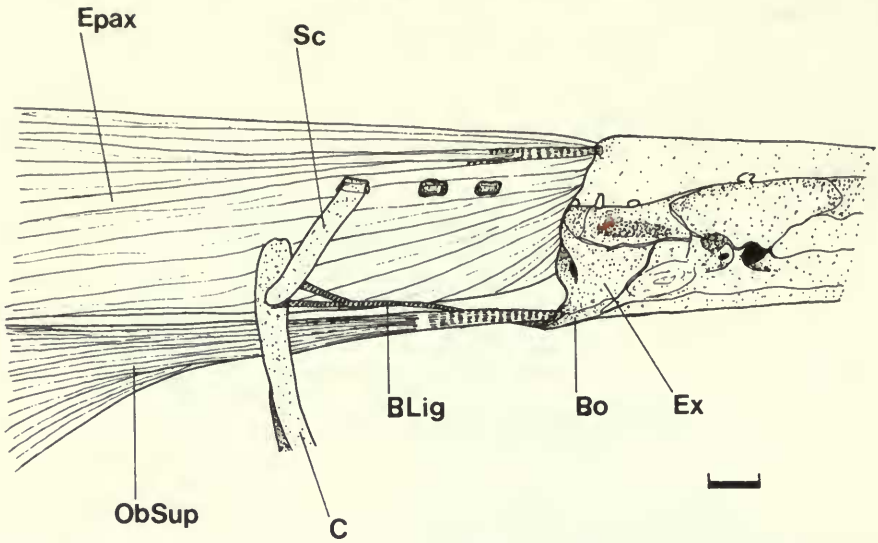

Fig. 83 *Mastacembelus mastacembelus,* epaxial musculature insertion on the basicranium and position of Baudelot's ligament; lateral aspect, right side.

The *obliquus superioris* (Fig. 83) has a particularly prominent point of insertion on the basicranium. The muscle tapers anteriorly from its posterior position along the ventrolateral wall of the body, the fibres merging into a strong aponeurosis adjacent to the medial face of the cleithrum. The aponeurosis passes along the ventral surface of the epaxial musculature, but is separated from it by the fascia covering the muscles. Anteriorly, the aponeurosis narrows into a strong tendon that inserts on the posteroventral base of the exoccipital, above its ventral border with the basioccipital.

Baudelot's ligament is small (Fig. 83), is closely associated with the prominent anterior tendon of the *obliquus superioris,* and is discernible only after careful dissection. It crosses the dorsal surface of the obliquus between its anterior connection to the basioccipital and its posterior connection to the pectoral girdle. The ligament attaches anteriorly to a shallow fossa on the posterior edge of the basioccipital, medial to the large obliquus tendon. A dense mass of adipose connective tissue in this region of the basicranium connects Baudelot's ligament to the *obliquus superioris* tendon. From its connection to the basioccipital the ligament runs posteriorly across the obliquus tendon and, anterior to the pectoral girdle, divides into an upper arm attaching to the ventromedial face of the supracleithrum, and a lower arm attaching to the dorsolateral face of the cleithrum.

Comparative myology of the Mastacembeloidei

Group one and two cephalic muscles in the majority of Asian and African mastacembeloids were examined and compared with those in *M. mastacembelus.* Unfortunately, this comparison only includes the most superficial muscles in specimens of *Chaudhuria* and *Pillaia,* partly because of their small adult size and partly because none could be serially sectioned.

Cephalic muscles

Group one muscles

The position and size of the maxillo-mandibular ligament in *M. mastacembelus* (Fig. 79a) is typical of that in the majority of mastacembeloids, including *Chaudhuria* and *Pillaia.* However, in two Tanganyikan species (*Mastacembelus albomaculatus* and *M. micropectus* Fig. 84a) and three from the lower Zairean rapids (*Mastacembelus brichardi,* Fig. 84b, *M.*

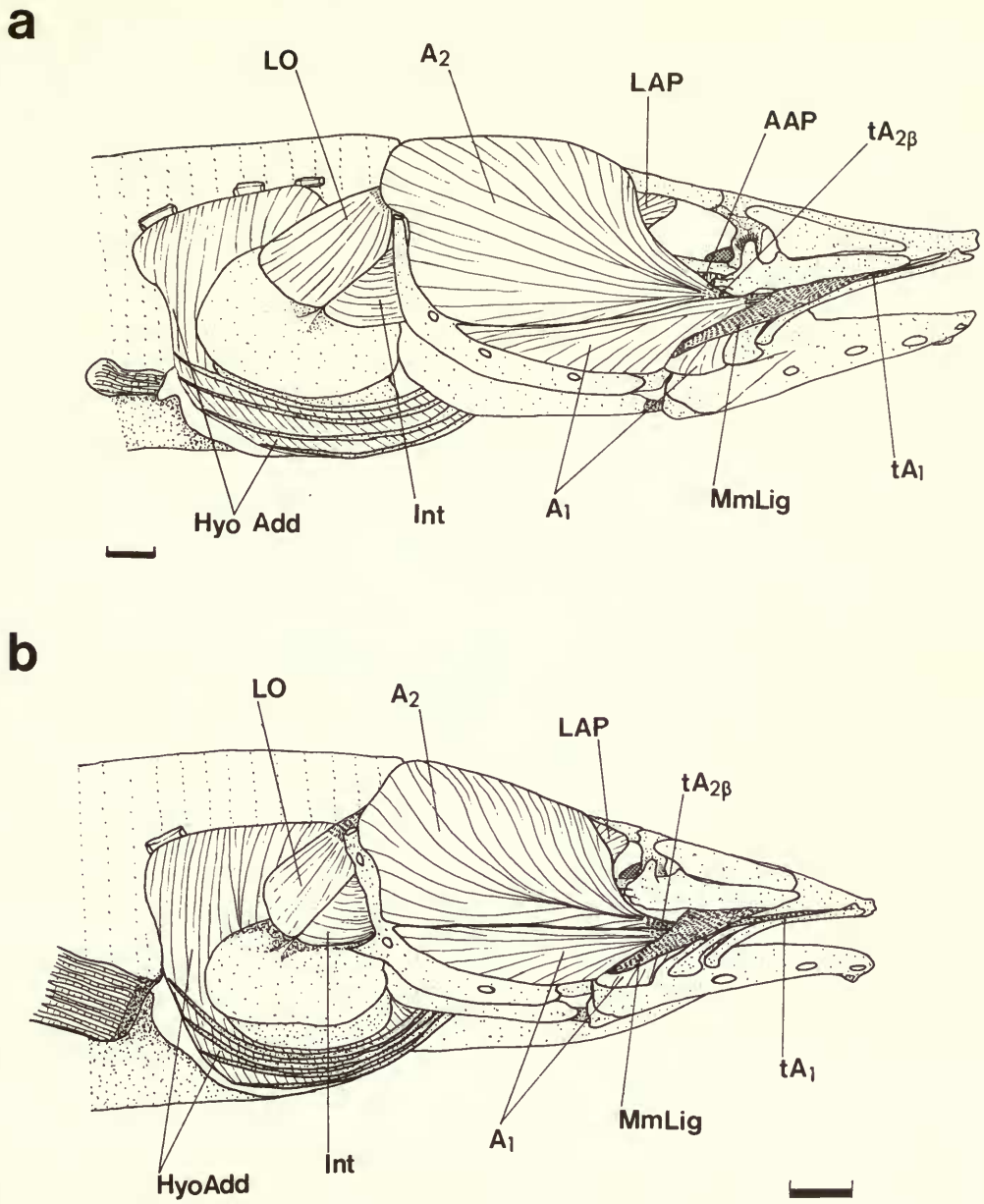

Fig. 84 Lateral view of the right superficial cephalic muscles, tendons and ligament after removal of the skin and eyeball, in (a) *Mastacembelus micropectus* and (b) *Mastacembelus brichardi*.

crassus and *M. aviceps*) the ventral attachment of the ligament is covered by the hypertrophied superficial adductor musculature. The maxillo-mandibular ligament is relatively narrow in *Mastacembelus moorii* (Fig. 85), and only attaches to the anterior end of the 1st infraorbital bone. The ligament is absent in *Mastacembelus sinensis, M. zebrinus, M. pancalus* and all *Macrognathus* species (Fig. 86a–c).

Interspecific variation in the morphology of the *adductores mandibulae* and their associated tendons is particularly noticeable in the superficial parts of that muscle complex.

The ventral position of A_1 is a diagnostic feature of all mastacembeloids. It is smaller than

A_2 in most taxa although some Asian species are exceptional. In the *Macrognathus* species (Fig. 86a), *Mastacembelus pancalus* (Fig. 86b) and *M. zebrinus* (Fig. 86c) A_1 is the largest element of the adductor complex. In these taxa it extends dorsally over the ventrolateral face of A_2, the upper edge lying on a level with the centre of the eye, and the large size of A_1 may be associated with the lack of the maxillo-mandibular ligament. Also, in these species the lateral fibres converge onto a sheet-like aponeurosis which is consolidated into a particularly long strap-like tA_1 tendon.

Part A_1 is also relatively large in a number of Tanganyikan and Zairean species (but does not exceed A_2 in size), and is a reflection of the generally hypertrophied adductor musculature in these species (see below).

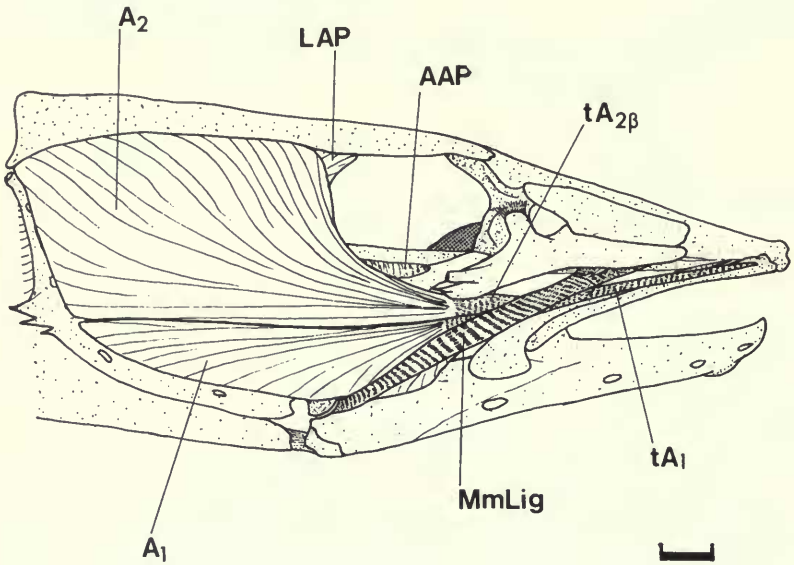

Fig. 85 *Mastacembelus moorii,* superficial *adductor mandibulae* muscle, tendons and associated ligament after removal of the skin and eyeball; lateral aspect, right side.

The inner slip of muscle originating from the anteromedial face of A_1 inserts musculously on the lateral face of the anterior tendinous part of A_2 in all mastacembeloid taxa. A_1 is small in *Mastacembelus moorii* (a Lake Tanganyikan species; Fig. 85), and has a restricted origin from the ventrolateral face of the quadrate, the anteroventral face of the preoperculum, and from the anguloarticular. In this species A_2 is large and originates from the lateral face of the symplectic and most of the preoperculum and quadrate.

The dorsolateral position of A_2 and its subdivision into two subsections ($A_{2\alpha}$ and $A_{2\beta}$) inserting tendinously on, respectively, the coronoid process and posterior tendon of A_w, are characteristic features of the superficial adductor musculature in all Asian and African mastacembeloids.

A_2 is exceptionally small in *Macrognathus* species, *Mastacembelus pancalus* and *M. zebrinus* (Fig. 86a–c), a feature combined with the enlarged A_1 in these taxa, and which may be correlated with the size and shape of the coronoid process (Travers, 1984). The posterodorsal fibres of A_2 in these taxa barely cover the *levator arcus palatini.* The fibres merge ventrorostrally and extend below the orbit, grading into a long strap-like tendon (tA_2). This tendon divides anteriorly, the small medial subsection ($tA_{2\alpha}$) inserting on the posterior aponeurosis of A_w, the larger lateral subsection ($tA_{2\beta}$) inserting on the lateral face of the broad, low coronoid process and on the dorsolateral face of the dentary.

The dorsal fibres of A_2 originate above the upper edge of the *levator arcus palatini* and part A_3, in the two Tanganyikan species *Mastacembelus moorii* and *M. ophidium.* The dorsal surface of the skull in these species is relatively narrow, and the expanded A_2 fibres originate from its dorsolateral margin.

The adductor muscles, particularly A_2, are hypertrophied to an unparalleled extent in the microphthalmic and cryptophthalmic mastacembeloids. *Pillaia* (from Asia; Fig. 87), *Mastacembelus micropectus* and *M. albomaculatus* (Lake Tanganyika; Fig. 84a) and *M. brachyrhinus, M. brichardi, M. crassus, M. aviceps* and probably *M. latens* (from the lower Zairean rapids; Fig. 84b).

The adductor musculature in *Mastacembelus brichardi* was described by Poll (1973). This species is markedly cryptophthalmic and its reduced eyes lie below A_2 and the *levator arcus palatini.*

In all the cryptophthalmic and microphthalmic taxa the roof of the skull slopes ventrally and the massive A_2 originates from the dorsal surface of the frontal postorbitally, and from the entire dorsal surface of the parietal. The dorsomedial face of each A_2 contacts its partner in the midline (their fibres not interconnecting) in all but *Pillaia* and *M. brachyrhinus,* in these species A_2 is not hypertrophied to such an extreme extent as it is in the others.

Part A_3 of the *adductor mandibulae* lies medial to the *levator arcus palatini* and has a similar origin and insertion in all mastacembeloids (p. 118). The size of the coronomeckelian is an indication of the size and strength of the A_3 muscle and its anterior tendon (tA_3). The extent to which the tendon of A_3 ossifies varies widely among the Asian and African taxa, (see above p. 80).

Part A_w shows no marked departure from the condition described for *M. mastacembelus* (p. 119).

In all species the *levator arcus palatini* lies between divisions A_2 and A_3 of the *adductor mandibulae*; it originates from the dorsolateral edge of the neurocranium and inserts musculously along the dorsolateral face of the suspensorium. The levator fibres merge ventrally into a wide, transparent, sheet-like aponeurosis which is particularly thin in a number of Asian (e.g. *Mastacembelus sinensis* and *M. armatus*) and African species (e.g. *M. frenatus, M. moorii* and *M. batesii*). This condition of the levator appears to have a mosaic distribution among the mastacembeloids. The posterodorsal fibres intermingle with those from the anterior margin of the *dilatator operculi* in all taxa.

The ventral apex of the *dilatator operculi* inserts tendinously on the dorsal surface of the opercular dilatator process in all mastacembeloids.

The extent to which the lateral face of the dilatator is covered by the preoperculum and the A_2 division of the *adductor mandibulae* depends on the degree to which the latter are developed. In those species with a protracted vertical arm of the preoperculum, for example *M. longicauda* and *M. reticulatus*, the lateral face of the dilatator is completely covered, as it is in those species with a particularly massive A_2 muscle (p. 87 & Fig. 84).

Group two muscles

The *levator operculi* shows little interspecific variation apart from slight differences in relative size. The muscle insertion on the dorsolateral face of the operculum, is a characteristic feature of all mastacembeloids. A large levator, (relative to its size in *M. mastacembelus*) occurs in *M. albomaculatus*; its ventrolateral fibres traverse the low opercular ridge in this species, and intermix with the dorsolateral fibres of the *'intraoperculi'* muscle.

The morphology of the *adductor operculi* also shows little interspecific variation. The fibres along the posterior margin of the muscle intermingle, in all species, with the dorsolateral part of the *hyohyoidei adductores* in a manner similar to that described in *M. mastacembelus* (p. 119). The pseudobranch lies between the posteromedial margin of the *adductor operculi* and anteromedial face of the *adductor hyomandibulae* in all the species investigated.

There is little interspecific deviation of the *adductor hyomandibulae*; it is particularly well-developed in all mastacembeloids. The muscle originates from the posteroventral region of

the parasphenoid and prootic (including the ventral surface of the otic bulla), and inserts on the medial face of the symplectic and hyomandibula (Fig. 81).

The marked interspecific variation in the arrangement of the *adductor arcus palatini* muscle involves, posteriorly, its site of origin along the ventrolateral face of the braincase, and anteriorly, its connection to the enlarged 1st infraorbital bone. The anterior region of the *adductor arcus palatini,* compared with its condition in *M. mastacembelus* (Fig. 81), is modified in a number of Asian taxa including the *Macrognathus* species, *Mastacembelus pancalus, M. zebrinus, M. keithi, M. caudiocellatus* and *M. maculatus* (see Figs 86 & 88). The anterior fibres of the muscle in these taxa extend from the anterolateral face of the parasphenoid across the ectopterygoid to insert musculously along the posterior edge of the 1st infraorbital. In *M. zebrinus* (Fig. 88a) this extension is little more than the lengthening of the anterolateral fibres of the adductor which form the orbital floor. However, in *Macrognathus* (particularly *M. aculeatus;* Fig. 88b) the anterior region of the *adductor arcus palatini* is unconnected to the fibres which form the orbital floor, apart from some slight contact along the anteromedial margin. The medial end of this virtually distinct anterior muscle in *Macrognathus aculeatus* is connected, tendinously, to the anterior end of the parasphenoid along its dorsolateral margin. The muscle fibres extend anterolaterally around the edge of the orbital cavity, crossing but not connecting to the anterodorsal face of the ectopterygoid. The anterior end of the fibres in this region merge into a broad aponeurosis which inserts on the attenuated posterior edge of the 1st infraorbital (Fig. 41a).

This anterior differentiation of the *adductor arcus palatini* may be correlated with the large rostral appendage in the species involved. The uniquely trunk-like rostral appendage in *Macrognathus,* where the muscle is found in its most highly developed form, lends support to this view. Contraction of the anterior adductor would result in movement of the large 1st infraorbital bone which contributes to the complex musculo-skeletal system that governs the movement of the highly mobile rostral appendage in these taxa.

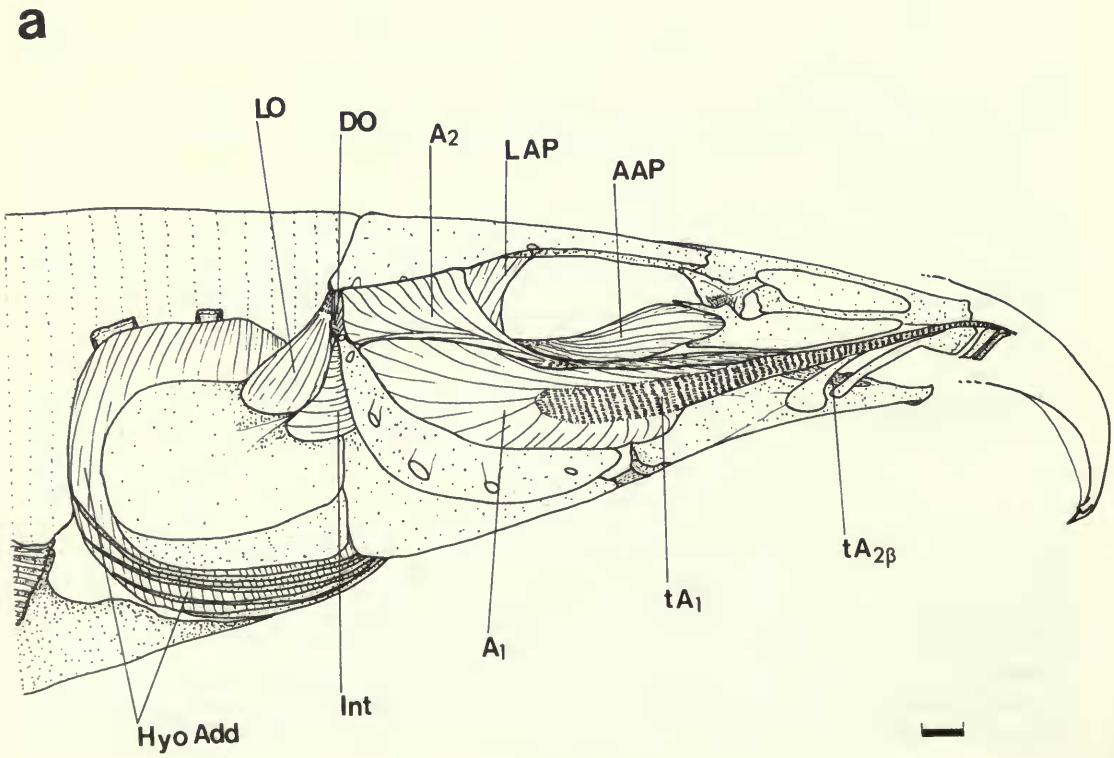

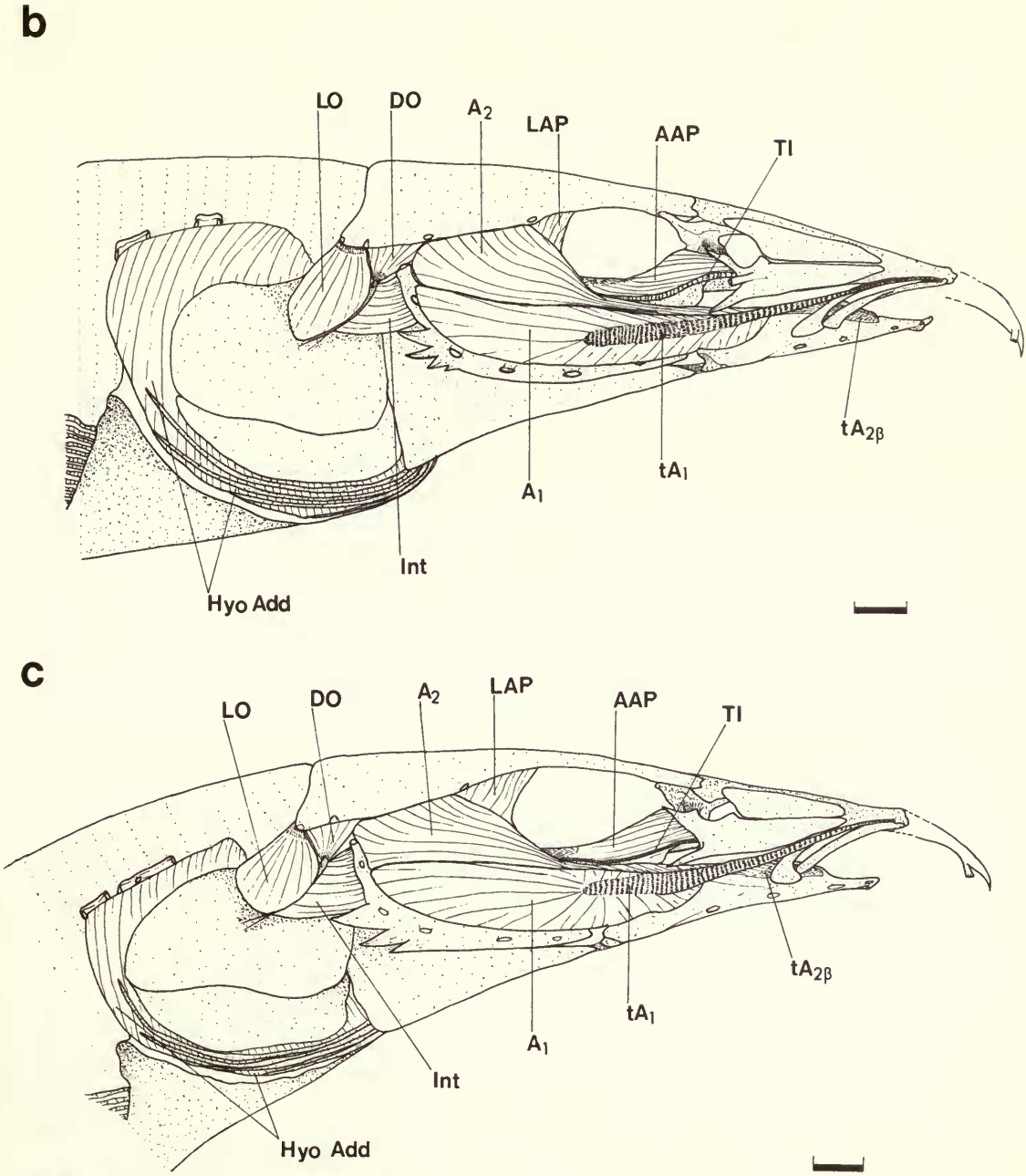

Fig. 86 Lateral view of the right superficial cephalic muscles, after removal of the skin and eyeball, in (a) *Macrognathus aculeatus,* (b) *Mastacembelus pancalus* and (c) *Mastacembelus zebrinus.*

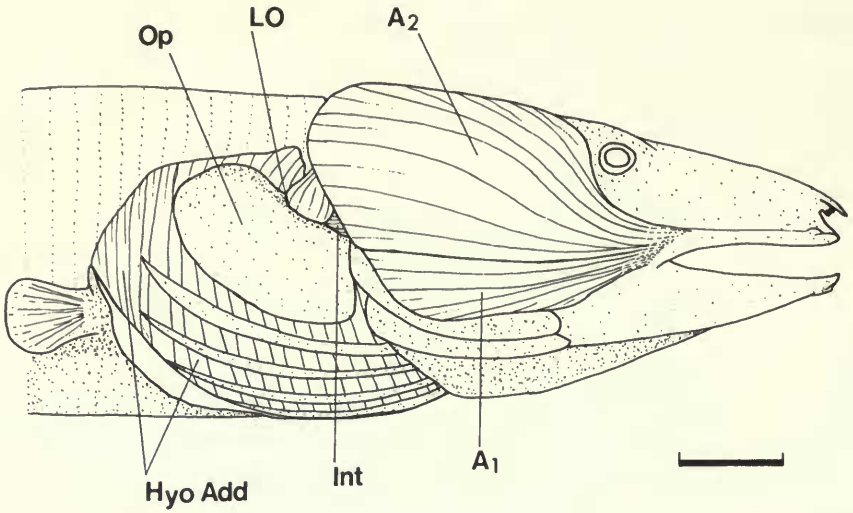

Fig. 87 *Pillaia indica,* superficial cephalic muscles after removal of the skin; lateral view, right side.

The anterior fibres of the *adductor arcus palatini* do not insert on the posterodorsal surface of the palatine in *Mastacembelus armatus* or *Mastacembelus erythrotaenia* and hence do not form the orbital floor in these species.

The *adductor arcus palatini* originates posteriorly, in the majority of mastacembeloids, along the ventrolateral face of the prootic and ventral surface of its anterior process (as described in *M. mastacembelus* p. 120). The lack of a long anterior prootic process in some species results in a smaller area available for the origin of the adductor. The absence of this process may be associated with the presence of only a relatively small rostral appendage and the lack of an enlarged anterior region of the adductor in these species (e.g. *Mastacembelus tanganicae* p. 61).

The need to provide an increased area of origin for the long *adductor arcus palatini* is probably a further factor influencing the development of the anterior process on the prootic generally found in mastacembeloids.

Of the other myological features; the *'musculus intraoperculi'* (p. 121) is a unique characteristic of all mastacembeloids. In the majority of taxa its fibres are unconnected to those of any other cephalic muscle (Figs 79a & 84–87).

The *hyohyoidei adductores* shows little interspecific variation in their arrangement. The dorsolateral expansion of the muscle, and its musculous insertion on the cleithrum, supracleithrum and posttemporal tubules are features common to all taxa, including *Chaudhuria* and *Pillaia.* This branchiostegal muscle is responsible for restricting the opercular opening since it extends over, and is inserted on, the ventrolateral face of the epaxialis musculature.

The *obliquus superioris* is similar in all mastacembeloids, and its anterior tendinous insertion on the posteroventral face of the exoccipital is a characteristic feature of the group. The wide anterior tendon inserts laterally in a shallow basioccipital fossa medial to which the basioccipital accommodates the anterior end of Baudelot's ligament.

A small, relatively weak Baudelot's ligament, as described in *M. mastacembelus* (p. 122), is present in all taxa. It is closely connected to the large anterior obliquus tendon ventrally, and with the ventral surface of the epaxialis musculature dorsally. In most species the ligament crosses the dorsal surface of the obliquus tendon before attaching to the pectoral girdle. However, in *Mastacembelus longicauda* it crosses ventrally, below the tendon. A divided posterior end of Baudelot's ligament, inserting on both the cleithrum and the supracleithrum, is also a feature common to all mastacembeloids.

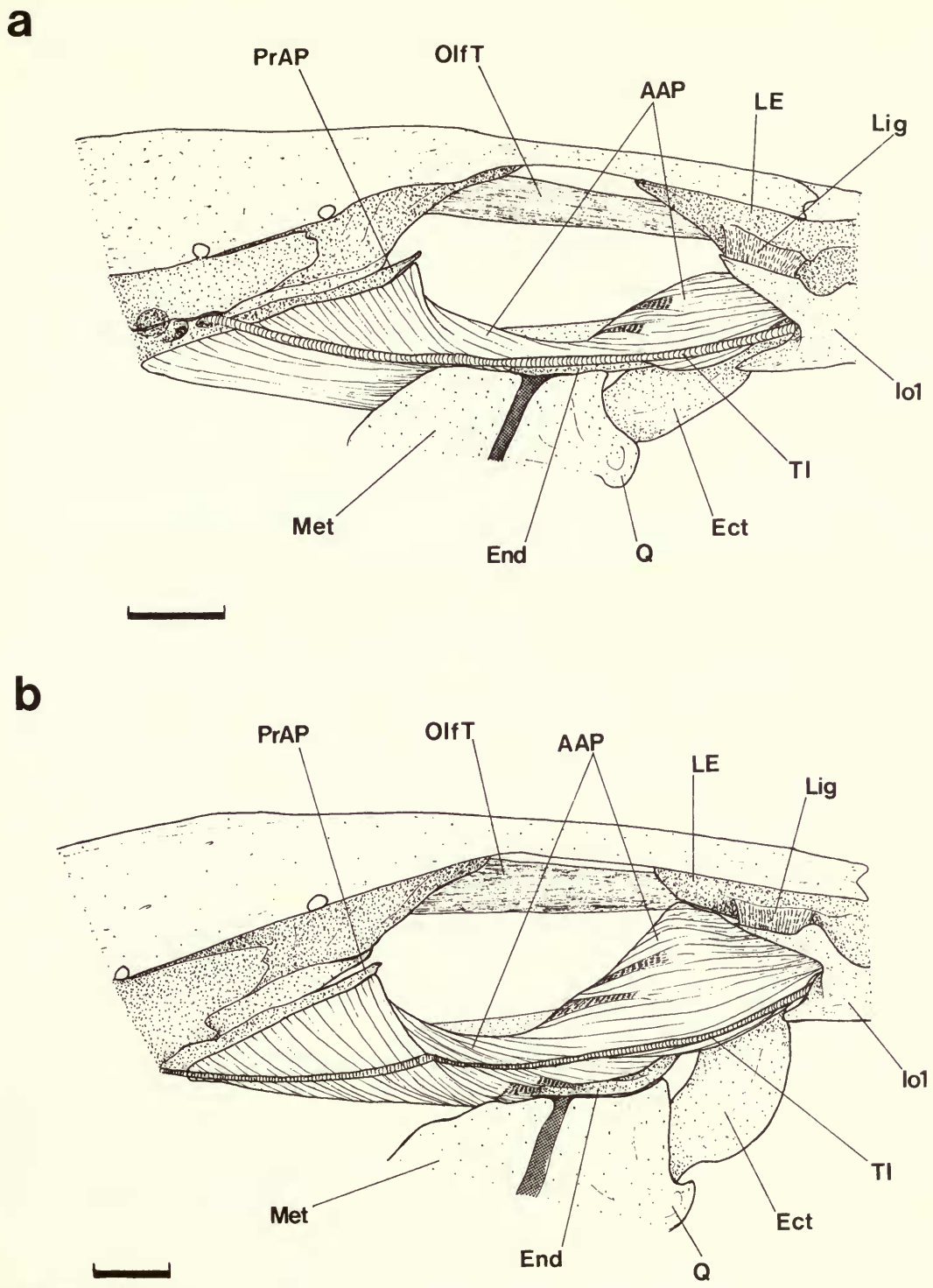

Fig. 88 Lateral view of the right *adductor arcus palatini* muscle in (a) *Mastacembelus zebrinus,* and (b) *Macrognathus aculeatus.*

Acknowledgements

I am indebted to the Trustees of the British Museum (Natural History) and the Keeper of Zoology for access to the collections and research facilities.

I acknowledge the assistance given me by Professor J. D. Pye (and staff in the Department of Zoology and Comparative Physiology, Queen Mary College) in whose department this study was initiated and I particularly thank Dr D. R. Kershaw for supervision and my initial introduction to the Fish Section at the British Museum (Natural History).

It is with great pleasure that I extend my sincere thanks and gratitude to the staff in the Fish Section (and all associated with it), under whose guiding influence I was fortunate enough to fall. In particular I thank Dr P. H. Greenwood (not least for his role as mentor and critic of an earlier draft) and Gordon Howes for their time and inspiring discussions.

Financial support from Queen Mary College (Drapers' Studentship) and the University of London (University Studentship) is also acknowledged with gratitude as is the Central Research Fund (Univ. of Lond.) and Godman Exploration Fund (BM[NH]) for financing fieldwork in East Africa.

Loans and gifts of specimens for this study were generously donated by: Dr P. H. Skelton (AM); Dr T. R. Roberts (CAS); Dr Hsien-Wen (IHW-h, China); Dr C. C. Swift (LACM); Prof K. F. Liem (MCZ); Dr D. Thys van den Audenaerde (RG) and Drs K. C. Jayaram & G. M. Yazdani (ZSI).

Finally, my parents Duilio and Helen Travers deserve special mention for without their active encouragement and support, over many years, this would surely not have been possible. To them and Kath I extend my warmest thanks.

References

Agrawal, V. P. & Dalela, R. C. 1966*a*. The heart of freshwater eel, *Macrognathus aculeatus* (Bl.). *Agra. Univ. J. Res.* **15** (1) : 83–89.

—— & —— 1966*b*. A study on the physiology of digestion in *Rhynchobdella aculeatus* (Bl.). *Proc. natn. Acad. Sci. India.* **36** (Sect. B) : 369–379.

—— & **Tyagi, A. P.** 1963. Studies on the morphology and physiology of the alimentary canal of *Mastacembelus pancalus* (Ham). *Agra. Univ. J. Res.* **12** : 105–114.

Annandale, N. 1918. Fish and fisheries in the Inle Lake. *Rec. Indian Mus.* **14** : 33–64.

—— & **Hora, S. L.** 1923. The systematic position of the Burmese fish *Chaudhuria. Ann. Mag. nat. Hist.* (9) **11** : 327–333.

Berg, L. S. 1940. *Classification of fishes both recent and fossil.* Russian & English Lithoprint, 1947. Ann Arbor, Michigan: J. W. Edwards.

Bertin, L. & Arambourg, V. 1958. Super-ordre des Teleosteens (Teleostei). In *Traite de Zoologie* by Grasse, P.–P. **13** : 2205–2500. Masson & Cie.

Bhargava, H. N. 1953. Pseudobranch in *Mastacembelus. Curr. Sci.* **22** : 343–344.

—— 1957*a*. The development of the chondrocranium of *Mastacembelus armatus* (Cuv. & Val.). *J. Morph.* **102** : 401–426.

—— 1957*b*. Studies on the development and morphology of the chondrocranium of *Mastacembelus armatus* (Cuv. & Val.). *J. Univ. Saugar* **11** *B. 6* : 86–89.

—— 1958. The morphology of the chondrocranium of *Mastacembelus armatus,* (Cuv. & Val.). *J. Morph.* **104** : 327–360.

—— 1962*a*. Studies on the nasal organ and infranasal chamber in the family Mastacembelidae. *Proc. 1st all-India Congr. Zool.* **2** : 169–177.

—— 1962*b*. Tubular and folded type of olfactory saccule in Mastacembelidae. *Curr. Sci.* **31** : 288–289.

—— 1963*a*. The cranial osteology of *Mastacembelus armatus. Morph. Jb.* **105** : 1–25, 8 figs.

—— 1963*b*. The development of the cephalic arteries in *M. armatus* (Cuv. & Val.). *Acta. Zool. Stockh.* **44** : 103–117.

Bleeker, P. 1859. Enumeratio specierum . . . *Act. Soc. Sc. Indo-Neerl.* **6** : 1–279.

Bloch, M. E. 1786. *Naturgeschichte der Austandichen Fische.* 2. Berlin.

—— 1801 (Ed. Schneider, J. G.). *Systema Ichthyologiae,* Berlin.

Boulenger, G. A. 1904. A synopsis of the suborders and families of teleostean fishes. *Ann. Mag. nat. Hist.* (7) **13** : 161–190.

—— 1912. A synopsis of the fishes of the genus *Mastacembelus. J. Acad. nat. Sci. Philad.* (*2*) **15** : 197–203.

Chandrasekhar, K. 1961. The structure of the kidney of some teleostean fishes. *Rec. Indian Mus.* **59** : 479–495.

Cuvier, M. le B. & Valenciennes, M. A. 1831. *Historie naturelle des poissons.* Paris, vol: 8.

Dalela, R. C. 1967*a*. The urinogenital system of Indian freshwater eel *M. aculeatus* (Bl.). *Vest. csl. Spol. zool* **31** :15–21.

—— 1967*b*. Studies on the afferent and efferent branchial vessels of the fresh water eel *Macrognathus aculeatus. Agra. Univ. J. Res.* **16** (1): 49–53.

—— 1968. Studies on the vertebral column of *Macrognathus aculeatus* (Bl.). *Zool. Anz.* **182**: 61–69.

—— **& Garg, P. C.** 1968. Studies on the vertebral column of *M. armatus (Lacép.). Vest. csl. Spol. zool* **32** : 312–318.

Datta Munshi, J. S. 1964. 'Chloride cells' in the gills of fresh water teleosts. *Q. Jl. microsc. Sci.* **105** (1) : 79–89.

Dingerkus, G. & Uhler, L. D. 1977. Enzyme clearing of Alcian Blue stained whole small vertebrates for demonstration of cartilage. *Stain. Tech.* **52** (4) : 229–232.

Dubale, M. S. 1952. Branchiomeric and hypobranchial muscles of certain Indian air-breathing fishes. *J. Univ. Bombay N.S.* **20B** (5) : 6–13.

Fink, W. L. 1981. Ontogeny and phylogeny of tooth attachment modes in actinopterygian fishes. *J. Morph.* **167** : 167–184.

Freihofer, W. C. 1963. Patterns of the ramus lateralis accessorius and their systematic significance in teleostean fishes. *Stanford Ichthyol. Bull.* **8** (2) : 80–89.

—— 1978. Cranial nerves of a percoid fish, *Polycentrus schomburgkii* (family Nandidae), a contribution to the morphology and classification of the order Perciformes. *Occ. Pap. Calif. Acad. Sci.* **128** : 1–78.

Frost, G. A. 1930. A comparative study of the otoliths of the neopterygian fishes. *Ann. Mag. nat. Hist.* (10) **5** (1930) : 621–627.

Goodrich, E. S. 1909. Cyclostomes and fishes. In *A treatise on zoology*: pt. 9. Lankester, R. (Ed.). Adam & Charles Black, London.

Gosline, W. A. 1971. *Functional morphology and classification of teleostean fishes.* Honolulu: Univ. Press. Hawaii.

Greenwood, P. H. 1976. A review of the family Centropomidae (Pisces, Perciformes). *Bull. Br. Mus. nat. Hist.* (Zool). **29** : 1–81.

—— **& Rosen, D. E.** 1971. Notes on the structure and relationships of the alepocephaloid fishes. *Am. Mus. Novit.* **2473** : 1–41.

——, **Rosen, D. E., Weitzman, S. H. & Myers, G. S.** 1966. Phyletic studies of teleostean fishes, with a provisional classification of living forms. *Bull. Am. Mus. nat. Hist.* **131** (4) : 339–456.

Gregory, W. K. 1933. Fish skulls: A study of the evolution of natural mechanisms. *Trans. Am. Phil. Soc.* **23** (Art 2) : 75–481.

Gronovius, L. T. 1763. *Zoophylacium Gronovianum* **1**: 132. Leiden.

Günther, A. 1861. *Catalogue of the acanthopterygian fishes* **3** (B) : 539–543.

Harrington, R. W. 1955. The osteocranium of the American cyprinid fish. *Notropis bifrenatus,* with an annotated synonymy of teleost skull bones. *Copeia* 1955 : 269–290.

Jarvik, E. 1980. *Basic structure and evolution of vertebrates.* Academic Press, London.

Job, T. J. 1941. Life-history and bionomics of the spiny eel, *Mastacembelus pancalus* (Hamilton). *Rec. Indian Mus.* **43** : 121–135.

Khanna, S. S. & Gill, T. S. 1973. Histology of the principle Islets of Langerhans in some freshwater teleosts. *Anat. Anz.* **133** (4) : 367–376.

Lacépède, B. 1800. *Histoire naturelle des poissons.* Paris, vol. 2.

Liem, K. F. 1974. Evolutionary strategies and morphological innovations: cichlid pharyngeal jaws. *Syst. Zool.* **22** : 425–441.

Linnaeus, C. 1758. *Systema Naturae.* 10th ed. Stockholm.

Maheshwari, S. C. 1963. The skull of *Mastacembelus armatus* (Lacép.). *Sci. & Cult.* **29** (1): 30–31.

—— 1965*a*. The head skeleton of *Mastacembelus armatus.* (Lacép.). *J. zool. Soc. India* **17** : 52–63.

—— 1965*b*. The cranial nerves of *Mastacembelus armatus* (Lacépède). *Jap. J. Ichthyol.* **12** : 89–98.

—— 1966*a*.The heart and venous system of *Mastacembelus armatus* (Lacép.). *Proc. Natn. Acad. Sci. India.* (Sect. B) **36** : 577–584.

—— 1966*b*. A case of abnormality in the testes of *Mastacembelus armatus* (Lacép.). *Jap. J. Ichthyol.* **14** : 101–102.

—— 1971. The cephalic sensory canals of *Mastacembelus armatus* (Lacépède). *J. Zool. Soc. India.* **23** (2): 163–166.

Matthes, H. 1962. Poissons nouveaux ou intéressants du lac Tanganika et du Ruanda. *Annls. Mus. r. Afr. Cent.* (in 8) *Zool.* **No. 111**: 27–88.

McAllister, D. E. 1968. Evolution of branchiostegals and classification of teleostome fishes. *Bull. Natn. Mus. Can.* **221**: 1–239.

Mitra, B. K. & Ghosh, E. 1931. On the internal anatomy of the families Opisthomi. *Rec. Indian Mus.* **33**: 291–300.

Müller, J. 1844. Uber den bau und die grenzen der ganoiden und uber das naturliche system der fische. *Ber. Akad. Wiss. Berlin:* 201–204.

Nagar, S. K. & Khan, W. M. 1957. The anatomy and histology of the alimentary canal of *Mastacembelus armatus* (Lacép). *Proc. Indian Acad. Sci.* **47B**: 173–187.

Nelson, G. J. 1969. Gill arches and the phylogeny of fishes, with notes on the classification of vertebrates. *Bull. Am. Mus. nat. Hist.* **141** (4): 475–552.

—— 1970. Gill arches of some teleostean fishes of the families Salangidae & Argentinidae. *Jap. J. Ichthyol.* **17** (2): 61–66.

Patterson, C. 1975. The braincase of pholidophorid and leptolepid fishes, with a review of the actinopterygian braincase. *Phil. Trans. R. Soc.* B **269** (No. 899): 275–579.

—— 1977. Cartilage bones, dermal bones and membrane bones, or the exoskeleton versus the endoskeleton. In *Problems in Vertebrate Evolution:* 77–121. Andrews, S. Mahala, Miles, R. S. & Walker, A. D. (Eds.). Academic Press, London.

—— **& Rosen, D. E.** 1977. Review of ichthyodectiform and other mesozoic teleost fishes and the theory & practice of classifying fossils. *Bull. Am. Mus. nat. Hist.* **158** (2): 83–172.

Poll, M. 1958. Description d'un poisson aveugle nouveau du Congo Belge appartenant à la famille des Mastacembelidae. *Revue Zool. Bot. Afr.* **57**: 388–392.

—— 1973. Les yeux des poissons aveugles Africains et de *Caecomastacembelus brichardi* Poll, en particulier. *Annls speleol.* **28** (2): 221–230.

Regan, C. T. 1912. The osteology of the teleostean fish of the order: Opisthomi. *Ann. Mag. nat. Hist.* (8) **9**: 217–219.

Regan, C. T. 1919. Notes on *Chaudhuria,* a teleostean fish of the order: Opisthomi. *Ann. Mag. nat. Hist.* (9) **3**: 198–199.

Roberts, T. R. 1980. A revision of the Asian mastacembeloid fish genus *Macrognathus. Copeia* 1980 **3**: 385–391.

—— **& Stewart, D. J.** 1976. An ecological and systematic survey of fishes in the rapids of the Lower Zaire or Congo River. *Bull. Mus. Comp. Zool.* **147** (6): 239–317.

Rosen, D. E. 1973. Interrelationships of higher euteleostean fishes. In *Interrelationships of fishes:* 397–513. Greenwood, P. H., Miles, R. S. & Patterson, C. (Eds.). Academic Press, London.

—— **& Greenwood, P. H.** 1976. A fourth neotropical species of synbranchid eel and the phylogeny and systematics of synbranchiform fishes. *Bull. Am. Mus. nat. Hist.* **157** (1): 1–69.

Russell, A. 1756. *The natural history of Aleppo, and parts adjacent.* 1st Ed. London.

Saxena, D. B. 1956. On the afferent branchial arteries in *Mastacembelus armatus. Curr. Sci.* **25**: 23.

Scopoli, J. A. 1777. *Introductio ad historiam naturalem.* Prague.

Skelton, P. H. 1976. A new species of Mastacembelus (Pisces: Mastacembelidae) from the Upper Zambezi River, with a discussion of the taxonomy of the genus from this system. *Ann. Cape Prov. Mus.* (*Nat. Hist.*). **11**: 103–116.

Smith, C. L. & Bailey, M. 1961. Evolution of the dorsal-fin supports of percoid fishes. *Pap. Mich. Acad. Sci.* **116**: 345–363.

Sriwastwa, V. M. S. 1970. Functional anatomy of digestive organs of a freshwater fish, *Rhynchobdella aculeata* (Ham.), Part 1B Histology. *Vest. csl. Spol. zool.* **34**: 136–142.

Swarup, K., Srivastava, S. & Das, V. K. 1971. Sexual dimorphism in the spiny eel *Mastacembelus pancalus. Curr. Sci.* **41** (2): 68–69.

Stiassny, M. L. J. 1981. The phyletic status of the family Cichlidae (Pisces Perciformes): A comparative anatomical investigation. *Neth. J. Zool.* **31** (2): 275–314.

Sufi, S. M. K. 1956. Revision of the Oriental fishes of the family Mastacembelidae. *Bull. Raffles Mus.* **27**: 93–146.

Talwar, P. M., Yazdani, G. M. & Kundu, D. K. 1977. On a new eel-like fish of the genus *Pillaia,* Yazdani (Pisces: Mastacembeloidei) from India. *Proc. Indian Acad. Sci.* **85** (*Sec. B.*) *No. 2*: 53–56.

Taverne, L. 1973. Sur la présence d'un dermosupraoccipital chez les Mastacembelidae (Teleosteans—Perciformes). *Revue Zool. Bot. afr.* **87** (4): 825–828.

—— 1980. Sur l'existence d'un basisphénoide chez les Mastacembelidae (téléostéens–acanthoptérygiens). *Bull. Inst. r. Sci. nat. Belg.* Biologie **52** : 1–2.

Travers, R. A. 1981. The interarcual cartilage; a review of its development distribution and value as an indicator of phyletic relationships in euteleostean fishes. *J. Nat. Hist.* **15** : 853–871.

—— 1984. A review of the Mastacembeloidei, a suborder of synbranchiform teleost fishes. Part II; Phylogenetic analysis. *Bull. Br. Mus. nat. Hist.* (Zool). **47** (1). Publication 28 June 1984.

Wheeler, A. C. 1956. The type species of *Mastacembelus* and the second edition of Russell's 'Natural History of Alleppo.' *Bull. Raffles Mus. No.* **27** : 91–92.

Whitehouse, R. H. 1918. The caudal fin of the eel *Chaudhuria. Rec. Indian Mus.* **14** : 65–66.

Winterbottom, R. 1974. A descriptive synonymy of the striated muscles of the Teleostei. *Proc. Acad. nat. Sci. Philad.* **125** (12) : 225–317.

Yazdani, G. M. 1972. A new genus of fish from India. *J. Bombay nat. Hist. Soc.* **69** (1) : 134–135.

Yazdani, G. M. 1975. Fishes of Khasi Hills Meghalya (India), with observations on their distributional pattern. *J. Bombay. nat. Hist. Soc.* **74** : 17–28.

—— 1976*a*. The upper jaw of Indian hill-stream eel *Pillaia indica,* Yazdani (Perciformes: Mastacembeloidei). *Bull. Zool. Surv. India.* **2** : 213–214.

—— 1976*b*. A new family of mastacembeloid fish from India. *J. Bombay nat. Hist. Soc.* **73** (1) : 166–170.

—— 1978. Adaptive radiation in the mastacembeloid fishes. *Bull. Zool. Surv. India.* **1** (3) : 279–290.

Manuscript accepted for publication 9 March 1983